

University of Windsor

Scholarship at UWindor

Electronic Theses and Dissertations

Theses, Dissertations, and Major Papers

2012

MODELING AND EXPERIMENTAL STUDY ON HEAT TRANSFER IN SQUEEZE CASTING OF MAGNESIUM ALLOY AM60 AND ALUMINUM ALLOY A443

Zhizhong Sun
University of Windsor

Follow this and additional works at: <https://scholar.uwindsor.ca/etd>

Recommended Citation

Sun, Zhizhong, "MODELING AND EXPERIMENTAL STUDY ON HEAT TRANSFER IN SQUEEZE CASTING OF MAGNESIUM ALLOY AM60 AND ALUMINUM ALLOY A443" (2012). *Electronic Theses and Dissertations*. 467.

<https://scholar.uwindsor.ca/etd/467>

This online database contains the full-text of PhD dissertations and Masters' theses of University of Windsor students from 1954 forward. These documents are made available for personal study and research purposes only, in accordance with the Canadian Copyright Act and the Creative Commons license—CC BY-NC-ND (Attribution, Non-Commercial, No Derivative Works). Under this license, works must always be attributed to the copyright holder (original author), cannot be used for any commercial purposes, and may not be altered. Any other use would require the permission of the copyright holder. Students may inquire about withdrawing their dissertation and/or thesis from this database. For additional inquiries, please contact the repository administrator via email (scholarship@uwindsor.ca) or by telephone at 519-253-3000ext. 3208.

**MODELING AND EXPERIMENTAL STUDY ON
HEAT TRANSFER IN SQUEEZE CASTING OF
MAGNESIUM ALLOY AM60 AND ALUMINUM
ALLOY A443**

by

Zhizhong Sun

A Dissertation

Submitted to the Faculty of Graduate Studies

through Engineering Materials

in Partial Fulfillment of the Requirements for

the Degree of Doctor of Philosophy at the

University of Windsor

Windsor, Ontario, Canada

2011

©2011 Zhizhong Sun

Modeling and Experimental Study on Heat Transfer in Squeeze Casting of Magnesium Alloy AM60 and Aluminum Alloy A443

by

Zhizhong Sun

APPROVED BY:

M. Sadayappan, External Examiner
CANMET Materials, Natural Resources Canada

H. Wu
Department of Electrical & Computer Engineering

V. Stoilov
Department of Mechanical, Automotive & Materials Engineering

J. Sokolowski
Department of Mechanical, Automotive & Materials Engineering

X. Niu, Industrial Advisor
Cosma International, MAGNA

H. Hu, Advisor
Department of Mechanical, Automotive & Materials Engineering

R. Carriveau, Chair of Defense
Department of Civil & Environmental Engineering

November 8, 2011

DECLARATION OF CO-AUTHORSHIP/PREVIOUS PUBLICATION

I. CO- AUTHORSHIP DECLARATION

I hereby declare that this dissertation does not incorporate material that is result of joint research. In all cases, the key ideas, primary contributions, experimental designs, data analysis and interpretation, were performed by the author and Dr. H. Hu as advisor.

I certify that, with the above qualification, this dissertation, and the research to which it refers, is the product of my own work.

II. DECLARATION OF PREVIOUS PUBLICATION

This dissertation includes 5 original papers that have been previously published/submitted for publication in peer reviewed journals/conference proceedings, as follows:

Thesis Chapter	Publication title/full citation	Publication status
Chapter 2	Zhizhong Sun , Xuezhi Zhang, Xiaoping Niu, Alfred Yu, Henry Hu, “Numerical simulation of heat transfer in pressurized solidification of Magnesium alloy AM50”, <i>Heat and Mass Transfer/Waerme- und Stoffuebertragung</i> , (2011) Vol. 47, pp. 1241-1249.	Published
Chapter 3	Zhizhong Sun , Xiaoping Niu, Henry Hu, “Estimation of heat transfer coefficient in squeeze casting of magnesium alloy AM60 by experimental polynomial extrapolation method”, <i>Magnesium Technology 2011</i> , (2011), p146-152. 140 th TMS 2011 conference proceedings.	Published
Chapter 4	Zhizhong Sun , Henry Hu, Xiaoping Niu, “Determination of heat transfer coefficients by extrapolation and numerical inverse methods in squeeze casting of magnesium alloy AM60”, <i>Journal of Materials Processing Technology</i> , (2011) Vol. 211, pp. 1432-1440.	Published
Chapter 5	Zhizhong Sun , Henry Hu, Xiaoping Niu, “Section thickness-dependant interfacial heat transfer in squeeze casting of aluminum alloy A443”, <i>The 3rd International Conference on</i>	Accepted

	<i>Advances in Solidification Processes(ICASP-3), Aachen, Germany (June 7-10, 2011).</i>	
Chapter 6	Zhizhong Sun , Xiaoping Niu, Henry Hu, “Effects of local pressure and wall-thickness on interfacial heat transfer in squeeze casting of magnesium alloy AM60”, <i>Proceedings of the 7th International Conference on Computational Heat and Mass Transfer(ICCHMT-7), Istanbul, Turkey, (July 18-22, 2011).</i>	Accepted
Chapter 7	Zhizhong Sun, Henry Hu, “Numerical simulation and experimental verification during squeeze casting of AM60 and A443”	Submitted

I hereby certify that I have obtained a written permission from the copyright owner(s) to include the above published material(s) in my dissertation. I certify that the above material describes work completed during my registration as graduate student at the University of Windsor.

I declare that, to the best of my knowledge, my dissertation does not infringe upon anyone’s copyright nor violate any proprietary rights and that any ideas, techniques, quotations, or any other material from the work of other people included in my dissertation, published or otherwise, are fully acknowledged in accordance with the standard referencing practices. Furthermore, to the extent that I have included copyrighted material that surpasses the bounds of fair dealing within the meaning of the Canada Copyright Act, I certify that I have obtained a written permission from the copyright owner(s) to include such material(s) in my dissertation.

I declare that this is a true copy of my dissertation, including any final revisions, as approved by my dissertation committee and the Graduate Studies office, and that this dissertation has not been submitted for a higher degree to any other University or Institution.

ABSTRACT

This study developed a solution algorithm based on the function specification method to solve the inverse heat conduction equations. By this solution, the casting-die interfacial heat transfer coefficients(IHTC) in light metal squeeze castings were determined accurately and the pressurized solidification was simulated precisely. This goal was accomplished in the four stages.

First, a model was developed to simulate fluid flow in forced convection and heat transfer in pressurized solidification of a cylindrical simple shape squeeze casting. Pressure-dependent heat transfer coefficients (HTC) and non-equilibrium solidification temperatures were determined by experimental measurements. With the measured HTC and temperatures under the different pressures, the temperature distributions and the cooling behaviours of squeeze cast were simulated.

In the second stage, a different wall-thickness 5-step casting mould was designed, and squeeze casting of magnesium alloy AM60 was performed under an applied pressure 30, 60 and 90 MPa in a hydraulic press. With measured temperatures, heat fluxes and IHTCs were evaluated using the polynomial curve fitting method and numerical inverse method. The accuracy of these curves was analyzed by the direct modeling calculation. The results indicated that heat flux and IHTCs determined by the inverse method were more accurately than those from the extrapolated fitting method.

In the third stage, the inverse method was applied to an aluminum alloy A443 and magnesium alloy AM60. As the applied hydraulic pressure increased, the IHTC peak value of each step was increased accordingly. Compared to the thin steps at the upper cavity, the relatively thick steps attained higher peak IHTCs and heat fluxes values due to

high local pressures and high melt temperature. The empirical equations relating IHTC to the local pressures and solidification temperature at the casting surface were derived and summarized.

Finally, the IHTC values calculated by inverse method were applied to simulate the solidification process of the 5-step casting model. The results showed that the numerical calculated temperatures were in well agreement with experimental ones. It is adequately demonstrated that the inverse method is a feasible and effective tool for determination of the IHTC.

DEDICATION

I would like to dedicate this dissertation to my parents for their unconditional love, support and encouragement.

I also would like to thank my wife, and my daughter. Their love and support enable me to go through the difficult time and finally complete this dissertation.

ACKNOWLEDGEMENTS

This study could not have done forward without the financial support from the Natural Sciences and Engineering Research Council of Canada(NSERC).

I would like to thank my doctoral advisor, Dr. Henry Hu, for his valuable suggestions and excellent supervision of this research work during my study.

Many thanks to my committee members(Dr. Jerry Sokolowski, Dr. Vesselin Stoilov, Dr. Huapeng Wu, and Dr. M. Sadayappan) for their helpful comments and careful review of this work.

In particular, I would like to thank Dr. Xiaoping Niu and Mr. Darren Womack from Promatek Research Centre of Cosma International, MAGNA for useful discussions.

I would like to thank Mr. Andy Jenner, Mr. Xuezhi Zhang, Mr. Zhijiang Wang, Mr. Jonathan Burns and Mr. Qiang Zhang from University of Windsor for their assistance with the experiments.

Finally, I am thankful to the faculty, staff and graduate students at the Department of Mechanical, Automotive and Materials Engineering of the University of Windsor, particularly my colleagues at the Light Metals Casting lab, for their support and encouragement.

TABLE OF CONTENTS

DECLARATION OF CO-AUTHORSHIP/PREVIOUS PUBLICATION.....	III
ABSTRACT.....	V
DEDICATION.....	VII
ACKNOWLEDGEMENTS	VIII
LIST OF TABLES	XII
LIST OF FIGURES	XIII
NOMENCLATURE.....	XVIII
ACRONYMS	XVIII
CHAPTER 1 INTRODUCTION.....	1
1. GENERAL OVERVIEW	1
2. MOTIVATION.....	2
3. OBJECTIVES	3
4. OUTLINE OF THIS DISSERTATION.....	4
5. INTERFACIAL HEAT TRANSFER COEFFICIENT	6
6. INVERSE METHOD	17
7. MODELING OF SQUEEZE CASTING	21
6. SUMMARY	25
REFERENCES.....	26
CHAPTER 2 NUMERICAL SIMULATION OF HEAT TRANSFER IN PRESSURIZED SOLIDIFICATION OF MAGNESIUM ALLOY AM50	35
1.INTRODUCTION	35
2. MATHEMATICAL MODELING.....	38
2.1. Governing equations	38
2.2. Enthalpy method	39
2.3. Initial and boundary conditions	40
3. SIMULATION RESULTS	44
3.1 Temperature distribution and solidification front	44
3.2 Effect of applied pressures on cooling behavior.....	50
4. EXPERIMENTAL VERIFICATION	53
5. RESULTS AND DISCUSSION	54
6. CONCLUSIONS	56
REFERENCES.....	58

**CHAPTER 3 ESTIMATION OF HEAT TRANSFER COEFFICIENT IN
SQUEEZE CASTING OF MAGNESIUM ALLOY AM60 BY EXPERIMENTAL
POLYNOMIAL EXTRAPOLATION METHOD 60**

1. INTRODUCTION	60
2. EXPERIMENTAL SETUP	62
2.1 5-Step casting	62
2.2 Casting Process	62
2.3 Casting process	63
3. DETERMINATION OF IHTC	64
3.1 Heat transfer model	66
3.2 Polynomial curve fitting method	67
4. RESULTS AND DISCUSSION	69
4.1 Experimental cooling curve	69
4.2 Typical Heat flux(q) & IHTC(h) curves	70
5. CONCLUSIONS	73
REFERENCES	75

**CHAPTER 4 DETERMINATION OF HEAT TRANSFER COEFFICIENTS BY
EXTRAPOLATION AND NUMERICAL INVERSE METHODS IN SQUEEZE
CASTING OF MAGNESIUM ALLOY AM60 78**

1. INTRODUCTION	78
2. EXPERIMENTS	82
2.1 Step casting model	82
2.2 CONFIGURATION OF DIE AND INSTALLATION OF MEASUREMENT UNIT	83
2.3 CASTING PROCESS	85
3. MATHEMATICAL MODELING OF IHTC	88
3.1 Inverse method	89
3.2 Polynomial curve fitting method	95
4. RESULTS AND DISCUSSION	97
4.1 Heat flux(q) & IHTC(h) curves	97
4.2 Accuracy verification	99
5. CONCLUSIONS	105
REFERENCES	107

**CHAPTER 5 SECTION THICKNESS-DEPENDANT INTERFACIAL HEAT
TRANSFER IN SQUEEZE CASTING OF ALUMINUM ALLOY A443 110**

1. INTRODUCTION	110
2. EXPERIMENTAL DESIGN	112
3. RESULTS AND DISCUSSION	114

CONCLUSIONS	119
REFERENCES	121
CHAPTER 6 EFFECTS OF LOCAL PRESSURE AND WALL-THICKNESS ON INTERFACIAL HEAT TRANSFER IN SQUEEZE CASTING OF MAGNESIUM ALLOY AM60.....	123
1.INTRODUCTION	123
2. EXPERIMENTAL DESIGN	126
3. RESULTS AND DISCUSSION	127
CONCLUSIONS	140
REFERENCE	142
CHAPTER 7 VERIFICATION OF IHTCS DETERMINED BY THE INVERSE METHOD	144
1. CASTING PARAMETER SPECIFICATION	144
2. COMPARISON OF COOLING CURVES MAGNESIUM ALLOY AM60	147
3. COMPARISON OF COOLING CURVES ALUMINUM ALLOY A443.....	154
4. SUMMARY	161
REFERENCE	161
CHAPTER 8 GENERAL CONCLUSIONS AND FUTURE WORK.....	163
1. GENERAL CONCLUSIONS	163
2. SUGGESTIONS FOR FUTURE WORK	165
CHAPTER 9 STATEMENT OF ORIGINALITY	163
APPENDIX A COPYRIGHT RELEASES FROM PUBLICATIONS.....	168
CHAPTER 2.....	168
CHAPTER 3.....	170
CHAPTER 4.....	171
CHAPTER 5.....	174
APPENDIX B SOURCE CODE OF INVERSE MODELING METHOD.....	177
APPENDIX C THE 5-STEP SQUEEZE CASTINGS EXPERIMENTAL RESULTS OF MAGNESIUM ALLOY AM60 & ALUMINUM ALLOY A443 UNDER DIFFERENT PRESSURES	189
PUBLICATION LIST	200
VITA AUCTORIS	203

LIST OF TABLES

Table 1- 1	IHTCs between light metal and mould dies or chills	9
Table 1- 2	Modeling method of squeeze casting processes	24
Table 2- 1.	Thermophysical properties of magnesium alloy AM50	44
Table 4- 1.	Chemical composition of magnesium alloy AM60	86
Table 4- 2.	Thermophysical properties of magnesium alloy AM60	86
Table 7- 1.	Parameters for filling simulation	145
Table 7- 2.	Parameters for solidification simulation.....	146
Table 7- 3.	Initial and boundary conditions for simulation	147

LIST OF FIGURES

Figure 1- 1 Heat flow across the metal-mould interface[4].	8
Figure 1- 2 Comparison of direct and inverse heat conduction problems[41].	18
Figure 2- 1. 3-D model of the squeeze cast cylindrical coupon.	41
Figure 2- 2. Schematic diagram of squeeze casting system employed in magnesium	41
Figure 2- 3. Temperature profiles(XZ section view) of the cylindrical coupon casting at different cavity filling percentage: (a) 10%, (b) 40%, (c) 60%, and (d) 80%.	47
Figure 2- 4. Temperature contours(XZ section view) of the cylindrical coupon casting after complete filling: (a)1 s, (b) 4s, (c) 10 s, and (d) 40 s, under applied pressure 60 MPa.	49
Figure 2- 5. Predicted cooling curves at the casting center solidified under an applied pressure 0, 30, 60, and 90 MPa.	51
Figure 2- 6. Predicted start and end solidification times at the casting center under an applied pressure 0, 30, 60, and 90 MPa.	52
Figure 2- 7. Predicted solidification time and cooling rates at the casting center under an applied pressure 0, 30, 60, and 90 MPa.	53
Figure 2- 8. Experimental results of temperature measurements at the center of a cylindrical casting of magnesium alloy AM50A solidified under applied pressures of 30, 60, and 90 MPa.	55
Figure 2- 9. Comparisons of total solidification time between computational and experimental results at the casting center under different pressures.	56
Figure 3- 1. 3-D model of 5-step casting with the round-shape gating system (A)XZ view; (B) YZ view; (C) isometric view	62
Figure 3- 2. Schematic diagram of squeeze casting machine	63
Figure 3- 3. A 5-step casting solidifying under applied pressure 30MPa.	64

Figure 3- 4. One-dimensional heat transfer at the interface between the casting and die, where temperature measurements were performed.	65
Figure 3- 5. Polynomial curve with various measured temperatures at a time of 4.1 seconds after pressurized solidification.	67
Figure 3- 6. Extrapolated temperature curve at the die surface(T_0) by the polynomial curve fitting method with applied pressure 30 MPa.	68
Figure 3- 7. Typical temperature versus time curves (Step 4, 30MPa) at metal surface, die surface, and various positions inside the die.	70
Figure 3- 8. Interfacial heat flux(q) and the heat transfer coefficient (IHTC) curves for step 4 with applied pressure 30 MPa.	71
Figure 3- 9. Heat flux(q) curves for step 3, 4, 5 estimated by the extrapolated fitting method.	72
Figure 3- 10. Heat transfer coefficient(IHTC) curves for step 3,4,5 estimated by the extrapolated fitting method.	73
Figure 4- 1. The 3-D model of 5-step casting with the round-shape gating system (A)XZ view; (B) YZ view; (C) isometric view	82
Figure 4- 2. Configuration of upper-dies and geometric installation of thermocouples and pressure transducers	84
Figure 4- 3. Installation of thermocouples measuring casting surface and inside die temperatures	84
Figure 4- 4. 5-step castings solidifying under applied pressure 30, 60, and 90MPa.	87
Figure 4- 5. One-dimensional heat transfer at the interface between the casting and die, where temperature measurements were performed.	89
Figure 4- 6. Flow chart showing an algorithm for the determination of IHTC at the casting-die interface	93
Figure 4- 7. Polynomial curve with various measured temperatures at a time of 4.1 seconds of solidification process.	95
Figure 4- 8. Typical temperature versus time curves (Step 4, 30 MPa) at metal surface, die surface, and various positions inside the die.	96

Figure 4- 9. Comparison of calculated temperature curve at the die surface by the inverse method and the extrapolated fitting method	98
Figure 4- 10. The interfacial heat flux(q) and the heat transfer coefficient (IHTC) curves estimated by extrapolated fitting method and inverse method	99
Figure 4- 11. The residual error of temperatures evaluated by the inverse method at the position $X_1=2\text{mm}$	100
Figure 4- 12. The residual error between the evaluated temperatures and the actual measured temperatures at $X_2=4\text{mm}$ beneath the die surface.....	101
Figure 4- 13. The residual error between the evaluated temperatures and the actual measured temperatures at $X_3=6\text{mm}$ beneath the die surface.....	102
Figure 4- 14. The residual error between the evaluated temperatures and the actual measured temperatures at $X_4=8\text{mm}$ beneath the die surface.....	103
Figure 4- 15. The heat transfer coefficient(IHTC) curves of 5 steps estimated by inverse method with applied pressure 30 MPa.	104
Figure 4- 16. The peak IHTC values of 5 steps estimated by inverse method with applied pressure 30, 60 and 90MPa.	105
 Figure 5- 1. (a) The isometric view of 5-step casting 3-D model with the round-shape gating system. (b) 5-step casting solidifying under applied pressure 60 MPa.	 113
Figure 5- 2. Typical temperature versus time curves (Step 4, 60 MPa) at metal surface, die surface, and various positions inside the die; The interfacial heat flux(q) and the heat transfer coefficient (IHTC) curves estimated by inverse method(Step 4, 60 MPa).	115
Figure 5- 3. Interfacial heat transfer coefficients(IHTC) curves of all steps under the applied pressure of 60MPa.....	116
Figure 5- 4. Peak IHTC values and local pressure peak values varying with different cross section thicknesses of the 5-step casting.....	117
Figure 5- 5. Peak IHTC values of 5 step-casting A443 with applied pressure 30, 60, and 90MPa.	119

Figure 6- 1. Typical temperature versus time curves (Step 4, 30 MPa) at metal surface, die surface, and various positions inside the die; The interfacial heat flux(q) and the heat transfer coefficient (IHTC) curves estimated by inverse method(Step 4, 30 MPa).	128
Figure 6- 2. Typical local pressure distributions and IHTC curve at the casting-die interface of step 4 under the applied hydraulic pressures of 30, 60, 90MPa.	129
Figure 6- 3. Typical effects of applied pressures on the heat transfer coefficients with casting surface temperature at the step 4.	130
Figure 6- 4. Interfacial heat transfer coefficients(IHTC) curves of 5 steps under the applied pressure of 30MPa.....	132
Figure 6- 5. The peak IHTC values of 5 steps estimated by inverse method with applied pressure 30, 60 and 90MPa.	133
Figure 6- 6. IHTC curve plane of Step 5 as a function of the local pressures and solidification temperature.	136
Figure 6- 7. IHTC curve plane of Step 4 as a function of the local pressures and solidification temperature.	137
Figure 6- 8. IHTC curve plane of Step 3 as a function of the local pressures and solidification temperature.	138
Figure 6- 9. IHTC curve plane of Step 2 as a function of the local pressures and solidification temperature.	139
Figure 6- 10. IHTC curve plane of Step 1 as a function of the local pressures and solidification temperature.	140
Figure 7- 1. A typical experimental cooling curve at the center of Step 5 (AM60) under an applied pressure of 60 MPa.	148
Figure 7- 2 Temperature distribution inside the 5-step casting (80% solidified) of AM60 simulated with the input of HTC's, (a) C7000, (b) Yu's research and (c) the Inverse Method.	150

Figure 7- 3 Comparison of the experimental and computational cooling curves at the center of Step 5(AM60) under an applied pressure of 60MPa, (a) the entire cooling period, and (b) the enlarged solidification region.	151
Figure 7- 4 Yu's IHTC data applied to MAGMASoft simulation (AM60).....	152
Figure 7- 5 IHTCs derived from the inverse method data applied to MAGMASoft simulation (AM60).....	153
Figure 7- 6 A typical cooling curve at the center of Step 5 of Al A443 squeeze cast under an applied pressure of 60 MPa.	155
Figure 7- 7 Temperature distribution inside the 5-step casting (80% solidified) of Al A443 simulated with the input of HTC's, (a) C7000, (b) Yu's research and (c) the Inverse Method.....	157
Figure 7- 8 Comparison of the experimental and computational cooling curves at the center of Step 5 (A443) under an applied pressure of 60MPa, (a) the entire cooling period, and (b) the enlarged solidification region.	158
Figure 7- 9 The Yu's IHTC data applied in MAGMASoft simulation(A443).	159
Figure 7- 10 The inverse method IHTC data applied in MAGMASoft simulation(A443).	160

NOMENCLATURE

V_F	volume fraction in the computational cell available for flow
r, θ, z	cylindrical coordinate system
A_r, A_θ, A_z	fractional areas available for flow in the cylindrical (r, θ , z) directions
u_r, u_θ, u_z	fluid velocities in the cylindrical (r, θ , z) directions
P	the pressure of the fluid
G_r, G_θ, G_z	body accelerations in the cylindrical (r, θ , z) directions
f_r, f_θ, f_z	viscous accelerations in the cylindrical (r, θ , z) directions
μ	dynamic viscosity
η	kinematic viscosity
T_{DIF}	heat conduction diffusion
C_s, C_b, C_m	heat capacities for liquid, solid and mushy phases, respectively
h	heat transfer coefficient
H	enthalpy
H_f	latent heat
k	thermal conductivity
R	radius
Re	Reynolds number
S	source term
t	time
T	temperature
ΔT	solidification range of temperature
λ	liquid fraction
ρ	density

ACRONYMS

<i>SC</i>	Squeeze casting
<i>HTC</i>	Heat transfer coefficient
<i>IHTC</i>	Interfacial heat transfer coefficient
<i>FDM</i>	Finite difference method
<i>FEM</i>	Finite element method

CHAPTER 1

INTRODUCTION

1. GENERAL OVERVIEW

The automotive industry has been developing towards to produce lighter vehicles due to market demand and government regulation. The weight reduction in vehicles can be achieved by new engineering designs and application of lighter materials such as aluminum and magnesium alloys. The growth of consumption in both aluminum and magnesium are mainly resulting from die casting, sand casting and other conventional processes. But, due to process limitation, there are problems associated with those casting processes. For example, die cast parts have poor mechanical properties due to the presence of entrapped gas and porosity. Thus they are not suitable for manufacturing large and thick automotive applications of which enhanced engineering performance is required.

Compared to other conventional casting processes, the most attractive feature of squeeze casting (SC) is that it can make castings virtually free of porosity. Hence, squeeze castings usually have excellent as-cast quality, and are heat treatable, which is difficult to achieve with other conventional casting processes. Application of squeeze cast aluminum automotive components, such as road wheels, steering wheel knuckles, and engine blocks, have been quite common[1]. Despite of many research activities on squeeze casting process, some fundamental questions still need to be answered and the process must be optimized so as to expand its application[2].

Mathematical modeling of casting processes started as early as the mid-60s. With the continuous prosperity and popularity of computers, especially after the 80s, more and more researchers have been involved in casting simulation in the way of either research, and development or application. Mathematical modeling has changed the way that casting industry works. Instead of trial with experience and then taking corrective action in years ago, now simulation helps do the analysis and optimization in advance and undertake preventive action. By shortening development time, eliminating product defects and reducing cost, the simulation can not only improve the product quality but also make the production more efficient [3].

A lot of casting simulation models have been developed, and some of them even are commercialized. Simulation of casting solidification offers the potential to optimize casting processes. In order to realize this potential, it is necessary to accurately represent all heat transfer phenomena within the casting system. A critical portion of heat transfer in the system is that at the metal/mould interface. Many complicating factors make the heat transfer at the cast metal/mould interface very difficult to measure or quantify. The interfacial heat transfer depends upon the alloy to be cast, the mould material and coating, the casting process parameters, and the casting geometry. However, for a unique cast metal system, an interfacial heat transfer coefficient(IHTC) can be defined.

2. MOTIVATION

In squeeze casting, an external pressure is applied during the whole stage of pressurized solidification upon the completion of cavity filling, which makes the condition at the casting-die interface different from other conventional casting processes.

When applying pressures in squeeze casting, only hydraulic pressure has been cited. As a result, a fixed constant value of heat transfer coefficient(HTC) is used as the boundary condition. By using these constant HTC in simulation, the accuracy of predicted results certainly is in question.

Simulation is a very important method for optimizing squeeze casting process. Since casting is a transient process, during the process, not only the metal itself changes its phase from liquid to solid, but also the casting-die interfacial heat transfer condition. The changes of these two factors affect each other. Generally, in casting simulation model, any minor change in the boundary conditions can significantly affect the numerical prediction results. Therefore, to obtain reliable and valid prediction through simulation, precisely casting-die interfacial heat transfer condition must be imposed.

3. OBJECTIVES

The main aim of this project was to accurately determinate the casting-die interfacial heat transfer coefficient(IHTC) for simulating squeeze casting processes for light metals, i.e., aluminum and magnesium alloys. The objectives of this study were:

- To develop an experimental technique to measure local cavity pressures in squeeze casting of aluminum and magnesium alloys;
- To develop an experimental technique to determine heat transfer coefficients at the casting-die interface;
- To investigate modeling methods to determine heat transfer coefficients at the casting-die interface; and

- To determine the interfacial heat transfer coefficient(IHTC) as a function of local pressures, and section wall-thicknesses of squeeze castings;

4. OUTLINE OF THIS DISSERTATION

This dissertation is organized in seven chapters. Chapter 1 is an introduction to the entire dissertation that starts with a general overview, literature review on interfacial heat transfer coefficient(IHTC), and an outline of the objectives. It then analyzes the modeling methodologies of IHTC used in the following chapters and influence factors in the heat transfer between the surface of the solidifying casting and the mould, which include different aluminum and magnesium alloys, mould materials, casting processes, and casting geometry shapes. Finally, this chapter focuses on the inverse method to estimate boundary conditions from knowledge of thermal history in the interior of the solid.

In Chapter 2, based on finite difference and control-volume scheme, a model was developed to simulate fluid flow in forced convection and heat transfer in pressurized solidification of a simple cylindrical coupon of magnesium alloy AM50. Experimentally determined pressure-dependent heat transfer coefficients (HTC) and non-equilibrium solidification temperatures were employed. With the measured HTC under the different pressures, the temperature distributions and the cooling behaviors of squeeze cast were simulated.

In an effort of investigating the section thickness effect on heat transfer under different pressures during squeeze casting, A real 5-step squeeze casting with various

section thicknesses was designed and computational methodologies of IHTC were explored in the Chapter 3 and Chapter 4.

In Chapter 3, a different wall-thickness 5-step (with thicknesses as 3, 5, 8, 12, 20 mm) casting mold was designed, and squeeze casting of magnesium alloy AM60 was performed under an applied pressure 30, 60 and 90MPa in a hydraulic press. The casting-die interfacial heat transfer coefficients (IHTC) in 5-step casting were determined based on experimental thermal histories data throughout the die which were recorded by fine type-K thermocouples. With measured temperatures, heat flux and IHTC were evaluated using the polynomial curve fitting method. In Chapter 4, with measured temperatures, heat flux and IHTC were evaluated using the numerical inverse method. A solution algorithm was developed based on the function specification method to solve the inverse heat conduction equations. Furthermore, the accuracy of these curves was analyzed by the direct modeling calculation. The results indicated that heat flux and IHTCs determined by the inverse method were more accurately than those from the extrapolated fitting method.

The inverse modeling method was demonstrated in Chapter 5 to determine the IHTC during 5-step squeeze casting of aluminum alloy A443. Compared to the thin steps at the upper cavity, the relatively thick steps in the lower die attained higher peak IHTC and heat fluxes values due to high local pressures and high melt temperature. The inverse method was employed in Chapter 6 to calculate the IHTC curves during 5-step squeeze casting of magnesium alloy AM60. The in-cavity local pressures measured by Kistler pressure transducers(6175A2) were explored at the casting-die interfaces of all five steps.

The empirical equations relating IHTC to the local pressures and solidification temperature at each Steps were derived and summarized.

In Chapter 7, the accuracy of the inverse method is further verified through the comparison between numerical calculated and experimental results by applying the identified IHTC values in Chapter 5 and Chapter 6. MAGMAsoft is employed as the simulation tool and the Step 5 is taken as an example to conduct the verification.

The summary of the preceding chapters is presented in Chapter 8, which enlists the main conclusions of this dissertation. In the same chapter, it also lists several recommendations for future work.

5. INTERFACIAL HEAT TRANSFER COEFFICIENT

Many researchers investigated the interfacial heat transfer coefficient(IHTC) between a solidifying casting and metal mould[4-39]. These studies have been analyzed for a variety of aluminum and magnesium alloys, metal moulds and chills, and casting geometries. The IHTC essentially quantifies the resistance to heat flow across the interface between the casting and the mould material surrounding it. Figure 1-1a shows a schematic representation of the two contacting surfaces[4]. Because the two surfaces in contact are not perfectly flat, when the interfacial contact pressure is reasonable high, most of the energy passes through a limited number of actual contact spots. The heat flow across the casting-mould interface can be characterized by a macroscopic average metal – mould interfacial heat transfer coefficient(IHTC) based on the following Equation 1-1:

$$h = \frac{q}{A(T_{cs} - T_{ds})} \quad (1-1)$$

where h is IHTC; q is average heat flux at the metal-die interface; A is section area; T_{cs} and T_{ds} are the casting surface temperature and die surface temperature, respectively. From Equation 1-1, the higher the value of h , the less resistance of the heat flow and the greater the heat flux from the casting to its surroundings.

The quantification of heat flux in terms of a heat transfer coefficient, as indicated in Figure 1-1b for the idealized temperature profile, requires that the heat capacity is zero so that the thermal diffusivity is infinite, and consequently heat fluxes entering and leaving the interface are equal.

The heat transfer coefficient shows a high value in the initial stage of solidification, the result of the good surface conformity between the liquid core and the solidified shell. As solidification progresses, the mould expands due to the absorption of heat and the solid metal shrinks during cooling. As a result, a gap develops because pressure becomes insufficient to maintain a conforming contact at the interface. Once the air gaps forms, the heat transfer across the interface decreases rapidly and a relatively constant value of h is attained. The mode of heat transfer across the metal–mould interface has been suggested mainly due to conduction through isolated metal–mould contacts and through gases present in the gap. During the subsequent stage of solidification a slight drop in the interfacial heat transfer coefficient with time can be observed. This might caused by the growth of oxide films on chill and mould surfaces, and by a reduction in the thermal conductivity of the interfacial gas with declining temperature[5].

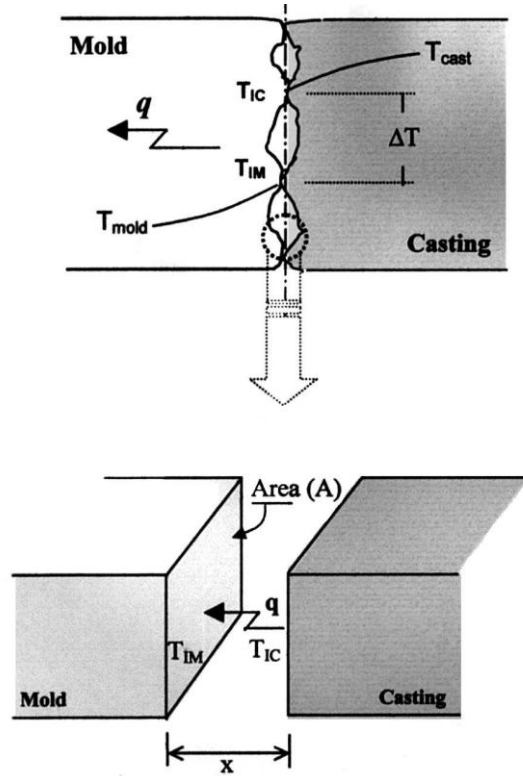


Figure 1- 1 Heat flow across the metal-mould interface[4].

A lot of techniques have been attempted to determine IHTC in metal mould and obtained widely divergent values. Initial IHTC ranging from 85,000 W/m²K to less than 2,000 W/m²K have been reported for solidifying aluminum and magnesium alloys in steel or cast iron moulds. Among these research of heat transfer coefficient at metal/mould interface, the most frequently investigated casting method has been that of permanent mould or chill casting. The IHTC for other casting methods have been listed in Table 1-1.

Table 1- 1 IHTCs between light metal and mould dies or chills

Researchers	Alloy	Die	Process	Casting geometry	IHTC(W/m ² K)
Sully[6]	Pure Al	Steel	permanent	plate	1,930
Nishida[7]	Pure Al	Steel	permanent	cylindrical plate	2,200 to 3,000 2,800
Sekhar[8]	Al-Si eutectic	H13	Squeeze (196MPa)	cylindrical	3,400 to 52,000
El-Mahallawy[9]	Pure Al	copper	permanent	cylindrical	12,000
Ho & Pehlke[10]	Pure Al	Copper	permanent	cylindrical	2,200(top) 5,000(bottom)
Chiesa[11]	A356	Cast iron	permanent	plate	2,700
Taha[12]	Al-4.5Cu	copper	permanent	cylindrical	14,000
Cho & Hong[13]	Al-4.5Cu	steel	Squeeze (50Mpa)	cylindrical	4,700
Santos[4]	Al-4.5Cu	Steel Copper	Permanent	plate	7,500(steel) 9,500(copper)
Kim[14]	A356	SKD61 steel	permanent	Hollow cylinder	2,700 (outer) 20,000(core wall)
Griffiths[15]	Al-7Si	Copper-water cool	permanent	cylindrical	3,400(top) 5,000(side) 7,100(bottom)
Trovant[16]	A356	copper	permanent	cylindrical	3,200
Hines [17]	Al-7Si-3Cu	H13	Low pressure	Wing shape	8,000
Hamasaiid[18]	AZ91D	H11	HPDC	plate	85,000
Dour[19]	Al-12Si	H13	HPDC	plate	46,000
Dargusch[20]	Al-9Si AZ91	steel	HPDC	plate	9,000(A380) 8,500(AZ91)
Guo[21]	ADC12 AM50	steel	HPDC	plate	20,760(ADC12) 12,900(AM50)
Aweda[22]	Pure Al	steel	Squeeze (85MPa)	cylindrical	3,400

In these investigations, the authors discuss the initial solidification of a thin skin at the interface and the conduction heat transfer through the points of contact of the rough surfaces of the casting and mould as well as through the voids between the contact points. The contact changes due to the variation of the relative thermal expansion and contraction of the casting and mould which eventually results in complete separation of the metal from the mould. This range in values can be due to a variety of factors and essentially result in a variation in the air gap at the interface between the solidifying casting and the mould.

Ho and Pehlke[10] described heat transfer at the interface as a function of the gap between casting and mould in their 1985 article. The author used Beck's nonlinear estimation technique[24] to calculate the transient IHTC from thermocouple measurements for pure aluminum and Al-5Cu casting. By measuring temperatures from top-chilled and bottom chilled castings, they concluded that contact conductance decreases significantly during early stages of solidification, and the heat transfer is a function of the interfacial gap. In 1988, Hou and Pelke[25] estimated the contact conductance in Al-13Si castings by measuring interfacial gap size and heat flux data obtained from inverse method. In a 1995 review of IHTC applications in permanent mould casting, Pehlke[26] reported how the IHTC numerical method is applied to solve for the IHTC, and how the results are used in IHTC analysis and its limitations. Finally, he demonstrated usefulness of the application of IHTC in permanent moulds by specific casting cases.

After that, many researchers have examined various processing parameters and their effect on IHTC.

El-Mahallawy[9] reported on many chill/casting IHTC investigations for pure Al, Al-Si alloys, and Al-Cu alloys. The influence of varied superheats on IHTC of pure aluminum solidifying against a copper chill was investigated. They observed that IHTC reaches a maximum value when the surface temperature nears that of liquidus. Their analysis suggests that the heat flow from the metal to the mould is mainly by conduction. Higher IHTC values and smaller gap sizes were obtained with higher superheats.

Taha[12] studied the solidification of Al-4.5Cu cylindrical castings with 12.5 mm diameter and length 95 or 230 mm in a vertical end-chill apparatus. IHTC values were assumed as a function of time and repeated computations were performed for varying IHTC values until experimental cooling curves matched those were computed. Then, the air gap and IHTC were computed using a numerical model which takes into consideration metal and mould shrinkage and expansion, gas film formation, and metallostatic pressure.

Kumar and Prabhu[27] investigated the IHTC of square bar casting of Al-13.2Si eutectic and Al-3Cu-4.5Si alloys during solidification against chills of cast iron, copper, and die steel of various thicknesses. They concluded that the maximum heat flux depended on the chill thickness and diffusivity. Heat flux values for the alumina coating were found to be higher than that for the fireclay coating of the same thickness.

Cho and Hong[28,29] studied the IHTC for a squeeze casting process using Al-4.5Cu alloy. The authors reported IHTC values of about 1000 W/m²K prior to pressurization which rapidly increased to around 4700 W/m²k at a pressure of 50 MPa for a cylindrical casting in a steel mould.

Krishnan and Sharma[30,31] reported the measurement of IHTC between iron chill and Al-11.5Si, Al-9Si-3.6Cu, and Al-2.7Li. The inverse method used required

temperature measurement on both sides of the interface. Their work yielded a time-dependent IHTC which varied over a range of 200 to 2000 W/m²K and increased with increasing section size. Reasonable agreement was found between their results and IHTC values obtained from previous air gap measurements.

Michel[32] investigated the IHTC for Al-Si alloys in steel mould with and without coatings. They found that no coating or thin graphite coating results in the highest maximum IHTC. For pure aluminum, a 100 micron vermiculite coating yielded higher IHTC values than a 300 micron coating. They also found that the mould initial temperature had a greater impact on the IHTC than the coating.

Kim and Lee[14] studied the IHTC between tube-shaped casting and steel moulds. They performed an extremely interesting investigation of the difference in heat transfer between concave and convex casting surfaces and found that the IHTC were substantially higher between the casting and mould when the casting is freezing onto the mould rather than away from it. 1-D heat flow analysis and the sequential function specification method was used to calculate IHTC at the inner and outer metal/mould interfaces for pure Al and three Al-Si alloys. While the outer surface exhibited normal heating and cooling curves, the temperature change at the inner surface was unusual by comparison. Overall, the IHTC at the inner mould wall increases with time. For wide freezing range alloys, the IHTC of 1000 W/m²K was observed during the experiment.

Carroll[33] examined the effect of interfacial contact pressure on the IHTC for aluminum alloy casting against steel moulds. The average IHTC increased as the pressure was increased. The IHTC versus temperature curves were divided into three zones. The first zone saw a steady decrease in IHTC due to decreasing interfacial heat flux and the

IHTC increased in the second zone, which has 35% to 60% solid fraction. After casting surface reached 60% solid, the interface start to transform from a condition of high conformity to low conformity. In low pressure experiments, the IHTC dropped rapidly with temperature in the third zone while an approximate plateau was reached for the high pressure experiment.

Krishna[34] estimated the IHTC for A356 during an indirect squeeze casting process. They calculated temperature histories inside the die and casting with varied IHTC values, and choose the best correlation one between measured and calculated values. The estimated IHTC was found to be close to those observed by Cho and Hong[29]. The authors conclude that there is a critical value of squeeze pressure beyond which the heat transfer will not significantly improve.

Santos[4, 35] investigated the effects of mould temperature and mould coating on the heat-transfer coefficient for solidifying castings of pure Al, Al-4.5Cu, Al-15Cu and Al-Cu eutectic alloys. The chill materials considered were steel and copper. The authors concluded that IHTC could be expressed as a power function of time given by the general form $IHTC = C_i(t)^{-n}$ where the IHTC is expressed in units of W/m^2K , t is time in seconds, and C_i and n are constants depending on alloy composition, chill material, and superheat. They reported lower IHTC in steel moulds compared to copper moulds and the IHTC profiles increased with increasing chill diffusivity.

Kim[36] conducted experiments of pure aluminum cast into a cylindrical copper mould to determine the effects of coating and superheat on the IHTC. While the cast alloy is liquid, the IHTC is influenced by mould surface roughness, the wettability of the alloy on the mould, and the physical properties of the coating layer. Due to the abrupt

surface deformation of the casting, an IHTC drop was observed at the onset of solidification. The air gap and the direct contact between the casting and mould affect IHTC values. They claim that when the cast metal is in the solid phase the ihtc is not affected by the type or thickness of the mould coating and that it only depends on the thermal conductivity and thickness of the air gap.

Griffiths[15] examined the effect of the direction of gravity in relation to the interface by investigating Al-Si castings that had been cast using a copper chill placed on the bottom, top, or side of a sand mold. The highest IHTC values were found for vertically upward solidification, intermediate values were found for horizontal solidification, and the lowest values were associated with vertically downward solidification. IHTC values varied from 2500 to 9000 W/m²K depending on direction of solidification. They also found that the surface of castings were convex toward the chill by around 10 to 20 microns. This convexity was attributed to the deformation of solidifying skin of the casting soon after its formation. This skin deformation was incorporated into a model and shown to be a significant factor in the interfacial heat transfer[37].

Broucuret [23] studied Al-Si alloys and also reported research on the effect of graphite and alumina coatings on heat transfer. They reported an inverse logarithmic relationship between the coating thickness and the heat-transfer coefficient: as the coating thickness increased, the heat-transfer coefficient decreased.

Gunasegaram and Nguyen[23] observed that an air gap did not form between the casting and the mold until the casting reached a temperature of around 545 °C regardless of whether the mold was force cooled. This temperature is also the solidus temperature of

the Al-7 pct Si alloy used in the study, suggesting that the permanent mold really only contributes to the heat transfer, while the immediate area around the interface is still in a liquid state. Once the gap initiates, the mold IHTC decreases significantly. This effect is particularly important in castings with thicker sections because the areas closest to the interface can freeze much too fast for heat from the center of the section to be removed.

Paray[38] observed similar effects when performing in-situ temperature measurements while using low pressure casting to cast aluminum plates of varying thicknesses (3 to 20 mm). They examined both 356 and 319 aluminum alloys. As expected, they found that the cooling rate was faster in thinner sections.

Trovant and Argyropoulos[16,39] expanded on that work by examining the development of the interfacial heat transfer between the mould and the metal in considerable detail and presented a sequence of events for the formation of an air gap. They contend that there are four stages of interfacial heat transfer between the metal and the mould. In stage 1, the metal is completely liquid and heat transfer occurs solely through conduction across the interface. In stage 2, a thin solid film is formed at the surface of the molten metal and the asperities on the film and the mould are the points of contact for thermal conduction. Contact pressure between the metal and the mould plays an important role here. Stages 3 and 4 are somewhat arbitrary because in stage 3 the metal is beginning to pull away from the mold but there is still some contact, while in stage 4, the air gap is large enough that the surface asperities play no role in the heat transfer.

This “air gap” formation is what determines the value of the interfacial heat-transfer coefficient between melt and mould at a given temperature and is clearly a

function of many parameters having to do with the particular casting situation and geometry. As molten metal cools and goes from the liquid to solid state, it shrinks in volume, pulling away from the interface. The newly formed air gap creates further resistance to heat flow out of the casting and the IHTC value decreases substantially as the air gap continues to increase. It is for this reason that IHTC are reported as a function of temperature or time.

Weng[40] investigated the IHTC between liquid and semisolid AZ91D magnesium alloy and a SKD-61 steel mould. Cylindrical castings that were chilled at one end by a water-cooled steel chill were considered. Beck's method was used to solve the IHTC. The authors presented one case of experimental results from a liquid magnesium alloy experiment and six cases demonstrating different IHTC values due to changes in the initial solid fraction and/or the casting pressure. For the semisolid cases that did not involve the application of high pressure, the results show an influence of the initial fraction of solid on the IHTC. For fractions of solid of 0.22, 0.45, and 0.6, the maximum IHTC is 2900, 3200, and 3600 W/m²K, respectively. For the high pressure semisolid experiments, the maximum IHTC reached 7000 W/m²k for casting pressure of 9.8MPa and around 13000 W/m²K for a casting pressure of 14.7MPa.

The accuracy of a solidification simulation depends on the accuracy of the heat transfer modeling. Modeling of the heat transfer at the metal/mould interface of a casting is very challenging due to a number of factors. One of the greatest modeling challenging is the handling air gap formation. Besides the different casting techniques, casting process parameters, and casting geometry shapes, some additional influencing factors need to be also considered in order to determine IHTC accurately. These factors include:

- the pressure at the interface(the applied pressure during squeeze casting, the orientation of the casting with respect to gravity casting);
- alloy characteristics(superheat, composition, mushy zone, liquid surface tension);
- mould processing conditions(mould materials, roughness of contacting surface, coating type and thickness, preheat temperatures).

Since so many factors play a role in the heat transfer between the surface of the solidifying casting and the mould, determining accurate IHTC is very specific to a given casting shape and process. Most of the studies have been performed using cylindrical or plate castings, of which IHTC results cannot be easily applied to complex casting geometries. Griffiths[37] pointed out that small errors in experimental measurements of temperatures in a casting or mould can result in very large differences in IHTC calculation. Therefore, it is essential to explore an effective method to reduce the experimental measurement errors and consequently increase the accuracy of IHTC.

6. INVERSE METHOD

Direct heat conduction problems are associated with the determination of temperature distribution inside a heat conducting body using appropriate boundary conditions. On the other hand, inverse problems are involved with the estimation of boundary conditions from knowledge of thermal history in the interior of the solid. A comparison of the direct and inverse heat conduction problem is shown in Figure 1-2[41].

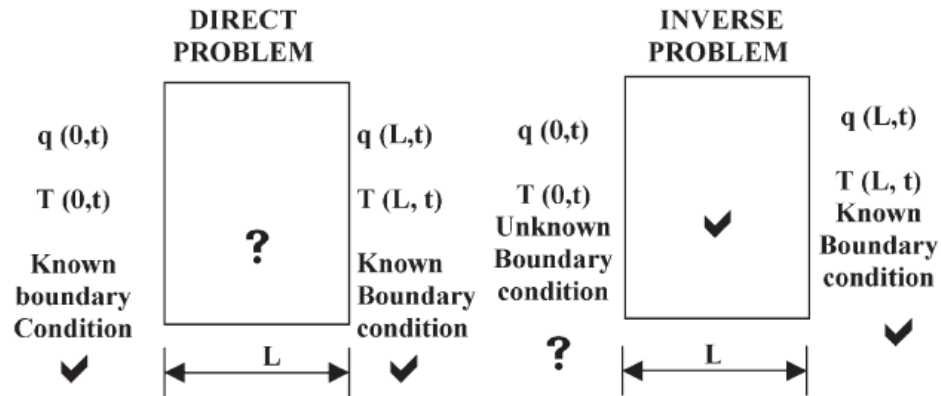


Figure 1- 2 Comparison of direct and inverse heat conduction problems[41].

In many engineering problems, an accurate determination of the thermal boundary condition may not be feasible[24, 42]. For example, the presence of a sensor may alter the thermal conditions in the boundary region affecting the true values of the temperatures to be measured.

Therefore, inverse methods in heat conduction are frequently employed in the field of materials processing because it can reveal information that is difficult or impossible to measure directly. Thermal properties of materials or heat transfer at the surface of a body are among the information which might be found by inverse methods. In the case of metal castings, the inverse method of heat conduction is useful in the determination of heat flux or heat transfer coefficient at the metal/mould interface. To characterize interfacial heat transfer with inverse method, the temperature history at one or more points within the domain body need to be supplied[37].

Inverse problems find a wide variety of applications in the field of materials processing. During casting process, heat transfer across the casting/mould interface plays an important role in the heat removal from the molten metal and in the filling and

solidification of a casting[43]. Especially, in the case of continuous casting, squeeze casting, and die casting, the metal/mould interface plays a dominant role in the removal of heat from the molten metal. Therefore, a reliable set of data on the casting/mould interfacial heat transfer coefficients are required for an accurate simulation of the solidification process[29,44].

The direct determination of casting/mold interfacial heat transfer coefficients is difficult due to the nonconforming contact existing at the interface[4]. As Figure 1-1 shown, the nature of the interface is very complex and it is not possible to determine the boundary temperatures directly. Instead, an inverse model could be adopted to estimate the interfacial heat flux and the surface temperatures utilizing the temperature distribution data inside the mould and the solidifying metal.

Inverse analysis is extensively used in materials modeling. However, the inverse heat conduction analysis is an ill-posed problem since it does not satisfy the general requirement of existence, uniqueness, and stability under small changes to the input data[24]. Furthermore, the output of an inverse solution to a heat conduction problem is very sensitive to measurement errors. To overcome such difficulties, many techniques for solving inverse heat conduction problems have been proposed[44].

From the measured interior temperature histories, the transient metal-die interface heat flux and temperature distribution can be estimated by the following techniques:

1. control volume method[45]: The energy balance was applied at each control volume. Partial heat conduction equations can be reduced to ordinary differential equations in time factor. But, it involves many complex equations (4th order

difference), which is difficult to program, and only can be applied to simple geometry shape.

2. polynomial extrapolation method[46]: Temperature was deducted by extrapolating to die-metal interface by polynomial curve fitting technique. This needs many measurement points inside the body. It was lacking in other mathematical tools to minimize measurement errors.
3. regularization method[47]: Based on Tikhonov regularization theory, established a regularized function to decrease the sensitivity of the measurement data, thus improve the accuracy and stability of the solution. It can get excellent solutions and applied to complex geometry, but the calculation takes long time.
4. boundary element method & Laplace Transform[18,19,23]: It can transform Equations to matrix which easy to be coded in program, which is an effective method to solve linear problem. Temperature data can tolerate more noise, but heat flux is fluctuated with measuring errors.
5. Beck's function specification with finite difference method(implicit & explicit)[5,9,10,12,15,21,31,41]: It is effective to minimize the sum of squares function with respect to heat flux (q) and the errors between calculated and measured data. It can be used for linear or non-linear problems. Also, it can achieve an accurate result with efficient computation.

Analytical and numerical methods are available for solving the heat flow equations. By using measured temperatures in both casting and mould, together with numerical [31,48-50] or analytical [51,52] solutions of the solidification problem, many

research workers have attempted to calculate metal–mould interfacial heat transfer in terms either of a heat transfer coefficient or heat flux.

The analytical procedures are to develop expressions for the boundary condition for a given temperature history in the body. A few temperature sensors are placed at arbitrary locations in the conducting body. However, the IHTC is difficult to solve analytically because the temperature response at an interior location in a body due to a given stimulus at the surface is both delayed and diminished in amplitude. Measurement of temperatures at discrete locations at discrete time intervals provides incomplete information for obtaining an accurate solution. The limitations exposed by the analytical solutions are overcome by the use of numerical methods.

For the numerical solution, an approximate form of the variation of the unknown boundary condition with time is assumed. Using this form of the boundary condition with unknown coefficient, the interior temperature field is determined in the domain by numerical procedures like the Finite Differences Method (FDM) or the Finite Element Method (FEM). An objective function based on the values of measured and calculated temperatures at various internal points is then determined. It is minimized or maximized as the case may be, by correcting the values chosen for coefficients used in the boundary conditions. This is carried out iteratively till a stationary value of the objective function is obtained. Thus, the measurement errors can be minimized by this numerical procedure.

7. MODELING OF SQUEEZE CASTING

The available publications show that simulation of squeeze casting did not start until early 90s. Tadayon et al [53] developed a finite element model for squeeze casting

process, in which the effect of pressure on thermophysical properties was incorporated. The model has been used for predicting thermal front during squeeze casting of an aluminum (AA 7000 series) vehicle road wheel. Gethin et al [54] continued this work by combining flow and heat transfer in squeeze casting process where the flow model was based on simple mass conservation. In the model, when the punch touched the metal surface (early stage), the heat transfer coefficient at the casting/die interface was assumed to be constant determined by the static head at the lower surface of the pool. During the pressurization stage, the heat transfer coefficient was assumed to linear with applied pressure.

Zhang and Cantor [55] developed a finite difference model to simulate the heat flow during squeeze casting aluminum alloy A356. An equation considering the heat transfer coefficients as a linear function of applied pressure was proposed and used in the model. Computed results showed that solidification and cooling rates during squeeze casting increased with increasing ingot/die heat transfer coefficients under high pressures. Lee et al. [56] applied a two-dimensional finite element code for heat transfer analysis in indirectly squeeze wrought aluminum alloy 5083. A pressure-dependent heat-transfer coefficient and the equivalent heat capacity method was employed by the model. The cooling behavior during squeeze casting process was simulated and compared with the measured results.

Maeng[57] investigated the effect of processing parameters on the microstructure and mechanical properties of modified B390 alloy in direct squeeze casting by using commercial finite volume method code for heat transfer analysis, and MAGMAsoft for

cooling curves. In this model, the heat transfer was considered constant for a specific applied pressure.

Hu and Yu [58] developed a 2-D finite difference model for heat transfer events in squeeze casting of magnesium alloy AZ91D. The model used the heat transfer coefficient as a linear function of applied pressure.

Lee et al [59] simulated melt flow by using the software MAGMAsoft for the direct squeeze casting an orbiting scroll compressor of aluminum alloy B390. In the model, only the melt flow during the pouring step and the solidification rate were calculated.

Youn et al. [60] conducted a die filling and solidification analysis of engine bracket mounting (aluminum alloy A356) in horizontal squeeze casting process by the commercial MAGAMsoft with add-on module high pressure die casting. In the model, constant heat transfer coefficients were employed for die/die and die/casting interfaces.

Postek et al [61] developed a coupled model to evaluate the effects of initial stresses in the pressurized casting process. An implicit time integration scheme is applied to solve the transient thermomechanical problem in a staggered form. The constitutive mechanical model is elasto-viscoplastic with hardening incorporated with a Von Mises yield function. In the model, the interfacial heat transfer coefficient was coupled with the contact between die and cast.

Table 1- 2 Modeling method of squeeze casting processes

Author(s)	Alloy /Part	Process	Features
Tadayon et al [53]	AA 7000 series /Vehicle wheel	Direct Squeeze Casting	Applied pressure: 55, 110 MPa; Incorporated the effect of pressure on the thermophysical properties; Calculate heat transfer only; No fluid flow included; Constant boundary conditions.
Gethin et al [54]	AA 7000 series /Vehicle wheel	Direct Squeeze Casting	Applied pressure: 55 MPa; Incorporated the effect of pressure on the thermophysical properties; Combined flow and heat transfer; Approximated flow calculation; Linear relationship between pressure and HTC.
Zhang and Cantor [55]	A356 /Coupon	Direct Squeeze Casting	Applied pressure: >50 MPa; Calculate heat transfer only; Linear relationship between pressure and HTC.
Lee et al [56]	5083 /Coupon	Indirect Squeeze Casting	Pressure range: 25-100 MPa; Calculate heat transfer only; Constant boundary conditions.
Maeng et al [57]	B390 /Coupon	Direct Squeeze Casting	Maximum Pressure 100 MPa; Validate cooling rate results; Constant boundary conditions.
Hu and Yu [58]	AZ91D /Coupon	Direct Squeeze Casting	Pressure range: 10-200 MPa; Calculated heat transfer only; Linear relationship between pressure and HTC.
Lee et al [59]	B390 /Scroll compressor	Direct Squeeze Casting	Pressure range: 10-50 MPa; Calculated heat transfer and fluid flow; Boundary condition was not clear.
Youn et al [60]	A356 /Engine bracket mounting	Horizontal Squeeze casting	Applied Pressure: 70-150 MPa; Included both filling and solidification; Constant boundary conditions.
Postek et al [61]	LM25 /Coupon	Direct Squeeze Casting	Applied Pressure: 200 MPa; HTC coupled with casting and die contact; Non-linear effect on solidification

6. SUMMARY

The above review in this chapter gives an overall perspective of heat transfer at the casting/mould interface and the development of squeeze casting simulation. Despite extensive utilization of computer simulation for various casting processes, published work on development of advanced models incorporating precise interfacial heat transfer coefficient(IHTC) for squeeze casting is limited.

Since the squeeze casting technology is relatively new for light alloys, aluminum and magnesium, more fundamental research is needed for a scientific understanding of the heat transfer at the casting/mould interface. In particular, advanced methodology of IHTC coupled with precisely boundary conditions have to be fully developed for the simulation of squeeze casting processes.

Therefore, the purpose of this study is to investigate the modeling methodology of IHTC and cavity pressure in 5-step squeeze casting, and establish a generalized relationship between local pressure, section thickness, and the casting/die interfacial heat transfer coefficient (HTC), then incorporate precise IHTC to simulate solidification phenomena occurring in squeeze casting of magnesium and aluminum alloys.

REFERENCES

- [1] R. DasGupta, "Squeeze Casting: Principles and Applications", Die casting Engineer, Vol. 48, No.1, 2004, 54-58.
- [2] H. Hu, "Squeeze casting of magnesium alloys and their composites", Journal of Materials Science, Vol. 33, No.6, 1998, 1597-1589.
- [3] A. Sholapurwalla, "Virtual Casting: Die Casting Process Simulation", Die Casting Engineer, Vol.46, 2002, 58-62.
- [4] C.A.Santos, J.M.V. Quaresma, A. Garcia, "Determination of transient interfacial heat transfer coefficients in chill mold castings", Journal of Alloys and Compounds, Vol.319, 2001, 174-186.
- [5] K. Hou, R.D. Pehlke, "Transient methods for determination of metal-mold interfacial heat transfer", AFS transactions, Vol. 91, 1983, 689-698.
- [6] L.D.J., Sully, "The thermal interface between castings and chill molds", AFS Transactions, Vol.84, 1976, 735-742.
- [7] Y., Nishida, H., Matsubara, "Effect of pressure on heat transfer at the metal mold casting surface", British Foundryman, Vol.69, 1976, 274-278.
- [8] J. A., Sekhar, G.J. , Abbaschian, R., Mehrabian, "Effect of pressure on metal-die heat transfer coefficient during solidification", Material Science and Engineering, Vol. 40, 1979, 105-110.
- [9] N.A., El-Mahallawy, A.M., Assar, "Effect of melt superheat on heat transfer coefficient for aluminum solidifying against copper chill", Journal of Material Science, Vol. 26, 1991, 1729-1733.

- [10] K. Ho, R.D. Pehlke, “ Metal-Mold interfacial heat transfer ”, Metallurgical Transaction, Vol.16B, 1985, 585-594.
- [11] F., Chiesa, “Heat Losses During Filling of Permanent Moulds”, AFS Transactions, Vol. 98, 1990, 193-200.
- [12] M. A., Taha, N.A., El-Mahallawy, A., Assar, R.M., Hammouda, “Effect of melt superheat and chill material on interfacial heat-transfer coefficient in end-chill Al and Al-Cu Alloy castings”, Journal of Materials Science, Vol.27, 1992, 3467-3473.
- [13] I.S., Cho.and C.P. Hong, “Evaluation of heat-transfer coefficients at the casting/die interface in squeeze casting”, International Journal of cast metals research, Vol.9, 1996, 227-232.
- [14] T.G., Kim, Z.H. Lee., “Time-varying heat transfer coefficients between tube-shaped casting and metal mold”, International Journal of Heat and Mass Transfer, Vol.40, 1997, 3513-3525.
- [15] W.D. Griffiths, “The heat-transfer coefficient during the unidirectional solidification of an Al-Si Alloy casting”, Metallurgical and Materials Transactions B, Vol.30B, 1999, 473-482.
- [16] M. Trovant, S. Argyropoulos, “Finding boundary conditions: A coupling strategy for the modeling of metal casting processes: Part I. Experimental study and correlation development”, Metallurgical and Materials Transactions B, Vol.31B, 2000, 75-86.
- [17] J. A. Hines, “Determination of interfacial heat-transfer boundary conditions in an aluminum low-pressure permanent mold test casting”, Metallurgical and materials transactions B, Vol. 35B, 2004, 299-311.

- [18] A. Hamasaiid, G. Dour, M.S. Dargusch, T. Loulou, C. Davidson, G. Savage, “ Heat-transfer coefficient and in-cavity pressure at the casting-die interface during high-pressure die casting of the magnesium alloy AZ91D”, *Metallurgical and Materials Transactions A*, Vol. 39A, 2008, 853-864.
- [19] G. Dour, M. Gargusch, C. Davidson, A. Nef, “Development of non-intrusive heat transfer coefficient gauge and its application to high pressure die casting effect of the process parameters”, *Journal of Materials Processing Technology*, Vol. 169, 2005, 223-233.
- [20] M. Dargusch, A. Hamasaiid, G. Dour, T. Loulou, C. Davidson, and D. StJohn, “The accurate determination of heat transfer coefficient and its evolution with time during high pressure die casting of Al-9%Si-3%Cu and Mg-9%Al-1%Zn alloys”, *Advanced Engineering Materials*. vol.9, 2007, No.11, 995-999
- [21] Z.P. Guo, S. Xiong, S. Cho, J. Choi, “Heat transfer between casting and die during high pressure die casting process of AM50 alloy-modelling and experimental results”, *Journal of Material Science Technology*, Vol.24, 2008, 131-135.
- [22] J. Aweda, M. Adeyemi, “Experimental determination of heat transfer coefficients during squeeze casting of aluminum”, *Journal of Materials Processing Technology*, Vol. 209, 2009, 1477-1483.
- [23] S. Broucayet, A. Michrafy, G. Dour, “Heat transfer and thermo-mechanical stresses in a gravity casting die influence of process parameters”, *Journal of Materials Processing Technology*. Vol.110, 2001, 211-217.
- [24] J.V. Beck, B. Blackwell, Jr. St. Clair, “Inverse heat conduction: ill-posed problems”, *Wiley Interscience: New York*. 1985. 1-50.

- [25] T.X. Hou, R.D. Pehlke, "Determination of mold-metal interfacial heat transfer and simulation of solidification of an aluminum-13% Silicon casting", AFS Transactions, Vol.96, 1988, 129-136.
- [26] R.D. Pehlke, "Heat transfer at the mold/metal interface in permanent mold casting", Modeling of casting, welding and advanced solidification processes VII, ed. M., Cross and J. Campbell, The Mineral, Metals and Materials society, 1995, 373-380.
- [27] P.T.S. Kumar, N. K. Prabhu, "Heat flux transients at the casting/chill interface during solidification of aluminum base alloys", Metallurgical Transactions B, Vol.22B, 1991, 717-727.
- [28] I.S. Cho, C.P. Hong, "Evaluation of heat-transfer coefficients at the casting/die interface in squeeze casting", International Journal of Cast Metals Research, Vol.9, 1996, 227-232.
- [29] I.S. Cho, C.P. Hong, "Modeling of microstructural evolution in squeeze casting of an Al-4.5mass%Cu Alloy", ISIJ International, Vol.37, 1997, 1098-1106.
- [30] M. Krishnan, D.G.R. Sharma, "Determination of heat transfer coefficient between casting and chill in unidirectional heat flow", AFS Transactions, Vol.102, 1994, 769-774.
- [31] M. Krishnan, D.G.R. Sharma, "Determination of interfacial heat transfer coefficient h in unidirectional heat flow by Beck's non linear estimation procedure", International Comm. Heat and Mass Transfer, Vol.23, 1996, 203-214.
- [32] F. Michel, P.R. Louchez, F.H. Samuel, "Heat transfer coefficient during solidification of Al-Si alloys: Effects of mold temperature, coating type and thickness", AFS Transactions, Vol.103, 1995, 275-283.

- [33] M. Carroll, C. Walsh, M.M. Makhlof, "Determination of effective interfacial heat transfer coefficient between metal moulds and Al alloy castings", AFS Transactins, Vol.107, 1999, 307-314.
- [34] P. Krishna, K.T. Bilkey, R.D. Pehlke, "Estimation of interfacial heat transfer coefficient in indirect squeeze casting", AFS Transactions, Vol.109, 2001, 131-139.
- [35] C.A. Santos, A. Garcia, C.R. Frick, J.A. Spim, "Evaluation of heat transfer coefficients along the secondary cooling zones in the continuous casting of steel billets", Inverse Problems, design and optimization symposium, 2004.
- [36] H.S. Kim, I.S. Cho, J.S. Shin, S.M. Lee, B.M. Moon, "Solidification parameters dependent on interfacial heat transfer coefficient between aluminum casting and copper mould", ISIJ International, Vol.45, 2005, 192-198.
- [37] W.D. Griffiths, "A model of the interfacial heat-transfer coefficient during unidirectional solidification of an aluminum alloy", Metallurgical and Materials Transactions B, Vol.31B, 2000, 285-295.
- [38] F. Paray, J. Clements, B. Kulunk, J.E. Gruzleski, "In-situ temperature measurement in low-pressure permanent-mold casting;", AFS Transactions, Vol.105, 1997, 791-801.
- [39] M. Trovant, S. Argyropoulos, "Finding boundary conditions: A coupling strategy for the modeling of metal casting processes: Part II. Numerical study and analysis", Metallurgical and Materials Transactions B, Vol.31B, 2000, 87-96.
- [40] R.J. Weng, J.H. Kuo, C.H. Wu, W.S. Hwang, "Effects of solid fraction and operating pressure on the heat transfer coefficient at the casting/mold interface for AZ91D magnesium alloy", AFS Transactions, Vol.113, 2005, 234-241.

- [41] K. Narayan Prabhu, A.A. Ashish, “Inverse modeling of heat transfer with application to solidification and quenching”, materials and manufacturing Processes, Vol.17, 2002, 469-481.
- [42] M. Ozisik Necati, “Inverse heat conduction problem(IHCP)”, Heat Conduction; John wiley & Sons Inc.: New York, 1993, 571-615.
- [43] E. Velasco, J. Talamantes, S. Cano, S. Valtierra, J.F. Mojica, R. Colas, “Casting-chill interface heat transfer during solidification of an aluminum alloy”, Metallurgical and Materials Transactions B, Vol.30B, 1999, 773-778.
- [44] J.V. Beck, “Inverse problems in heat transfer with application to solidification and welding”, In Modeling of casting, welding and advanced solidification processes V, ed. Rappaz M.,Ozgu M.R., Mahin K.W., The Mineral, Metals and Materials society, 1991, 503-513.
- [45] R. Rajaraman, R. Velraj, “Comparison of interfacial heat transfer coefficient estimated by two different techniques during solidification of cylindrical aluminum alloy casting”, Heat Mass Transfer, Vol.44, 2008, 1025-1034.
- [46] J. Aweda, M. Adeyemi, “Experimental determination of heat transfer coefficients during squeeze casting of aluminum”. Journal of Materials Processing Technology. vol.209, 2009, 1477-1483.
- [47] D.S. Sui, Z.S. Cui, “Regularized determination of interfacial heat transfer coefficient during ZL102 solidification process”, Transactions of nonferrous metals society of China, Vol.18, 2008, 399-404.

- [48] A.V. Reddy, C. Beckermann, "Measurements of metal-mold interfacial heat transfer coefficients during solidification of Sn and Sn-Pb alloys", *Experimental Heat Transfer*, Vol.6, 1993, 111-129.
- [49] M.A. Taha, N.A. El-Mahallawy, M.T. El-Mestekawi, A.A. Hassan, "Estimation of air gap and heat transfer coefficient at different faces of Al and Al-Si castings solidifying in permanent mould", *Material Science and Technology*, Vol.17, 2001, 1093-1101.
- [50] J.F. Evans, D.H. Kirkwood, J. Beech, "The determination of metal/mold interfacial heat transfer coefficients and the prediction of gross shrinkage cavities in chill mold castings", *Modeling of casting, Welding and Advanced solidification Processes V*, ed. Pappaz M., Ozgu M.R., Mahin K.W., The Minerals, Metals and Materials Society, 1991, 531-538.
- [51] A. Garcia, T.W. Clyne, M. Prates, "Mathematical model for the unidirectional solidification of metals: II. Massive molds", *Metallurgical Transactions*, Vol.10B, 1979, 85-91.
- [52] A. Garcia, T.W. Clyne, "A versatile technique for characterization of metal/mould heat transfer and correlation with thermal and structural effects", in *Solidification Technology in the Foundry and Casthouse*, ed. Charles J.A., The Metals Society, London, 1982.
- [53] M.R. Tadayan, D.T. Gethin, R.W. Lewis, "A finite element model of the squeeze forming process including the effect of pressure on thermophysical properties", *Seventh International Conference(Proc. Conf.)*, Stanford, Connecticut, USA, 8-12 July 1991, *Numerical Methods in Thermal Problems*, Vol.7.1, 1991, 302-314.

- [54] D.T. Gethin, R.W. Lewis, M.R. Tadayan, "A finite element approach for modeling metal flow and pressurized solidification in the squeeze casting process", *International Journal for Numerical Methods in Engineering*, Vol.35, 1992, 939-950.
- [55] D.L. Zhang, B. Cantor, "A numerical heat flow model for squeeze casting aluminum alloys and Al alloy/SiCp composites", *Model. Simul. Mater. Sci. Eng.*, Vol.3,1995, 121-130.
- [56] J.H. Lee, H.S. Kim, S.I. Hong, C.W. Won, S.S. Cho, B.S. Chun, "Effect of die geometry on the microstructure of indirect squeeze cast and gravity die cast 5083 wrought Al alloy and numerical analysis of the cooling behavior", *Journal of Materials Processing Technology*, Vol.96, 1999, 188-197.
- [57] D.Y. Maeng, J.H. Lee, C.W. Won, S.S. Cho, B.S. Chun, " The effect of processing parameters on the microstructure and mechanical properties of modified B390 alloy in direct squeeze casting", *Journal of Materials Processing Technology*, Vol. 105, 2000, 196-203.
- [58] H. Hu, A. Yu, "Numerical simulation of squeeze cast magnesium alloy AZ91D", *Modeling Simul. Mater. Sci. Eng.* Vol.10, 2002, 1-11.
- [59] J.H. Lee, C.W. Won, S.S. Cho, B.S. Chun, S.W. Kim, "Effects of melt flow and temperature on the macro and microstructure of scroll compressor in direct squeeze casting", *Materials Science and Engineering: A*, Vol. 281, 2000, 8-16.
- [60] S.W. Youn, C.G. Kang, P.K. Seo, "Thermal fluid/solidification analysis of automobile part by horizontal squeeze casting process and experimental evaluation", *Journal of Materials Processing Technology*, Vol. 146, 2004, 294-302.

- [61] E.W. Postek, R.W. Lewis, D.T. Gethin, R.S. Ransing, "Influence of initial stresses on the cast behavior during squeeze forming processes", *Journal of Materials Processing Technology*, Vol. 159, 2005, 338-346.

CHAPTER 2

NUMERICAL SIMULATION OF HEAT TRANSFER IN PRESSURIZED SOLIDIFICATION OF MAGNESIUM ALLOY AM50

1.INTRODUCTION

Due to low density and high strength-to-weight ratio, magnesium castings in the automotive application increase rapidly. Currently, high pressure die casting(HPDC) is the dominating production process for the most of magnesium automotive components. However, based on Zhou's experiment results[1], die castings have relatively high gas and shrinkage porosity, particularly in an area with relatively thick cross section. After reviewing the automotive applications of magnesium casting, which lowers their mechanical properties, Hu[2] noted a major limitation on the use of magnesium die castings in some critical areas of the vehicle where high dynamic loading is present.

Compared with the HPDC, the squeeze casting process with high applied pressure is a promising solution for thick magnesium castings. Hu[3] concluded that the squeeze casting process is capable of eliminating micro-porosity and making sound castings. Ghomashchi[4] reviewed squeeze casting metallurgical features including porosity, recrystallisation and grain refinement. Yong[5] reported that the UTS value were 50% higher than those magnesium alloy casting under atmospheric pressure, and the cell size of magnesium alloy was reduced from 127 to 21 μm with increasing the applied pressure from 0.1 to 60 MPa. Due to the elimination of air gap between the metal and die interface, the heat transfer coefficient is increased, which enhances cooling rates and solidification. Zhou and Hu presented the tensile test result and microstructure of squeeze

casting which indicates that squeeze casting can improve mechanical properties effectively[6]. The squeeze casting has been commercially succeeded in manufacturing aluminum automotive components such as road wheels, engine blocks, pistons and knuckle. However, rare squeeze cast magnesium components have been used in real engineering applications.

The squeeze casting process parameters should be optimized before the full economic and applicable squeeze casting can be achieved in industry. Among various processing parameters, such as applied pressure, die and pouring temperatures, alloy composition, die coating thickness, the pressure and die temperature are two primary parameters. To obtain high quality squeeze castings, the varying processing parameters must be optimized. Among these parameters, the heat transfer and temperature gradient needs to be well controlled primarily in squeeze castings. Guo analyzed the effect of wall thicknesses and process parameters to the interfacial heat transfer coefficient during the HPDC process[7]. For the squeeze casting, Dasgupta summarized that the heat transfer between the die and molten metal plays a critical role in understanding and modeling the development of casting microstructure[8]. Yu and Hu reported that heat flow in boundary layers is affected significantly by applied pressures and summarized the empirical equations on relationship of heat transfer coefficient (HTC), melt temperature, and applied pressure during squeeze casting for magnesium and aluminum alloys[9].

Recently, the numerical simulation has increasingly become an effective tool in the casting manufacturing, by which some primitive and time-consuming procedures for finding the appropriate set of process parameters are avoided. Sun optimized the parameters of gating system on magnesium alloy castings based on the simulation[10].

Despite many application of mathematical simulation modeling in HPDC process, the publication on squeeze casting is very limited. Zhang and Cantor reported a flow model for squeeze casting of aluminum alloys[11]. However, their model failed to take into consideration a variation in thermophysical properties with a change in phases. Certain simulation work on squeeze casting of magnesium alloys was performed by Hu and Yu[12]. But, no consideration was given to the influence of the applied pressures on heat transfer coefficients.

Nowadays in most engineering applications, recourse for solving the moving boundary problems has been made to numerical analyses that utilize the finite difference and finite element methods. The success of finite element and boundary element methods lies in their ability to handle complex geometries, but they are acknowledged to be more time consuming in terms of computing and programming. Because of their simplicity in formulation and programming, finite difference and control volume scheme are still the most popular at the present[13].

In this study, the formulation of a mathematical model developed based on the finite difference and control-volume scheme for squeeze casting of magnesium alloys is described with consideration of pressure-dependent heat transfer coefficient and non-equilibrium solidification temperature. The numerical prediction of fluid flow in forced convection and heat transfer in pressurized solidification of a cylindrical squeeze casting of magnesium alloy AM50 under the applied pressures of 0, 30, 60, and 90 MPa is presented. The effect of applied pressure levels on solidification and cooling behavior of squeeze cast AM50 is discussed. The predicted result is validated with experiment measurements.

2. MATHEMATICAL MODELING

2.1. GOVERNING EQUATIONS

According to the fluid flow equations from Patankar[14], due to the cylindrical shape of the squeeze cast AM50 coupon employed in this study, the cylindrical coordinate(r, θ, z) is chosen to take advantage of symmetry. With the assumption of no tangential velocity ($u_\theta = 0$), the dimensionless governing equations for laminar(non-turbulent) and incompressible flow with no viscous dissipation in the cylindrical coordinate system can be expressed as following:

Continuity equation:

$$\frac{1}{r} \frac{\partial}{\partial r} (r u_r A_r) + \frac{\partial}{\partial z} (u_z A_z) = 0 \quad (2-1)$$

Momentum equation:

$$\text{R component: } \frac{\partial u_r}{\partial t} + \frac{1}{V_F} \left[u_r A_x \frac{\partial u_r}{\partial r} + u_z A_z \frac{\partial u_r}{\partial z} \right] = -\frac{1}{\rho} \frac{\partial P}{\partial r} + G_r + f_r \quad (2-2)$$

Z component:

$$\frac{\partial u_z}{\partial t} + \frac{1}{V_F} \left[u_r A_x \frac{\partial u_z}{\partial r} + u_z A_z \frac{\partial u_z}{\partial z} \right] = -\frac{1}{\rho} \frac{\partial P}{\partial z} + G_z + f_z$$

where, (G_r, G_θ, G_z) are body gravity accelerations, (f_r, f_θ, f_z) are viscous accelerations which are defined as following, where $\eta = \mu / \rho$.

$$f_r = \eta \left[\frac{1}{r} \frac{\partial}{\partial r} \left(r \frac{\partial u_r}{\partial r} \right) + \frac{\partial^2 u_r}{\partial z^2} - \frac{u_r}{r^2} \right]$$

$$f_z = \eta \left[\frac{1}{r} \frac{\partial}{\partial r} \left(r \frac{\partial u_z}{\partial r} \right) + \frac{\partial^2 u_z}{\partial z^2} \right]$$

Energy equation:

$$V_F \frac{\partial}{\partial t} (\rho H) + u_r A_r \frac{\partial}{\partial r} (\rho H) + u_z A_z \frac{\partial}{\partial z} (\rho H) = T_{DIF} + S \quad (2-3)$$

where T_{DIF} is thermal conduction diffusion which is defined as

$$T_{DIF} = \frac{1}{r} \frac{\partial}{\partial r} (k r A_r \frac{\partial T}{\partial r}) + \frac{\partial}{\partial z} (k A_z \frac{\partial T}{\partial z})$$

2.2. ENTHALPY METHOD

Based on thermodynamics equation, $dH = C(T)dT$, Hu[12,13] proposed that the phase change is used to convert the energy equation to a non-linear equation with only one variable (H). If a constant specific heat for each phase is considered and $H=0$ is chosen to correspond to alloy at its solidus temperature, the relation between temperature and enthalpy becomes:

$$T = \begin{cases} T_s + H / C_s; & H \leq 0 \\ T_s + H [\Delta T / (C_m \Delta T + H_f)]; & 0 < H < H_f + C_m \Delta T \\ T_s + (H - H_f - (C_m - C_l) \Delta T) / C_l; & H \geq H_f + C_m \Delta T \end{cases} \quad (2-4)$$

where $\Delta T = T_1 - T_s$ is the solidification range of the alloy.

According to the equation (2-4), the energy equation (2-3) can be rewritten as equation (2-5):

$$V_F \frac{\partial}{\partial t} (\rho H) + u_r A_r \frac{\partial}{\partial r} (\rho H) + u_z A_z \frac{\partial}{\partial z} (\rho H) = \left[\frac{1}{r} \frac{\partial}{\partial r} (\gamma r A_r \frac{\partial H}{\partial r}) + \frac{\partial}{\partial z} (\gamma A_z \frac{\partial H}{\partial z}) \right] + \left[\frac{1}{r} \frac{\partial}{\partial r} (r A_r \frac{\partial S}{\partial r}) + A_z \frac{\partial^2 S}{\partial z^2} \right] \quad (2-5)$$

Where

$$\begin{cases} \text{solid phase} & H \leq 0; & \gamma = k_s / C_s; & S = 0 \\ \text{solid / liquid phase} & 0 < H < H_f + C_m \Delta T; & \gamma = k_{in} / (C_m \Delta T + H_f); & S = 0 \\ \text{liquid phase} & H \geq H_f + C_m \Delta T; & \gamma = k_l / C_l; & S = -\frac{k_l}{C_l} [H_f + (C_m - C_l) \Delta T] \end{cases}$$

The properties of the alloy in mushy region are defined as:

$$\begin{aligned}k_m &= \lambda k_l + (1 - \lambda)k_s \\C_m &= \lambda C_l + (1 - \lambda)C_s \\\rho_m &= \lambda \rho_l + (1 - \lambda)\rho_s \\\lambda &= \frac{H}{H_f}\end{aligned}$$

During the forced-flow filling and mushy zone solidification stage, the energy equation is expressed only in terms of a single variable, H , and one source term, S . The transformation of energy equation simplifies the numerical solution of the present case and makes it possible to use the existing algorithm.

2.3. INITIAL AND BOUNDARY CONDITIONS

A squeeze cast cylindrical coupon with a diameter of 10 cm and a height of 8 cm , as shown in Figure 2-1, was employed in this study. The material selected for squeeze cast coupons was commercially-available magnesium alloy AM50 (Mg-5.0wt.%Al-0.38wt.%Mn-0.2wt.%Zn) due to its extensive usage in the automotive industry. The mold material was tool steel H13.

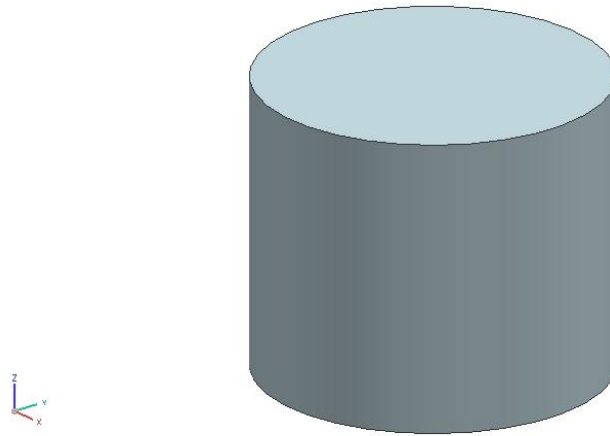


Figure 2- 1. 3-D model of the squeeze cast cylindrical coupon.

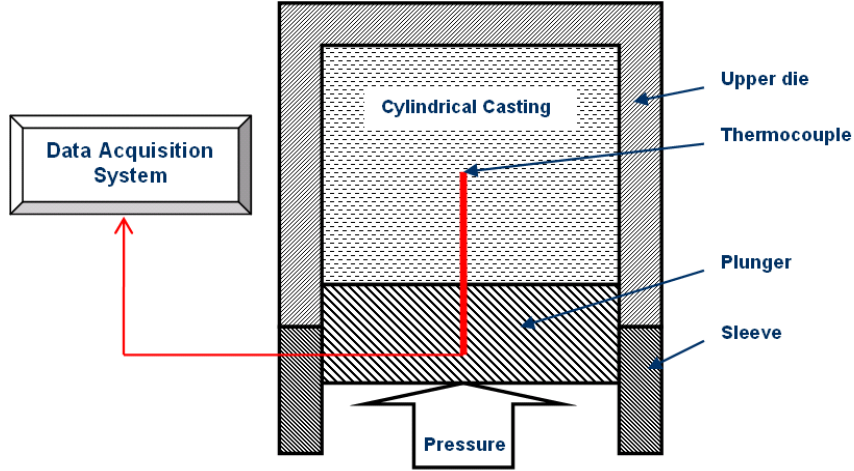


Figure 2- 2. Schematic diagram of squeeze casting system employed in magnesium alloy AM50 coupon.

During the cavity filling, molten metal was poured into the sleeve and then forced into the upper die cavity by the movement of the plunger with a speed of 5.5 cm/s in an upward direction as illustrated in Figure 2-2. The filling velocity of the melt instantly decreased to zero once the cavity filling was completed. The initial temperature of the AM50 melt was 695°C; the initial die temperature was 275°C and the plunger temperature was 150°C. Newton's law of cooling was applied at boundaries between the casting and the die, which was of the form in equation (2-6):

$$q = -k \frac{\partial T}{\partial r} = h_{c/d}(T_c - T_d), \quad \text{or} \quad q = -k \frac{\partial T}{\partial z} = h_{c/d}(T_c - T_d) \quad (2-6)$$

where q is the heat flux across the casting/die interface, k is the thermal conductivity of the magnesium alloy, $h_{c/d}$ is the heat transfer coefficient across the casting/die

interface, T_c is the casting temperature at the casting/die interface, and T_d is the die temperature at the casting/die interface.

The heat transfer coefficient ($h_{c/d}$) in equation (2-6) is an important factor which controls the solidification and cooling rates in squeeze casting processes. The determination of heat transfer coefficient is a troublesome task since it depends on numerous factors, such as pressure, pouring temperature, die material, coating and air gap on the die surface, etc. The study by Yu and Hu [9, 15] indicates that the heat transfer coefficient ($h_{c/d}$) of squeeze casting of light alloys are primarily affected by pressure levels. For squeeze casting of magnesium alloy AM50 with the application of moderate pressures (0 ~ 100 MPa), a polynomial relationship between heat transfer coefficient ($h_{c/d}$) and the applied pressure levels applied in magnesium squeeze casting is proposed:

$$h_{c/d} = 1996.6 + 169.56P - 0.78P^2 \quad (2-7)$$

where $h_{c/d}$ is the heat transfer coefficient between the casting and die surface (W/m^2K), and P is the applied pressure (MPa). Equation (2-7) was incorporated into the heat transfer models of the simulation software in this study. Since the applied pressure also increases liquidus temperature, a linear relation between the liquidus temperatures and applied pressures was employed:

$$T_l = 0.092P + T_m \quad (2-8)$$

where T_l is the liquidus temperature of magnesium alloy AM50A under applied pressures, P is the applied pressure (MPa), T_m is the non-equilibrium solidification temperature ($625.1^\circ C$) at 0 MPa. A similar linear relation between the solidus

temperatures and applied pressures was available in the range of the pressures (0 – 100 MPa):

$$T_s = 0.072P + T_{s,m} \quad (2-9)$$

where T_s is the solidus temperature of magnesium alloy AM50A under applied pressures, P is the applied pressure, $T_{s,m}$ is the solidus temperature (427.8°C) at 0 MPa.

Once the molten metal completes filling the cylindrical die cavity, the solid shell formed at the interface between die and metal ($u_r = 0$; $u_z = 0$; $S = 0$), from equation (2-3), the heat transfer and temperature distribution was simply governed by the heat conduction equation (2-6), where $\gamma = k / C$.

$$V_F \frac{\rho}{\gamma} \left(\frac{\partial T}{\partial t} \right) = \frac{1}{r} A_r \frac{\partial}{\partial r} \left(r \frac{\partial T}{\partial r} \right) + A_z \frac{\partial^2 T}{\partial z^2} \quad (2-10)$$

The governing equations are discretized with control volume implicit finite difference procedure. The computation is done on a domain with 28 x 34 nodes. The stability and convergence for each iteration were assured with dimensionless time step under 8×10^{-7} . In addition to this criterion of convergence discussed above, a grid refinement study was performed by doubling the number of nodal points used. In other words, computations were also carried out using a domain 56 x 68 nodes. No significant differences were evident between the predictions made using the 56 x 68 nodes and those made on the basis of the smaller 28 x 34 node grid. Simulations were performed with the filling velocity of 5.5 cm/s and the filling time of 1.5 second. The predictions for the temperature, velocity, and time did not differ by more than 4% between the two grid sizes. The thermophysical properties of the cast magnesium alloy AM50 listed in Table 2-1 were used in simulation.

Table 2- 1. Thermophysical properties of magnesium alloy AM50

Properties	Mg Alloy AM50	
	Solid	Liquid
Thermal Conductivity (W/m K)	80	100
Specific Heat (J/kg K)	1220	1320
Density (kg/m ³)	1710	1650
Latent Heat (J/kg)	3.7x10 ⁵	
Liquidus Temperature at 0MPa (°C)	620	
Solidus Temperature at 0MPa (°C)		435

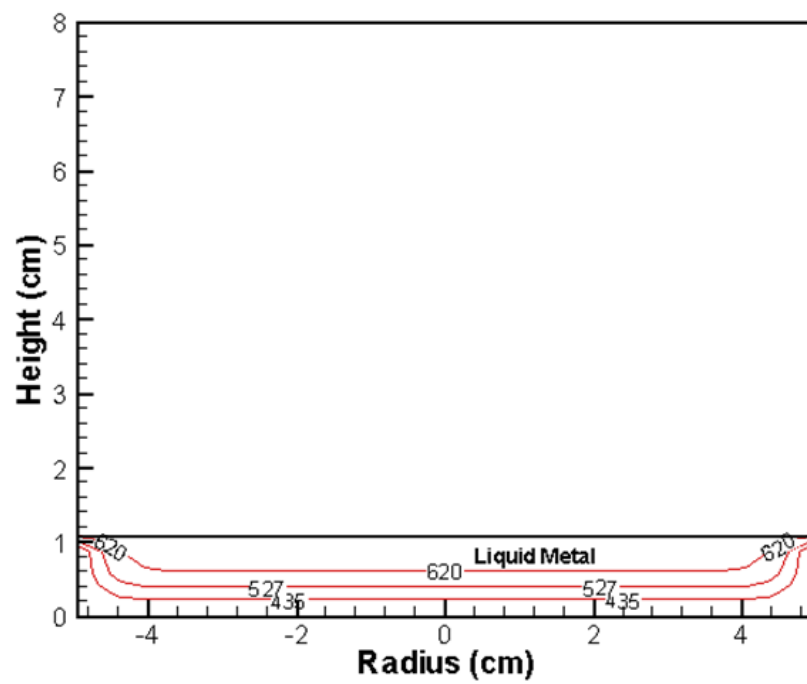
3. SIMULATION RESULTS

3.1 TEMPERATURE DISTRIBUTION AND SOLIDIFICATION FRONT

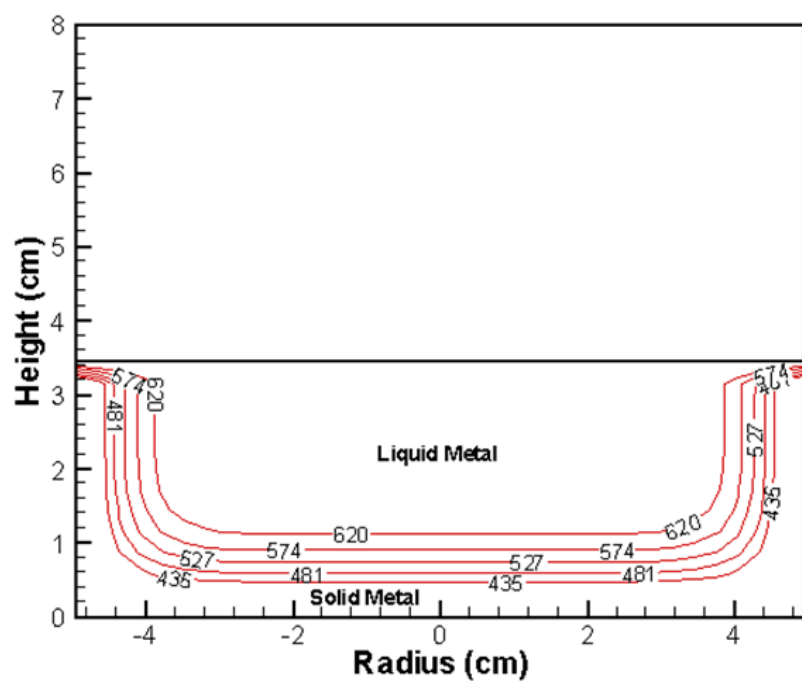
Figure 2-3 shows the filling sequence in the cavity with different filling percentage. The red lines in figures illustrate the temperature profile of the liquid-solid zone (mushy zone) where the metal shell solidifies outside and liquid metal inside. During the initial filling stage, the top of the casting is experiencing natural convection with the cover gas, while its side and bottom are releasing heat to the sleeve through convection and the plunger by conduction, respectively. Thus, during the whole filling process, the temperature profile almost maintains the same top-opened shell shape although the metal height is different. After 40% filling percentage ie, in the later stage of the cavity filling, the bottom solidified layer becomes thicker than the side solidified layer due to the lower plunger initial temperature (150°C) than the cylindrical sleeve initial temperature (275°C). Due to slow heat transfer caused by natural convection between the top surface of the metal and the air, the natural convective heat transfer coefficient ($h_{cov} = 150 \text{ Wm}^{-2}\text{K}^{-1}$) between top surface and the air and the heat transfer

coefficient ($h_{\text{die}} = 2000 \text{ Wm}^{-2}\text{K}^{-1}$) between melt and die were employed during calculating the filling process.

Figure 2-4 shows the temperature isocontours at different instants of time during the stage of pressurized solidification AM50 with applied pressure 60 MPa. As can be seen from prediction of figure 2-4(a), the temperature profiles are almost vertically symmetric resulting from pre-solidification shell at the bottom and side of cylindrical coupon. This is because, in the sleeve cavity, heat conduction-dominated rapid chill takes place at the bottom and along the side surfaces, and the top surface is slowly cooled by natural convection. As shown in figure 2-4(b), once the die cavity is filled completely, the firm contact between the top surface of the melt and the die surface is formed under the applied pressure. This results in a rapid cooling on the top surface of the casting through heat conduction to the die. As the time goes on, the rapid cooling from the top surface moves the hot area downward, which distorts the vertically symmetric temperature profile formed at the early stage of the process. The distorted temperature profiles are mainly attributed to the differences in the initial heat transfer conditions between the top, side and bottom surfaces of the casting.



(a)



(b)

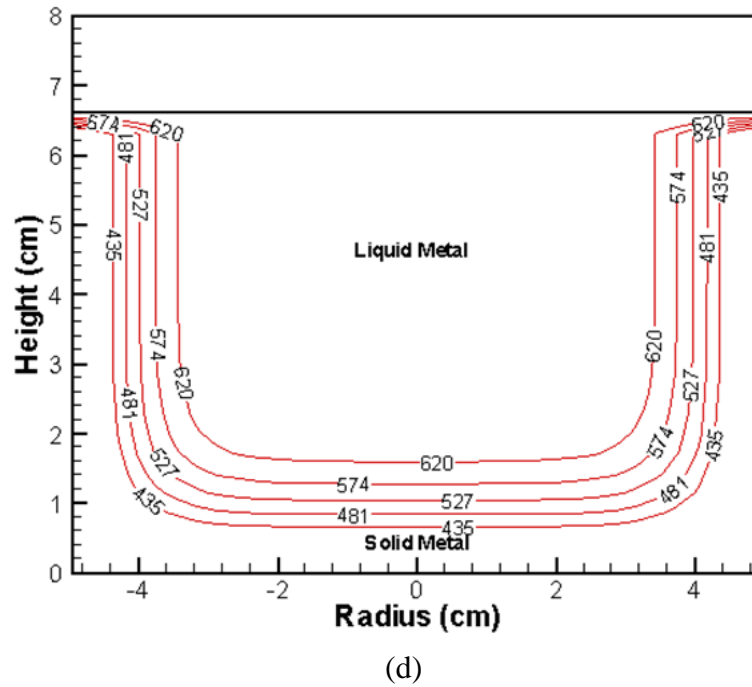
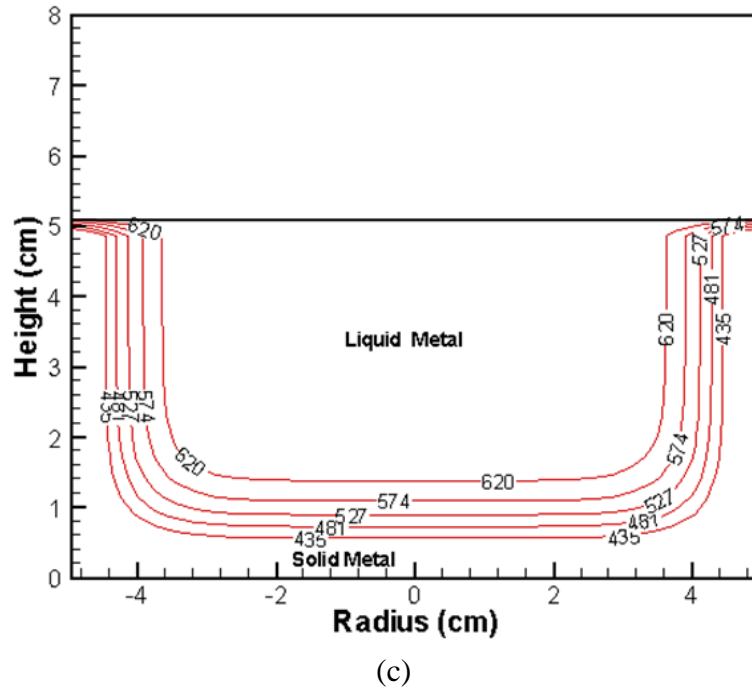
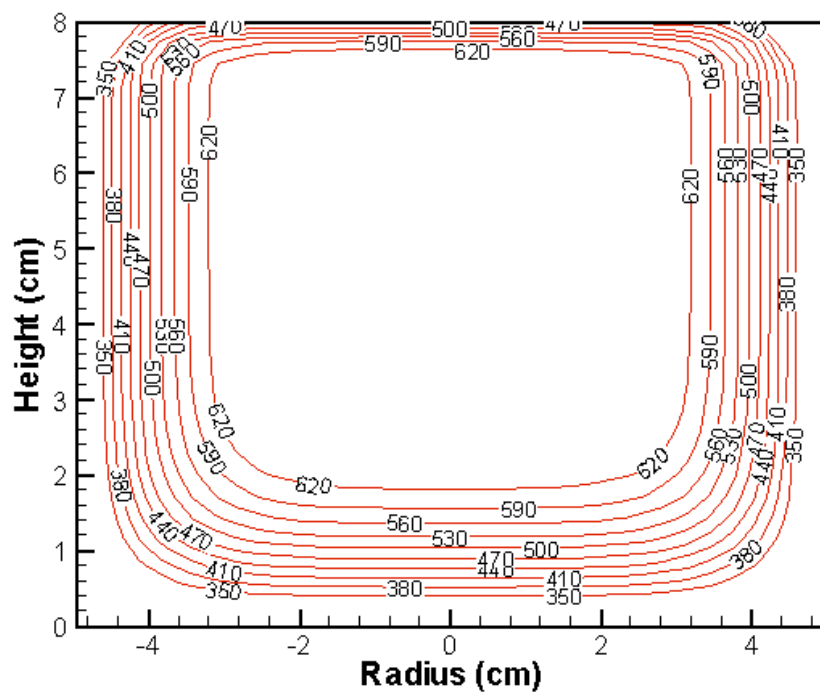
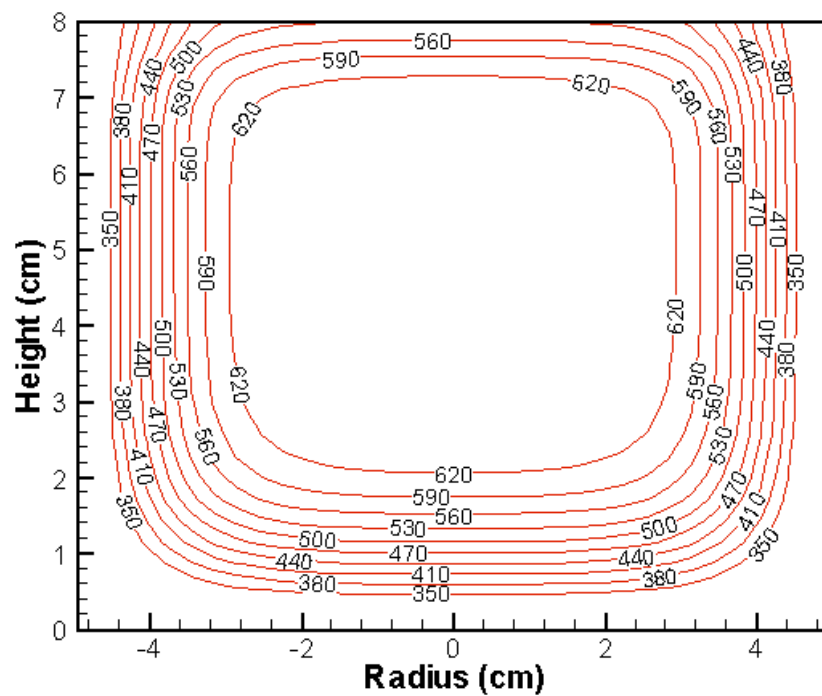


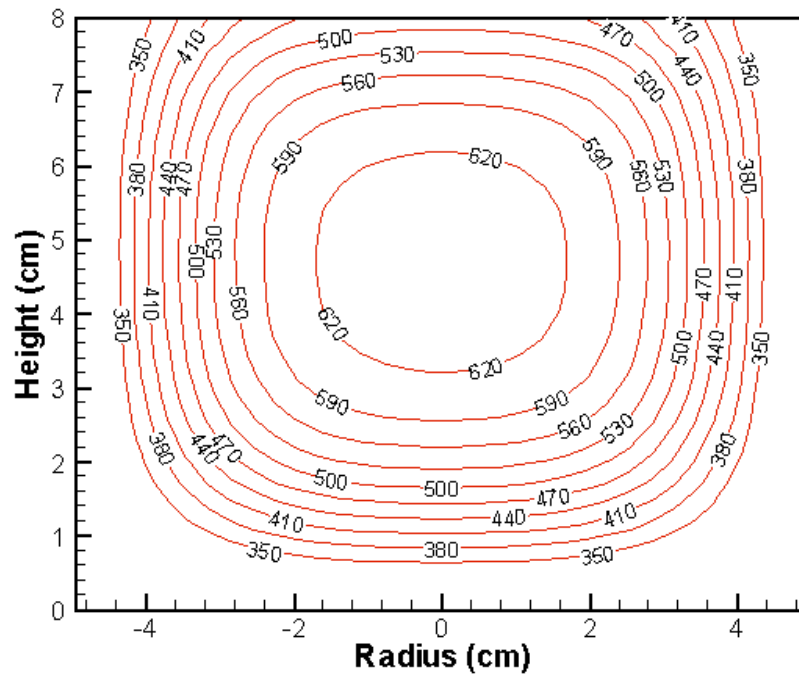
Figure 2- 3. Temperature profiles(XZ section view) of the cylindrical coupon casting at different cavity filling percentage: (a) 10%, (b) 40%, (c) 60%, and (d) 80%.



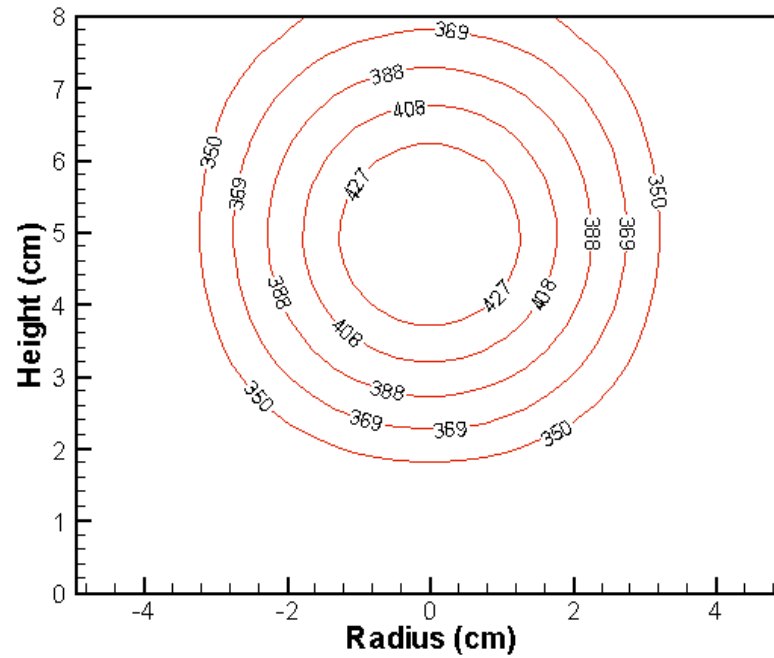
(a)



(b)



(c)



(d)

Figure 2- 4. Temperature contours(XZ section view) of the cylindrical coupon casting after complete filling: (a)1 s, (b) 4s, (c) 10 s, and (d) 40 s, under applied pressure 60 MPa.

For the top, the heat transfer coefficients ($h_{top} = 8400 \text{ Wm}^{-2}\text{K}^{-1}$, $9400 \text{ Wm}^{-2}\text{K}^{-1}$, and $10090 \text{ Wm}^{-2}\text{K}^{-1}$) were employed during calculating the solidification process under applied pressure 30, 60, and 90MPa, respectively. The heat transfer coefficients on side and bottom die ($h_{top} = 6900 \text{ Wm}^{-2}\text{K}^{-1}$, $7026 \text{ Wm}^{-2}\text{K}^{-1}$, and $7257 \text{ Wm}^{-2}\text{K}^{-1}$) were employed during calculating the solidification process under applied pressure 30, 60, and 90MPa, respectively.

As the solidification proceeds, the high temperature area tends to move towards the center of the casting. It can be indicated from figure 2-4(c) that the solidification of the top portion of the casting is accelerated and dictated by heat conduction between the top surface and die surface under the applied pressure instead of natural convection. The conduction-controlled solidification of the top portion tends to move the phase front downward. Meanwhile, the ongoing solidification at the bottom and side surface of the casting pushes the front upward and inward, respectively. As a result shown in figure 2-4(d), the last solidified point is present at 3 cm down from top surface of the casting due to initial uneven temperature distribution between the top and bottom of the die.

3.2 EFFECT OF APPLIED PRESSURES ON COOLING BEHAVIOR

Figure 2-5 predicts the cooling curves at the 4 cm(casting center) down from top surface along the central line of the cylindrical casting during pressurized solidification under 0, 30, 60, 90MPa. It is indicated that the casting center reaches its liquidus temperature 7.02, 7.40, 8.58, and 8.92 seconds after the cast filling process with applied pressure 90, 60, 30, and 0 MPa, respectively. Their liquidus temperature can be maintained for about 2 to 3 seconds.

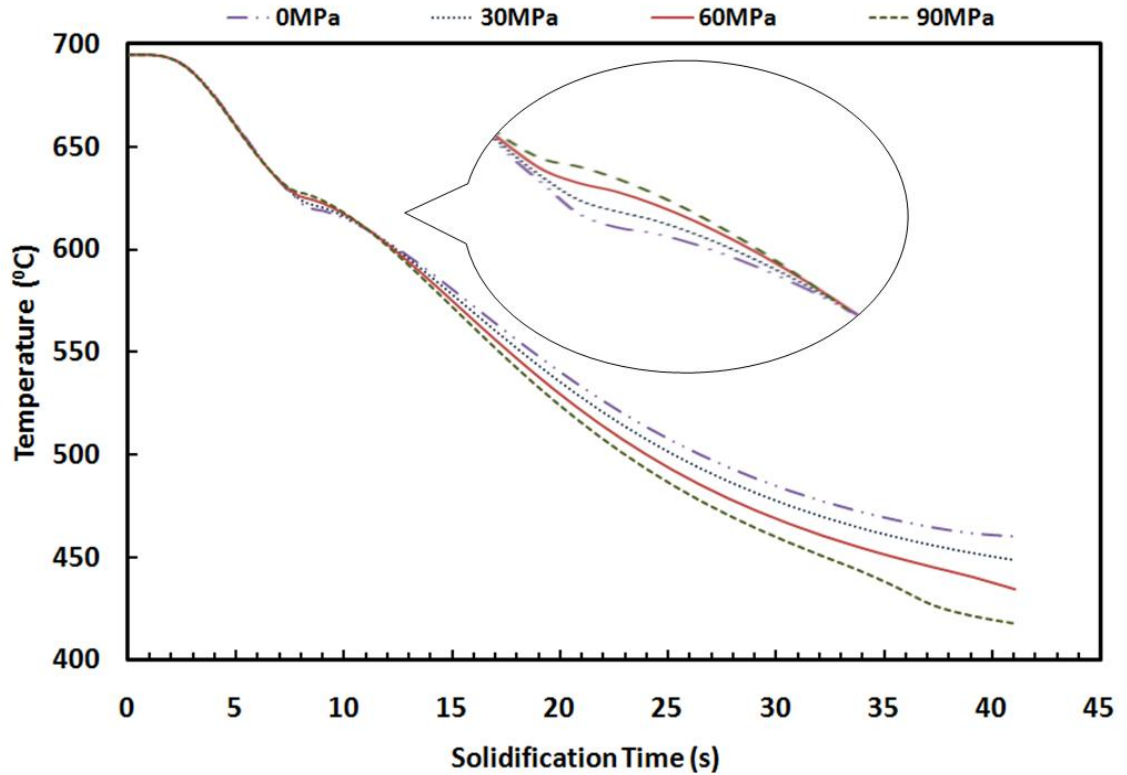


Figure 2- 5. Predicted cooling curves at the casting center solidified under an applied pressure 0, 30, 60, and 90 MPa.

As can be seen from the enlarged insert in figure 2-5, the application of 90 MPa pressure enables the casting center to reach the liquidus temperature earlier. This earlier arrival at the liquidus temperature might be due to the fact that the relatively large increase in the non-equilibrium liquidus temperature results from the high applied pressure of 90 MPa compared to those under 60 and 30 MPa. As the pressurized solidification proceeds, the temperature of the casting center under 90 MPa drops faster than the other two temperatures with the pressures of 60 and 30 MPa. It is evident that, 40 seconds after the onset of the pressurized solidification, the temperatures of the casting center becomes 417.9, 434.5, and 448.7⁰C under the applied pressures of 90, 60, and 30

MPa, respectively. The enhanced heat transfer at the casting/die interface due to the high applied pressure should be responsible for the quick temperature decrease and consequently the rapid solidification.

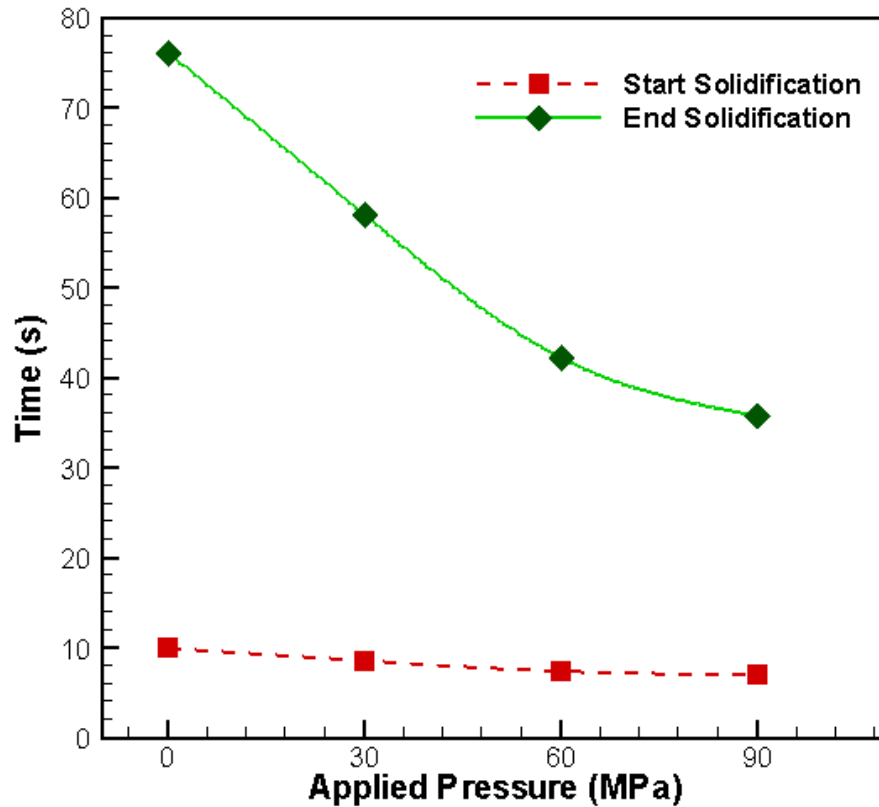


Figure 2- 6. Predicted start and end solidification times at the casting center under an applied pressure 0, 30, 60, and 90 MPa.

Figure 2-6 and 2-7 illustrate the effect of applied pressure on the solidification time of the casting. As indicated in figure 2-6, the high levels of applied pressures lower both the start and the end solidification times. It appears from the predicted results given in figure 2-7 that an applied pressure 60 MPa reduces solidification time and increases cooling rate more effectively than 30 and 90 MPa. The study by Hu[13] indicates that

further increase in the pressure beyond the value of 80 MPa has a minor influence on solidification rate of the magnesium squeeze castings.

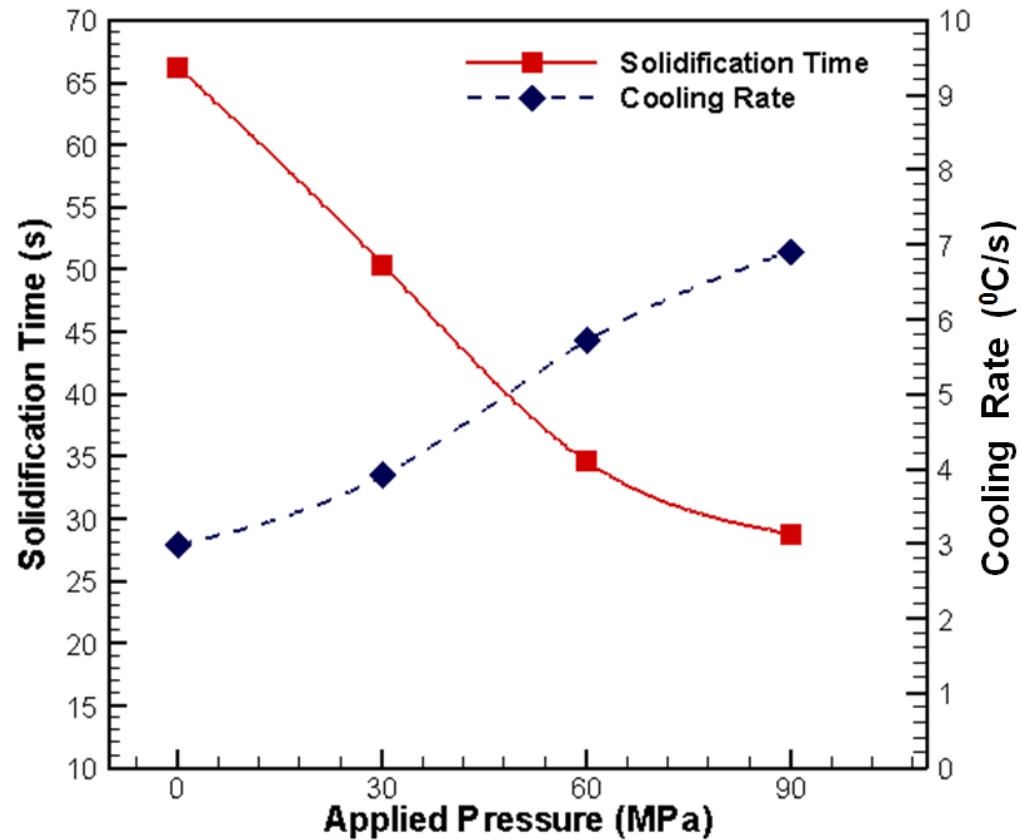


Figure 2- 7. Predicted solidification time and cooling rates at the casting center under an applied pressure 0, 30, 60, and 90 MPa.

4. EXPERIMENTAL VERIFICATION

To verify the simulation results, a squeeze casting experiment system was conducted. The integrated system consists of a 75 tons laboratory hydraulic press, a die, an electric resistance furnace and a data acquisition system. Figure 2-2 illustrates schematically the cylindrical squeeze casting and thermocouple location. The

experimental procedure includes pouring molten metal into the bottom sleeve, close the dies, cavity filling, squeezing solidification with applied pressure, and ejecting the casting from the top mould of the die. The temperature in the casting center was measured by Omega KTSS-116U thermocouples. Thermocouples were inserted from the plunger to the center of the casting under applied pressures 0, 30, 60, 90MPa, respectively. Real-time pressure and temperature data were recorded by a LabVIEW- based data acquisition system with a pouring temperature of 695⁰C, sleeve die temperature of 275⁰C, and plunger temperature of 150⁰C.

5. RESULTS AND DISCUSSION

Figure 2-8 shows typical cooling curves measured in the center of the casting solidified under the different applied pressures of 0, 30, 60, 90 MPa which were recorded by thermocouples. It can be seen for all three cases that, once the pressure is applied starting at 0 second, the temperature increases rapidly until reaching a plateau, i.e., the liquidus temperature. Then, the temperature is kept almost constant for a certain period of time before starting to decrease. However, the variation of applied pressures influences the attainable level and the holding duration of the liquidus temperature plateau. With the highest liquidus temperature, the applied pressure of 90 MPa accelerates the temperature of the casting center in a cooling rate faster than the pressures of 60 and 30 MPa during the pressurized solidification. As a result, at the 40th second after the solidification beginning, the temperatures of the casting center drops to 403.6, 412.3 and 438.7⁰C under the applied pressures of 90, 60 and 30 MPa, respectively.

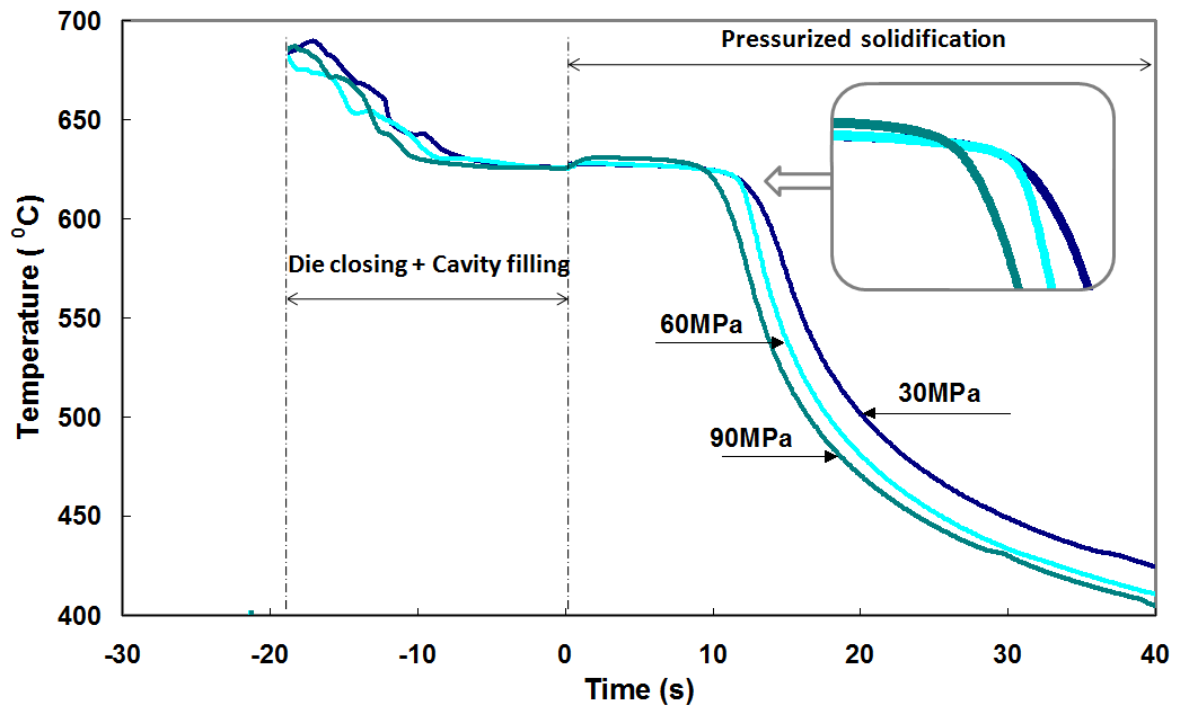


Figure 2- 8. Experimental results of temperature measurements at the center of a cylindrical casting of magnesium alloy AM50A solidified under applied pressures of 30, 60, and 90 MPa.

The total solidification time between the computational results and the experimental data is compared in Figure 2-9. The agreement is reasonably good between the predicted and the measured results. It can be found that the computed total solidification times are longer than those which are experimentally determined.

Compared the simulation result with the experimental data, during the stage of pressurized solidification, the predicted and measured temperature histories are in a good agreement. However, there is deviation between the prediction and experimental data, especially around the liquidus and solidus temperatures. This may be, at least partly, because the heat transfer coefficient used in the computation upon the completion of

filling was set as a function of the applied hydraulic pressure instead of local pressures. Thus may result in the underestimation of the heat transfer coefficients used in computation. Yu and Hu[9] indicated recently that local pressures can vary considerably during squeeze casting of magnesium alloys. Assuredly, further work is needed on experimentally determining an accurate relationship between the heat transfer coefficient and local pressure levels for magnesium squeeze casting.

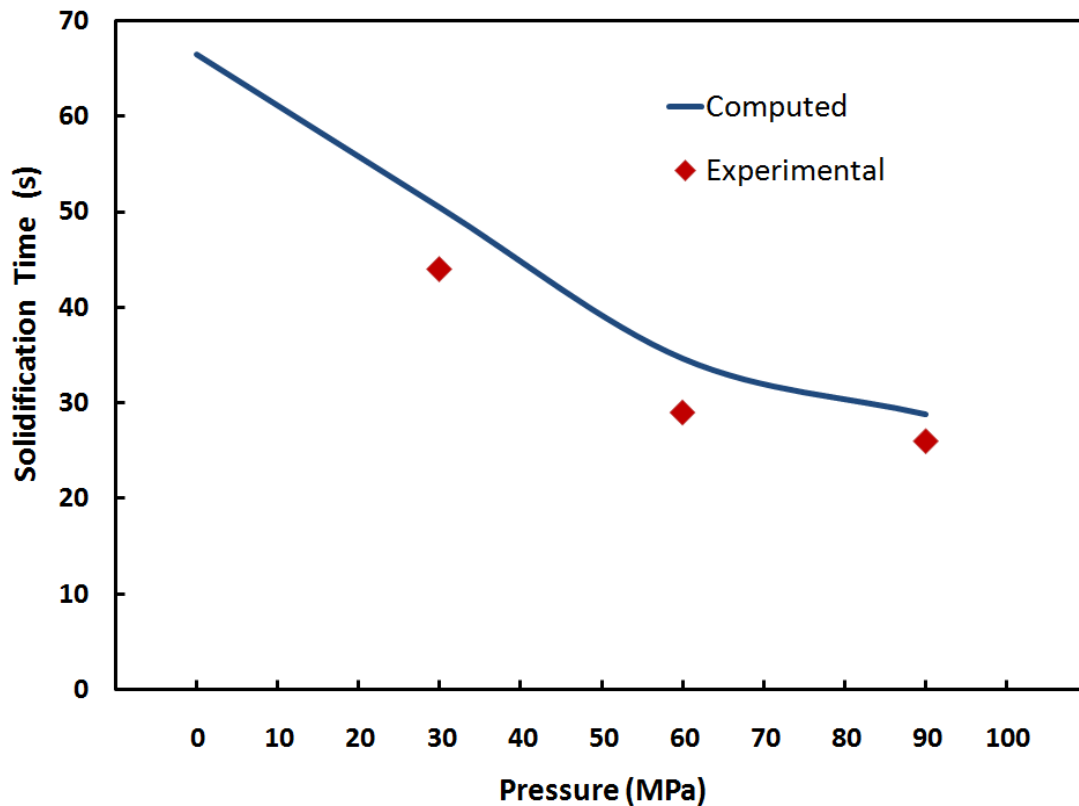


Figure 2- 9. Comparisons of total solidification time between computational and experimental results at the casting center under different pressures.

6. CONCLUSIONS

A mathematical model has been developed based on the finite difference and the enthalpy method to simulate heat transfer, and solidification phenomena taking place during squeeze casting magnesium alloy (AM50) involving two primary steps, which are cavity filling and pressurized solidification. With the help of experimentally determined heat transfer coefficients, the filling and pressurized solidification phenomena of squeeze cast magnesium alloy AM50 are simulated. The results show that the pre-solidified shell forms during cavity filling in the squeeze casting of magnesium alloy AM50 due to the involvement of both convection and conduction in heat transfer. The application of high pressure upon the completion of cavity filling results in rapid heat transfer across casting/die interface, and consequently increase solidification and cooling rates. To verify simulation result, temperature measurements inside an experimental squeeze casting were performed. Comparisons of the numerical results with the experimental measurements show close agreement.

REFERENCES

- [1] M. Zhou, N. Li, and H. Hu, (2005) Effect of Section Thicknesses on Tensile Behavior and Microstructure of High Pressure Die Cast Magnesium Alloy AM50. Materials Science Forum. Vol.476, 463-468.
- [2] H. Hu, A. Yu, N. Li, J. E. Allison, (2003) Potential Magnesium Alloys for High Temperature Die Cast Automotive Applications: A Review. Materials and Manufacturing Processes, Vol.18, No.5, 687-717.
- [3] H. Hu, (1998) Squeeze casting of magnesium alloys and their composites, J. of Materials Science, Vol. 33, 1579-1589.
- [4] M. R. Ghomashchi, A. Vikhrov, (2000) Squeeze casting: an overview. J. of Materials Processing Technology, 101, 1-9.
- [5] M. S. Yong, A. J. Clegg, (2004) Process optimization for a squeeze cast magnesium alloy. J. of Material processing Technology. 145, 134-141.
- [6] M. Zhou, H. Hu, N. Li, J. Lo, (2005) Microstructure and tensile properties of squeeze cast magnesium alloy AM50, [Journal of Materials Engineering and Performance](#). Vol. 14, 539-545.
- [7] Z. Guo, S. Xiong, B. Liu, M. Li, J. Allison, (2008) Effect of Process Parameters, Casting Thickness, and Alloys on the Interfacial Heat-transfer Coefficient in the High-pressure Die Casting Process. Metallurgical and materials transactions, Vol.39A, 2896-2905.
- [8] A. Dasgupta, and Y. Xia, (2004) Squeeze Casting: Principles and Applications, Die Casting Engineers. Vol. 48, No.1, 54-58.

- [9] A. Yu, H. Hu, (2007) Mathematical Modeling and Experimental Study of Squeeze Casting of Magnesium Alloy AM50A and Aluminum Alloy A356. Ph.D. dissertation, Department of Mechanical, Automotive & Materials Engineering, University of Windsor.
- [10] Z. Sun, H. Hu, and X. Chen, (2007) Numerical Optimization of Gating System Parameters for a Magnesium Alloy Casting with Multiple Performance Characteristic, J. of Materials and Processing Technology, Vol.199, Issue 1-3, 256-264.
- [11] D. Zhang, B. Canter, (1995) A numerical heat flow model for squeeze casting Al alloys and Al alloy/SiCp composites. Modelling Simul. Mater. Sci. Eng. Vol.3 121-126.
- [12] H. Hu, and A. Yu, (2002) Numerical Simulation of Squeeze Cast Magnesium Alloy AZ91D. Modeling Simul. Mater. Sci. Eng. Vol.10, 1-11.
- [13] H. Hu, and S.A. Argyropoulos, (1997) Mathematical Simulation and Experimental Verification of Melting Resulting from the Coupled Effect of Natural Convection and Exothermic Heat of Mixing. Metallurgical and Materials Transactions B, Vol. 28B, 135-148.
- [14] S.V. Patankar, (1980) Numerical Heat Transfer and Fluid Flow, McGraw-Hill, New York.
- [15] A. Yu, S. Wang, N. Li, H. Hu, (2007) Pressurized Solidification of Magnesium Alloy AM50A. J. of Material processing Technology. 191, 247-250.

CHAPTER 3

ESTIMATION OF HEAT TRANSFER COEFFICIENT IN SQUEEZE CASTING OF MAGNESIUM ALLOY AM60 BY EXPERIMENTAL POLYNOMIAL EXTRAPOLATION METHOD

1.INTRODUCTION

The squeeze casting process with high applied pressures is a promising solution for magnesium castings. Compared to other conventional casting processes, the most attractive features of squeeze casting (SC) are slow filling velocities and the pressurized solidification. Before the solid fraction of the casting is high enough, the applied pressure squeezes liquid metal feed into the air or shrinkage porosities effectively. Therefore, squeeze casting can make castings virtually free of porosity and usually have excellent as-cast quality, and are heat treatable, which is difficult to achieve with other conventional casting processes[1]. Although many research activities on squeeze casting process, some fundamental questions still need to be answered and the process must be optimized so as to expand its application, especially for emerging magnesium alloys.

Numerical simulation improved the productivity and optimized casting process greatly in the last decade. Beside the correct thermophysical property data, the estimating of the interfacial heat transfer coefficients(IHTCs) at the metal-mold interface is also necessary to simulate the solidification process accurately. IHTCs are usually very roughly set in the available FEM/FDM commercial codes. An accurate prediction of the boundary conditions is required to determine temperature distribution, solidification path, formation of shrinkage porosity, microstructure development, and residual stress. The pressure-transfer path is affected by applied hydraulic pressures, pouring and die initial

temperatures, alloy and die materials, and casting orientation. Thermal barriers include coating applied on the die surface and air gap caused by shrinkage. The process parameters, such as the applied hydraulic and local pressures, pouring temperatures, and die initial temperatures, have an influence on the formation of pressure-transfer path, which consequently affects heat transfer at the metal-mold interface and the final quality of squeeze castings[2,3]. In various casting process, the contact between the liquid metal and mold die is imperfect because of the coating applied on the die surface and air gap caused by shrinkage[4]. These thermal barriers may decrease the heat transfer between metal and die and cooling rate of the casting surface, which affect microstructure and quality of the casting significantly. Hence, precise determination of heat transfer coefficients at the metal-mold interface is a critical consideration to simulate the solidification process and model the microstructure of die castings accurately[5-10]. Especially, for thin-wall castings, the evaluation of IHTC becomes vital due to very limited solidification time.

However, many studies only focused on the simple shape die casting[11-14]. Little attention has been paid to variation of casting thicknesses and hydraulic pressures. Actually, in the die casting practice, various section thicknesses at different locations of castings result in significant variation of the local heat transfer coefficients. Therefore, it would be essential to investigate the influence of casting thickness, pressure value, and process parameters on the IHTC. In this study, a special 5-step squeeze casting was designed for understanding casting thickness-dependant IHTC, and the temperature measuring units and the pressure transducers were employed to accurately measure the temperatures and the local pressures during squeeze casting of magnesium alloy AM60.

2. EXPERIMENTAL SETUP

2.1 5-STEP CASTING

A 5-step shape casting was designed special for this study. Figure 3-1 shows the 3-D model of 5-step casting, which consists of 5 steps(from top to bottom designated as steps 1 to 5) with dimensions of 100x30x3 mm, 100x30x5 mm, 100x30x8 mm, 100x30x12 mm, 100x30x20 mm accordingly. The molten metal fills the cavity from the bottom cylindrical shape sleeve with diameter 100 mm.

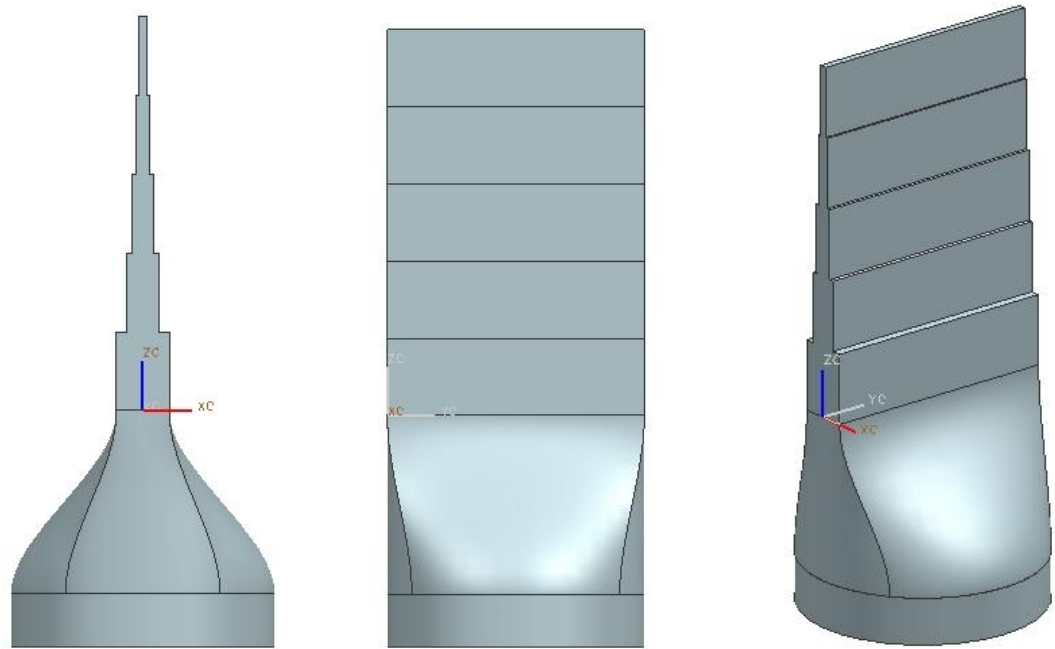


Figure 3- 1. 3-D model of 5-step casting with the round-shape gating system (A)XZ view; (B) YZ view; (C) isometric view

2.2 CASTING PROCESS

The integrated system included a laboratory hydraulic press, upper-lower die, an electric resistance furnace and a data acquisition system. As Figure 3-2 shows, the mold

assembly was composed of three parts. The two upper die of casting cavity split along the center. The bottom sleeve has a diameter of 0.1016 m and a height of 0.127 m. The chill vent was located on the top of the step casting, which can discharge the gas inside the upper die cavity. Both the upper die and the bottom sleeve were heated by cartridge heaters, in which the temperatures were separately controlled by Shinko Temperature Controllers.

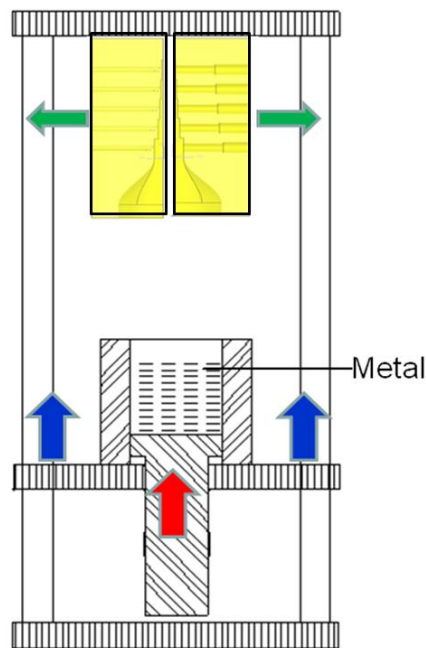


Figure 3- 2. Schematic diagram of squeeze casting machine

2.3 CASTING PROCESS

The 75- ton heavy duty hydraulic press and commercial magnesium alloy AM60 were used in the experiment. Figure 3-3 shows a typical 5-step casting poured under above mentioned process condition with applied hydraulic pressure of 30 MPa.



Figure 3- 3. A 5-step casting solidifying under applied pressure 30MPa.

3. DETERMINATION OF IHTC

Based on the principle of heat transfer, the interfacial heat transfer coefficients(IHTC) between metal and die surface can be determined by above mentioned Equation 1-1(Chapter 1). But, determination of IHTC using measurements of T_{cs} , T_{ds} , and $q(t)$ directly is difficult. As a result, a polynomial curve fitting method needs to be employed to determine the IHTC based on the temperatures measured inside the die or casting[10,12,15]. The direct heat transfer modeling also was involved to calculate heat flux at the casting-die interface, which requires numerical or analytical methods to be solved. In this study, from the measured interior temperature histories, the transient

metal-die interface heat flux and temperature distribution were estimated by the polynomial extrapolation method. To evaluate the IHTC effectively as a function of solidification time in the squeeze casting process, the finite difference method(FDM) was employed as follows based on the heat transfer equations[16].

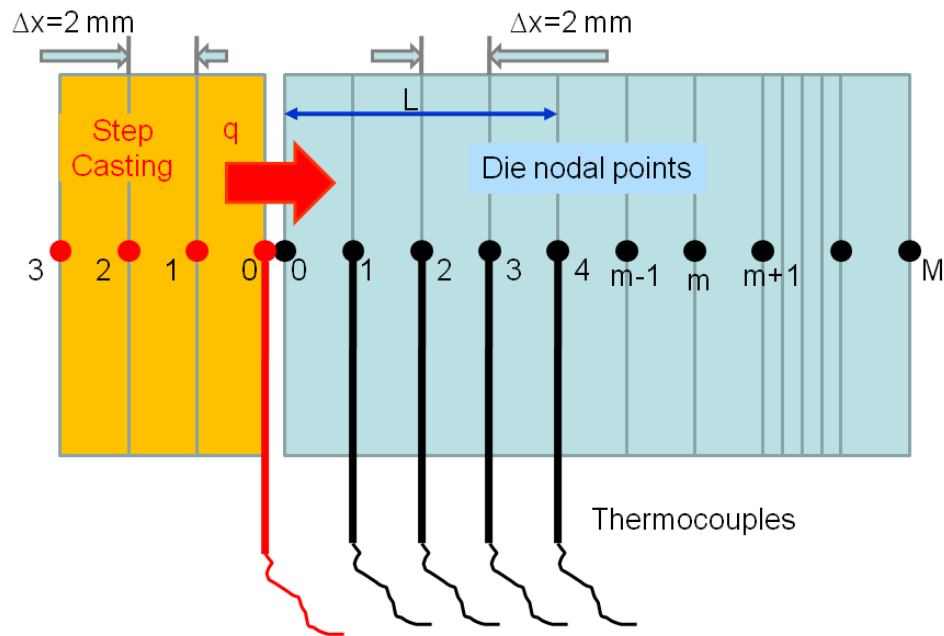


Figure 3- 4. One-dimensional heat transfer at the interface between the casting and die, where temperature measurements were performed.

Since the thickness of each step is much smaller than the width or length of the step, it can be assumed that the heat transfer at each step is one-dimensional. The heat transfer across the nodal points of the step casting and die is shown in Figure 3-4. The temperatures were measured at 2, 4, 6, 8 mm beneath die surface and the heat flux transferred to the die mould can be evaluated by heat transfer equations. Please refer the Chapter IV for detailed information.

3.1 HEAT TRANSFER MODEL

The heat flux for both the casting and die interface can be calculated from the temperature gradient at the surface and sub-surface nodes by Equation 3-1:

$$q(t) = -k \frac{dT}{dx} = -k \frac{T_m^t - T_{m-1}^t}{\Delta x} \quad (3-1)$$

where k is thermal conductivity of the casting or die materials. The superscript t is solidification time. The subscript m means the number of the discrete nodal points. The heat flux at the casting-die interface(q) at each time step was obtained by applying segregated heat conduction Equation 3-2.

$$\rho c \frac{\partial T(x,t)}{\partial t} = \frac{\partial}{\partial x} \left(k \frac{\partial T(x,t)}{\partial x} \right) \quad (3-2)$$

For the surface node of the die, Equation 3-2 can be rearranged as Equation 3-3:

$$(1 + 2F_0)T_0^{p+1} - 2F_0T_1^{p+1} = 2F_0 \frac{\Delta x}{k} q_0 + T_0^p \quad (3-3)$$

For any interior node of the die, Equation 3-2 can be solved as Equation 3-4:

$$(1 + 2F_0)T_m^{p+1} - F_0(T_{m-1}^{p+1} + T_{m+1}^{p+1}) = T_m^p \quad (3-4)$$

where the superscript p is used to denote the time dependence of T. F_0 is a finite different form of the Fourier number:

$$F_0 = \frac{\alpha \Delta t}{(\Delta x)^2} = \frac{k}{c\rho} \frac{\Delta t}{(\Delta x)^2} \quad (3-5)$$

The heat flux at the casting-die interface(q) at each time step was obtained by applying Equations 3-3 and 3-4. Thus, with T_{ds} estimated by the polynomial curve fitting method, the segregated IHTC values were evaluated by Equation 1-1.

3.2 POLYNOMIAL CURVE FITTING METHOD

For example, beneath the step 4 die surface, as Figure 3-4 showed, thermocouples were positioned at $X1 = 2\text{mm}$, $X2 = 4\text{mm}$, $X3 = 6\text{mm}$, and $X4 = 8\text{mm}$ away from the die surface. From the temperature versus time curves obtained at each position inside the die, the temperature at the die surface($X0 = 0\text{mm}$) can be extrapolated by using a polynomial curve fitting.

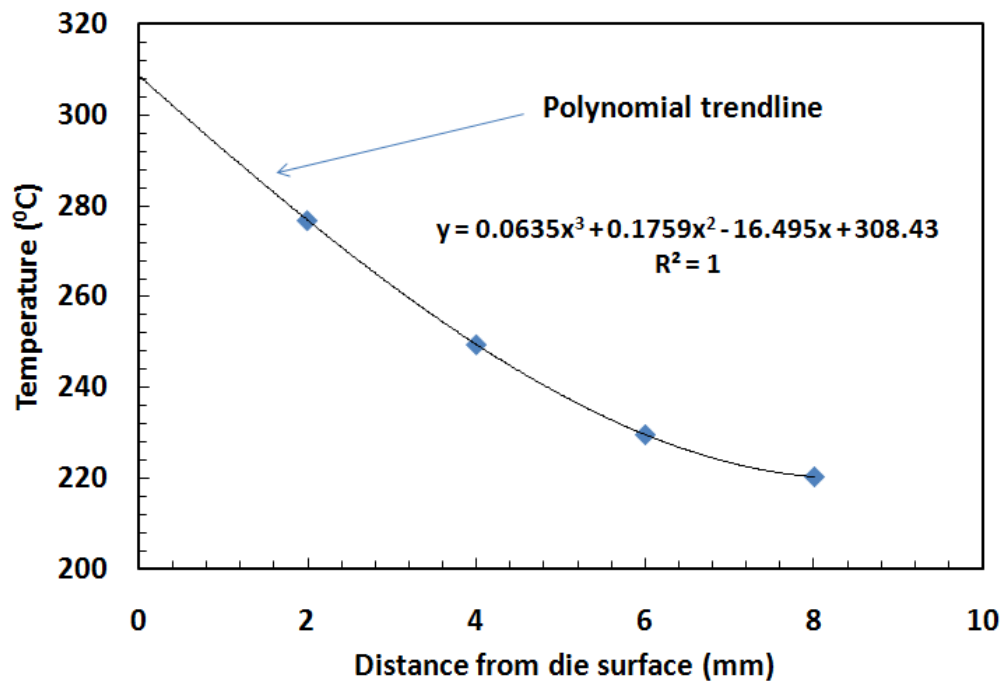


Figure 3- 5. Polynomial curve with various measured temperatures at a time of 4.1 seconds after pressurized solidification.

After the completion of filling, by selecting a particular time of solidification process, for example $t = 4.1$ seconds, the values of temperatures were read from the temperature-time data at position $X1$, $X2$, $X3$, and $X4$. Figure 3-5 shows the temperature

values against distance X which were fitted by the polynomial trendline. The temperature at the die surface($T_0=308.430^\circ\text{C}$) was determined by substituting the value of $x=0$ in the polynomial curve fitting Equation 3-6 obtained from the temperature values at various distances inside the die at a chosen time of 4.1 seconds after pressurized solidification.

$$y = 0.0635x^3 + 0.1759x^2 - 16.495x + 308.43 \quad (3-6)$$

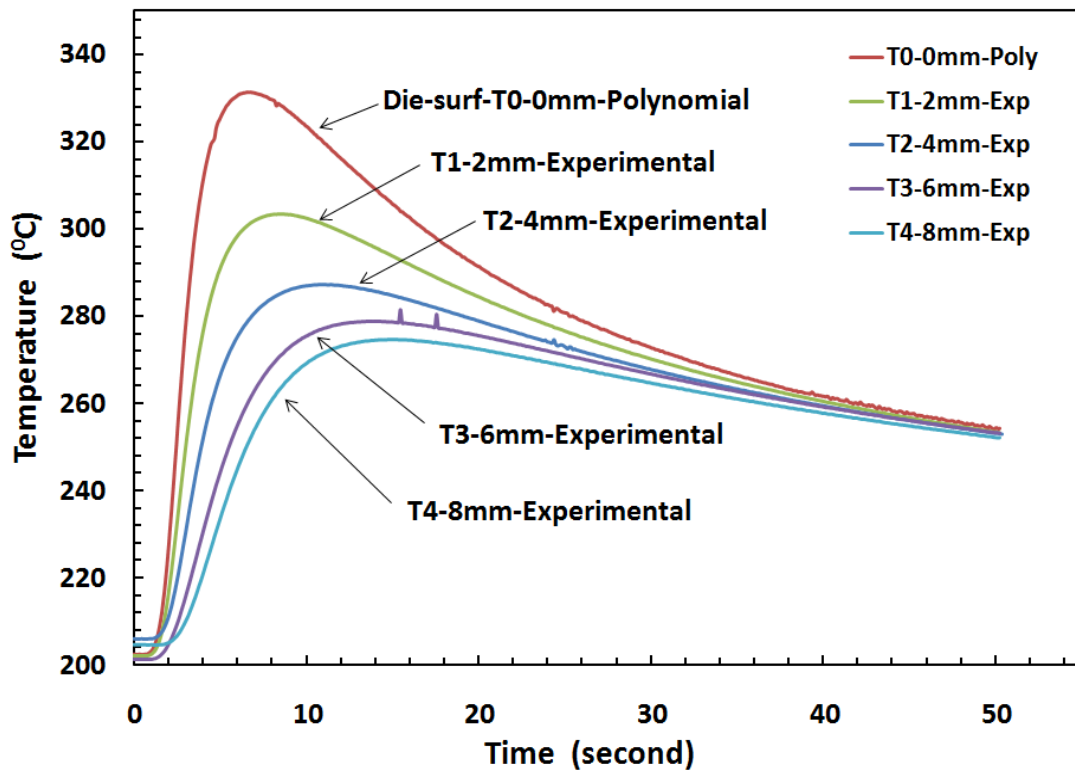


Figure 3- 6. Extrapolated temperature curve at the die surface(T_0) by the polynomial curve fitting method with applied pressure 30 MPa.

This procedure was repeated for a number of time increments to get series of such temperatures with corresponding times. As Figure 3-6 shows, for the step 4 under pressure 30 MPa, the temperature curve versus time at the die surface($X_0 = 0\text{mm}$) was extrapolated as “Die-surf- T_0 -0mm-polynomial” based on the experimental data

T1(X1=2mm), T2(X2=4mm), T3(X3=6mm), and T4(X4=8mm) beneath the die surface. By extrapolation, the evaluated peak temperature value of the die surface is 333.39⁰C at the solidification time t=6.1 seconds.

4. RESULTS AND DISCUSSION

4.1 EXPERIMENTAL COOLING CURVE

Figure 3-6 and 3-7 show typical temperatures versus time curves at the metal-die interface of Step 4 for solidifying magnesium alloy AM60 and the steel die respectively with an applied hydraulic pressure of 30 MPa. The measured locations are described in Figure 3-4, which include casting surface temperature(Metal-surface-Experimental), T1, T2, T3, and T4 inside the die. The following analysis was also based on this typical data at Step 4 with pressure 30MPa. This information includes measurements of the casting surface temperature in addition to temperature measurements obtained at different depths under the die surface. Since molten metal filled the cavity from the bottom, pre-solidification occurred upon the completion of cavity filling. No die surface temperatures exceeded 340⁰C, and the highest temperature of the casting surface was 532.97⁰C.

From Figure 3-7, it can be observed that the temperature curve at casting surface increases abruptly and drops faster than the temperature measurements obtained at different depths under the die surface. The curves indicated the dynamic temperature change at the metal-die interface.

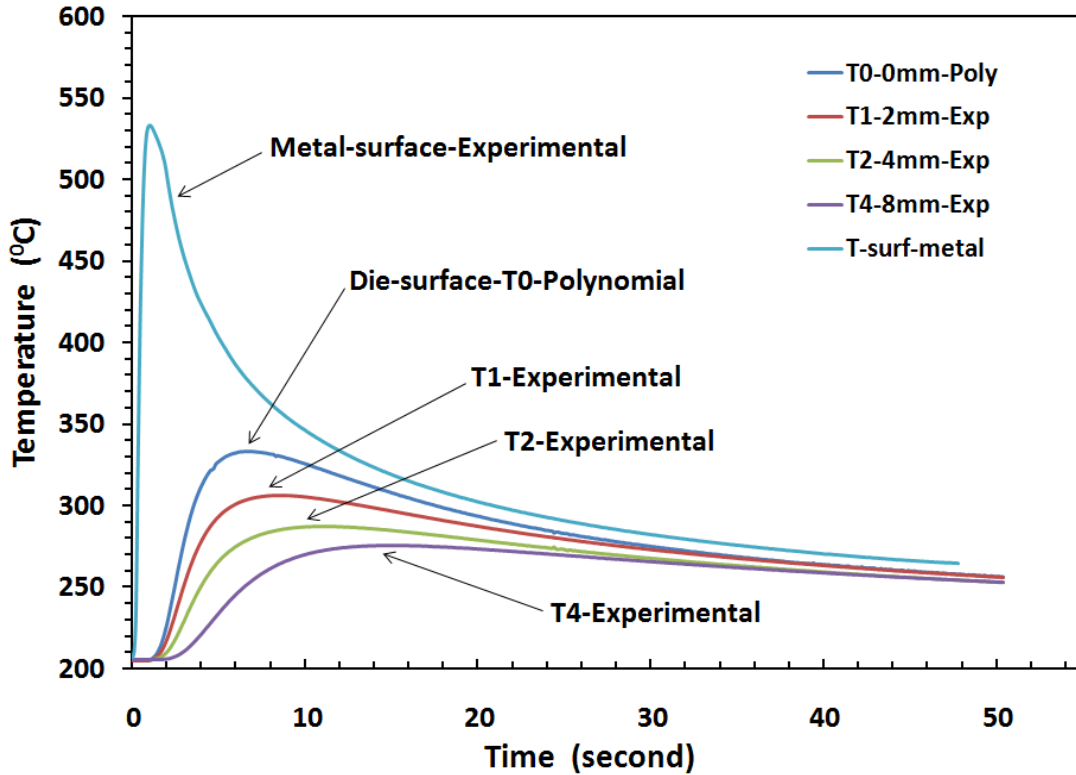


Figure 3- 7. Typical temperature versus time curves (Step 4, 30MPa) at metal surface, die surface, and various positions inside the die.

4.2 TYPICAL HEAT FLUX(Q) & IHTC(H) CURVES

Substituting the estimated die surface temperature(T_0) and the measured temperature at $T_1=2$ mm to Equation 3-2, the interfacial heat flux(q) was calculated. Figure 3-8 shows the interfacial heat flux(q) and the heat transfer coefficient(IHTC) versus solidification time of Step 4 with applied pressure 30 MPa. The curves were estimated by extrapolated fitting method based on the data in Figure 3-7. For step 4, the peak heat flux value was $3.4E+05$ W/m², and the peak value of IHTC was 6,450 W/ m²K. From Figure 3-8, it can be observed that the heat flux(q) curve reached its peak value abruptly within 2.3 seconds and decreased rapidly to a lower level($5.0E+04$ W/m²) after

20 seconds. While the heat transfer coefficients(h) curve reached its peak value gradually at 12.3 seconds and vibrated around that peak value for about 6.5 seconds, then decreased slowly to the level 3,000 W/ m²K after 28 seconds. It is noted that the uncertainty and error of the polynomial extrapolated method should be responsible for the significant variation presented in the heat flux & IHTC curve in Figure 3-8.

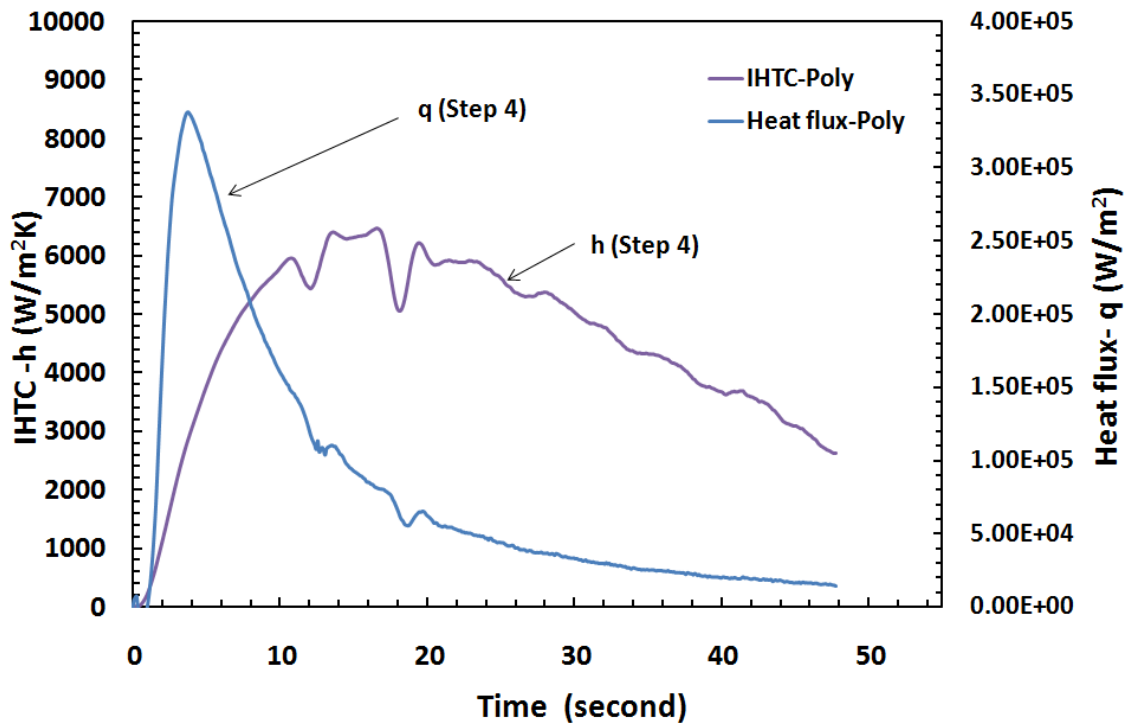


Figure 3- 8. Interfacial heat flux(q) and the heat transfer coefficient (IHTC) curves for step 4 with applied pressure 30 MPa.

Figure 3-9 shows the heat flux(q) versus solidification time of step 3, step 4, and step 5 with an applied pressure of 30 MPa. The curves were estimated by extrapolation of the experimental data. For Steps 3, 4, and 5, the peak heat flux values were 1.8E+05 W/m², 3.4E+05 W/m², 5.25E+05 W/m², respectively. From Step 3 to Step 5, the heat flux(q) curves reached to their peak value abruptly between 2.4, and 3.8 second and

decreased rapidly to the lower level ($5.0\text{E}+04 \text{ W/m}^2$) at 16, 28, and 42 seconds, respectively.

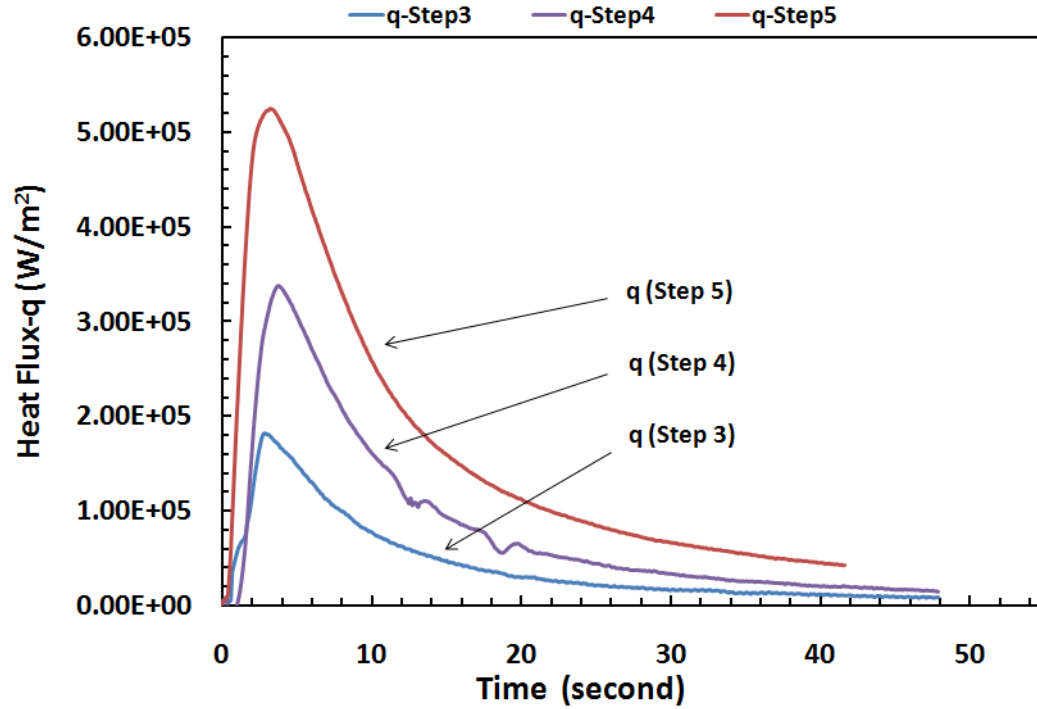


Figure 3- 9. Heat flux(q) curves for step 3, 4, 5 estimated by the extrapolated fitting method.

Figure 3-10 shows that the heat transfer coefficient(IHTC) curves of Steps 3,4,5 estimated by the extrapolated fitting. For Step 3, IHTC began increasing, and reached its peak value of $3,200 \text{ W/ m}^2\text{K}$ at 12.5 seconds, maintained that value for about 6 seconds, then decreased slowly to the level $1,600 \text{ W/ m}^2\text{K}$ at 48 seconds. For Step 4, IHTC value increased and reached its peak value($6,450 \text{ W/ m}^2\text{K}$) at about 12.3 seconds, remained at that value for about 6.5 seconds, then decreased slowly to the level $3,000 \text{ W/ m}^2\text{K}$ at 48 seconds. For step 5, IHTC curve increased sharply to the peak value of $7,915 \text{ W/ m}^2\text{K}$ at 11.2 seconds and then decreased to the lower level $2,230 \text{ W/ m}^2\text{K}$ at 48 seconds.

From steps 3 to 5, the peak IHTC value varied from 3,200 W/m²K to 7,850 W/m²K. Therefore, the wall thickness affects IHTC peak values significantly. The peak IHTC value decreased from the bottom to the top of the step casting as the step thickness reduced.

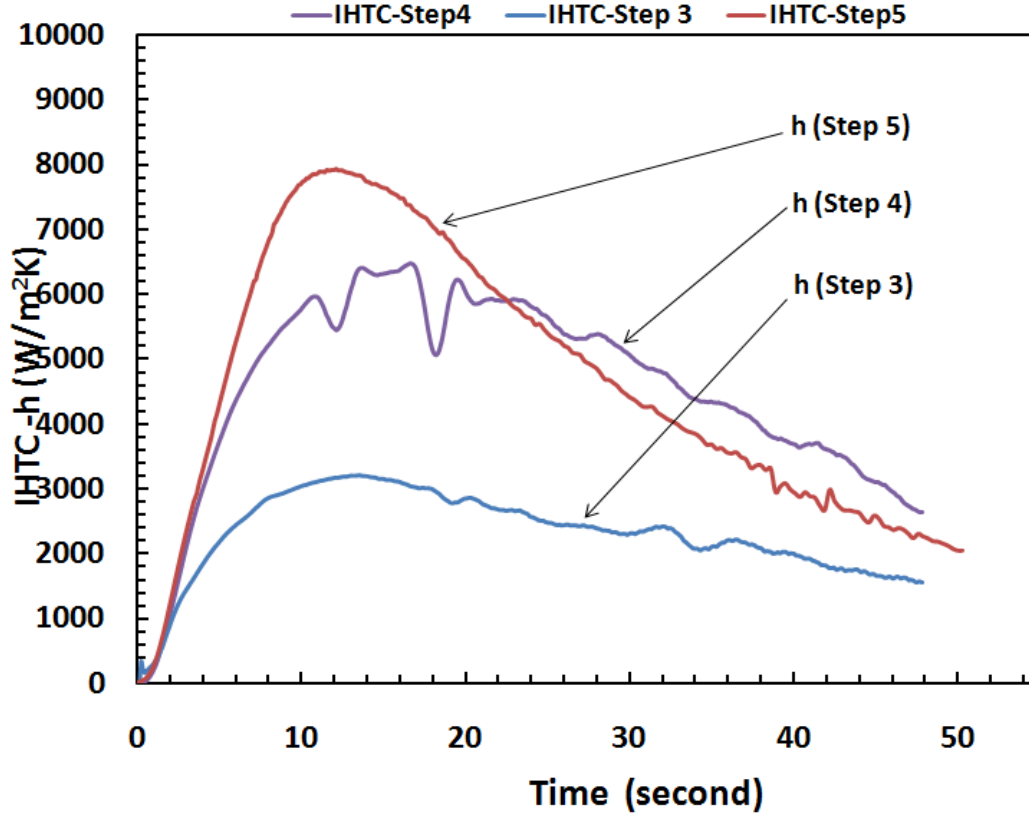


Figure 3- 10. Heat transfer coefficient(IHTC) curves for step 3,4,5 estimated by the extrapolated fitting method.

5. CONCLUSIONS

1. The heat flux and IHTC at metal-die interface in squeeze casting were determined based on an extrapolation method.

2. For all steps, IHTC increased first, and reached its peak value, then dropped gradually until it arrived at a low value.
3. For steps 3, 4, and 5, the peak heat flux values were $1.8\text{E}+05 \text{ W/m}^2$, $3.4\text{E}+05 \text{ W/m}^2$, $5.25\text{E}+05 \text{ W/m}^2$, respectively.
4. For step 3, with a section thickness of 8mm, IHTC began with a increasing stage, and reached its peak value of $3,200 \text{ W/ m}^2\text{K}$ at 12.5 seconds, maintained that value for about 6 seconds, then decreased slowly to the level $1,600 \text{ W/m}^2\text{K}$ at 48 seconds. For step 4 of the thickness 12mm, IHTC value increased and reached its peak value($6,450 \text{ W/m}^2\text{K}$) at about 12.3 seconds, remained at that value for about 6.5 seconds, then decreased slowly to the level $3,000 \text{ W/m}^2\text{K}$ at 48 seconds. From step 3 to 5, the peak IHTC value varied from $3,200 \text{ W/m}^2\text{K}$ to $7,850 \text{ W/m}^2\text{K}$.
5. The wall thickness of squeeze cast magnesium alloy AM60 affected IHTC peak values significantly. The peak IHTC value decreased in a direction from the bottom to top as the step thickness reduced.

REFERENCES

- [1] I. Cho, C. Hong, "Evaluation of heat-transfer coefficients at the casting/die interface in squeeze casting", *Int. J. Cast Metals Res*, 1996, Vol.9, 227-232
- [2] J. Aweda, M. Adeyemi, "Experimental determination of heat transfer coefficients during squeeze casting of aluminum", *J. of Materials and Processing Technology*, 2009, vol.209, p1477-1483.
- [3] Z. Guo, S. Xiong, B. Liu, M. Li, J. Allison, "Effect of Process Parameters, Casting Thickness, and Alloys on the Interfacial Heat-transfer Coefficient in the High-pressure Die Casting Process", *Metallurgical and materials transactions*, Vol.39A, 2008, p2896-2905.
- [4] M. Trovant, S. Argyropoulos, "Finding boundary conditions: A coupling strategy for the modeling of metal casting processes: Part I. Experimental study and correlation development", *Metallurgical and materials transactions B*, Vol.31B, 2000, p75-86.
- [5] A.Yu, "Mathematical Modeling and experimental study of squeeze casting of magnesium alloy AM50A and aluminum alloy A356", Ph.D. dissertation, Department of Mechanical, Automotive & Materials Engineering, University of Windsor, 2007.
- [6] D. Browne, D. O'Mahoney, "Interface heat transfer in investment casting of aluminum", *Metall.Mater.Trans. A*, 32A, 2001, p3055-3063
- [7] G. Dour, M. Dargusch, C. Davidson, and A. Nef, "Development of a non-intrusive heat transfer coefficient gauge and its application to high pressure die casting", *J. of Materials and Processing Technology*, 2005, vol.169, p223-233.

- [8] A. Hamasaiid, M. Dargusch, C. Davidson, S. Tovar, T. Loulou, F. Rezai-aria, and G. Dour, "Effect of mold coating materials and thickness on heat transfer in permanent mold casting of aluminum alloys", *Metallurgical and materials transactions A*, Vol.38A, 2007, p1303-1316
- [9] M. Dargusch, A. Hamasaiid, G. Dour, T. Loulou, C. Davidson, and D. StJohn, "The accurate determination of heat transfer coefficient and its evolution with time during high pressure die casting of Al-9%Si-3%Cu and Mg-9%Al-1%Zn alloys", *Advanced Engineering Materials*, 2007, Vol.9, No.11, p995-999
- [10] J. Taler, W. Zima, "Solution of inverse heat conduction problems using control volume approach", *Int. J. Heat Mass Transf.*, 1999, Vol.42, p1123-1140
- [11] R. Rajaraman, R. Velraj, "Comparison of interfacial heat transfer coefficient estimated by two different techniques during solidification of cylindrical aluminum alloy casting", *Heat Mass Transfer*, 2008, Vol.44, p1025-1034
- [12] J. Su, F. Geoffrey, "Inverse heat conduction problem of estimating time varying heat transfer coefficients", *Numer Heat Transf Part A*, 2004, Vol.45, p777-789
- [13] D. Sui, Z. Cui, "Regularized determination of interfacial heat transfer coefficient during ZL102 solidification process", *Transactions of Nonferrous Metals Society of China*, 2008, Vol.18, p399-404
- [14] S. Broucaret, A. Michrafy, G. Dour, "Heat transfer and thermo-mechanical stresses in a gravity casting die influence of process parameters", *J. of Materials Processing Technology*, 2001, vol.110, p211-217
- [15] J. Beck, "Nonlinear estimation applied to the nonlinear inverse heat conduction problem", *Int. J. Heat Mass Transfer*, 1970, Vol.13, 703-715

- [16] J. Beck, B. Blackwell, A. Haji-sheikh, "Comparison of some inverse heat conduction methods using experimental data", Int. J. Heat Mass Transfer, 1996, Vol.39, 3649-3657.

CHAPTER 4

DETERMINATION OF HEAT TRANSFER COEFFICIENTS BY EXTRAPOLATION AND NUMERICAL INVERSE METHODS IN SQUEEZE CASTING OF MAGNESIUM ALLOY AM60

1. INTRODUCTION

Compared to other conventional casting processes, the most attractive features of squeeze casting (SC) are slow cavity filling and pressurized solidification. Before the solid fraction of the casting becomes high enough, the applied pressure squeezes liquid metal feed into the air or shrinkage porosities effectively. Therefore, squeeze casting can make castings virtually free of porosity and usually have excellent as-cast quality, and are heat treatable, which is difficult to achieve with other conventional high pressure casting processes. Despite of many squeeze casting research activities of Cho and Hong[1] and Yu [2], certain fundamental questions still need to be answered and the process must be optimized so as to expand its application, especially for emerging magnesium alloys.

To solve the obstacles of squeeze casting application, the optimized process parameters and interfacial heat transfer coefficient (IHTC) at the metal-mold interface need to be further studied. The process parameters, such as the applied hydraulic and local pressures, pouring temperatures, and die initial temperatures, have an influence on the formation of pressure-transfer path, which consequently affects heat transfer at the metal-mold interface and the final quality of squeeze castings[3-5]. In various casting processes, the contact between the liquid metal and die inner surface is usually imperfect because of coating applied on the die surface and air gap caused by shrinkage. These

thermal barriers may decrease the heat transfer between metal and die and cooling rates of the casting surface, which influence microstructure and quality of the casting significantly[6]. Hence, precise determination of heat transfer coefficients at the metal-mold interface is essential to accurately simulate solidification process and model microstructure evolution of die castings. Especially, for thin-wall castings, Guo[7] described that the accuracy of IHTC is critically vital due to very limited solidification time.

Although the IHTC has been studied extensively by many researchers, rare experiment has been carried on to determine the IHTC in squeeze die casting processes because it is hard to perform and the operation procedure is complicated for magnesium alloys. Cho and Hong[8] estimated heat transfer coefficients at the molten metal-die interface in aluminum alloy(Al-4.5%Cu) squeeze casting. The IHTC values were about 1,000 W/m²K prior to pressurization which rapidly increased to around 4,700 W/m²K at a single hydraulic pressure(50 MPa) for a cylindrical casting with a heated steel die. Then, it was concluded that IHTC increased with the application of pressure. Kim and Lee[4] investigated the tube shape casting and found that the heat transfer coefficients at the interface of the inner mould decreased temporarily and then increased, while the one at the outer interface of the mould decreased monotonously. Browne and O'Mahoney[9] carried out experiments with different solidification ranges of aluminum alloys. After investigating the effect of alloy solidification ranges, metal static heads, initial die temperatures and interface geometry shapes, they found that the metal static head affected IHTC significantly for long freezing range alloys and initial temperatures also had alloy-dependent effects on IHTC.

By applying the Laplace Transform of the heat conduction equation, Broucayet and Dour[10] estimated the unidirectional heat flux exchanged between plate shape die and aluminium-silicon(AS7G06) casting. Dour[11] developed a heat-transfer gage which used an infrared probe incorporated into a Pyrometric chain. They claimed that the inside die temperature and molten metal surface temperature can be measured accurately without any intrusion into the casting. By this method, Dargusch[12] measured surface die temperature and determined IHTC during high pressure die casting of magnesium alloy AZ91 and Al-9%Si-3%Cu alloy. The results showed that the peak IHTC reached close to 9,000 W/m²K and 8,500 W/m²K for aluminum alloy A380 and magnesium alloy AZ91, respectively.

Hamasaidd[13] measured IHTC peak values in permanent mold casting of aluminum alloys Al-9Si-3Cu(A380) and Al-7Si-0.3Mg(A356) are 3,000 W/m²K and 4,000 W/m²K, respectively. In high pressure die casting process, Guo[7] investigated the IHTC of a step-shape high pressure die casting in magnesium alloy AM50 and aluminum alloy ADC12. The results indicated that the IHTC value increased during initial stage, followed by fluctuation period at the peak values, then dropped abruptly to a lower level. Within the peak value fluctuation period, the maximum IHTC values are 12,900 W/m²K for AM50 and 20,760 W/m²K for ADC12, respectively. In thinner steps, a faster shot velocity led to a higher IHTC peak value. Higher initial die temperatures, lower the IHTC peak values for the thick sections.

Yu[2] studied the IHTC of a cylindrical shape coupon in the squeeze casting of magnesium alloy AM50. When the applied pressure changed from 30 to 90 MPa, the IHTC peak values of the top coupon varied from 8,400 W/m²K to 10,090 W/m²K, and

the IHTC peak values of the side casting varied from 6,900 W/m²K to 7,257 W/m²K, accordingly.

Aweda[14] carried out the experiments on a cylindrical shape squeeze casting of commercially pure aluminum. With the measured temperatures inside a steel die, the die surface temperature was deducted by extrapolating to die-metal interface by polynomial curve fitting technique. The IHTC obtained by extrapolating method under no pressure application was 2,998 W/m²K, which agreed with 2,975 W/m²K obtained from numerical inverse method. He also observed that the effect of applied pressure became more significant at temperature close to the liquidus temperature. Within this temperature range, the measured peak values of IHTC varied from 3,000 W/m²K to 3,400 W/m²K with the applied pressure range from 0 to 85 MPa.

Beck[15,16] proposed the function specification method which can be used for linear or non-linear problems. Briefly, the method was to minimize the sum of squares function with respect to heat flux (q) and the errors between calculated and measured data. It was concluded that the function specification method gave the similar results avoid time-consuming calculation.

However, these studies only focused on castings with simple geometries. Little attention has been paid to variation of casting thicknesses and hydraulic pressures. Actually, in the die casting practice, the different thicknesses at different locations of castings results in significant variation of the local heat transfer coefficients. Therefore, it would be important to investigate the influence of casting thickness, pressure value, and process parameters on the IHTC. In this study, a special 5-step squeeze casting was

designed for understanding casting thickness-dependant IHTC. The temperature measuring units to hold multiple thermocouples simultaneously and the pressure transducers were employed to accurately measure the temperatures and the local pressures during squeeze casting of magnesium alloy AM60.

2. EXPERIMENTS

2.1 STEP CASTING MODEL

Figure 4-1 shows the 3-D model of 5-step casting, which consists of 5 steps(from top to bottom designated as steps 1 to 5) with dimensions of 100x30x3mm, 100x30x5mm, 100x30x8mm, 100x30x12mm, 100x30x20mm accordingly. The molten metal was filled the cavity from the bottom cylindrical shape sleeve with diameter 100 mm.

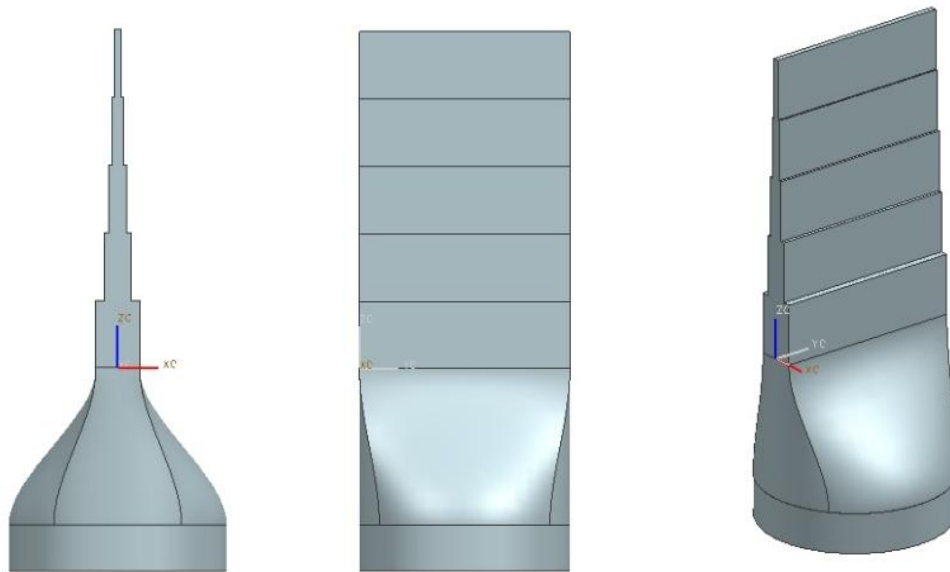


Figure 4- 1. The 3-D model of 5-step casting with the round-shape gating system (A)XZ view; (B) YZ view; (C) isometric view

2.2 CONFIGURATION OF DIE AND INSTALLATION OF MEASUREMENT UNIT

To measure the temperatures and pressures at the casting-die interface accurately and effectively, a special thermocouple holder was developed. It hosted 3 thermocouples simultaneously to ensure accurate placement of thermocouples in desired locations of each step. The thermocouple holders were manufactured using the same material P20 as the die to ensure that the heat transfer process would not be distorted. Figure 4-2 illustrates schematically the configuration of the upper die(left and right parts) mounted on the top ceiling of the press machine. It also reveals the geometric installation of pressure transducers and thermocouple holders. Pressures within the die cavity were measured using Kistler pressure transducers 6175A2 with operating temperature 850⁰C and pressures up to 200 MPa.

As shown in Figure 4-2, pressure transducers and temperature thermocouples were located opposite each other so that measurements from sensors could be directly correlated due to the symmetry of the step casting. Five pressure transducers and temperature measuring units were designated as PT1 through PT5, and TS1 through TS5, respectively. Each unit was inserted into the die and adjusted until the front wall of the sensor approached the cavity surface. The geometry shape of thermocouples holders was purposely designed the same as the pressure transducer, so that they could be exchangeable at different locations.

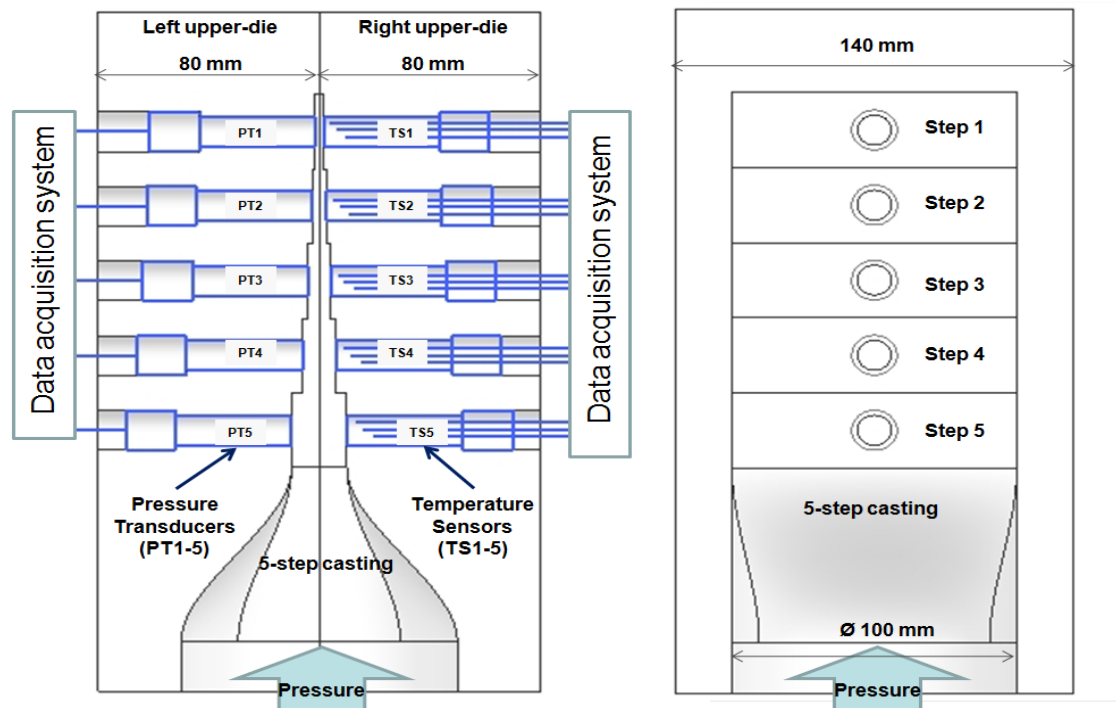


Figure 4- 2. Configuration of upper-dies and geometric installation of thermocouples and pressure transducers

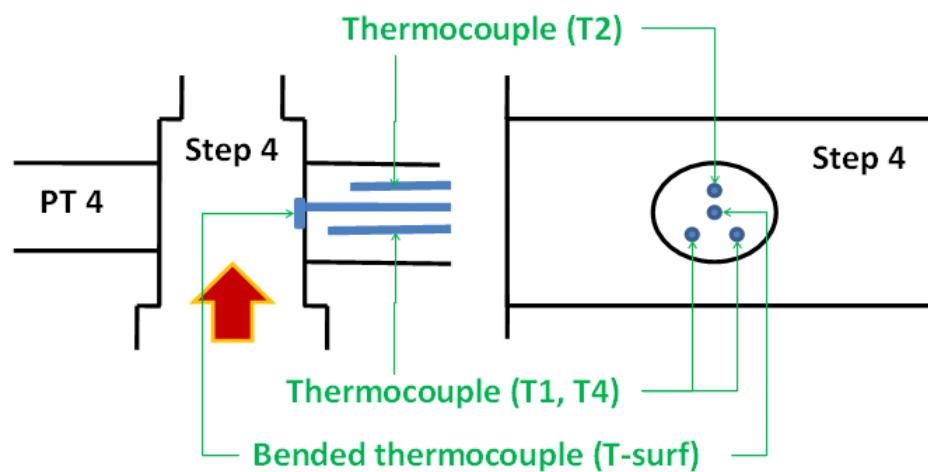


Figure 4- 3. Installation of thermocouples measuring casting surface and inside die temperatures

The thermocouples(Omega KTSS-116U-24) installed inside the die and casting surface were type K with 1/16 inch diameter, stainless steel sheath, ungrounded junction, and 24 inch sheath length. To measure the casting surface temperature, the thermocouples were inserted into the cavity through the center hole of each temperature measuring unit. As shown in Figure 4-3, the thermocouple head was bent down to 90 degree and attached to the die surface tightly. The designed installation method minimized the disturbance of the temperature field in the step casting cavity. On the right part of the die, the thermocouples was installed to measure casting surface(T-surf) and inside die temperatures(T1,T2,T4). To ensure the accuracy, temperature measurements were also carried out simultaneously in both the right and the left parts of the die. During the simultaneous measurements, the bended thermocouple was absent in the left part of the die, but was inserted only in the right part. The difference in the measured temperatures for step 4 between the right and left parts of the die was 1.97°C , which gave the percentage error($(T1L-T1R)/T1L$) of 0.64%. For the thinnest step 1, the temperature difference is 4.82°C and the percentage error is 2.77%. Thus, using bended thermocouples in the cavity to measure the surface casting temperature caused almost no interference on the temperature field in the casting and heat transfer inside the die. This thermocouple head bending method enables to acquire relatively accurate data of the casting surface temperature.

2.3 CASTING PROCESS

The integrated casting system consisted of a 75 tons laboratory hydraulic press, a two halves split upper die forming a 5-step cavity, one cylindrical sleeve lower die, an

electric resistance furnace and a data acquisition system. The 75- ton heavy duty hydraulic press made by Technical Machine Products (TMP, Cleveland, Ohio, USA) used in the experimental study. The die material was P20 steel. Commercial magnesium alloy AM60 was used in experiment. The chemical composition of AM60 is shown in Table 4-1. Table 4-2 gives the thermal properties of the related materials in this study. Based on Yu[2]'s work, the thermal conductivity(K) of AM60 has the linear relationship with its temperature and follows equations($K=192.8-0.187T$) in semisolid temperature range($540-615^{\circ}\text{C}$); ($K=0.0577T+60.85$) below the solidus temperature($<540^{\circ}\text{C}$), and ($K=0.029T+59.78$) for the liquid temperature range($>615^{\circ}\text{C}$).

Table 4- 1. Chemical composition of magnesium alloy AM60

Mg	Al(%)	Mn(%)	Si(%)	Cu(%)	Zn(%)
balance	5.5-6.5	0.13	0.5	0.35	0.22

Table 4- 2. Thermophysical properties of magnesium alloy AM60

Properties	Mg Alloy AM60	
	Solid	Liquid
Thermal Conductivity (W/m K)	62	90
Specific Heat (J/kg K)	1020	1180
Density (kg/m^3)	1790	1730
Latent Heat (KJ/kg)	373	
Liquidus Temperature at 0MPa ($^{\circ}\text{C}$)	615	
Solidus Temperature at 0MPa ($^{\circ}\text{C}$)		540

Before the pouring, the dies were pre-heated to 210°C using four heating cartridges installed inside the dies. The experimental procedure included pouring molten magnesium alloy AM60 into the bottom sleeve with a pouring temperature 720°C , closing the dies, cavity filling, squeezing solidification with the applied pressure,

lowering the sleeve die, splitting the two parts of the upper die, Finally the 5-step casting can be shaken out from the cavity. The temperatures inside the die and casting were measured by Omega KTSS-116U thermocouples with response time below 10 ms. Real-time in-cavity local pressures and temperature data were recorded by a LabVIEW- based data acquisition system.



Figure 4- 4. 5-step castings solidifying under applied pressure 30, 60, and 90MPa.

The mold coating used in step castings is Boron Nitride lubrication(Type S_f) which was sprayed manually onto the surface of the mold cavity before heating the dies to the initial temperature. To minimize the thermal barrier effect of mold coating, the coating thickness applied in this study was relatively thin(below 50um). As shown in Figure 4-4, totally 15 castings were poured with 30, 60 and 90MPa pressurized

solidification. The chill vent and all five steps were filled completely. X-ray radiography examination reveals the soundness of the step castings.

3. MATHEMATICAL MODELING OF IHTC

Based on the principle of heat transfer, the interfacial heat transfer coefficient(IHTC) between metal and die surface can be determined by Equation 4-1:

$$h(t) = \frac{q(t)}{T_{cs} - T_{ds}} \quad (4-1)$$

where h is IHTC; q is heat flux at the metal-die interface; T_{cs} and T_{ds} are the casting surface temperature and die surface temperature, respectively; and t is the solidification time. With the known boundary conditions in the form of temperatures or the heat fluxes, the temperature field inside the die or casting can be obtained by direct heat conduction method. But the values of T_{cs} and T_{ds} can not be measured directly because the insertion of thermocouples of finite mass at the interface may distort the temperature field at the interface. Further, the heat flow at the interface may not be unidirectional due to complex geometry shape. Therefore, determination of IHTC using measurements of T_{cs} , T_{ds} , and $q(t)$ directly is difficult. As a result, inverse heat conduction method needs to be employed to determine the IHTC based on the temperatures measured inside the die or casting. To solve the direct heat conduction and inverse heat conduction problems, the numerical or analytical method needs to be employed.

From the measured interior temperature histories, the transient metal-die interface heat flux and temperature distribution were estimated by two different techniques in this work: (1)polynomial extrapolation; and(2)inverse algorithm using function specification model, coupling with implicit finite difference method(FDM).

3.1 INVERSE METHOD

Because solidification of squeeze casting of magnesium alloy involves phase change and its thermal properties are temperature-dependent, the inverse heat conduction is a non-linear problem. To evaluate the IHTC effectively as a function of solidification time in the squeeze casting process, the finite difference method(FDM) was employed based on the Beck's algorithm.

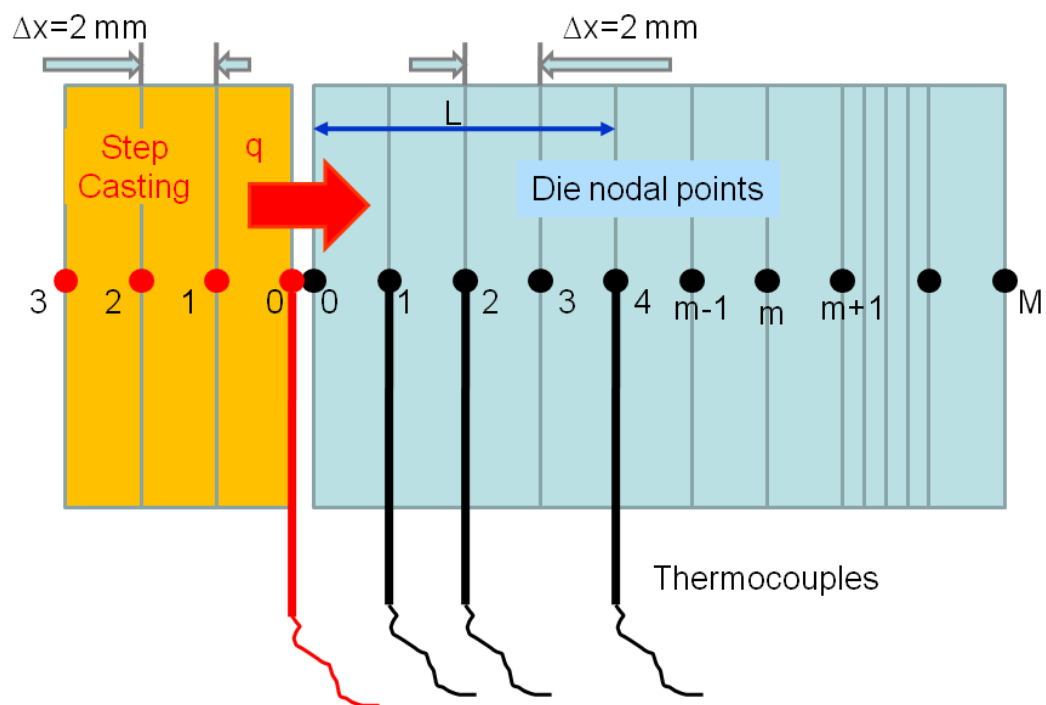


Figure 4- 5. One-dimensional heat transfer at the interface between the casting and die, where temperature measurements were performed.

Since the thickness of each step was much smaller than the width or length of the step, it can be assumed that the heat transfer at each step was one-dimensional. The heat transfer across the nodal points of the step casting and die is shown in Figure 4-5. The temperatures were measured at 2, 4, 8 mm beneath die surface and the heat flux

transferred to the die mould can be evaluated by the inverse method. Then, the temperatures at different locations were calculated by the direct model. Compared to the actual temperatures measured, the calculated errors at all locations were evaluated, which were less than 10⁰C.

The heat flux for both the casting and die interface can be calculated from the temperature gradient at the surface and sub-surface nodes by Equation 4-2:

$$q(t) = -k \frac{dT}{dx} = -k \frac{T_m^t - T_{m-1}^t}{\Delta x} \quad (4-2)$$

where k is thermal conductivity of the casting or die materials; T_m^t is the temperature value on time t at the nodal point m . With the heat flux value, the segregated IHTC value can be evaluated from Equation 1.

3.1.1 Heat transfer inside the die

The heat transfer inside the die at each step is transient conduction through one-dimensional steps which can be described by Equation 4-3:

$$\rho c(T) \frac{\partial T(x, t)}{\partial t} = \frac{\partial}{\partial x} \left(k(T) \frac{\partial T(x, t)}{\partial x} \right) \quad (4-3)$$

where ρ is density of conducting die, T is the temperature, t is the time and x is the distance from the die surface to the node point; $c(T)$, $k(T)$ are specific heat capacity and thermal conductivity of the die changed with temperature, respectively.

The initial and boundary conditions were described by the following Equations 4-4a to 4-4c:

$$T(x, 0) = T_i(x) \quad (4-4a)$$

$$q(0,t) = -k(T) \frac{\partial T}{\partial x} \Big|_{x=0} \quad (4-4b)$$

$$T(L,t) = Y(L,t) \quad (4-4c)$$

where T_i is the initial temperature of the die; q is the heat flux at the casting-die interface; L is the distance from the last temperature measurement point to the die surface; Y is the measured temperature at distance L from die surface. The measured region ($0 \leq x \leq L$) in the die is divided into M equal size meshes ($L=M\Delta x$), and n subscripts are used to designate the x location of the discrete nodal point. With the proper time step (Δt), the time can also be discretized as $t=p\Delta t$. Thus, the finite differential format to the time derivatives of Equation 4-3 can be expressed as Equation 4-5.

$$\frac{\partial T}{\partial t} \Big|_m \approx \frac{T_m^{p+1} - T_m^p}{\Delta t} \quad (4-5)$$

The superscript p was used to denote the time dependence of T . The subscript m means the number of the discrete nodal points. The implicit form of a finite difference method was applied to solve Equation 4-3. For the surface node of the die, Equation 3 can be rearranged as Equation 4-6a:

$$(1 + 2F_0)T_0^{p+1} - 2F_0T_1^{p+1} = 2F_0 \frac{\Delta x}{k} q_0 + T_0^p \quad (4-6a)$$

For any interior node of the die, Equation 4-3 can be solved as Equation 4-6b:

$$(1 + 2F_0)T_m^{p+1} - F_0(T_{m-1}^{p+1} + T_{m+1}^{p+1}) = T_m^p \quad (4-6b)$$

where F_0 is a finite different form of the Fourier number:

$$F_0 = \frac{\alpha \Delta t}{(\Delta x)^2} = \frac{k}{c\rho} \frac{\Delta t}{(\Delta x)^2} \quad (4-6c)$$

The heat flux at the casting-die interface(q) at each time step can be obtained by the Beck's function specification method. At the first time step, a suitable initial value of heat flux q was assumed which was maintained constant for a definite integer number($u=2-5$) of the subsequent future time steps. According to Equations 4-6(a), 4-6(b), and 4-6(c), with the measured initial die temperature($p=0$), the temperature distribution at each node of the next time step was calculated with this assumed q . The assumed heat flux value was changed by a small value(εq) where ε was a small fraction and the new temperature distribution value corresponding to $(q+\varepsilon q)$ was determined accordingly. Thus, the sensitivity coefficient(X) can be calculated by Equation 4-7. To minimize the calculation error, the calculated temperatures were compared with measured temperature at the same position, and the assumed heat flux(q) was corrected by the Equation 4-8. The corrected heat flux of the same time step was obtained by Equation 4-9:

$$X^{p+j-1} = \frac{\partial T}{\partial q} = \frac{T_{est}^{p+j-1}(q^p + \varepsilon q^p) - T_{est}^{p+j-1}(q^p)}{\varepsilon q^p} \quad (4-7)$$

$$\Delta q^p = \frac{\sum_{j=1}^u (Y_{mea}^{p+j-1} - T_{est}^{p+j-1}) X^{p+j-1}}{\sum_{j=1}^u (X^{p+j-1})^2} \quad (4-8)$$

$$q_{corr}^p = q^p + \Delta q^p \quad (4-9)$$

where $T_{est}(q)$ was estimated temperatures on p time step at the measuring node points inside die with a boundary constant heat flux q ; Y_{mea} was measured temperatures at the same measuring node points. The corrected heat flux and the new temperature

distribution were used as initial value for next cycle of calculation. The calculation process was repeated until the following condition given by Equation 4-10 was satisfied:

$$\frac{\Delta q^p}{q^p} \leq \varepsilon \quad (4-10)$$

Therefore, for all time steps, the surface heat flux and die surface temperature were determined according to the above procedures.

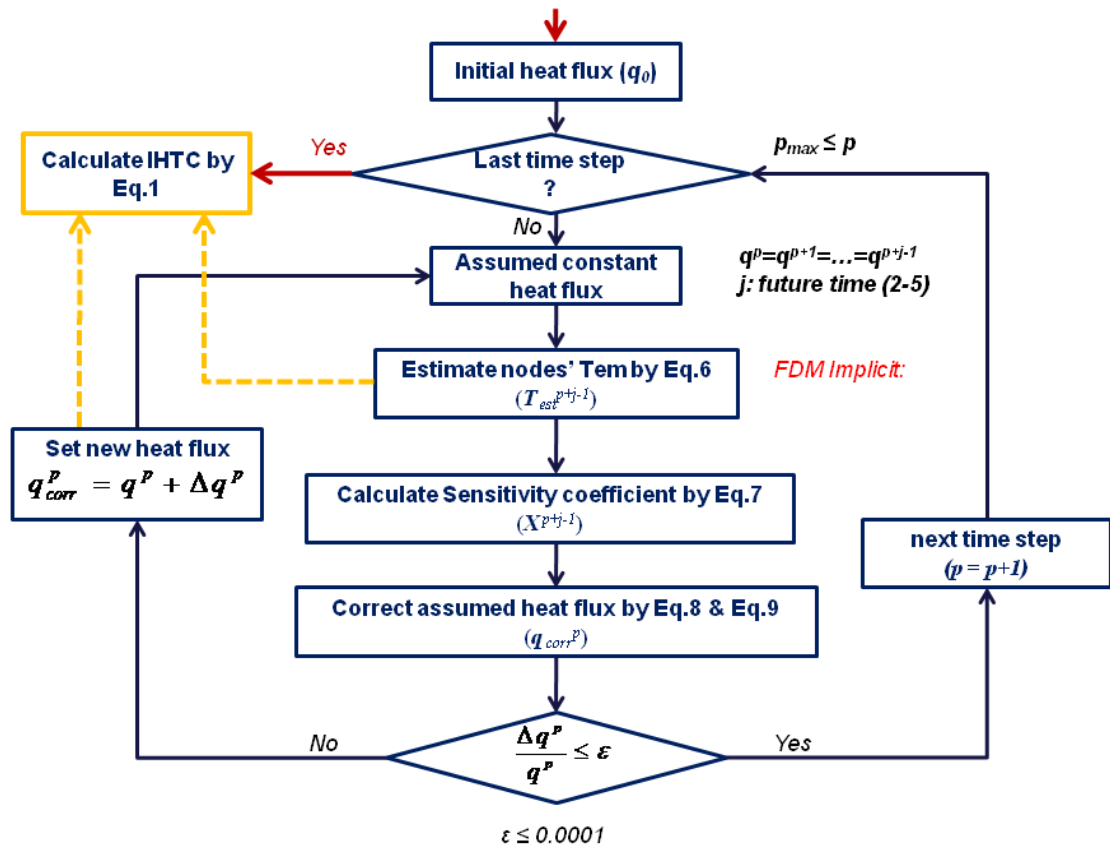


Figure 4- 6. Flow chart showing an algorithm for the determination of IHTC at the casting-die interface

The flow chart shown in Figure 4-6 gives an overview of the solution procedure. The j in Equation 4-7 is the integer subsequent future time steps ($j=1, 2, \dots, u$) and j should not be bigger than u (a definite integer number). The inverse modeling is to calculate heat flux (q) using the present temperatures and the future temperatures. The future temperatures are the calculated temperatures at time steps greater than the present time steps estimated using the known boundary condition $T(L,t)=T_1, T_4$ and the assumed constant heat flux ($q^p=q^{p+1}=\dots=q^{p+j-1}$), which set some future q^{p+1} is equal to q^{p+j-1} . But p is the present time steps for all nodal points. Only after the calculated heat flux satisfied Equation 4-10, the present time can go to next step ($p=p+1$).

3.1.2 Heat transfer inside the casting

To evaluate the IHTC, the temperatures inside the casting, especially the surface temperatures need to be estimated. Due to phase change of the casting, the heat source term related with the latent heat of solidification must be added to Equation 4-3. The heat transfer equation can be rewritten as Equation 4-11:

$$\rho c(T) \frac{\partial T(x,t)}{\partial t} = \frac{\partial}{\partial x} \left(k(T) \frac{\partial T(x,t)}{\partial x} \right) + S_l \quad (4-11)$$

where

$$S_l = \rho l \frac{\partial f_s}{\partial t} \quad (4-12)$$

where l is the latent heat of fusion and f_s is the solid fraction in the casting. Substitution of Equation 4-12 into Equation 4-11 led to the formation of Equation 4-13:

$$\rho \left[c(T) - l \frac{\partial f_s}{\partial T} \right] \frac{\partial T(x,t)}{\partial t} = \frac{\partial}{\partial x} \left(k(T) \frac{\partial T(x,t)}{\partial x} \right) \quad (4-13)$$

The term $\partial f_s / \partial T$ can be calculated at each step of the casting by its solidification curve. With the measured temperature data inside the step casting, the temperature profile on the surface of the step casting can be determined by applying Equations 4-6(a) through 4-6(c) given in the previous section.

3.2 POLYNOMIAL CURVE FITTING METHOD

Beneath the die surface, as Figure 4-5 shown, thermocouples were positioned at $X1 = 2\text{mm}$, $X2 = 4\text{mm}$, $X3 = 6\text{mm}$, and $X4 = 8\text{mm}$ away from the die surface. From the temperature versus time curves obtained at each position inside the die, the temperature at the die surface ($X0 = 0\text{mm}$) can be extrapolated by using polynomial curve fitting method.

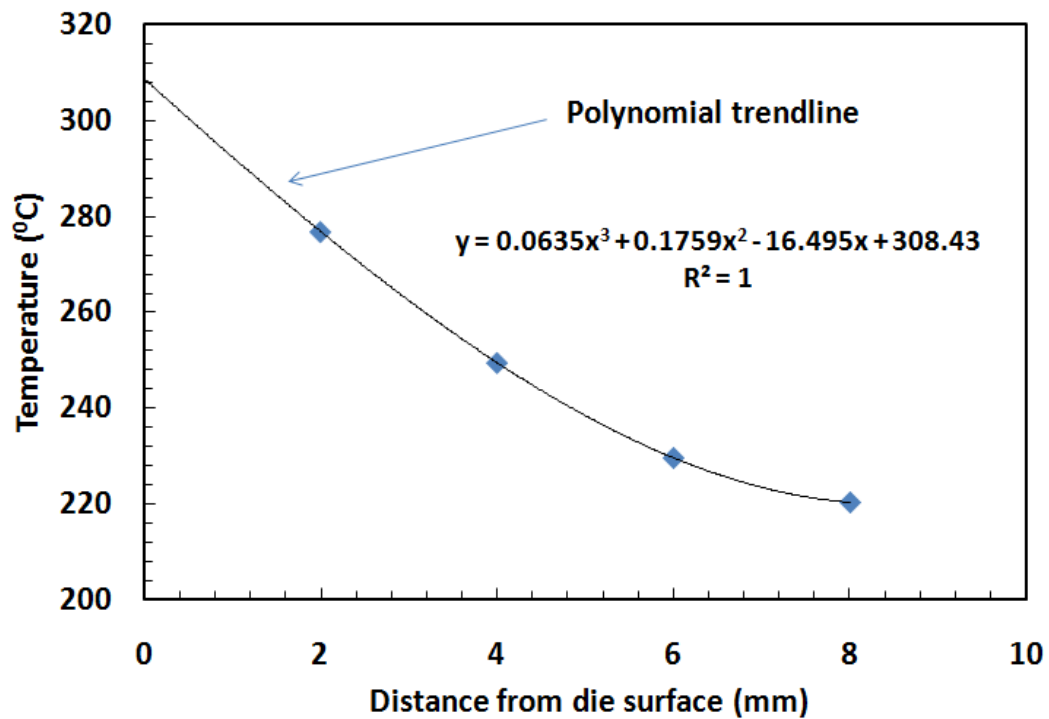


Figure 4- 7. Polynomial curve with various measured temperatures at a time of 4.1 seconds of solidification process.

After the completion of filling, by selecting a particular time of solidification process, for example $t = 4.1 \text{ seconds}$, the values of temperatures were read from the temperature-time data at position X1, X2, X3, and X4. Figure 4-7 shows the calculated temperatures against distance X which were fitted and extrapolated by a polynomial trendline. The temperature at the die surface ($T_0 = 308.43^\circ\text{C}$, $t = 4.1\text{s}$) was determined by substituting the value of $X=0$ in the polynomial curve fitting Equation 4-14 obtained from the temperature values at various distances inside the die at a chosen time of 4.1 seconds.

$$y = 0.0635x^3 + 0.1759x^2 - 16.495x + 308.43 \quad (4-14)$$

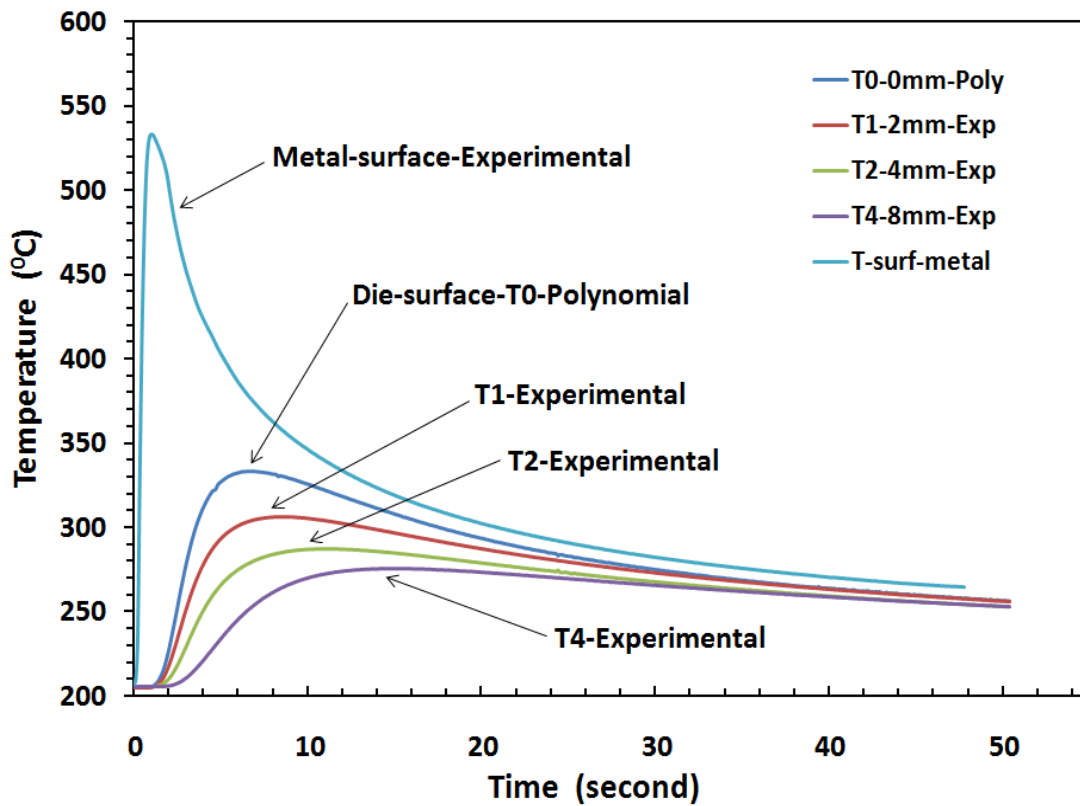


Figure 4- 8. Typical temperature versus time curves (Step 4, 30 MPa) at metal surface, die surface, and various positions inside the die.

This procedure was repeated for a number of time increments to get series of such temperatures with corresponding times. The extrapolated temperature curve versus time was drawn at die surface($X_0 = 0\text{mm}$) as “Die-surface-T0-polynomial” in Figure 4-8, which indicated the dynamic temperature change at the metal-die interface.

4. RESULTS AND DISCUSSION

4.1 HEAT FLUX(Q) & IHTC(H) CURVES

Figure 4-8 shows typical temperatures versus time curves at the metal-die interface of Step 4 for solidifying magnesium alloy AM60 and steel die respectively with an applied hydraulic pressure of 30 MPa. The following analysis was also based on this typical data at Step 4 with pressure 30 MPa. This information includes measurements of the casting surface temperature in addition to temperature measurements obtained at different depths under the die surface. Since molten metal filled the cavity from the bottom, pre-solidification occurred upon the completion of cavity filling. No die surface temperatures exceeded 340°C , and the highest temperature of the casting surface was 532.97°C .

Figure 4-9 shows the comparison of calculated temperatures at the die surface(T_0) by the inverse method and the extrapolated fitting method. The curves obtained by these two methods are in relatively poor agreement and their deviation values ranges from 0.46 to 57°C , which was indicated by temperature difference(Inv-Poly) curve in Figure 4-9. The peak temperature value(321.61°C) obtained by extrapolated fitting method was found to be lower than that temperature(327.97°C) estimated by the inverse

method. Compared to inverse method, the temperature estimated by the extrapolated fitting method reached its peak point 1.8 second later.

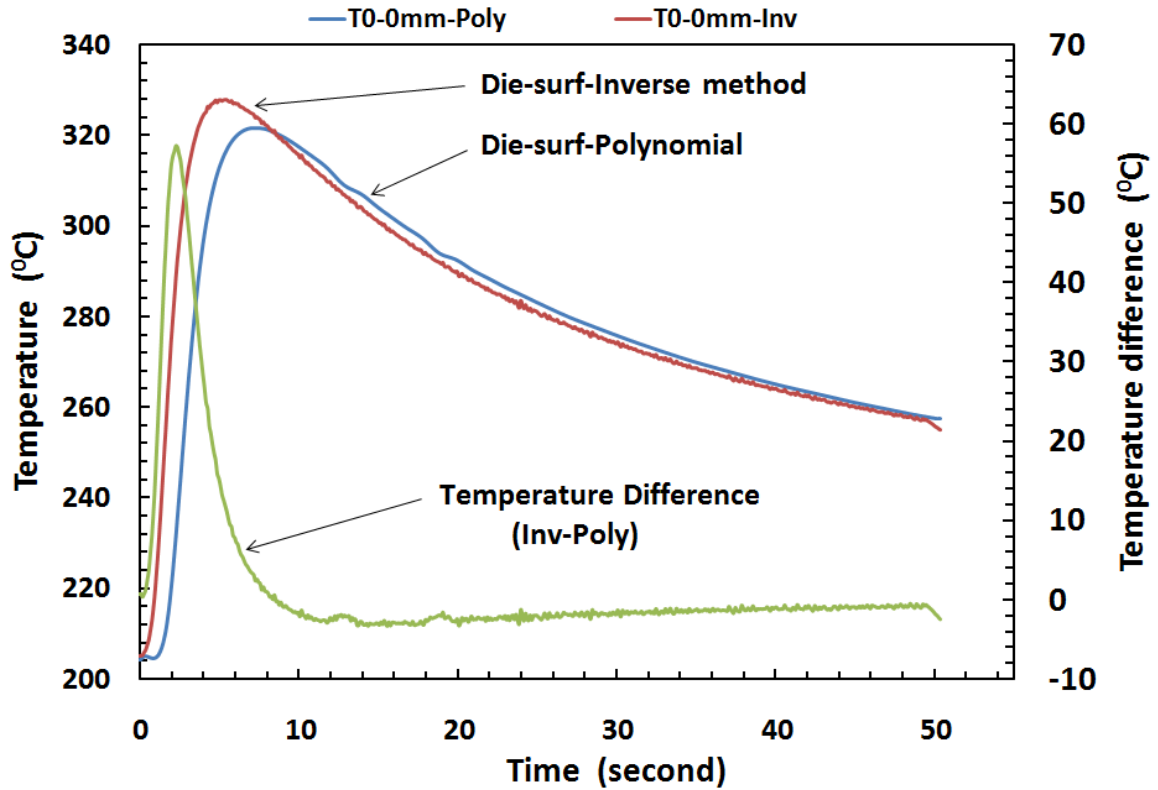


Figure 4- 9. Comparison of calculated temperature curve at the die surface by the inverse method and the extrapolated fitting method

Inserting the estimated die surface temperature(T_0) and the measured temperature at $T_1=2\text{mm}$ into Equation 4-6, the interfacial heat flux(q) was calculated. Figure 4-10 shows the interfacial heat flux(q) and the heat transfer coefficient(IHTC) versus solidification time estimated by extrapolated fitting method and inverse method, based on the data in Figure 4-8. By extrapolated fitting method, the peak heat flux value was $3.31\text{E}+05 \text{ W/m}^2$, and the peak value of IHTC was $6450 \text{ W/ m}^2\text{K}$. By the inverse method,

the peak heat flux value was $7.38\text{E}+05 \text{ W/m}^2$, and the peak value of IHTC was $6005 \text{ W/m}^2\text{K}$. From Figure 4-10, it can be observed that the heat flux and IHTC of inverse method curves reached to their peak value faster than those of extrapolated fitting method. The inverse method resulted in a high peak heat flux value and a low peak heat transfer coefficient compared with the extrapolated fitting method.

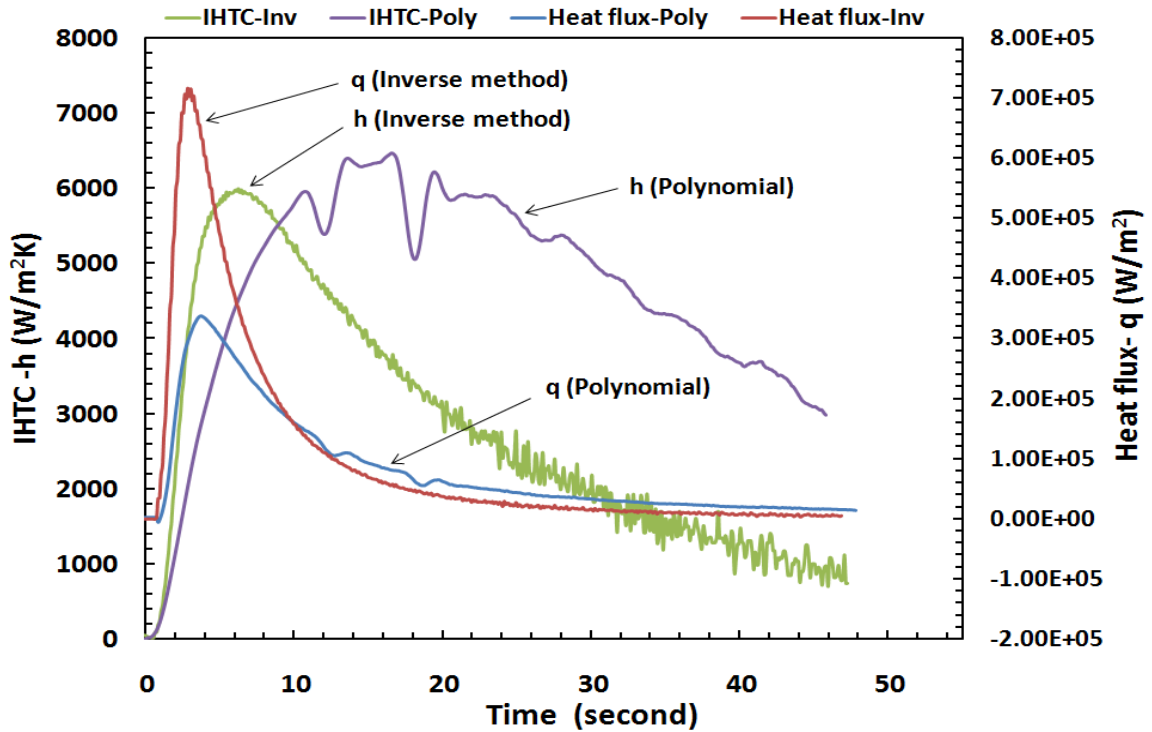


Figure 4- 10. The interfacial heat flux(q) and the heat transfer coefficient (IHTC) curves estimated by extrapolated fitting method and inverse method

4.2 ACCURACY VERIFICATION

The accuracy of IHTC evaluation by the inverse method and extrapolated fitting method was analyzed based on the residual error between the evaluated temperatures and the actual measured temperatures at various locations. With the die surface temperature

and heat flux evaluated by two methods as a boundary condition, direct heat transfer modeling was applied to Equations 4-6(a) to 4-6(c) and recalculated the temperature distribution at different locations($X_2 = 4\text{mm}$, $X_3 = 6\text{mm}$, $X_4 = 8\text{mm}$) inside the die.

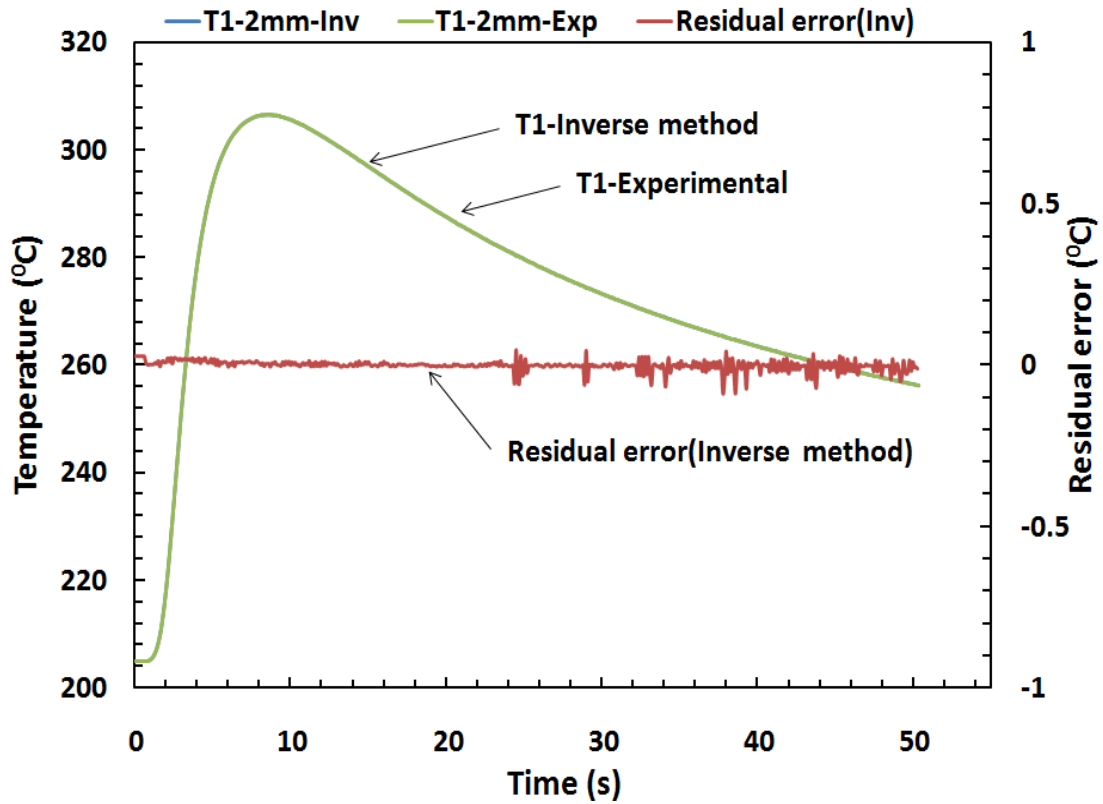


Figure 4- 11. The residual error of temperatures evaluated by the inverse method at the position $X_1=2\text{mm}$.

From Figure 4-11, the residual error of temperatures evaluated by the inverse method was less than 0.2°C at the position $X_1 = 2\text{mm}$. Since the extrapolated fitting method needs to take the measured temperature at X_1 as the initial input data, the residual error could not be evaluated.

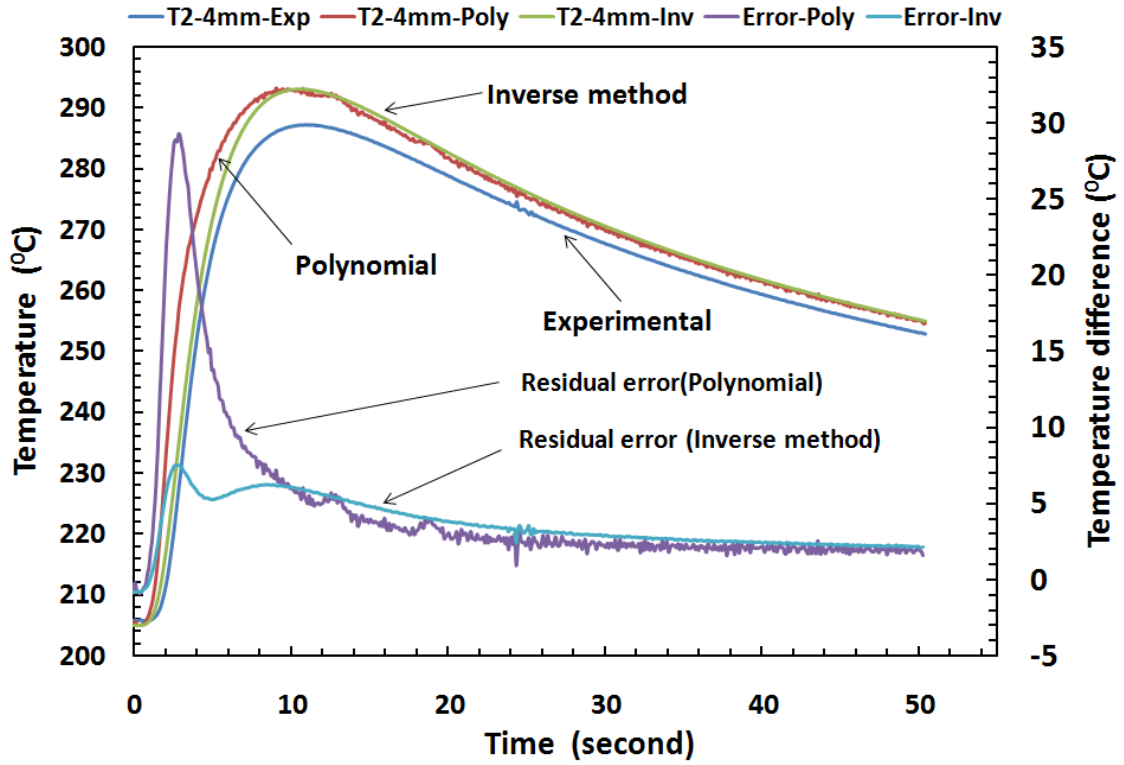


Figure 4- 12. The residual error between the evaluated temperatures and the actual measured temperatures at X2=4mm beneath the die surface.

As shown in Figures 4-12 to 4-14, the residual error of temperature evaluated by the inverse method was below 7.4°C at the position X2=4mm, while that residual error achieved 14.9°C evaluated by the extrapolated fitting method. The residual error of temperature evaluated by the inverse method was less than 3.3°C at the position X3=6mm, and that residual error increased to 33.2°C when evaluated by the extrapolated fitting method. At the position X4=8mm, the residual error of temperature evaluated by the inverse method was below 0.7°C . But that residual error was as high as 55.2°C when the extrapolated fitting method was employed.

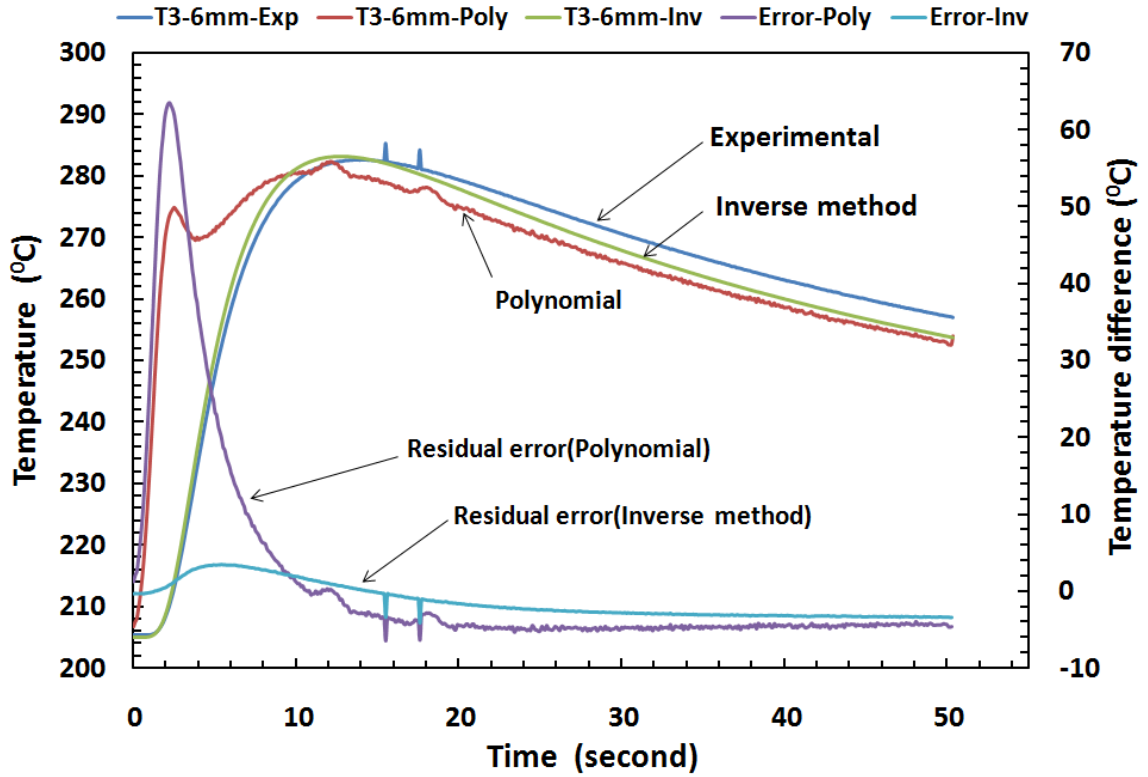


Figure 4- 13. The residual error between the evaluated temperatures and the actual measured temperatures at X3=6mm beneath the die surface.

For the inverse method, the residual error of temperature at X1 and X4 was less than one degree, which indicates that the thermal history was estimated accurately by the inverse method. For the extrapolated fitting method, the residual error increased from 14.9°C to 55.2°C with the depth below the die from 4mm to 8mm. Thereafter, the heat flux(q) and IHTC calculated by the extrapolated fitting method could not accurately represent the actual heat transfer at the metal-die interface.

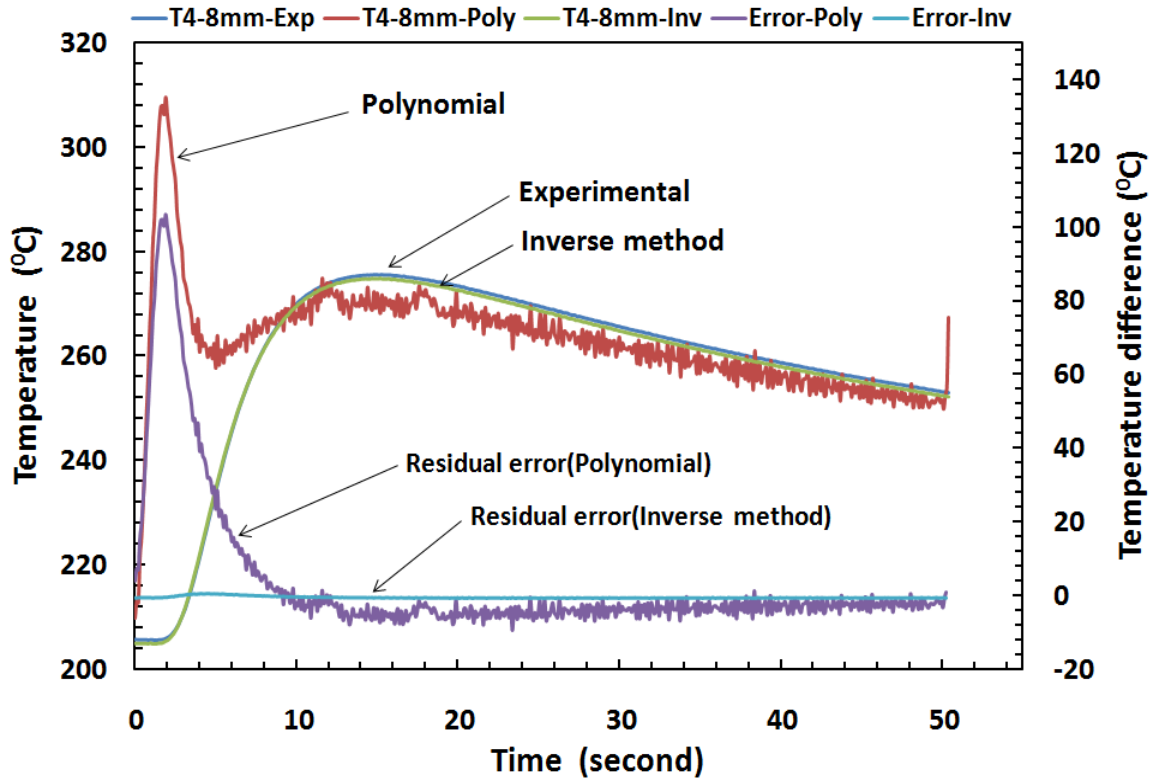


Figure 4- 14. The residual error between the evaluated temperatures and the actual measured temperatures at X4=8mm beneath the die surface.

Figure 4-15 shows that the heat transfer coefficient(IHTC) curves of 5 steps estimated by inverse method. For all steps, IHTC began with increasing stage and reached their peak value, then dropped gradually until the value became a low level. From steps 1, 2, 3, 4, to 5 with 30MPa pressure, the peak IHTC values varied from 2807W/m²K, 2962W/m²K, 3874W/m²K, 6005W/m²K to 7195W/m²K, indicating that the closer contact between the casting and die surface at thicker steps. Therefore, the wall thickness affected IHTC peak values significantly. The peak IHTC value decreased as the step became thinner. For the steps 1, 2, 3, 4 and 5, it took 4.1, 4.2, 4.7, 6.1, and 8.2

seconds to reach their peak values, respectively. Beside the different peak values, the time for IHTC to obtain the peak value during initial stage increased as the step became thicker. Thicker step spent longer time to reach its peak IHTC value and its IHTC curve dropped slower to a low level as well.

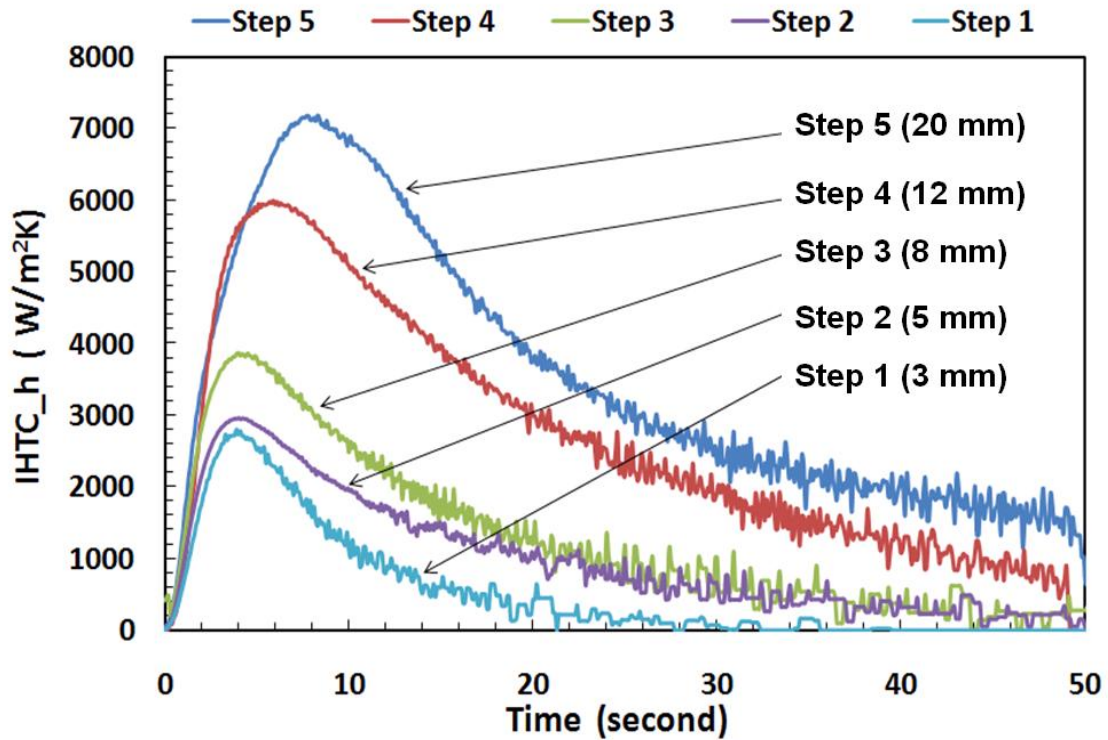


Figure 4- 15. The heat transfer coefficient(IHTC) curves of 5 steps estimated by inverse method with applied pressure 30 MPa.

Figure 4-16 shows the IHTC peak values at step 1 through 5 with applied pressure 30, 60 and 90MPa. Similar characteristics of IHTC peak values can be observed at 30, 60 and 90MPa applied pressures. With applied pressure 60MPa, the peak IHTC values at steps 1, 2, 3, 4, and 5 (section thickness 3, 5, 8, 12, and 20 mm) varied from 4662 W/m²K, 5001 W/m²K, 5629 W/m²K, 7871 W/m²K and 8306 W/m²K. With applied

pressure 90MPa, the peak IHTC values varied from 5623 W/m²K, 5878 W/m²K, 6783 W/m²K, 9418 W/m²K and 10649 W/m²K. With the applied pressure increased, the IHTC peak value of each step was increased accordingly. It can be observed that the peak IHTC value and heat flux increased as the step became thick. The large difference in temperatures between the melt and the die with thick cavity section as well as relatively high localized pressure should be responsible for the high peak IHTC values observed at the thick steps.

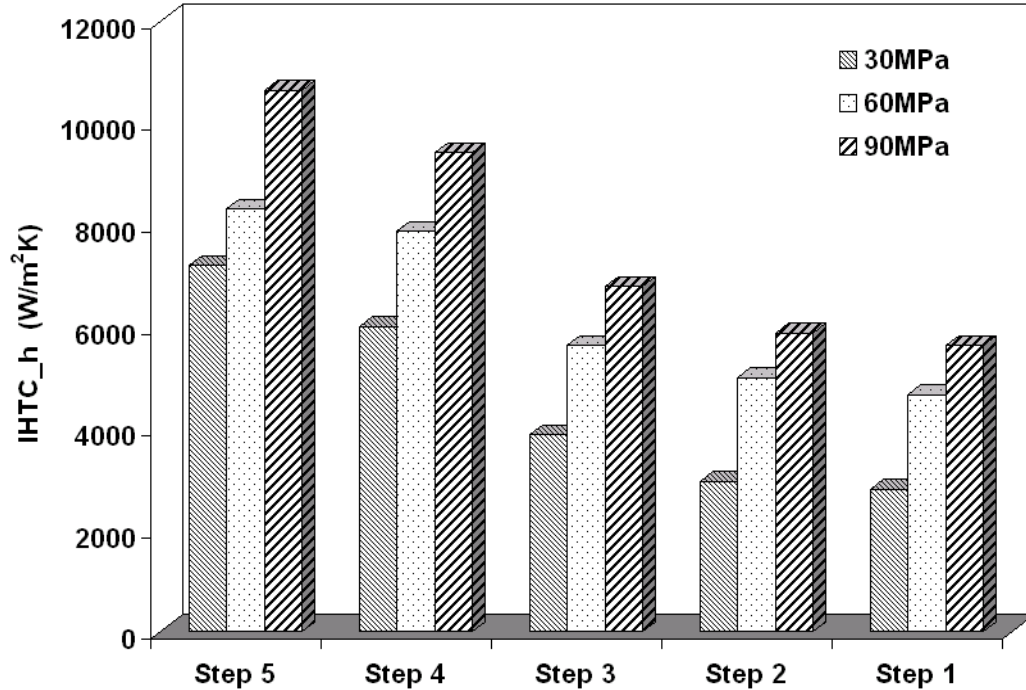


Figure 4- 16. The peak IHTC values of 5 steps estimated by inverse method with applied pressure 30, 60 and 90MPa.

5. CONCLUSIONS

The heat flux and IHTC at metal-die interface in squeeze casting were successfully determined based on the numerical inverse method and extrapolated fitting method.

For the inverse method, a solution algorithm has been developed based on the function specification method to solve the inverse heat conduction equations.

The IHTC curve increased and reached its peak value, then dropped gradually. For applied pressure 30MPa, the peak IHTC values at steps 1, 2, 3, 4, and 5 (section thickness 3, 5, 8, 12, and 20 mm) varied from 2807W/m²K, 2962W/m²K, 3874W/m²K, 6005W/m²K to 7195W/m²K. With applied pressure 60MPa, the peak IHTC values varied from 4662 W/m²K, 5001 W/m²K, 5629 W/m²K, 7871 W/m²K and 8306W/m²K. With applied pressure 90MPa, the peak IHTC values varied from 5623 W/m²K, 5878 W/m²K, 6783 W/m²K, 9418 W/m²K and 10649W/m²K. The peak IHTC value decreased as the step became thinner. With the applied pressure increased, the IHTC peak value of each step was increased accordingly.

For the steps 1, 2, 3, 4 and 5, it took 4.1, 4.2, 4.7, 6.1, and 8.2 seconds to reach their peak values, respectively. Beside the different peak values, the time for IHTC to obtain the peak value during initial stage increased as the step became thicker.

To verify estimation results, temperature distribution inside the die was recalculated by the direct modeling based on the estimated heat flux(q). After comparison with experimental data, the result showed that the heat flux and IHTC evaluated by the inverse method were more accurately than those of the extrapolated fitting method.

REFERENCES

- [1] I. Cho, C. Hong, 1996. Evaluation of heat-transfer coefficients at the casting/die interface in squeeze casting. *Int. J. Cast Metals Res.* Vol.9, 227-232.
- [2] A. Yu, 2007. Mathematical Modeling and experimental study of squeeze casting of magnesium alloy AM50A and aluminum alloy A356. Ph.D. dissertation, Dept. of Mechanical, Automotive & Materials Engineering, University of Windsor.
- [3] R. Rajaraman, R. Velraj, 2008. Comparison of interfacial heat transfer coefficient estimated by two different techniques during solidification of cylindrical aluminum alloy casting. *Heat Mass Transfer*, Vol.44, p1025-1034
- [4] J. Su, F. Geoffrey, 2004. Inverse heat conduction problem of estimating time varying heat transfer coefficients. *Numer Heat Transf Part A.* Vol.45, p777-789
- [5] D. Sui, Z. Cui, 2008. Regularized determination of interfacial heat transfer coefficient during ZL102 solidification process. *Transactions of Nonferrous Metals Society of China.* Vol.18, p399-404
- [6] J. Taler, W. Zima, 1999. Solution of inverse heat conduction problems using control volume approach. *Int. J. Heat Mass Transf.* Vol.42, p1123-1140
- [7] Z. Guo, S. Xiong, B. Liu, M. Li, J. Allison, 2008. Effect of Process Parameters, Casting Thickness, and Alloys on the Interfacial Heat-transfer Coefficient in the High-pressure Die Casting Process. *Metall. and Mater. Trans.* Vol.39A, p2896-2905.
- [8] T. Kim, Z. Lee, 1997. Time-varying heat transfer coefficients between tube-shaped casting and metal mold. *Int. J. Heat Mass Transf.* Vol.40, p3513-3525

- [9] D. Browne, D. O'Mahoney, 2001. Interface heat transfer in investment casting of aluminum. *Metall. and Mater. Trans. A*, 32A, p3055-3063
- [10] S. Broucaret, A. Michrafy, G. Dour, 2001. Heat transfer and thermo-mechanical stresses in a gravity casting die influence of process parameters. *J. Mater. Process. Technol.* vol.110, p211-217
- [11] G. Dour, M. Dargusch, C. Davidson, and A. Nef, 2005. Development of a non-intrusive heat transfer coefficient gauge and its application to high pressure die casting. *J. Mater. Process. Technol.* vol.169, p223-233.
- [12] M. Dargusch, A. Hamasaiid, G. Dour, T. Loulou, C. Davidson, and D. StJohn, 2007. The accurate determination of heat transfer coefficient and its evolution with time during high pressure die casting of Al-9%Si-3%Cu and Mg-9%Al-1%Zn alloys. *Advanced Engineering Materials*. vol.9, No.11, p995-999
- [13] A. Hamasaiid, M. Dargusch, C. Davidson, S. Tovar, T. Loulou, F. Rezai-aria, and G. Dour, 2007. Effect of mold coating materials and thickness on heat transfer in permanent mold casting of aluminum alloys. *Metall. and Mater. Trans. A*, Vol.38A, p1303-1316
- [14] J. Aweda, M. Adeyemi, 2009. Experimental determination of heat transfer coefficients during squeeze casting of aluminum. *J. Mater. Process. Technol.* vol.209, p1477-1483
- [15] J. Beck, 1970. Nonlinear estimation applied to the nonlinear inverse heat conduction problem. *Int. J. Heat Mass Transfer*, Vol.13, 703-715

- [16] J. Beck, B. Blackwell, A. Haji-sheikh, 1996. Comparison of some inverse heat conduction methods using experimental data. *Int. J. Heat Mass Transfer*. Vol.39, 3649-3657.

CHAPTER 5

SECTION THICKNESS-DEPENDANT INTERFACIAL HEAT TRANSFER IN SQUEEZE CASTING OF ALUMINUM ALLOY A443

1.INTRODUCTION

The heat transfer coefficient at casting-die interface is the most important factor influencing the solidification process. The accuracy of a solidification simulation depends on the precise determination of interfacial heat transfer coefficients between the casting and die. The complexity of heat transfer in solidification of a casting is often present at the casting/mold interface. Modeling of the interfacial heat transfer coefficient(IHTC) is very challenging due to a number of factors, such as air gap, casting geometry, alloy characteristics, mold material, coating, preheat temperature, and other process parameters. During the squeeze casting process, the applied pressures, mold conditions, alloy characteristics and processing parameters are considered to influence the IHTC strongly at the casting/mold interface[1]. Compared to other conventional casting processes, the most attractive features of squeeze casting are slow filling velocities and the pressurized solidification. Before the solid fraction of the casting becomes high enough, the applied high pressure squeezes liquid metal into the air or shrinkage porosities effectively. Therefore, squeeze casting can make castings virtually free of porosity and usually have excellent as-cast quality, and are heat treatable, which is difficult to achieve with other conventional high pressure casting processes[2].

Cho and Hong[3] used aluminum alloy Al-4.5%Cu to measure IHTC for a squeeze casting process. They reported IHTC values of about 1000 W/m²K prior to

pressurization which rapidly increased to around 4700 W/m²K at a pressure of about 50MPa for a cylindrical casting in a steel mold. Krishnan and Sharma[4] measured IHTC between a cast iron chill and aluminum alloy Al-11.5%Si. The inverse method was applied on both sides of the interface. Their work yielded a time-dependent IHTC which varied over a range of 200 to 2000 W/m²K. Reasonable agreement was found between their results and IHTC values obtained from previous air gap measurements. Krishna[5] simulated the IHTC for an indirect squeeze casting process for aluminum alloy A356. They computed temperature histories in the die and casting with varied IHTC values and corrected IHTC by minimizing the errors between measured and calculated values. The IHTC estimated values were found to be close to those observed by Cho and Hong[3]. The authors concluded that there was a critical value of squeeze pressure beyond which the heat transfer was not significantly improved. Chattopadhyay[6] simulated the squeeze casting process numerically on A-356 with variable heat transfer coefficient, and used heat transfer coefficient values 20,000 to 40,000 W/m²K for applied pressures of 25-100 MPa, respectively, and suggested that pressures of up to 60-100MPa were optimal for the squeeze casting process.

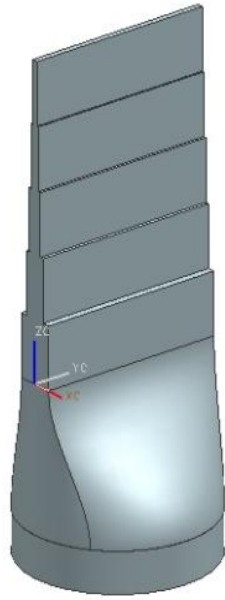
Netto[7] found the IHTC values ranged from 700 to 5000 W/m²K during horizontal strip continuous casting experiments using aluminum alloys. The various coatings roughness and thermoconductivity were contributed to the wide range of IHTC values reported. The heat transfer coefficient was found to increase with initial superheat, thickness of strip and smoother coatings. Kim[8] conducted experiments of pure aluminum cast into a cylindrical copper mold to determine the effects of coating and superheat on the IHTC. While the cast alloy was liquid, the IHTC was influenced by

mold surface roughness, the wettability of the alloy on the mold, and the physical properties of the coating layer. Attributed to the abrupt surface deformation of the casting, an IHTC drop was observed at the onset of solidification. The air gap and the direct contact between the casting and mold account for the IHTC. The authors claim that when the cast metal is in the solid phase the IHTC is not affected by the type or thickness of the mold coating and that it only depends on the thermal conductivity and thickness of the air gap.

However, studies of IHTC dependence on cross section thicknesses of aluminum squeeze castings are limited. In the present work, a special 5-step indirect squeeze casting was designed, in which different cross section thicknesses(2, 6, 8, 10, 20 mm) were included. Based on temperature measurements at each step, an inverse method was employed to numerically determine casting section thickness-dependant IHTCs.

2. EXPERIMENTAL DESIGN

The 5-step shape casting was used during the experiment. Figure 5-1 (a) shows the 3-D model of 5-step casting, which consists of 5 steps(from top to bottom designated as steps 1 to 5) with dimensions of 100x30x2mm, 100x30x6mm, 100x30x8mm, 100x30x10mm, 100x30x20mm accordingly. The molten metal was filled the cavity from the bottom cylindrical shape sleeve with diameter 100 mm. A real 5-step squeeze casting solidified under 60MPa is given in Figure 5-1(b).



(a)



(b)

Figure 5- 1. (a) The isometric view of 5-step casting 3-D model with the round-shape gating system. (b) 5-step casting solidifying under applied pressure 60 MPa.

The upper die(left and right parts) mounted on the top ceiling of the press machine. To measure the temperatures at the casting-die interface accurately, a special thermocouple holder was developed. The thermocouple holders were manufactured using the same material P20 as the die to ensure that the heat transfer process would not be distorted. The temperatures inside the die and casting were measured by Omega KTSS-116U-24 thermocouples with response time below 10 ms. Real-time temperature data were recorded by a LabVIEW- based data acquisition system. The detailed installation procedure and accuracy verification of the thermocouples installed inside the die and at casting surface were described in reference 9.

The integrated casting system consisted of a 75-ton laboratory hydraulic press, a two halves split upper die forming a 5-step cavity, one cylindrical sleeve lower die, an electric resistance furnace and a data acquisition system. Commercial aluminum alloy A443 was used in experiment with chemical composition (5.29%Si-0.11%Ti-0.1%Fe-balanceAl). Before metal pouring, the dies were pre-heated to 210⁰C by four heating cartridges installed inside the dies. The casting procedure included pouring melt into the bottom sleeve at 720⁰C, closing the dies, filling cavity, holding the applied pressure for 180 seconds, lowering the sleeve lower die, splitting the two parts of the upper die for casting ejection. Finally, the 5-step casting was shaken out from the cavity.

3. RESULTS AND DISCUSSION

Figure 2 shows typical temperatures versus time curves at the metal-die interface of Step 4 for solidifying aluminum A443 and inside the steel die with an applied hydraulic pressure of 60 MPa. The results include the measured temperatures of casting surface and temperature measurements obtained at different depths underneath the die surface(T1-2mm, T4-8mm). Since molten metal filled the cavity from the bottom, pre-solidification occurred upon the completion of cavity filling. No die surface temperatures exceeded 380⁰C, and the highest temperature of the casting surface was 541.7⁰C.

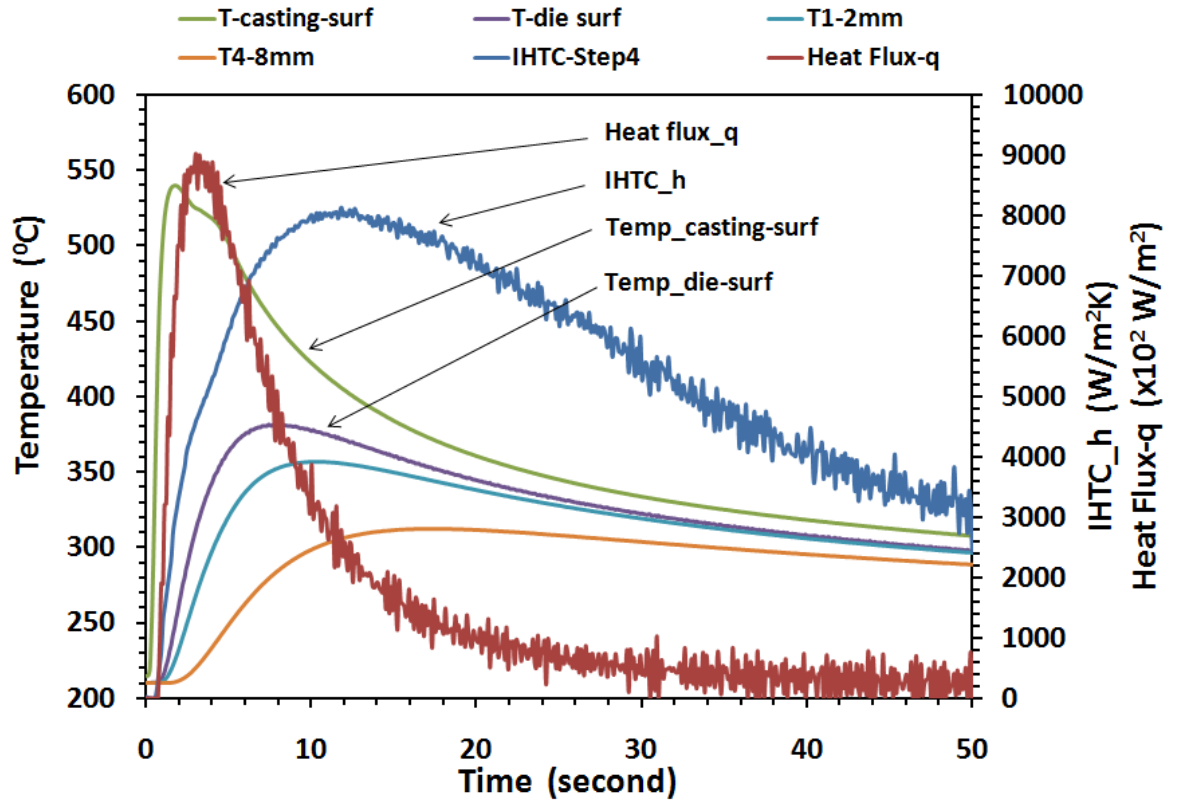


Figure 5- 2. Typical temperature versus time curves (Step 4, 60 MPa) at metal surface, die surface, and various positions inside the die; The interfacial heat flux(q) and the heat transfer coefficient (IHTC) curves estimated by inverse method(Step 4, 60 MPa).

The die surface temperature(T_0) and the heat flux(q) transferred at the interface between the molten metal and die were determined by the inverse method, which references 2 and 9 discussed in detail. Figure 5-2 shows the estimated result of the interfacial heat flux(q) and the heat transfer coefficient(IHTC) versus time. The peak heat flux value was $9.01\text{E}+05 \text{ W/m}^2$, and the peak value of IHTC was $8125 \text{ W/ m}^2\text{K}$. It

can be observed that the heat flux and IHTC curves reached to their peak value promptly and then dropped gradually until their values dropped to a low level, respectively.

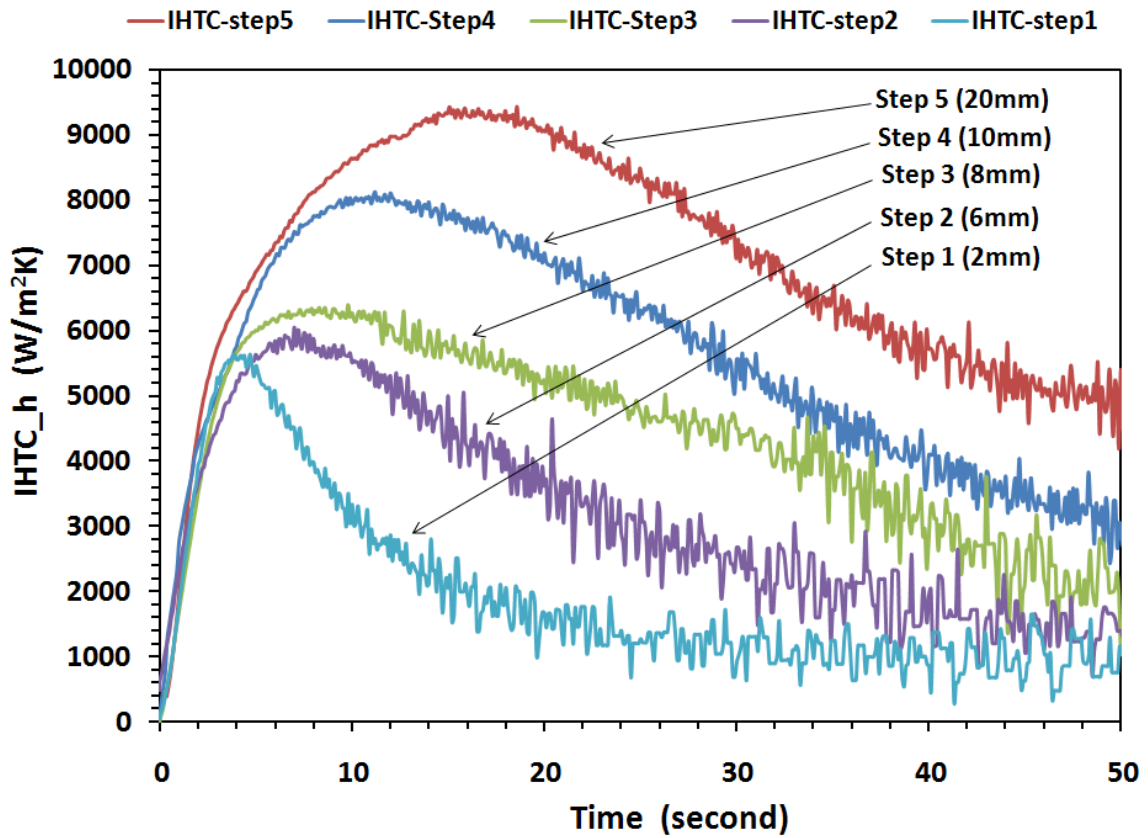


Figure 5- 3. Interfacial heat transfer coefficients(IHTC) curves of all steps under the applied pressure of 60MPa.

Figure 5-3 shows that the heat transfer coefficient(IHTC) curves of 5 steps determined by inverse method under applied pressure 60MPa. For all the steps, IHTCs began with an increasing stage and reached their peak value, then dropped gradually until the value became relative low level. From steps 1, 2, 3, 4, to 5 with 60MPa pressure, the peak IHTC values varied from 5629W/m²K, 6037W/m²K, 6351W/m²K, 8125W/m²K to 9419W/m²K, indicating that the closer contact between the casting and die surface at

thicker steps. Therefore, the section thickness affected IHTC peak values significantly. The peak IHTC value increased as the step became thicker. This effect can be associated to greater local pressure application experienced at the thicker step. For the steps 1, 2, 3, 4 and 5, it took 4.2, 7.9, 9.3, 12.1, and 16.8 seconds to reach their peak values, respectively. Besides the different peak values, the time for IHTC to obtain the peak value during the initial stage increased as the step became thicker. The thicker steps needed relatively long time to reach the high peak IHTC values since additional time was required for pressure transfer.

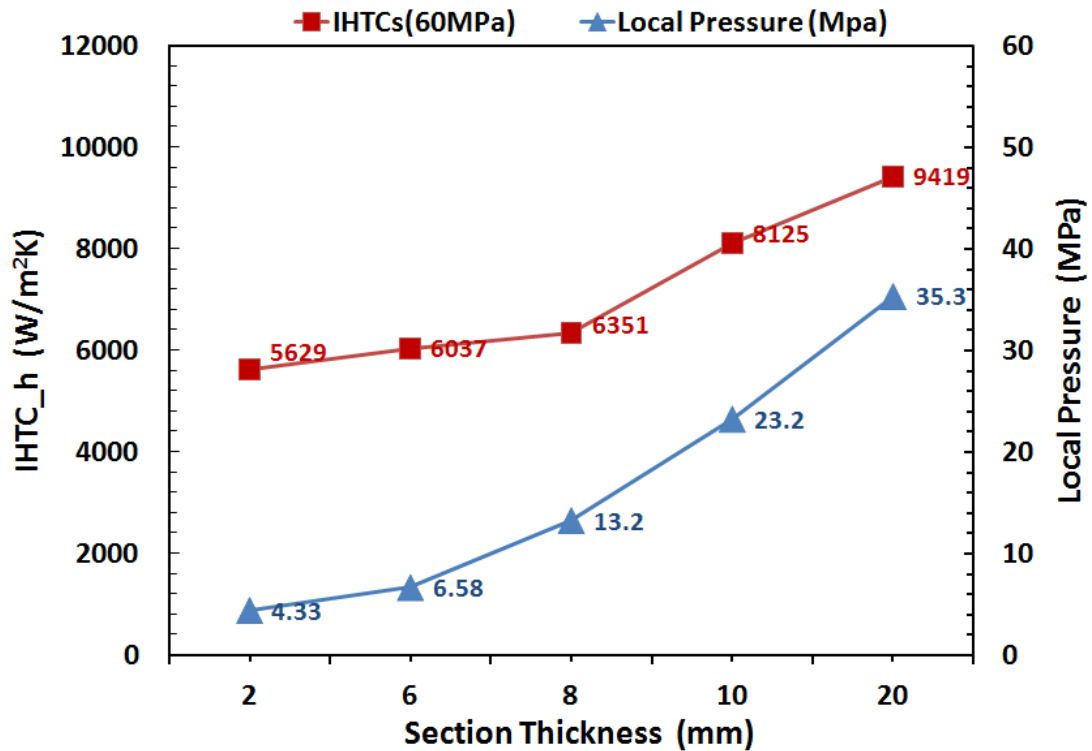


Figure 5- 4. Peak IHTC values and local pressure peak values varying with different cross section thicknesses of the 5-step casting.

The in-cavity local pressures at the interface of step casting and die were measured using the Kistler pressure transducers which were conducted calibration before the experiment. Upon the completion of the cavity filling, the local pressure increased abruptly to reach its peak value, then decreased gradually until the pressure-transfer path died out.

As Figure 5-4 was shown, the peak IHTC values and the local in-cavity pressure peak values at the casting-die interface were varied with different section thickness of steps 1, 2, 3, 4, and 5 under the applied pressure of 60MPa. As section thickness varied from 2 mm to 20 mm, the peak IHTC values increased from 5629 W/m²K to 9419 W/m²K, accordingly. With different casting section thicknesses 2, 6, 8, 10, and 20 mm, the local pressure peak values measured at the casting-die interface were 4.3, 6.6, 13.2, 23.2, and 35.3MPa, respectively.

The pressure difference between the instantaneous experimental measurements and the hydraulic applied pressures was a pressure loss($P_{loss}=(P-P_{local})/P$). When the melt filled the 5 steps cavity from the bottom sleeve with the hydraulic pressure 60MPa, the pressure loss at the casting-die interface was 41.2%, 61.3%, 78%, 89%, and 92.8% from the lowest thick step 5 to the uppermost step thin step 1, accordingly. A large percentage of the pressure loss occurred at a relatively upper thin steps compared to lower thick steps. The pressure loss rose significantly as the section thickness decreased since the pressure-transfer path inside the casting shrank quickly as the melt travelled to the upper thin steps.

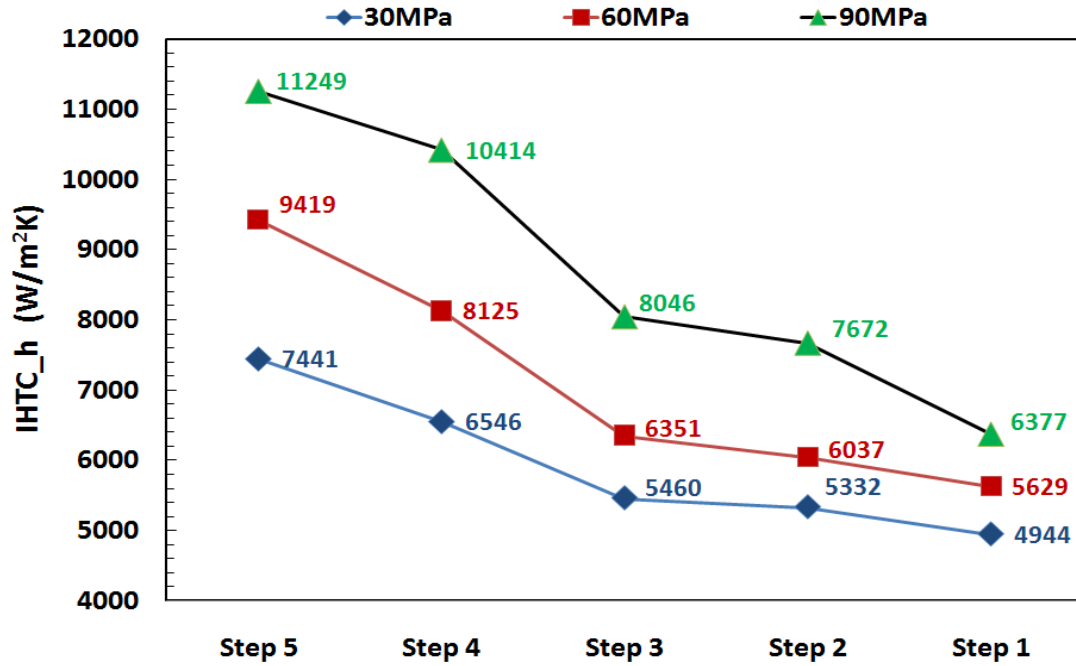


Figure 5- 5. Peak IHTC values of 5 step-casting A443 with applied pressure 30, 60, and 90MPa.

As Figure 5-5 shown, with increasing the applied pressures, the IHTC peak value of each step was increased accordingly. Peak IHTC value increased as the step became thick. The section thickness affected IHTC peak values significantly. The large difference in temperatures between the melt and the die with thick cavity section as well as relatively high localized pressure should be responsible for the high peak IHTC values observed at the thick steps.

CONCLUSIONS

1. Experimental investigation on 5-step castings of aluminum alloy A443 with different section thicknesses (2, 6, 8, 10, 20 mm) was conducted under the

hydraulic pressure of 60 MPa. The heat fluxes and IHTCs determined by inverse method reached to their peak values promptly and then dropped gradually to a low level.

2. From steps 1, 2, 3, 4, to 5, the peak IHTC values varied from 5629W/m²K, 6037W/m²K, 6351W/m²K, 8125W/m²K to 9419W/m²K, indicating that the closer contact between the casting and die surface at thicker steps. The time for IHTC to obtain the peak value during the initial stage increased as the step became thicker. The thicker steps needed relatively long time to reach the high peak IHTC values since additional time was required for pressure transfer.
3. The pressure loss rose significantly as the section thickness decreased since the pressure-transfer path inside the casting shrank quickly as the melt travelled to the upper thin steps.
4. The section thickness affected IHTC peak values significantly. The large difference in temperatures between the melt and the die with thick cavity section as well as relatively high localized pressure should be responsible for the high peak IHTC values observed at the thick steps.

REFERENCES

- [1] W. Griffiths, K. Kawai, 2010. "The effect of increased pressure on interfacial heat transfer in the aluminium gravity die casting process". *J. Mater. Sci.* Vol. 45, 2330-2339.
- [2] Z.Z. Sun, X.Z. Zhang, X.P. Niu, A. Yu, H. Hu, 2011. "Numerical simulation of heat transfer in pressurized solidification of Magnesium alloy AM50". *Heat and Mass Transfer*. In press. DOI 10.1007/s00231-011-0787-7.
- [3] I.S. Cho, and C.P. Hong, 1996. "Evaluation of heat transfer coefficients at the Casting/Die interface in squeeze casting," *International Journal of Cast Metals Research*, Vol.9, pp227-232.
- [4] M. Krishnan, and D.G.R. Sharma, 1996. "Determination of the Interfacial Heat transfer coefficient h in Unidirectional heat flow by Beck's Non Linear estimation procedure", *International Comm. Heat and Mass Transfer*, Vol.23, n.2, pp203-214.
- [5] P. Krishna, K.T. Bilkey, and R.D. Pehlke, 2001. "Estimation of interfacial heat transfer coefficient in indirect squeeze casting", *AFS transactions*, Vol.109, pp131-139.
- [6] H. Chattopadhyay, 2007. Simulation of transport process in squeeze casting. *J Mat Proc Technol* 186:174-178
- [7] P.G.Q. Netto, R.P. Tavares, M. Isac, and R.I.L. Guthrie, 2001., "A technique for the evaluation of instantaneous heat fluxes for the horizontal strip casting of aluminum alloys", *ISIJ international*, vol. 41, n.11, pp1340-1349.
- [8] H-S. Kim, I-S. Cho, J-S. Shin, S-M. Lee, and B-M. Moon, 2005. "Solidification parameters dependent on interfacial heat transfer coefficient between aluminum casting and copper

mold”, *ISIJ international*, vol. 45, n.2, pp192-198.

- [9] Z. Z. Sun, H. Hu, X.P. Niu, 2011. “Determination of heat transfer coefficients by extrapolation and numerical inverse methods in squeeze casting of magnesium alloy AM60”, *J. Mater. Process. Technol.* Vol. 211, pp. 1432-1440.

CHAPTER 6

EFFECTS OF LOCAL PRESSURE AND WALL-THICKNESS ON INTERFACIAL HEAT TRANSFER IN SQUEEZE CASTING OF MAGNESIUM ALLOY AM60

1.INTRODUCTION

The mechanical properties of magnesium castings are strongly dependent on the heat extraction rates that occur during solidification. The heat transfer coefficient for high pressure die casting(HPDC) can be expected to be much higher than that for gravity permanent mold casting process. Compared to other conventional casting processes, the most attractive features of squeeze casting are slow filling velocities and the pressurized solidification. Before the solid fraction of the casting becomes high enough, the applied pressure squeezes liquid metal into the air or shrinkage porosities effectively. Therefore, squeeze casting can make castings virtually free of porosity and usually have excellent as-cast quality, and are heat treatable, which is difficult to achieve with high pressure casting processes.

The accuracy of a solidification simulation depends on the accuracy of the heat transfer modeling. The critical portion of heat transfer in the casting is that at the metal/mold interface. Modeling of the interfacial heat transfer coefficient(IHTC) is very challenging due to a number of factors, such as air gap, casting geometry, alloy characteristics, mold material, coating, preheat temperature, and other process parameters. For the squeeze casting process, the applied hydraulic and local pressures, pouring temperatures, and die initial temperatures, are believed to be strongly influence the pressure-transfer behavior inside the casting[1]. In various casting

processes, the contact between the liquid metal and mould is imperfect because of coating applied on the die surface and air gap caused by shrinkage. These thermal barriers may decrease the heat transfer between metal and die and cooling rates of the casting surface, which influences microstructure and quality of the casting significantly. Hence, precise determination of heat transfer coefficients at the metal-mold interface is essential to accurately simulate solidification process.

The interfacial heat transfer depends on actual contact situation between the rough surface of the mold and the casting. In the case of relatively low melting temperature light alloys, the mechanism of heat transfer would be by conduction through the points of interfacial contact, and by conduction through the interfacial gas in the regions between the contact points. Radiation would not be expected to be a significant heat transfer mechanism in the case of Al or Mg alloys[2].

The effect of many casting parameters on the interfacial heat transfer coefficient have been studied experimentally. Browne and O'Mahoney[3] examined the effect of alloy freezing range and head height during solidification of an aluminum alloy in investment casting. Ferreira[4,5] analyzed the effect of alloy composition, melt superheat, mould material, mould roughness, mould coatings, and mould initial temperature distribution on the interfacial heat transfer coefficient. Arunkumar[6] examined two-dimensional heat transfer in gravity die casting, and studied how the initial nonuniform temperature field that typically results after filling of the mould caused the distribution of heat flux and initiation of air-gap formation around a casting-mould interface nonuniformly.

Other researchers aimed at examining the effect of increased pressure on interfacial heat transfer. Meneghini[7] concluded that increased metal head height increased the interfacial heat transfer coefficient and delayed the onset of air-gap formation during gravity aluminum alloy die casting. Chattopadhyay[8] simulated the squeeze casting process numerically on A-356 with variable heat transfer coefficient, and used heat transfer coefficient values 20,000 to 40,000 W/m²K for applied pressures of 25-100 MPa, respectively, and suggested that pressures of up to 60-100MPa were optimal for the squeeze casting process. Aweda[9] found only a small(14%) increase in interfacial heat transfer coefficient on pure aluminum with applied pressure 86MPa. Guo[10] found that heat transfer coefficient initially reached a maximum value of about 10,000 to 20,000 W/m²K on ADC12 aluminum alloy with 2 to 14mm section thickness, followed by a rapid decline to low values of about a few hundred W/m²K. In the case of high pressure die casting of Mg alloy(AM50) in H13 tool steel dies, an initial peak heat transfer coefficient value reached 12,000 W/m²K, then decreased to less than 1,000 W/m²K over 7 seconds. Dour[11] measured the interfacial heat transfer coefficient values of 45,000-60,000 W/m²K on Al-12%Si alloy within the 33-90MPa pressure range, but observed that the pressure variation did not have a significant impact on the heat transfer. A “saturation effect” where increased pressure did not lead to increased heat transfer, was suggested to occur above 5MPa local in-cavity pressure at the interface of H13 die and aluminum alloy. Hamasaiid[12] and Dargusch[13] reported the peak heat transfer coefficient value of 90,000-112,000 W/m²K during the HPDC of magnesium alloy AZ91D with section thickness 2-5mm, declining to low values within 2 seconds. In high pressure die casting(HPDC) the

typical behavior of the heat transfer coefficient is to increase to a peak value, then followed by a rapid decline. This may be explained by increasing solidification and fraction solid in the mould cavity causing a reduction in the pressure transmitted from the piston to the casting-mould interface.

Although the IHTC has been studied extensively by many researchers for magnesium alloys, these studies only focused on castings with simple geometries. Little attention has been paid to variation of casting thicknesses and hydraulic pressures. Actually, in the die casting practice, the different thicknesses at different locations of castings results in significant variation of the local heat transfer coefficients. Therefore, it is essential to investigate the influence of casting thickness, pressure levels, and process parameters on the IHTC. In this study, a special 5-step squeeze casting was designed for numerical determination of casting thickness-dependant IHTCs. The temperature measuring units to hold multiple thermocouples simultaneously and the pressure transducers were employed to accurately measure the temperatures and the local pressures during squeeze casting of magnesium alloy AM60.

2. EXPERIMENTAL DESIGN

Figure 4-1 shows the 3-D model of 5-step casting, Figure 4-2 illustrates schematically the configuration of the upper die(left and right parts) mounted on the top ceiling of the press machine. It also reveals the geometric installation of pressure transducers and thermocouple holders. The detailed information was provided in Chapter 4.

The experiments were designed to measure both in-cavity local pressure and heat flux simultaneously at the die-casting interface of each step. As shown in Figure 4-2, pressure transducers and temperature thermocouples were located opposite each other so that measurements from sensors could be directly correlated due to the symmetry of the step casting. Five pressure transducers and temperature measuring unit were designated as PT1 through PT5, TS1 through TS5, respectively. Each unit was inserted into the die and adjusted until the front wall of the sensor approached the cavity surface. The geometry shape of thermocouples holders was purposely designed the same as the pressure transducer, so that they could be exchangeable at different locations. The detailed installation procedure and accuracy verification of the thermocouples installed inside the die and at casting surface were described in reference 14.

Before the pouring, the dies were pre-heated to 210°C by four heating cartridges installed inside the dies. The casting procedure included pouring molten magnesium alloy AM60 into the bottom sleeve at 720°C , closing the dies, filling cavity, holding the applied pressure for 180 seconds, lowering the sleeve lower die, splitting the two parts of the upper die. Finally the 5-step casting can be shaken out from the cavity.

3. RESULTS AND DISCUSSION

Figure 6-1 shows typical temperatures versus time curves at the metal-die interface of Step 4 for solidifying magnesium alloy AM60 and inside the steel die with an applied hydraulic pressure of 30 MPa. The results include the measured temperature of casting surface and temperature measurements obtained at different depths underneath the die surface(T1-2mm, T2-4mm, and T4-8mm). Since molten metal filled the cavity

from the bottom, pre-solidification occurred upon the completion of cavity filling. No die surface temperatures exceeded 340°C , and the highest temperature of the casting surface was 532.97°C .

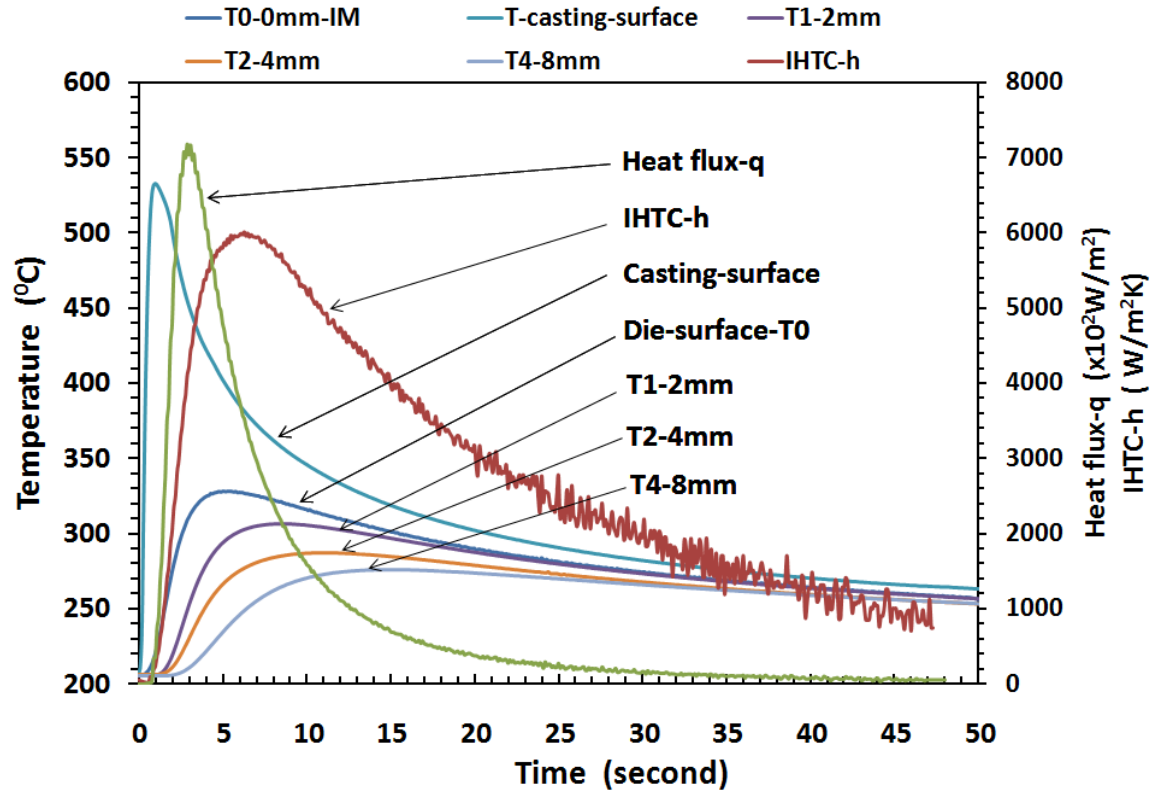


Figure 6- 1. Typical temperature versus time curves (Step 4, 30 MPa) at metal surface, die surface, and various positions inside the die; The interfacial heat flux(q) and the heat transfer coefficient (IHTC) curves estimated by inverse method(Step 4, 30 MPa).

The die surface temperature($T0$) and the heat flux(q) transferred at the interface between the molten metal and die were determined by the inverse method, which reference 14 discussed in detail. Figure 6-1 shows the estimated result of the interfacial heat flux(q) and the heat transfer coefficient(IHTC) versus solidification time. The peak heat flux value was $7.38\text{E}+05 \text{ W/m}^2$, and the peak value of IHTC was $6005 \text{ W/ m}^2\text{K}$. It

can be observed that the heat flux and IHTC curves reached to their peak value promptly and then dropped gradually until their values dropped to a low level, respectively.

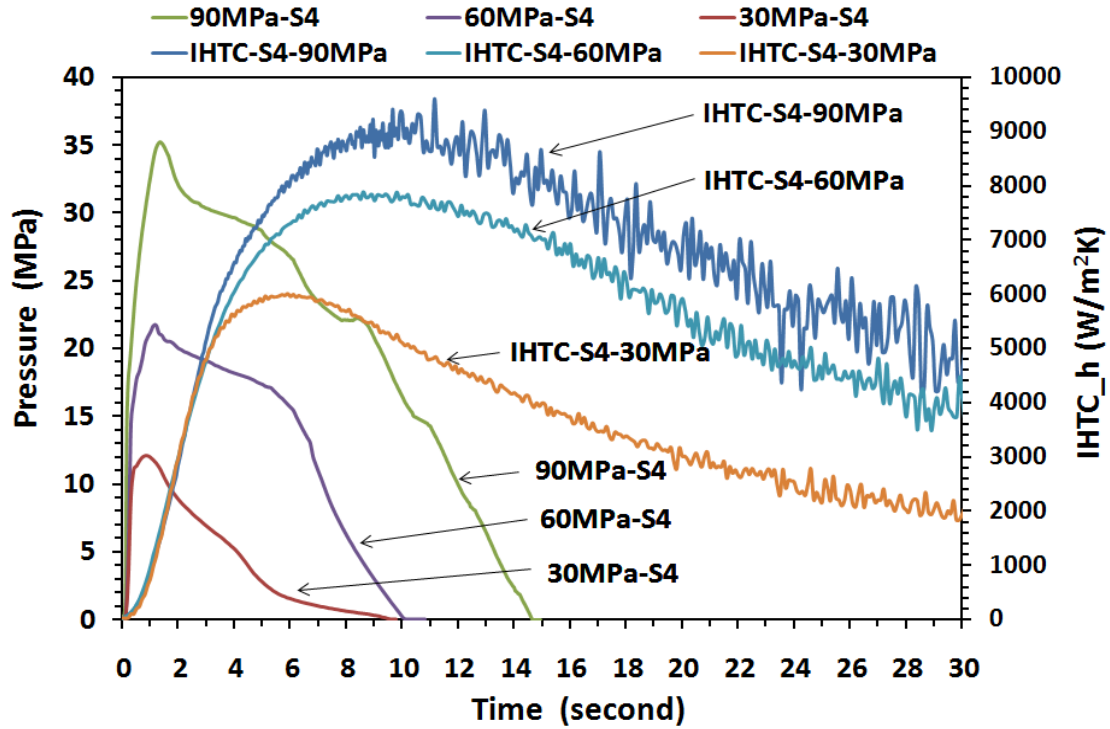


Figure 6- 2. Typical local pressure distributions and IHTC curve at the casting-die interface of step 4 under the applied hydraulic pressures of 30, 60, 90MPa.

The in-cavity local pressures at the interface of step casting and die were measured using the Kistler pressure transducers of which calibration was conducted before the experiment. Figure 6-2 shows the local pressure distributions at the casting-die interface of step 4 under the applied hydraulic pressures of 30, 60, 90MPa. Upon the completion of the cavity filling, the local pressure increased abruptly to reach its peak value, then decreased gradually until the pressure-transfer path died out. For the hydraulic pressures of 30, 60, and 90MPa, the local pressure peak value were 12.1, 21.7, and 35.2MPa, respectively. With the applied hydraulic pressure increased from 30 to 90MPa,

the IHTC peak value of step4 was increased from 6005 to 9418 W/m²K, accordingly. This effect can be associated to greater local pressure application experienced for higher applied hydraulic pressure.

Under the applied hydraulic pressure of 30MPa, the pressure-transfer path inside the casting shrank quickly(9.1 s) as the solidification proceeded. The pressure-transfer path existed longer(14.6 s) when the applied hydraulic pressure increased to 90MPa, indicating that a good heat transfer condition can be achieved. From the hydraulic pressure 30 to 90MPa, the local pressure peak value at step 5 casting-die interface was varied from 20 to 50MPa.

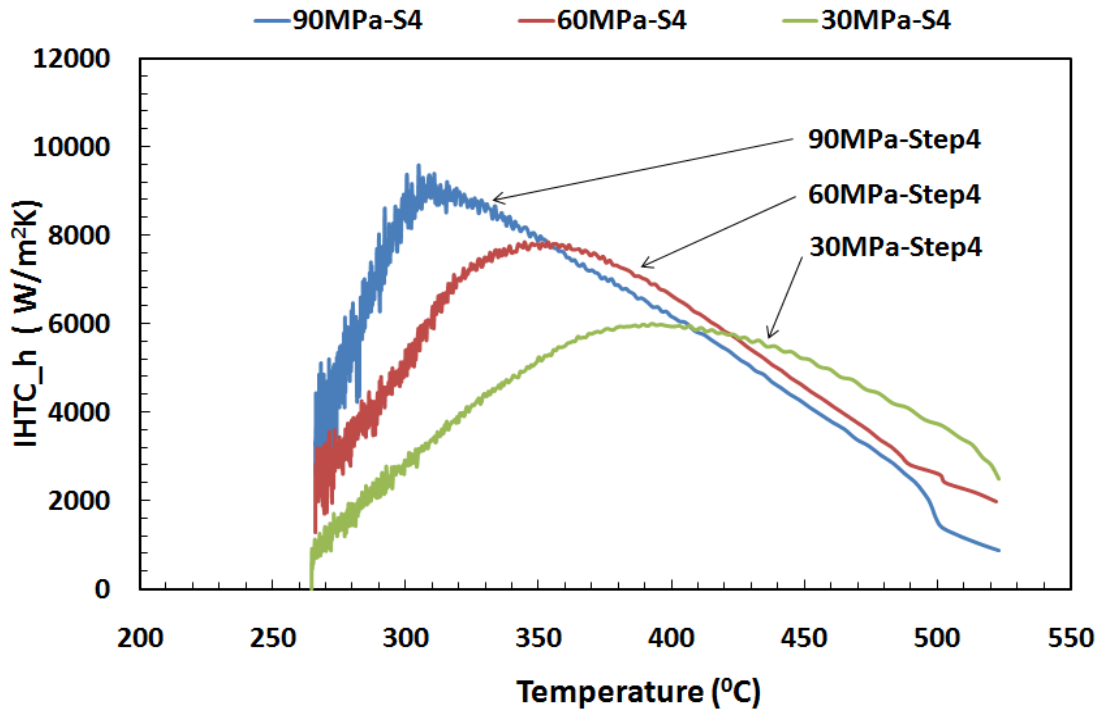


Figure 6- 3. Typical effects of applied pressures on the heat transfer coefficients with casting surface temperature at the step 4.

Figure 6-3 shows the variation of interfacial heat transfer coefficients as a function of casting surface solidifying temperature at the step 4 under applied hydraulic pressures 30, 60, and 90MPa. It can be observed that the interfacial heat transfer coefficients values increased gradually after the cavity filled. When the maximum IHTC values reached at different casting surface temperatures under various applied pressures, the IHTC values decreased to a low value level. For the applied pressures 30, 60, and 90MPa, the peak IHTC values(6005, 7871, and 9418 W/m²K) were found at 392, 353, and 304⁰C, respectively. As the applied pressure was relatively small(30MPa), the peak value of the IHTC was low(6005W/m²K) and appeared at a high die surface temperature(392⁰C). However, under the high applied pressure(90MPa), the peak value of the IHTC was increased to 9418 W/m²K and occurred at a low die surface temperature(304⁰C). This observation should be attributed to the presence of long pressure transfer path as the high pressure was applied.

Figure 6-4 shows that the heat transfer coefficient(IHTC) curves of 5 steps determined by inverse method under applied pressure 30MPa. For all the steps, IHTC began with increasing stage and reached their peak value, then dropped gradually until the value became a low level. From steps 1, 2, 3, 4, to 5 with 30MPa pressure, the peak IHTC values varied from 2807W/m²K, 2962W/m²K, 3874W/m²K, 6005W/m²K to 7195W/m²K, indicating that the closer contact between the casting and die surface at thicker steps. Therefore, the wall thickness affected IHTC peak values significantly. The peak IHTC value increased as the step became thicker. This effect can be associated to greater local pressure application experienced at the thicker step.

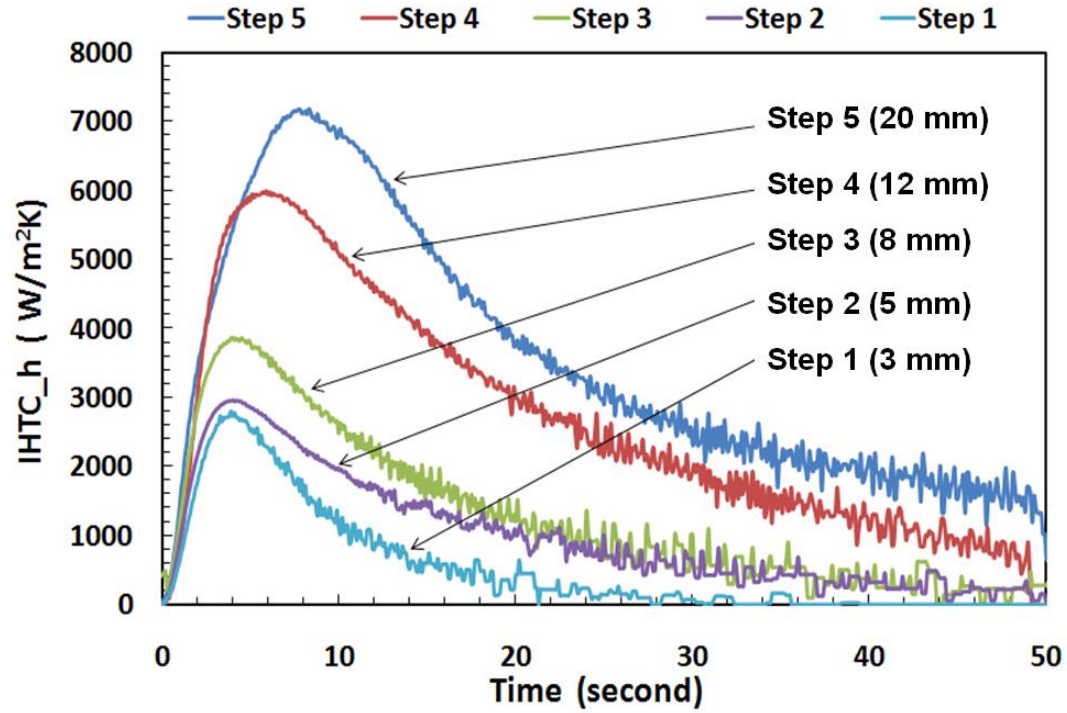


Figure 6- 4. Interfacial heat transfer coefficients(IHTC) curves of 5 steps under the applied pressure of 30MPa.

For the steps 1, 2, 3, 4 and 5, it took 4.1, 4.2, 4.7, 6.1, and 8.2 seconds to reach their peak values, respectively. Besides the different peak values, the time for IHTC to obtain the peak value during the initial stage increased as the step became thicker. The thicker steps needed relatively long time to reach the high peak IHTC values since additional time was required for pressure transfer.

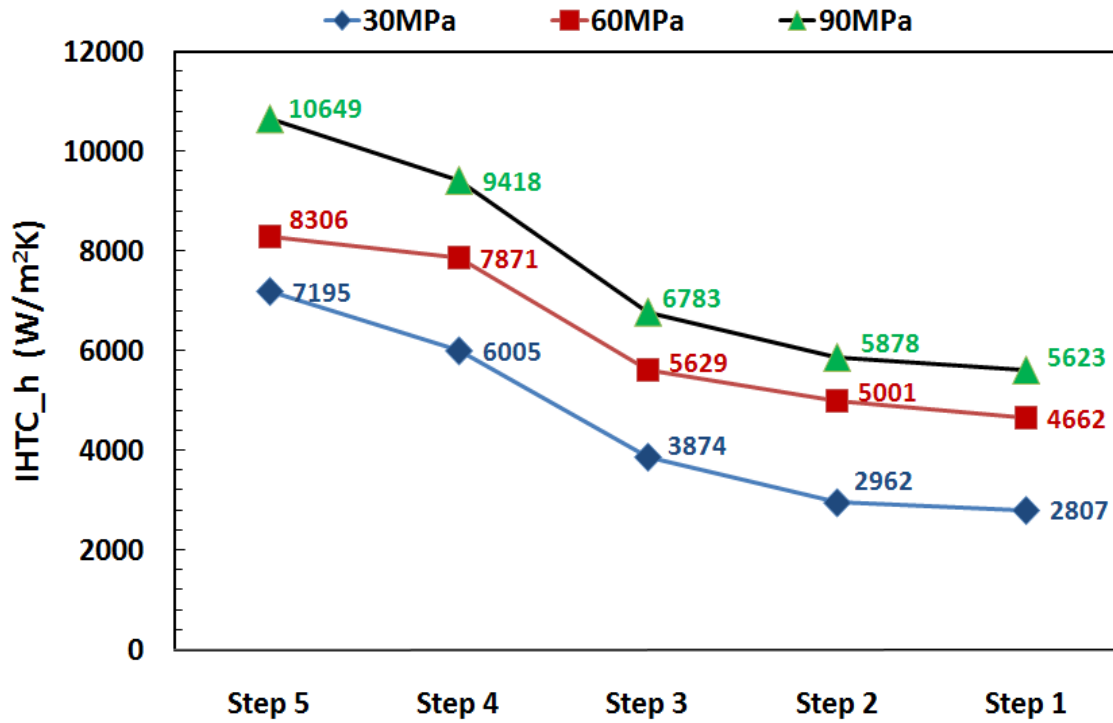


Figure 6- 5. The peak IHTC values of 5 steps estimated by inverse method with applied pressure 30, 60 and 90MPa.

Figure 6-5 shows the IHTC peak values at step 1 through 5 with applied pressure 30, 60 and 90MPa. Similar characteristics of IHTC peak values can be observed at 30, 60 and 90MPa applied pressures. With applied pressure 60MPa, the peak IHTC values at steps 1, 2, 3, 4, and 5 varied from 4662 W/m²K, 5001 W/m²K, 5629 W/m²K, 7871 W/m²K and 8306 W/m²K. With applied pressure 90MPa, the peak IHTC values varied from 5623 W/m²K, 5878 W/m²K, 6783 W/m²K, 9418 W/m²K and 10649 W/m²K.

With increasing the applied hydraulic pressures, the IHTC peak value of each step was increased accordingly. This results from exertion of larger pressures locally at each

step as the high hydraulic pressure applied. The wall thickness affected IHTC peak values significantly. It also can be observed that the peak IHTC value and heat flux increased as the step became thick. The large difference in temperatures between the melt and the die with thick cavity section as well as relatively high localized pressure should be responsible for the high peak IHTC values observed at the thick steps.

From the above interfacial heat transfer coefficient(IHTC) curves obtained with temperatures and pressures, the peak IHTC value(h) empirical equation as a function of local pressures and solidification temperatures can be derived for all steps by multivariate linear and polynomial regression.

For the step 5 with thickness 20mm,

$$h_{step5} = (0.000044P - 0.0028)T^3 + (3.118 - 0.0633P)T^2 + (25.66P - 1053.33)T - 3131P + 112616 \quad (0MPa < P < 50MPa, \quad 20^\circ C < T < 540^\circ C, \\ \text{the correlation coefficient } R = 0.9026)$$

For the step 4 with thickness 12mm,

$$h_{step4} = (0.00017P - 0.0022)T^3 + (2.297 - 0.2048P)T^2 + (76.17P - 738.08)T - 8983P + 75045 \quad (0MPa < P < 36MPa, \quad 20^\circ C < T < 540^\circ C, \\ \text{the correlation coefficient } R = 0.9586)$$

For the step 3 with thickness 8mm,

$$h_{step3} = (0.000014P + 0.0011)T^3 - (1.35 + 0.0178P)T^2 + (8.44P + 506.66)T - 623P - 68705 \quad (0MPa < P < 25MPa, \quad 20^\circ C < T < 510^\circ C, \\ \text{the correlation coefficient } R = 0.8625)$$

For the step 2 with thickness 5mm,

$$h_{step2} = (0.0039 - 0.00003P)T^3 + (0.016P - 3.473)T^2 + (945 - 0.87P)T - 185P - 89714 \quad (0MPa < P < 15MPa, \quad 20^\circ C < T < 450^\circ C, \\ \text{the correlation coefficient } R = 0.8563)$$

For the step 1 with thickness 3mm,

$$h_{step1} = (0.000087P + 0.0015)T^3 - (0.075P + 1.24)T^2 + (20.13P + 344)T - 1632P - 30051 \quad (0MPa < P < 10MPa, \quad 20^\circ C < T < 360^\circ C, \\ \text{the correlation coefficient } R = 0.8694)$$

where P is the local pressure with the range from 0MPa to 50MPa(hydraulic pressure from 0MPa to 90MPa), T is the solidification temperatures with the range from $0^\circ C$ to $540^\circ C$, and the correlation coefficient R varies from 0.85 to 0.95.

Figure 6-6 to Figure 6-10 displays three-dimensional(3-D) curve planes for the purpose of demonstrating the combining effect of the local pressures and solidification temperatures on IHTC values (h), which are predicted by the above empirical equations.

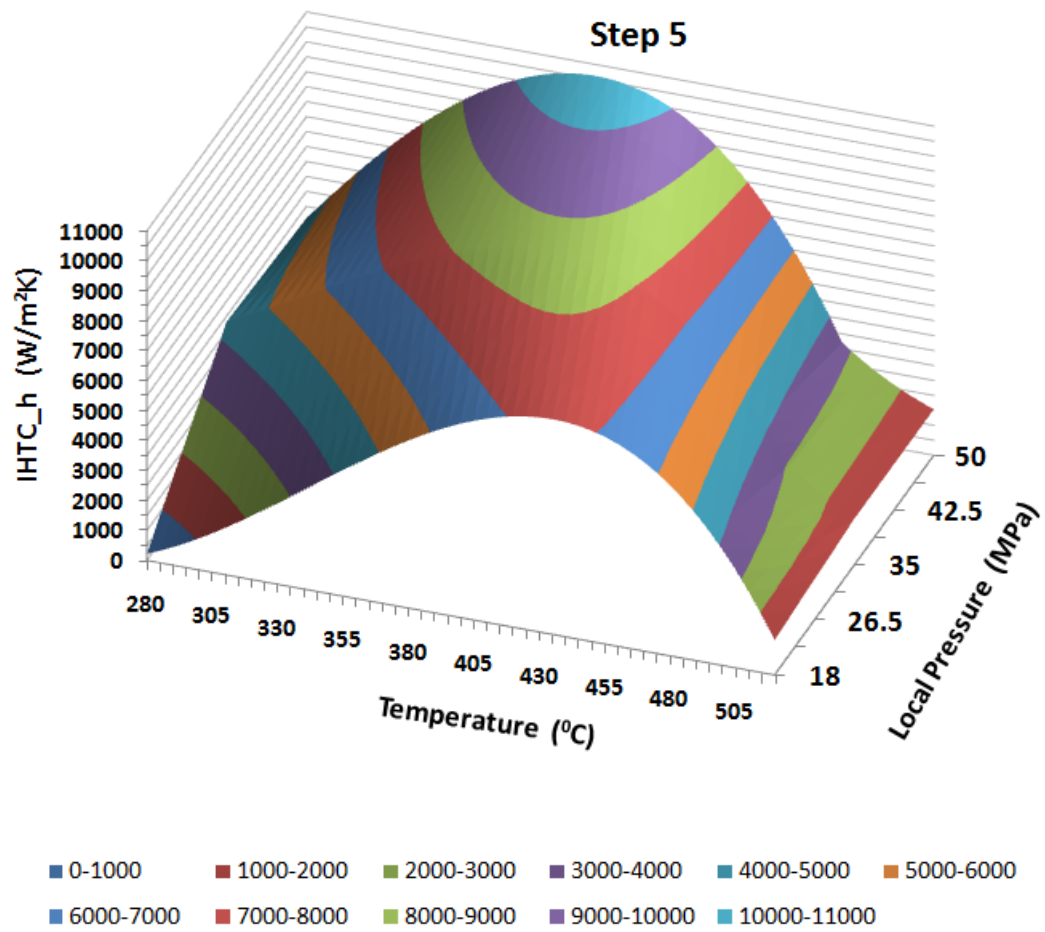


Figure 6- 6. IHTC curve plane of Step 5 as a function of the local pressures and solidification temperature.

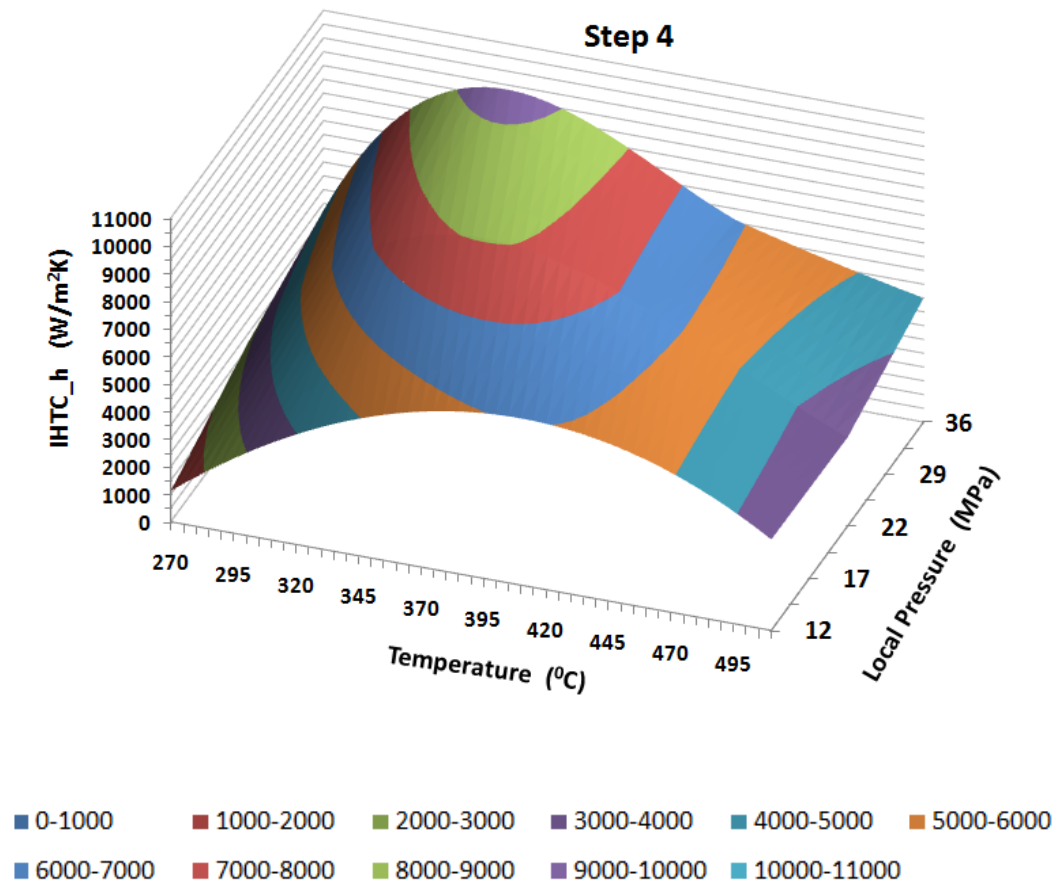


Figure 6- 7. IHTC curve plane of Step 4 as a function of the local pressures and solidification temperature.

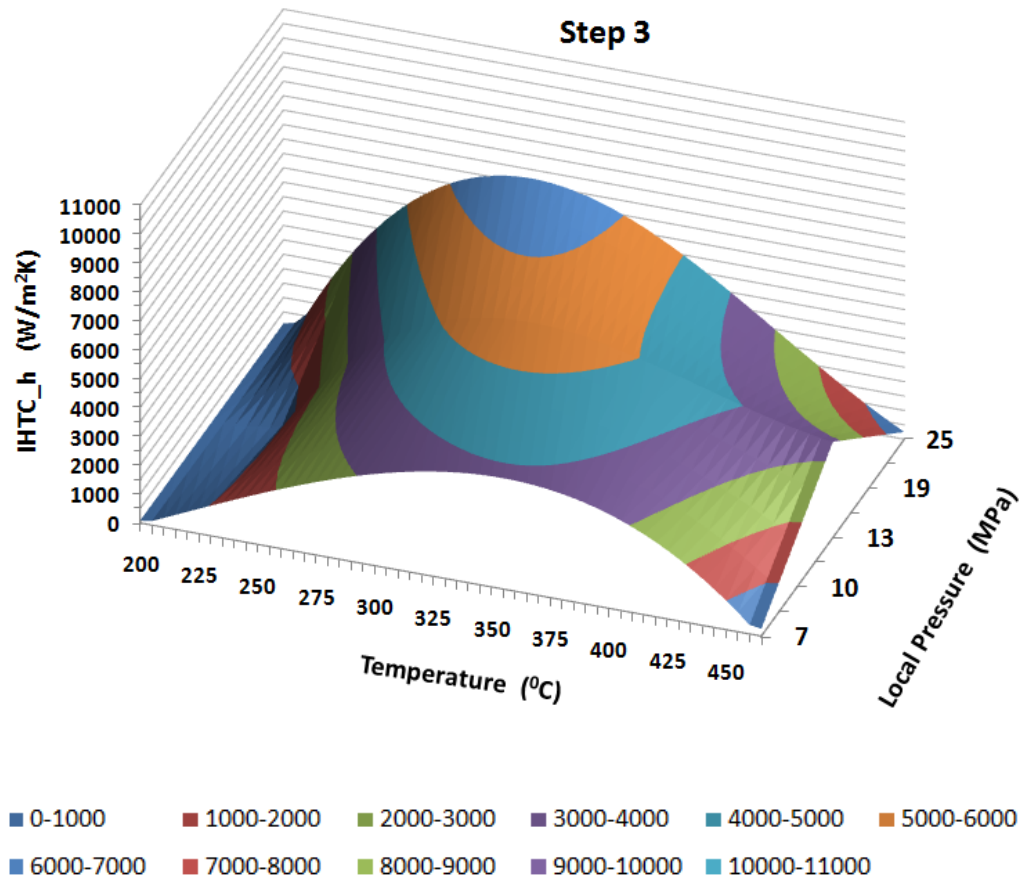


Figure 6- 8. IHTC curve plane of Step 3 as a function of the local pressures and solidification temperature.

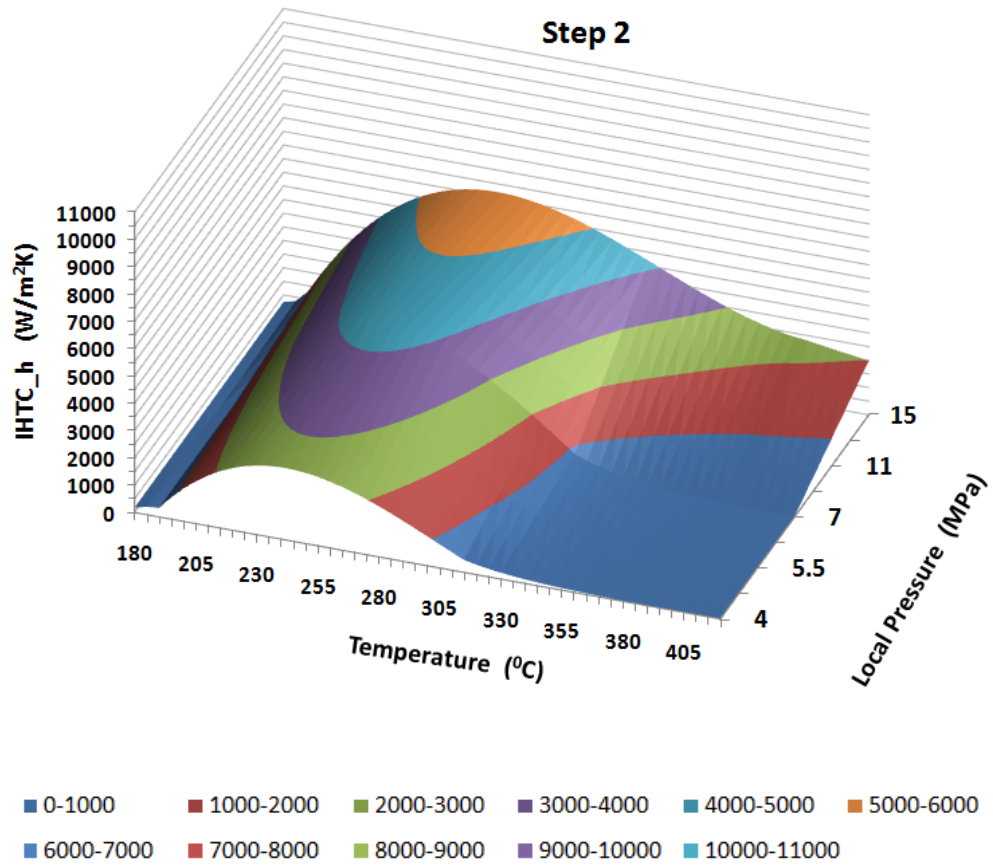


Figure 6- 9. IHTC curve plane of Step 2 as a function of the local pressures and solidification temperature.

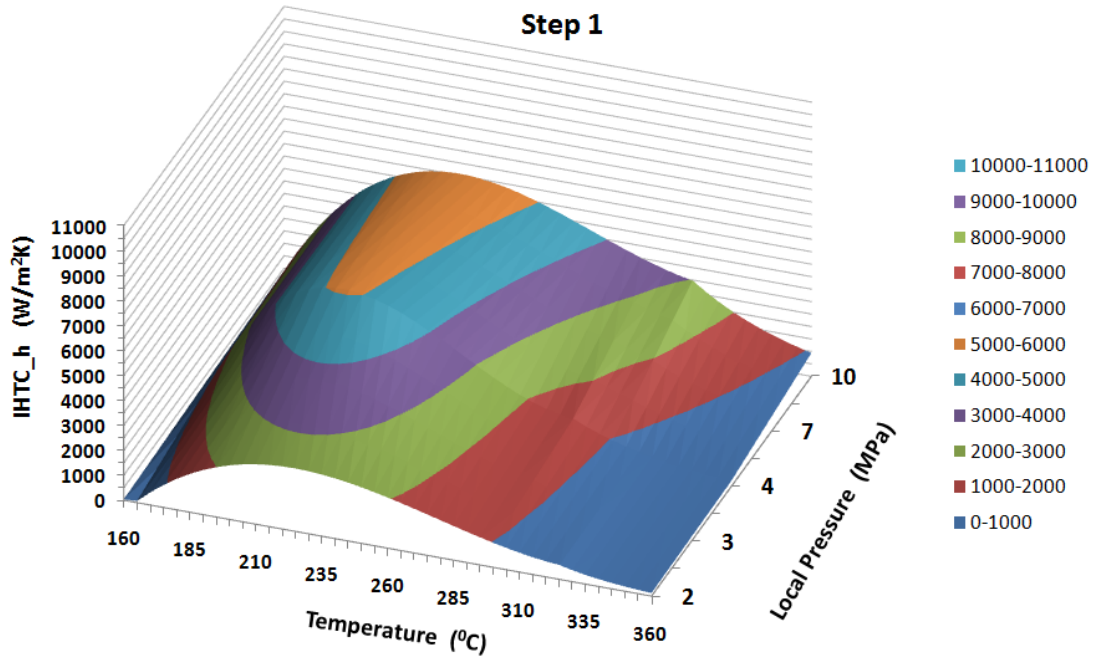


Figure 6- 10. IHTC curve plane of Step 1 as a function of the local pressures and solidification temperature.

CONCLUSIONS

1. The 5 step casting of magnesium alloy AM60 with different wall-thicknesses (3, 5, 8, 12, 20 mm) were prepared under various hydraulic pressures(30, 60, and 90 MPa) using indirect squeeze casting process. The IHTC versus time and temperature curves have been successfully determined by the inverse method. The heat flux and IHTC reached to their peak values promptly and then dropped gradually to a low level.
2. The in-cavity local pressures at the interface of step casting and die rose abruptly to its peak value, then decreased gradually until the pressure-transfer path died

out. The pressure-transfer path extended longer as the applied hydraulic pressure increased.

3. As the applied hydraulic pressure increased, the high IHTC peak value of each step was obtained accordingly. This effect can be attributed to the exertion of greater pressure locally at each step for higher applied hydraulic pressure.
4. The casting wall thickness affected IHTC peak values significantly. The peak IHTC values and heat fluxes increased as the steps became thick. The large difference in temperatures between the melt and the die with thick cavity sections as well as relatively high localized pressure should be responsible for the high peak IHTC values observed at the thick steps.
5. The empirical equations of all steps relating IHTC to the local pressures and solidification temperature at the casting surface were developed.

REFERENCE

- [1] Z.Z. Sun, X.Z. Zhang, X.P. Niu, A. Yu, H. Hu, 2011. Numerical simulation of heat transfer in pressurized solidification of Magnesium alloy AM50. Heat and Mass Transfer. DOI: 10.1007/s00231-011-0787-7
- [2] W. Griffiths, K. Kawai, 2010. The effect of increased pressure on interfacial heat transfer in the aluminium gravity die casting process. J. Mater. Sci. Vol. 45, 2330-2339.
- [3] D. Browne, D. O'Mahoney, 2001. Interface heat transfer in investment casting of aluminum. Metall. and Mater. Trans. A, 32A, p3055-3063
- [4] I.L Ferreira, J.E. Pinelli, B. Nestler, A. Garcia, 2008. Influences of solute content, melt superheat and growth direction on the transient metal/mold interfacial heat transfer coefficient during solidification of Sn–Pb alloys. Mat. Chem. Phys. Vol. 111, p444-454.
- [5] I.L. Ferreira, J.E. Spinelli, L.C. Pires, A. Garcia, 2005. The effect of melt temperature profile on the transient metal/mold heat transfer coefficient during solidification. Mat. Sci. Eng. A. Vol.408, p317-325.
- [6] S. Arun kumar, K.V. Sreenivas Rao, T.S. Prasanna Kumar., 2008. Spatial Variation of Heat Flux at the Metal-Mold Interface due to Mold Filling Effects in Gravity Die Casting Int. J. Heat Mass Transf. Vol.51, p2676-2685.
- [7] A. Meneghini, L. Tomesani, 2005. Chill material and size effects on HTC evolution in sand casting of aluminium alloys, Journal of Materials Processing Technology 162-163, p534-539.

- [8] H. Chattopadhyay, 2007. Simulation of transport process in squeeze casting. *J Mat Proc Technol* 186:174-178
- [9] J. Aweda, M. Adeyemi, 2009. Experimental determination of heat transfer coefficients during squeeze casting of aluminum. *J. Mater. Process. Technol.* vol.209, p1477-1483
- [10] Z.P. Guo, S.M. Xiong, B.C. Liu, M. Li, J. Allison, 2008. Effect of Process Parameters, Casting Thickness, and Alloys on the Interfacial Heat-transfer Coefficient in the High-pressure Die Casting Process. *Metall. and Mater. Trans.* Vol.39A, p2896-2905.
- [11] G. Dour, M. Dargusch, C. Davidson, and A. Nef, 2005. Development of a non-intrusive heat transfer coefficient gauge and its application to high pressure die casting. *J. Mater. Process. Technol.* vol.169, p223-233.
- [12] A. Hamasaiid, M. Dargusch, C. Davidson, S. Tovar, T. Loulou, F. Rezai-aria, and G. Dour, 2007. Effect of mold coating materials and thickness on heat transfer in permanent mold casting of aluminum alloys. *Metall. and Mater. Trans. A*, Vol.38A, p1303-1316
- [13] M. Dargusch, A. Hamasaiid, G. Dour, T. Loulou, C. Davidson, and D. StJohn, 2007. The accurate determination of heat transfer coefficient and its evolution with time during high pressure die casting of Al-9%Si-3%Cu and Mg-9%Al-1%Zn alloys. *Advanced Engineering Materials*. vol.9, No.11, p995-999
- [14] Z.Z. Sun, H. Henry, X.P. Niu, 2011. Determination of heat transfer coefficients by extrapolation and numerical inverse methods in squeeze casting of magnesium alloy AM60. *J. Mater. Process. Technol.* (2011) Vol. 211, pp. 1432-1440.

CHAPTER 7

VERIFICATION OF IHTCS DETERMINED BY THE INVERSE METHOD

The inverse modeling method developed in this study was aimed to determine the interfacial heat transfer coefficient(IHTC) precisely. In this Chapter, by applying the identified IHTC values presented in Chapters 4-6[1, 2, 3], the accuracy of the inverse method is verified through the comparison between numerical predictions and experimental results. MAGMAsoft, the most popular casting simulation software, was employed as the simulation tool and the Step 5 is taken as an example to conduct the verification.

As per the configuration of the dies mentioned at Chapter 3, the thermocouples installed inside mould of the 5-step squeeze casting were type K with 1/16 inch diameter, stainless steel sheath, ungrounded junction, and 24 inch sheath length. To measure the temperature at the center of Step 5, a thermocouple was inserted into the cavity through the center hole of the temperature measuring unit of Step 5.

1. CASTING PARAMETER SPECIFICATION

Before the simulation was performed, casting process parameters were defined, including the thermophysical properties of the casting and mould material and their initial temperature conditions. The heat transfer coefficients also had to be input as the boundary condition for the casting configuration. Specifications for the filling and solidification processes included the filling time or pouring rate, the filling direction, the feeding effectivity, criterion temperatures and the solver types. The feeding effectivity

defined the maximum ratio of the volume available for feeding and the actual volume of the top chill vent. The filling time was determined based on the casting size and the hydraulic plunger moving speed. The fill direction indicates the flow of metal into the mold and is defined here in the positive Z direction to match the orientation of the squeeze casting system. The filling and solidification simulation parameters used in this study are listed in Tables 7-1 and 7-2[4,5].

Table 7- 1. Parameters for filling simulation

Filling Definition	
Parameter	Value
Solver	Solver 5
Filling Depends on	Time
Filling Time	1.8 s
Storing Data	10% increments of % Filled
Fill Direction-X	0
Fill Direction-Y	0
Fill Direction-Z	+1

Simulation of the mold filling and solidification process required geometrical models of the casting, the gating system and the mould. The preprocessor module of simulation software then read the STL files as geometry. After the establishment of the full casting models, the whole geometry was enmeshed automatically with about 200,000 elements using Solver 5.

Table 7- 2. Parameters for solidification simulation

Solidification Definition	
Parameter	Value
Temperature from Filling	Yes
Solver	Solver 5
Stop Simulation	Automatic
Stop Value	433°C
Calculate Feeding	Yes
Feeding Effectivity	70%
Criterion Temperature 1#	451.6°C
Criterion Temperature 2#	621.0°C
Storing Data	10% increments of % Solidified

Then, the three different Heat Transfer Coefficient(HTC) were defined according to the MAGMASoft database[4], Yu's research[6] , and the current work. The thermophysical properties of the magnesium alloy AM60 and aluminum alloy A443 was selected from the database of simulation software. The initial and boundary conditions for simulation are listed in Table 7-3.

Table 7- 3. Initial and boundary conditions for simulation

1	Material definitions (Initial Temperature) [$^{\circ}\text{C}$]	Cast Alloy (AM60) Cast Alloy (A443)	620
		Mould (HPDC)	210
2	Boundary definitions (Heat Transfer Coefficient) [$\text{W}/\text{m}^2\text{K}$]	Casting – Mould	(1)C7000 (2) Yu's Curve (3) IM curve
3	Filling definitions (pouring time) (s)	Use solver 5	1.8

Once the meshed geometries and the necessary process parameters were established, the actual filling and solidification simulations were carried out. The type of numerical calculations employed was based on the algorithm (Solver) type chosen. Solver 5 was selected for speed and accuracy.

2. COMPARISON OF COOLING CURVES MAGNESIUM ALLOY AM60

Figure 7-1 presents typical magnesium alloy AM60 experimental results of temperature measurements while the 5-step casting was squeezed under an applied pressure of 60 MPa with a melt temperature of 620°C and a die temperature of 210°C . The temperature history at the center of the fifth step of the 5-step casting is represented in Figure 7-1.

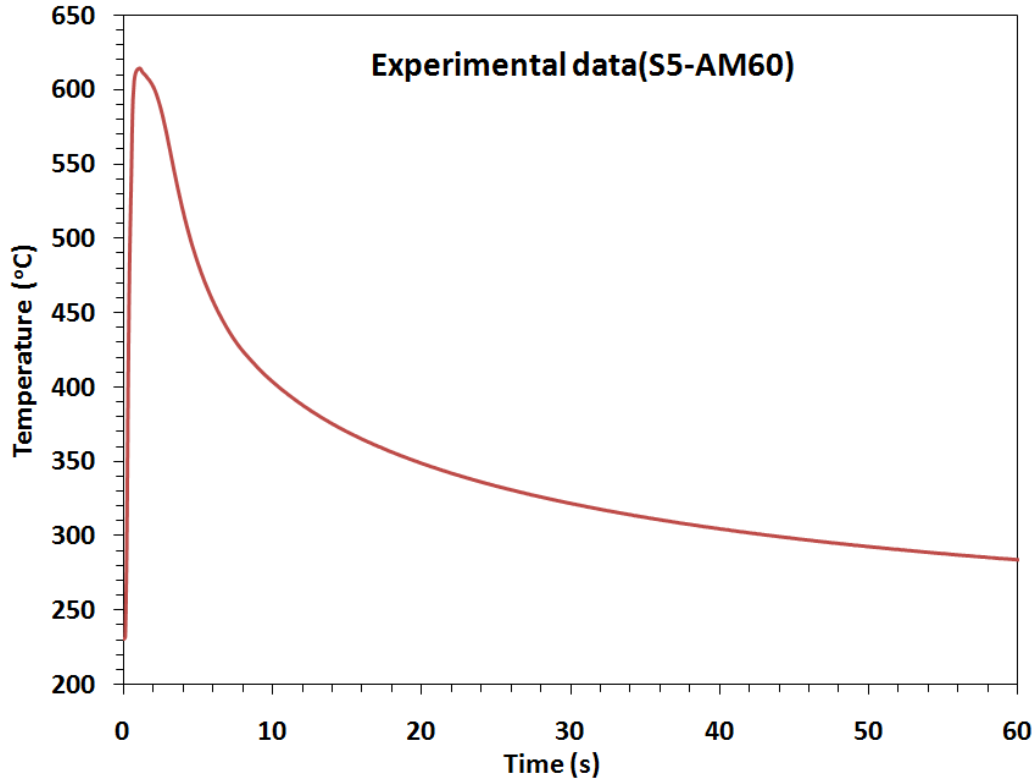
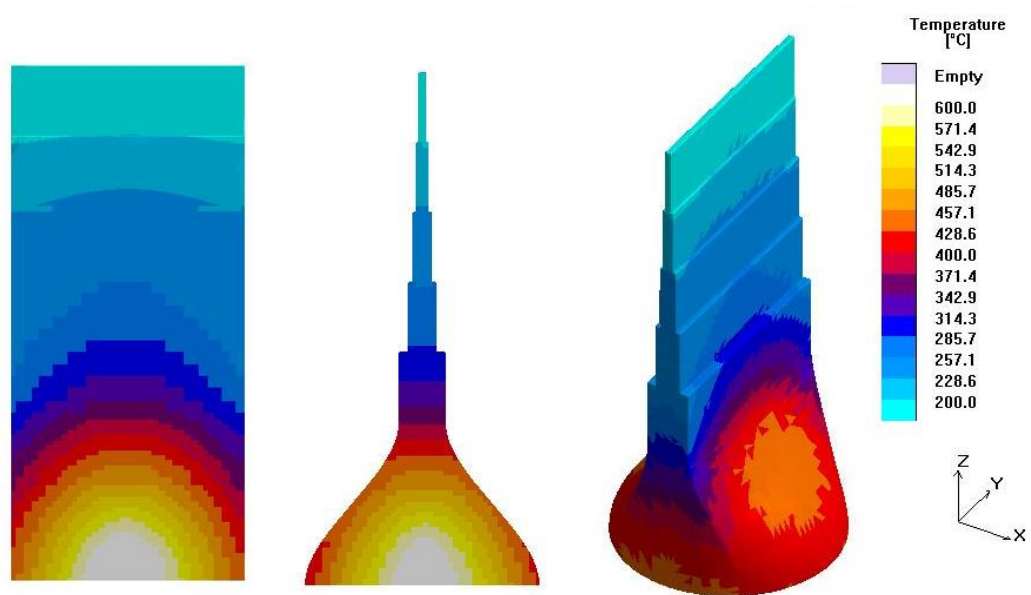


Figure 7- 1. A typical experimental cooling curve at the center of Step 5 (AM60) under an applied pressure of 60 MPa.

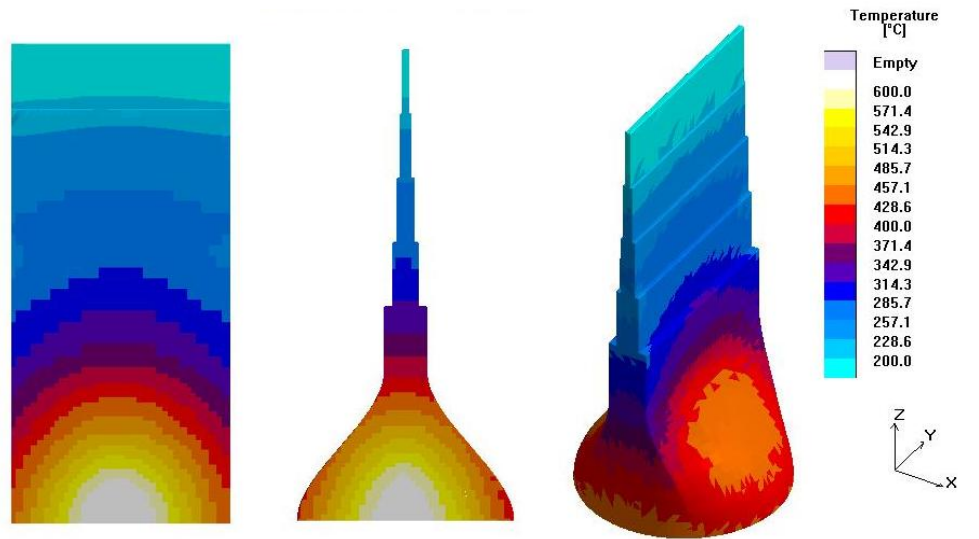
During experiments, after the commencement of the process, the temperature increase at the center of Step 5 was recorded by the first segment of cooling curve till the melt was filled into cavity. Before the filling was completed, the center of the casting as the last solidification area was cooled at a slower rate than its outer portion. The highest temperature of 614.8 °C just around the liquidus temperature (615°C) at the center was able to maintain at the liquidus solidus mush state and then dropped quickly[5]. This observation indicates that pre-solidification occurred in the 5-step casting adjacent to the casting/die interface during filling. As solidification time further increased, the temperature at the center of Step 5 decreased toward the solidus temperature within 6 seconds and the temperature decreased below 300°C after 60 second.

To compare the simulation prediction with the experimental data, MAGMASoft was employed to conduct the simulation. For the verification of the identified IHTC, the temperature distribution was calculated by feeding the different IHTC into the MAGMASoft with the same materials and process parameters, and then compared to the measured temperatures at the corresponding location.

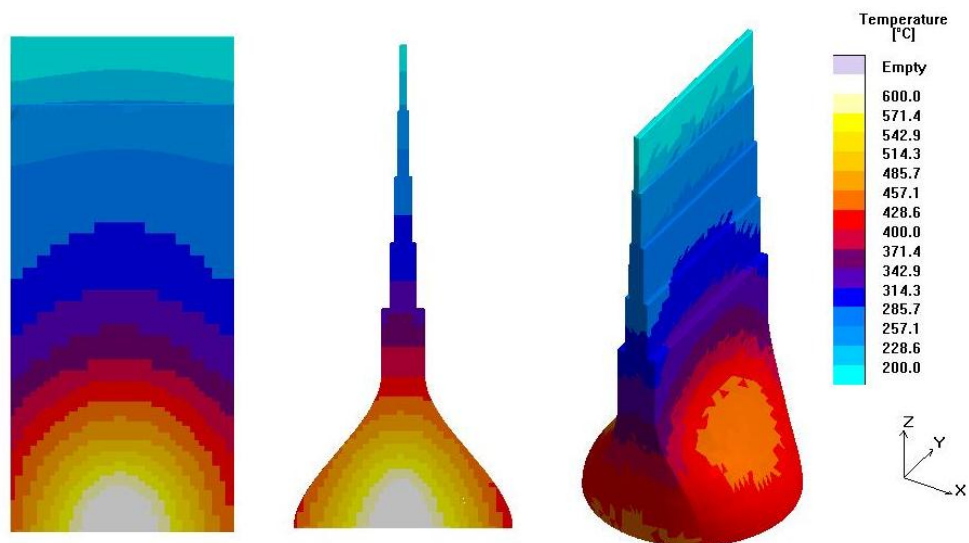
Three different heat transfer coefficient(HTC) values were applied to the prediction calculation: (1) a constant of C7000 from MAGMASoft database[4]; (2) the heat transfer coefficient calculated from Alfred Yu[6]’s research; (3) the heat transfer coefficients calculated by the inverse method presented in Chapters 4 and 6[1,3]. Figure 7-2 shows the temperature distribution inside the 5-step casting simulated with the input of three selected different HTC values when 80% volume of the casting was solidified.



(a)



(b)



(c)

Figure 7- 2 Temperature distribution inside the 5-step casting (80% solidified) of AM60 simulated with the input of HTC, (a) C7000, (b) Yu's research and (c) the Inverse Method.

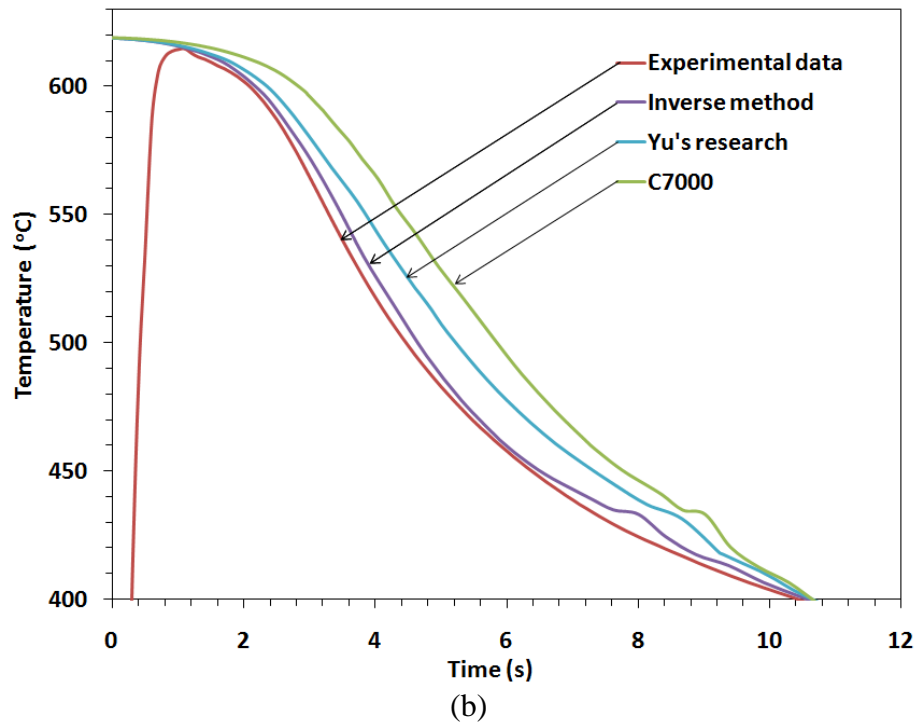
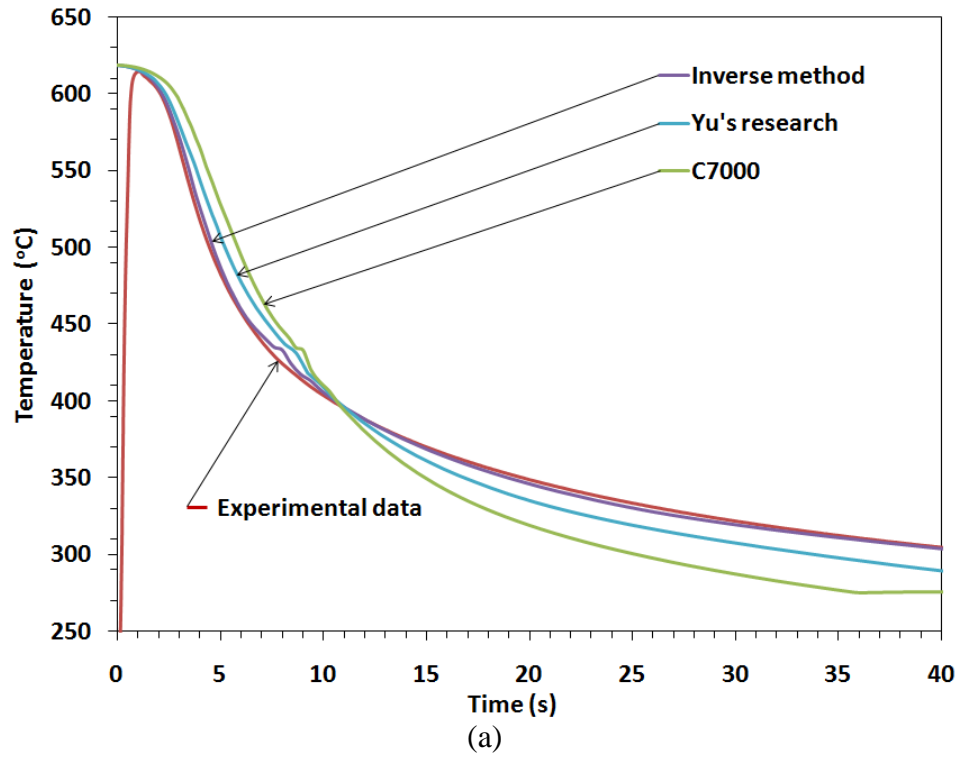


Figure 7- 3 Comparison of the experimental and computational cooling curves at the center of Step 5(AM60) under an applied pressure of 60MPa, (a) the entire cooling period, and (b) the enlarged solidification region.

As shown in Figure 7-3, the green curve presents the computed results by applying the constant HTC C7000 from the MAGMASoft database. It appeared that, an underestimation of the HTC ($7000 \text{ W/m}^2\text{K}$) occurred at the early stage of the solidification process since the computed temperatures were quite higher than the experimental measurements. As the solidification proceeded after 11 seconds, however, the measured temperature history moved upward and stayed above the numerical prediction. The input of $7000 \text{ W/m}^2 \text{ K}$ seemed to be overestimated.

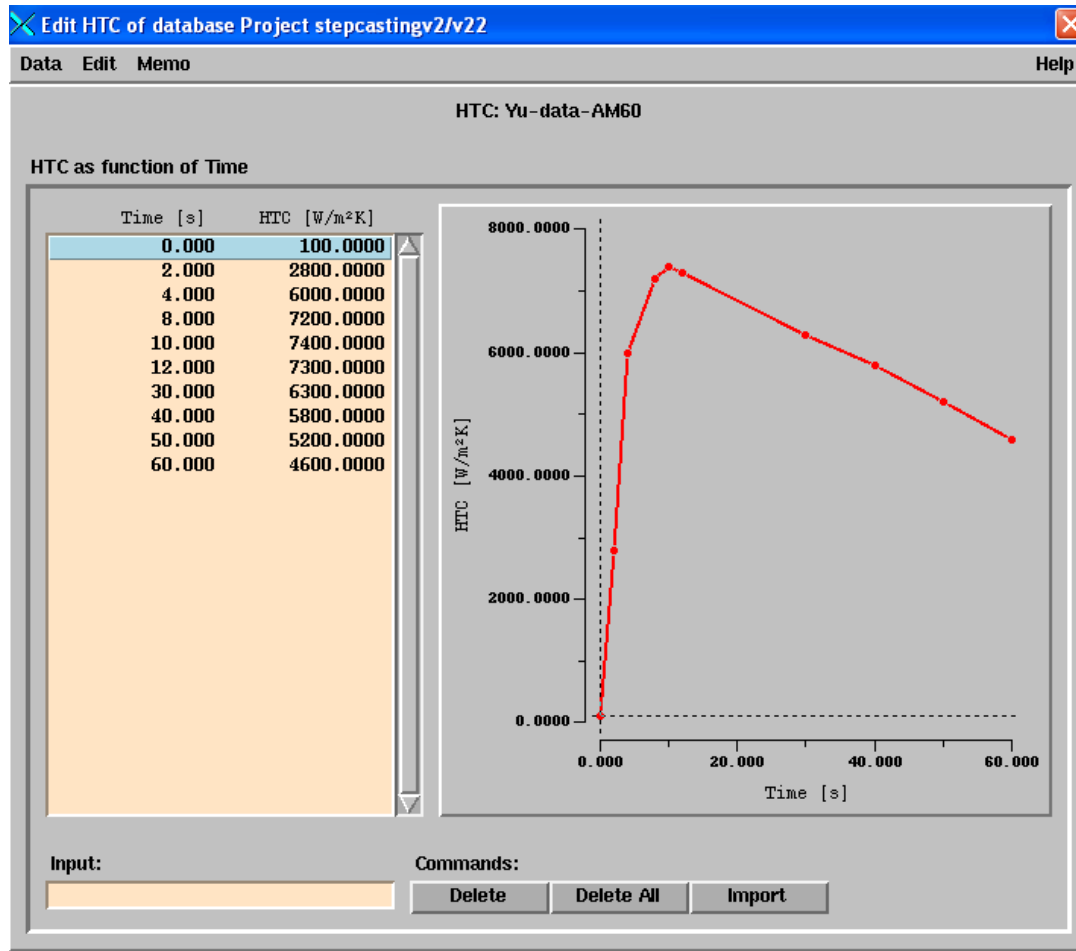


Figure 7- 4 Yu's IHTC data applied to MAGMASoft simulation (AM60).

Figure 7-4 shows the IHTC curve of Yu's research data[6] applied in MAGMASoft when calculate the solidification temperature at the center of Step 5. The blue curve was predicted by applying Yu's research data. It can be observed that a small deviation between the prediction and experimental data. The simulation was improved by Alfred Yu's research data over the adoption of a simple constant (7000 W/m² K). But, the underestimation and overshooting of the HTC also took place at the early and later stages of the solidification process, respectively.

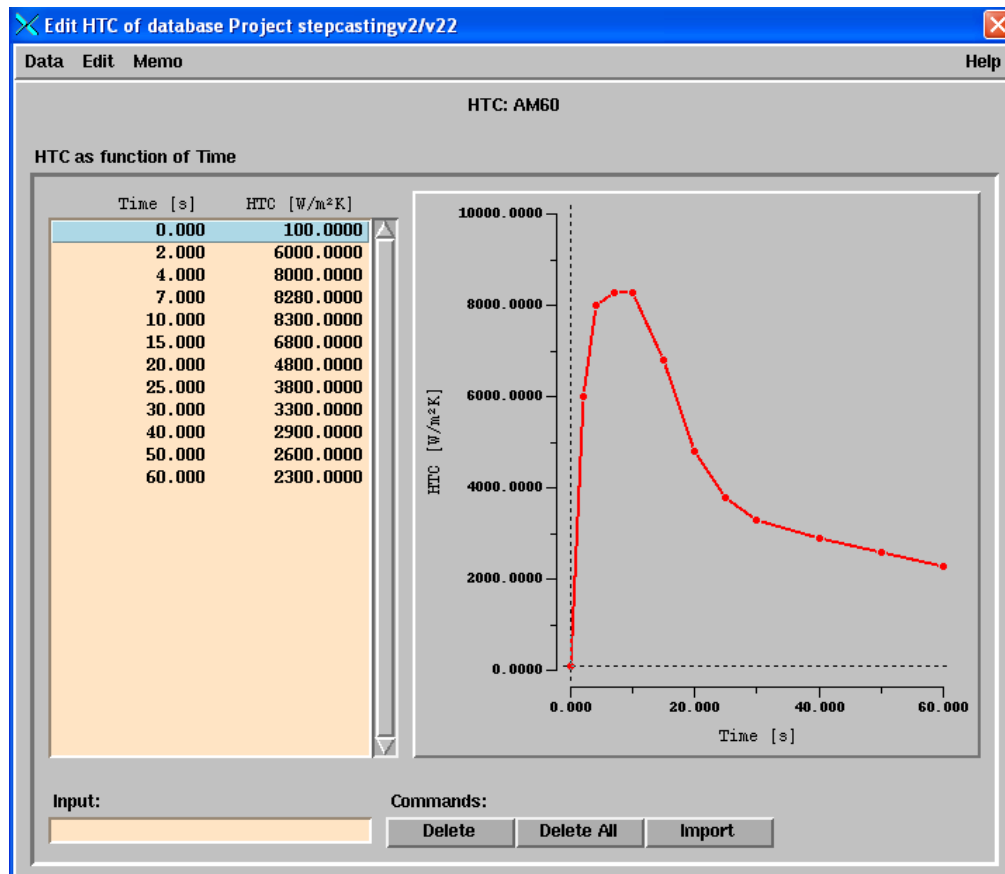


Figure 7- 5 IHTC derived from the inverse method data applied to MAGMASoft simulation (AM60).

Figure 7-5 shows the IHTC curve data applied in MAGMASoft when calculate the solidification temperature at the center of Step 5. All the IHTC data were derived from Chapter 4 by the inverse method. The purple curve in Figure 7-3 represents the simulated temperatures by applying the inverse method and the HTC data from Chapter 4. A little deviation between the experimental measurements and the computed temperatures was observed in the region of the solidus temperature. This may be attributed to the fact that the inverse method calculated the HTCs based on the temperatures measured in the mould which is outside the casting, because it is almost impossible to precisely measure the temperatures at the casting centre.

The computational output from the inverse method has the best agreement with experimental data compared to those resulting from other methods. The maximal temperature differences were less than 9°C and the mean temperature differences were less than 3.8°C between the numerical calculation of the inverse method and experimental measurements. The results confirm that the inverse method can be applied to determine the IHTC between the castings and mould accurately and reliably.

3. COMPARISON OF COOLING CURVES ALUMINUM ALLOY A443

Figure 7-6 presents the typical experimental results of temperature measurements while the 5-step casting of aluminum alloy A443 was squeezed under an applied pressure of 60MPa with a melt temperature of 620°C and a die temperature of 210°C .

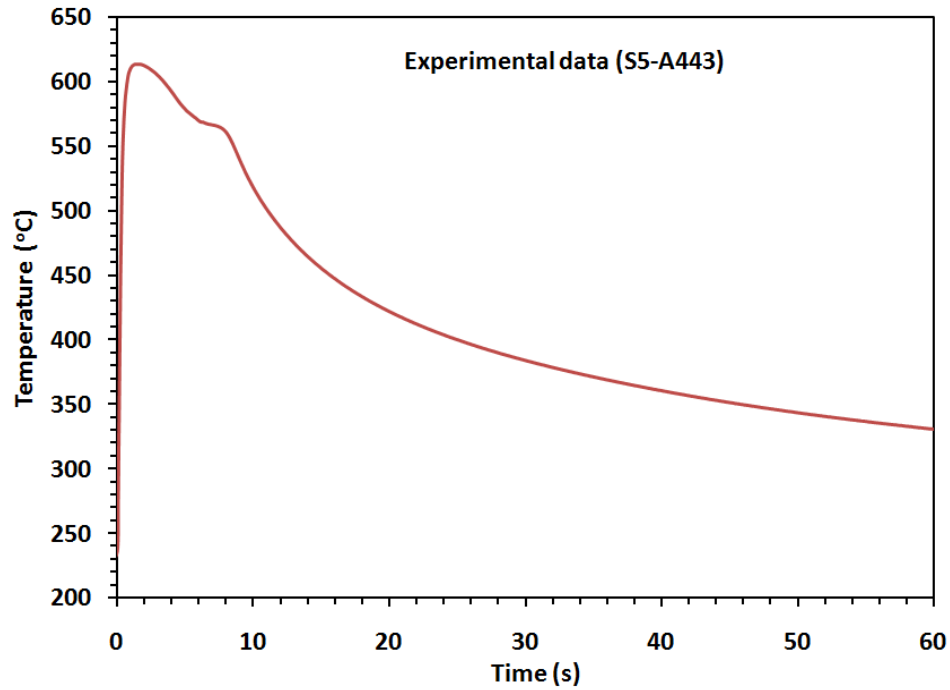
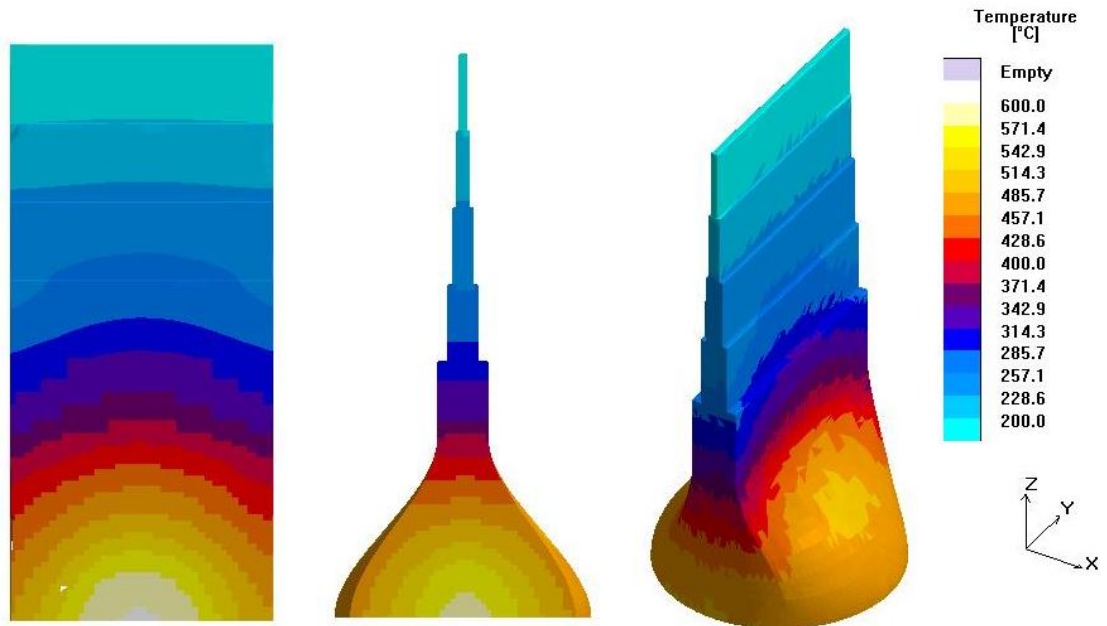


Figure 7- 6 A typical cooling curve at the center of Step 5 of Al A443 squeeze cast under an applied pressure of 60 MPa.

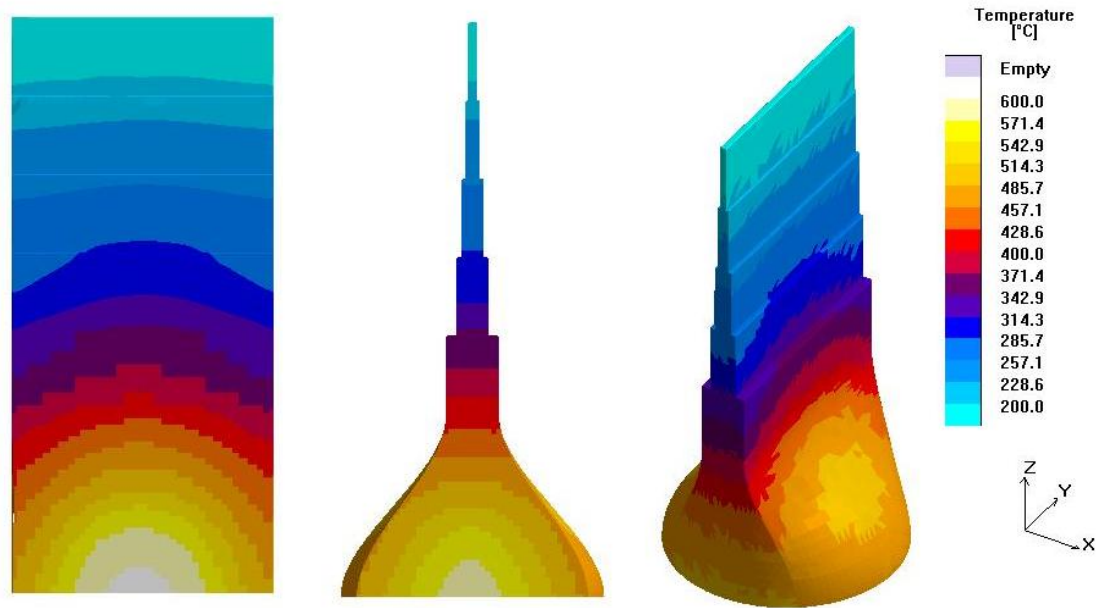
During the experiment, after the commencement of the process, the temperature rise at the center of Step 5 was recorded by the first segment of cooling curve till the melt was filled into the mould cavity. The temperature of 619.3 °C just around the liquidus temperature (619°C) at the center was able to maintain the melt at the liquidus temporarily and then dropped quickly. The second plateau of the solidus temperature(574°C) was maintained for 3 seconds. This observation indicates that the solidification completion occurred in the center of 5-step casting during this stage. As solidification time further increased, the temperature at the center of Step 5 decreased smoothly below 350°C after 60 seconds.

To compare the numerical prediction with the experimental data, MAGMASoft was employed to conduct the simulation of the step casting. For the verification of the identified IHTC, the temperature distribution was calculated by feeding the different IHTCs into the MAGMASoft with the same materials and process parameters, and then compared to the measured temperatures at the corresponding location.

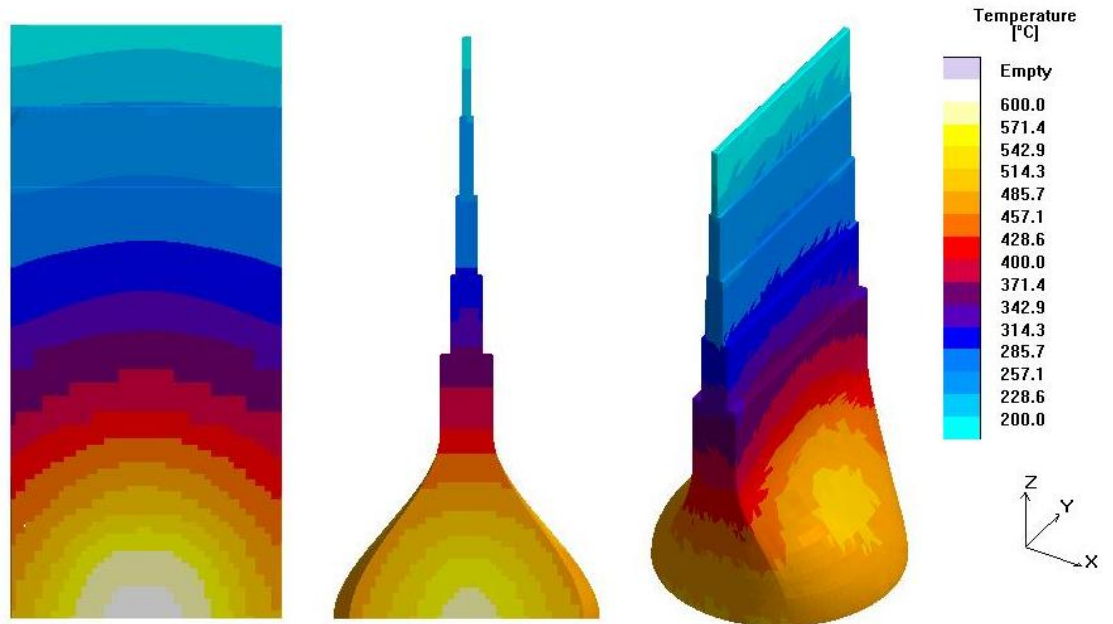
Three types of heat transfer coefficient(HTC) were applied in the prediction calculation: (1) the constant C7000 from MAGMASoft database[4]; (2) the heat transfer coefficient calculated from Alfred Yu[6]’s research; and (3) the heat transfer coefficient calculated by the inverse method presented in Chapter 5 [1,2]. The temperature profiles inside the casting of aluminum alloy A443 are shown in Figure 7-7, which were computed with the boundary conditions of different HTC values when 80% volume of the casting was solidified.



(a)

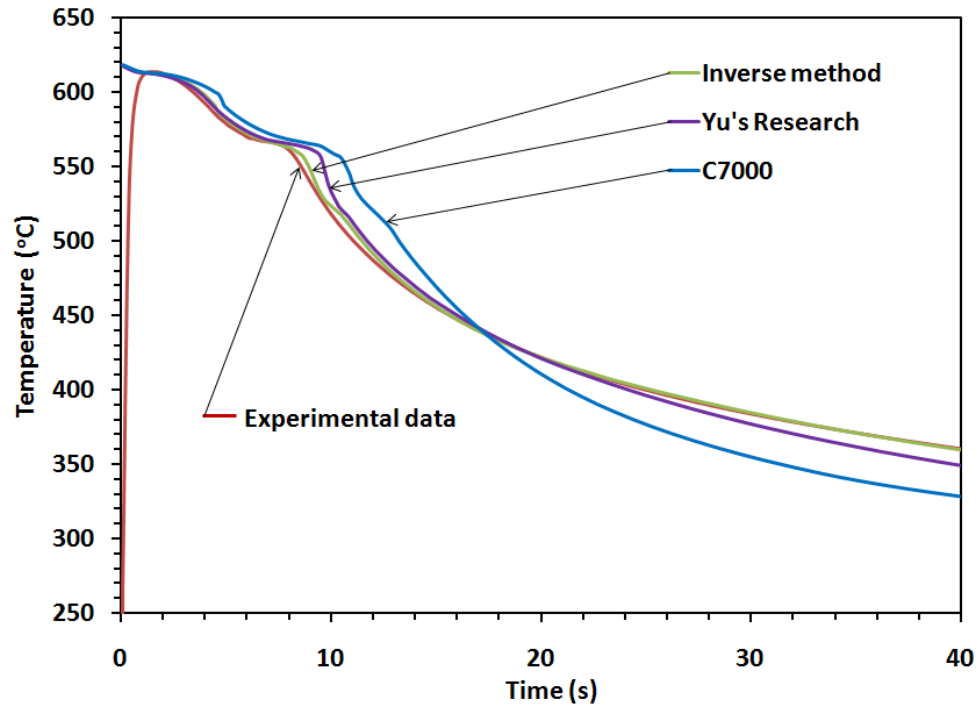


(b)

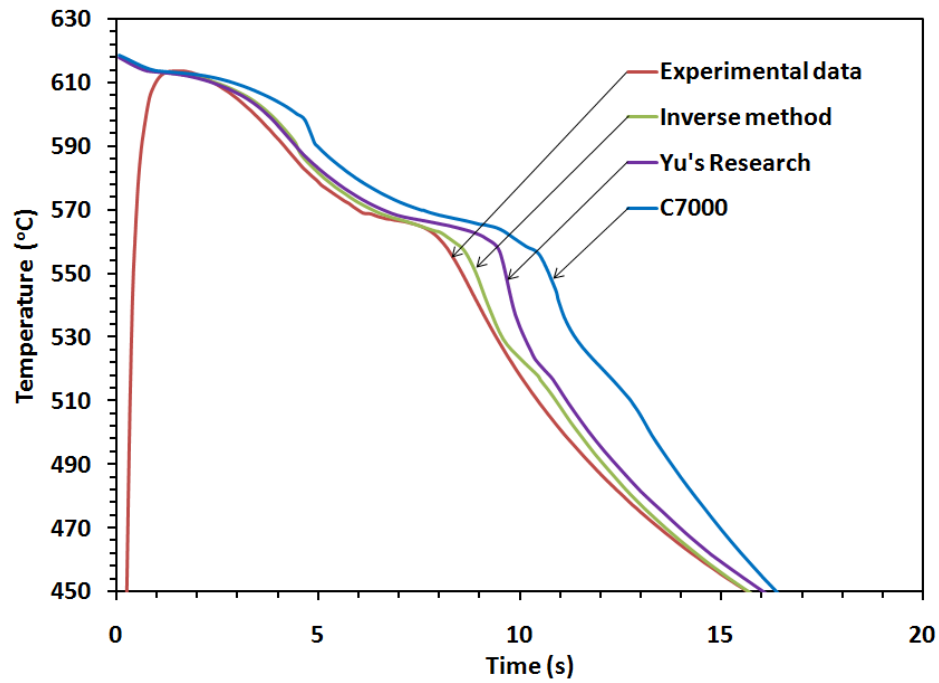


(c)

Figure 7- 7 Temperature distribution inside the 5-step casting (80% solidified) of Al A443 simulated with the input of HTC, (a) C7000, (b) Yu's research and (c) the Inverse Method.



(a)



(b)

Figure 7- 8 Comparison of the experimental and computational cooling curves at the center of Step 5 (A443) under an applied pressure of 60MPa, (a) the entire cooling period, and (b) the enlarged solidification region.

The curve in Figure 7-8 representing the predicted temperatures by applying the constant HTC C7000 from the MAGMASoft database somewhat deviates from the experimental measurements. It seems that the implementation of a constant HTC failed the precise prediction.

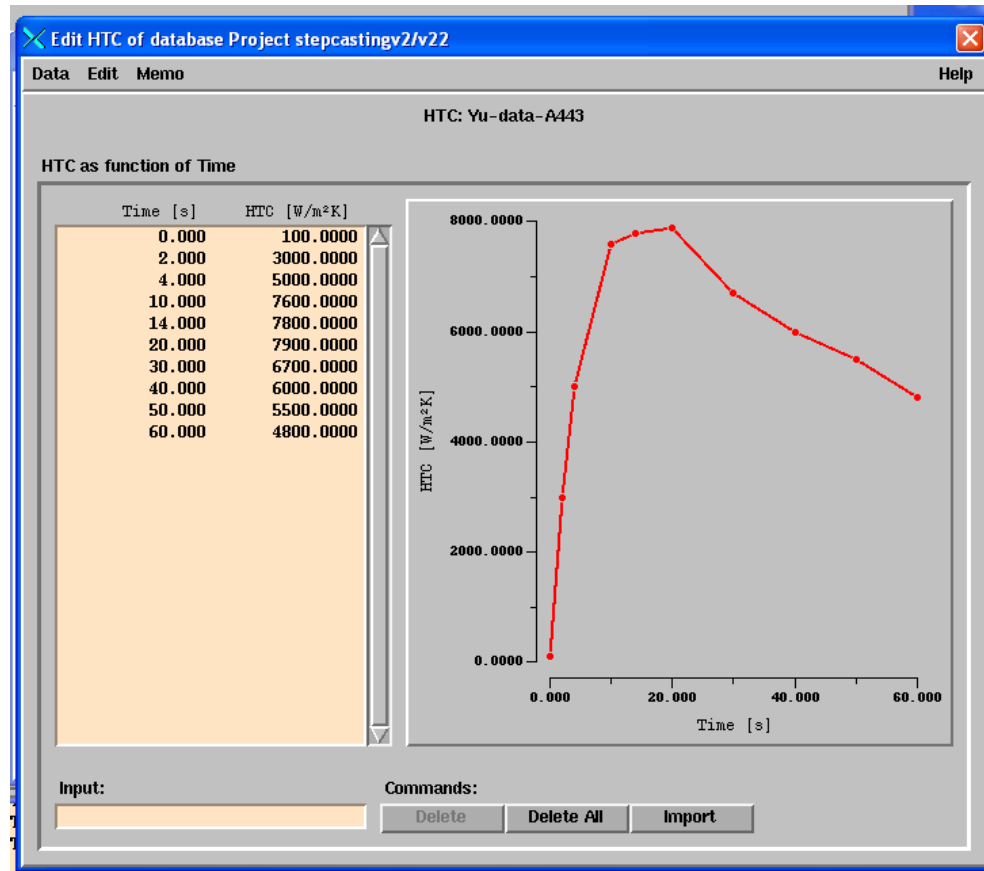


Figure 7- 9 The Yu's IHTC data applied in MAGMASoft simulation(A443).

Figure 7-9 shows the IHTC curve from Yu's research data[6] applied to MAGMASoft for the calculation of the solidification temperatures at the center of Step 5. The curve simulated by applying the Yu's research data[6] indicated an reduction in the deviation between the prediction and experimental data.

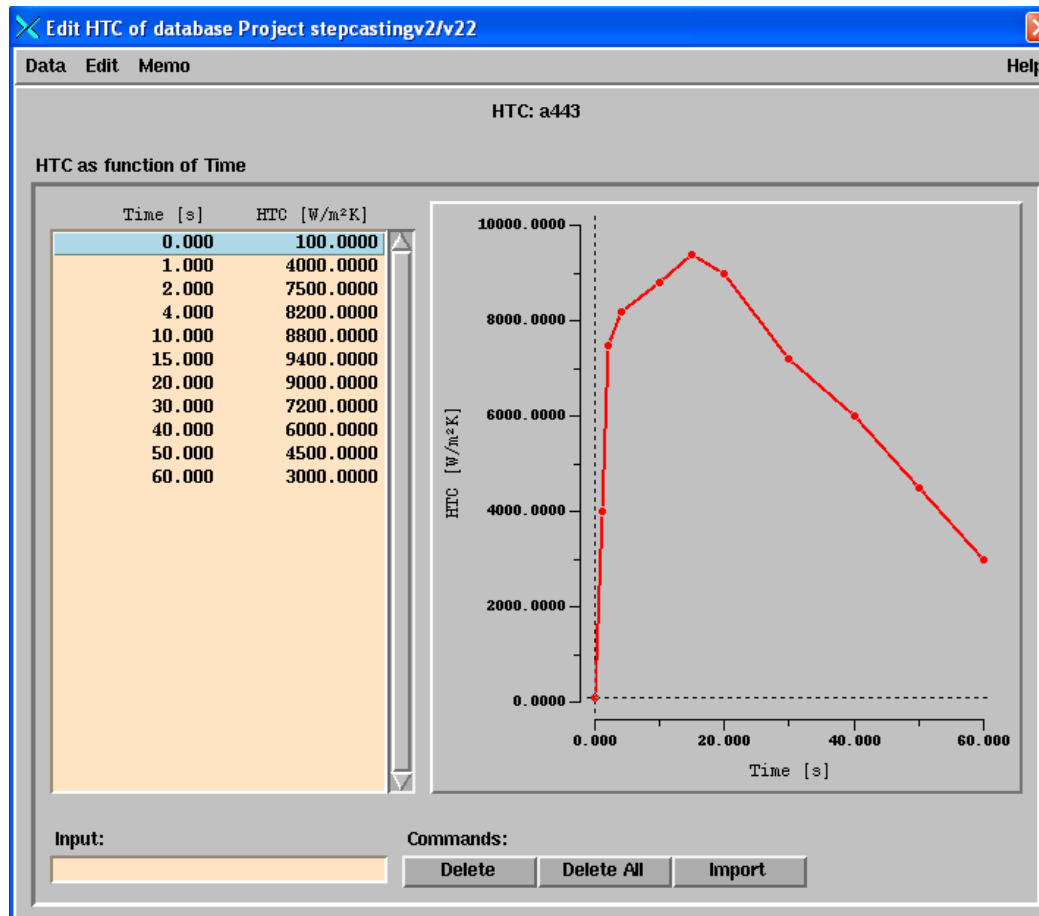


Figure 7- 10 The inverse method IHTC data applied in MAGMASoft simulation(A443).

Figure 7-10 shows the IHTC data were derived by the inverse method presented in Chapter 5. The cooling curve in Figure 7-8 computed by applying the IHTC data of the inverse method shows a good agreement between the predictions and the measured temperature history. The average temperature differences are less than 4.5°C between the numerical calculation and measurements.

The results confirm again that the inverse method can be applied to identify the IHTCs between the aluminum castings and mould accurately and reliably as well. The inaccuracy in the determination of IHTC should be responsible for the deviation.

4. SUMMARY

The correctness of inverse method has been verified through the comparison between numerical calculated and experimental results based on the various IHTC values obtained from three methods. The results show that the IHTC values derived from the inverse method provide the best agreement with the experimental measurements for squeeze casting both magnesium AM60 and aluminum A443 alloys . It is adequately demonstrated that the inverse method is a feasible and effective tool for determination of the casting-mould IHTC.

REFERENCE

- [1] Z.Z. Sun, H. Henry, X.P. Niu, 2011. Determination of heat transfer coefficients by extrapolation and numerical inverse methods in squeeze casting of magnesium alloy AM60. *J. Mater. Process. Technol.* (2011) Vol. 211, pp. 1432-1440.
- [2] Z. Z. Sun, X. P. Niu, H. Hu, “Effects of local pressure and wall-thickness on interfacial heat transfer in squeeze casting of magnesium alloy AM60”, *Proceedings of the 7th International Conference on Computational Heat and Mass Transfer(ICCHMT-7), Istanbul, Turkey, (July 18-22, 2011)*, Accepted.
- [3] Z. Z. Sun, H. Hu, X.P. Niu, “Section thickness-dependant interfacial heat transfer in squeeze casting of aluminum alloy A443”, *The 3rd International Conference on Advances in Solidification Processes(ICASP-3), Aachen, Germany (June 7-10, 2011)*, Accepted.
- [4] MAGMASOFT® (version 4.4) Release Notes and Manual, (2006).
- [5] Magnesium and Magnesium Alloys. ASM Speciality Handbook, ed. M.M. Avedesian and H. Baker. ASM International, 2000.
- [6] A. Yu, “Mathematical modeling and experimental study of squeeze casting of magnesium alloy AM50A and aluminum alloy A356”, Ph.D. dissertation, Dept. of mechanical, automotive & materials engineering, University of Windsor. 2007.

CHAPTER 8

GENERAL CONCLUSIONS AND FUTURE WORK

1. GENERAL CONCLUSIONS

In order to fulfill the objectives stated in Chapter 1, a 5-step casting was developed to characterize the IHTC, local in-cavity pressures, and observe heat transfer phenomena taking place in squeeze casting of magnesium alloy AM60 and aluminum alloy A443. The inverse modeling method developed in this study was aimed to determinate the interfacial heat transfer coefficient(IHTC) precisely. The main conclusions from this study can be summarized as following:

1. A mathematical model based on FDM and inverse method has been developed for numerical determination of IHTCs for squeeze casting of light alloys;
2. A comparative study of polynomial and inverse method was carried out. The calculated results show that the heat flux and IHTC evaluated by the inverse method were more accurate than those of the extrapolated fitting method;
3. The effect of section thicknesses on the IHTCs of two light alloys, AM60 and A443, was determined successfully by employing the 5-step casting design;
4. For magnesium alloy AM60, the IHTC values increased and reached its peak value, then dropped gradually. With applied pressure 30MPa, the peak IHTC values at steps 1, 2, 3, 4, and 5 (section thickness 3, 5, 8, 12, and 20 mm) varied from 2807 W/m²K, 2962 W/m²K, 3874 W/m²K, 6005 W/m²K to 7195 W/m²K. With applied pressure 60MPa, the peak IHTC values varied from 4662 W/m²K, 5001 W/m²K, 5629 W/m²K, 7871 W/m²K and 8306 W/m²K. With applied pressure 90MPa, the peak IHTC values varied from 5623 W/m²K, 5878 W/m²K,

6783 W/m²K, 9418 W/m²K and 10649 W/m²K. The peak IHTC value decreased as the step became thinner. With the applied pressure increased, the IHTC peak value of each step was increased accordingly.

5. For aluminum alloy A443, with applied pressure 30MPa, the peak IHTC values at steps 1, 2, 3, 4, and 5 (section thickness 3, 5, 8, 12, and 20 mm) varied from 4944 W/m²K, 5332 W/m²K, 5460 W/m²K, 6546 W/m²K to 7441 W/m²K. With applied pressure 60MPa, the peak IHTC values varied from 5629 W/m²K, 6037 W/m²K, 6351 W/m²K, 8125 W/m²K and 9419 W/m²K. With applied pressure 90MPa, the peak IHTC values varied from 6377 W/m²K, 7672 W/m²K, 8046 W/m²K, 10414 W/m²K and 11249 W/m²K. Compared with AM60, higher IHTC values were achieved between die and casting. It took longer time to reach their peak values and decrease slower than those of AM60.
6. The in-cavity local pressures at the interface of step casting and die rose abruptly to its peak value, then decreased gradually until the pressure-transfer path died out. The pressure-transfer path extended longer as the applied hydraulic pressure increased. For aluminum alloy A443, with applied hydraulic pressure 30 MPa, the local pressure values at steps 1, 2, 3, 4, and 5 varied from 2.4, 5.3, 8.4, 12.9, 21.2 MPa. With applied hydraulic pressure 60 MPa, the local pressure values at steps 1, 2, 3, 4, and 5 varied from 4.5, 9.2, 14.6, 24.7, 36.4 MPa. With applied hydraulic pressure 90 MPa, the local pressure values at steps 1, 2, 3, 4, and 5 varied from 10.1, 18.8, 28.7, 38.2, 52.1 MPa. For magnesium alloy AM60, with applied hydraulic pressure 30 MPa, the local pressure values at steps 1, 2, 3, 4, and 5 varied from 2.3, 4.2, 7.1, 12.1, 17.3 MPa. With applied hydraulic pressure 60

MPa, the local pressure values at steps 1, 2, 3, 4, and 5 varied from 3.7, 7.1, 13.3, 21.7, 34.6 MPa. With applied hydraulic pressure 90 MPa, the local pressure values at steps 1, 2, 3, 4, and 5 varied from 9.8, 15.2, 25.1, 35.2, 49.8 MPa.

7. The wall thickness affected IHTC peak values significantly. The peak IHTC values and heat fluxes increased as the steps became thick.
8. The large difference in temperatures between the melt and the die with thick cavity sections as well as relatively high localized pressure should be responsible for the high peak IHTC values observed at the thick steps.
9. The time for IHTC to obtain the peak value during the initial stage increased as the step became thicker.
10. The empirical equations and curve planes diagrams of all steps relating IHTC to the local pressures and temperature at the casting surface were developed and demonstrated.

In conclusion, the IHTCs application to the solidification simulation of the 5-step casting verified that the inverse method developed in this study is an effective and precise approach for the determination of interfacial heat transfer coefficients(IHTCs) in light metal squeeze casting.

2. SUGGESTIONS FOR FUTURE WORK

Suggested future work for the squeeze casting process may include the following:

- Extending the developed inverse method to determine the IHTC in squeeze casting of complex industrial components;
- Improving the local in-cavity pressure model by extending the experimental study of in-cavity pressures to the real casting components;
- Developing a mathematical model to simulate the casting internal pressure distribution so that it can be used to predict local pressures accurately in advance during squeeze casting;
- Incorporating the developed IHTC data based on the inverse method to the database of simulation software, such as MAGMASoft, and Flow3D;
- Analyzing microstructures in individual steps to establish the correlation between microstructures and section-thicknesses;
- Developing a heat transfer-related phase change model based on the relation between microstructures and section-thicknesses to predict microstructure evolution of magnesium and aluminum alloys during pressurized solidification and the formation of defects inside the castings.

CHAPTER 9

STATEMENT OF ORIGINALITY

The following aspects of this study, in the author's opinion, are novel and distinct contributions to original knowledge:

- A mathematical model was developed to simulate heat transfer phenomena which took place during squeeze casting of magnesium and aluminum alloys. In the model, inverse algorithm was employed to numerical determination of interfacial heat transfer coefficients(IHTCs) based on function specification method.
- Establishment of a technique involving both experiment and computation to determine the characteristics of IHTCs and local cavity pressures at various wall thicknesses during squeeze casting of aluminum and magnesium alloys.
- The empirical equations at different casting thicknesses relating IHTCs to the local pressures and temperatures were developed.

APPENDIX A

COPYRIGHT RELEASES FROM PUBLICATIONS

CHAPTER 2

License Number	2790320934326
License date	Nov 15, 2011
Licensed content publisher	Springer
Licensed content publication	Heat and Mass Transfer
Licensed content title	Numerical simulation of heat transfer in pressurized solidification of Magnesium alloy AM50
Licensed content author	Zhizhong Sun
Licensed content date	Jan 1, 2011
Volume number	47
Issue number	10
Type of Use	Thesis/Dissertation
Portion	Full text
Number of copies	5
Author of this Springer article	Yes and you are the sole author of the new work
Order reference number	PhD-Diss
Title of your thesis / dissertation	MODELING AND EXPERIMENTAL STUDY ON HEAT TRANSFER IN SQUEEZE CASTING OF MAGNESIUM ALLOY AM60 AND ALUMINUM ALLOY A443
Expected completion date	Nov 2011
Estimated size(pages)	200
Total	0.00 USD

From: <CustomerCare@copyright.com>
Subject: RE: Request for permission to include the paper in my dissertation [pfCase:324051, pfTicket:5395607]
Date: Tue, 15 Nov 2011 11:06:12 -0500
To: Sun Zhizhong <sun11@uwindsor.ca>



Dear Sun Zhizhong

Thank you for contacting Copyright Clearance Center's Rightslink® service. Rightslink is a licensing service that provides permission for the reproduction and distribution of copyrighted materials in print and electronic formats on behalf of rightsholders who list their titles with us. Rightslink is a service that is accessed directly through a publisher's website. Please be aware that the types of licenses offered are established by each individual rightsholder, and will vary.

As the author of the published paper, you have the right to include the article in full or in part in a thesis or dissertation (provided that this is not to be published commercially).

Getting Started:

Please go to the participating publisher's website and search for 1) the journal and 2) the article of interest by volume/issue/page number. Click on "Request Permission" (or similar link), and you will be directed to the Rightslink order page.

You can obtain a price quote in advance by using the "quick price" button. Please note that any fees are set by the publisher, and not by Rightslink, which is a service that acts on behalf of the publisher. Before you can place a license order, kindly create an account with Rightslink (click "Create Account"). After you complete the 2-page account creation, you will be able to submit your order.

For your convenience the following is a link to the article where you will find the Permissions & Reprints link:
<http://www.springerlink.com/content/k8w00v8410137171/>.

If you have any further questions, please contact a Rightslink Customer Care Representative at 978-646-2777, Monday-Friday 8:00 to 6:00 EST, or email customercare@copyright.com.

Sincerely,

Ben Delatizky

Customer Service Representative, Rightslink

Copyright Clearance Center

222 Rosewood Drive

Danvers, MA 01923

+1 877-622-5543 Toll Free

+1 978-646-2600 Main

+1 978-646-8600 Fax

www.copyright.com

****Please include all prior email correspondence in your reply so that we may better serve you and provide you with a more timely response.**

From: Sun Zhizhong [mailto:sun11@uwindsor.ca]
Sent: Tuesday, November 15, 2011 09:08 AM
To: permissions.dordrecht@springer.com; permissions.heidelberg@springer.com
Cc: customercare@copyright.com
Subject: Request for permission to include the paper in my dissertation [pfCase:324051, pfTicket:5395607]

Dear Sir/Mdm,

I am completing a doctoral dissertation at the University of Windsor entitled " Modeling and Experimental Study on Heat Transfer in Squeeze Casting of magnesium alloy AM60 and aluminum Alloy A443" I would like your permission to include in my dissertation the following paper:

Zhizhong Sun, Xuezhi Zhang, Xiaoping Niu, Alfred Yu, Henry Hu, "Numerical simulation of heat transfer in pressurized solidification of Magnesium alloy AM50", *Heat and Mass Transfer/Waerme- und Stoffuebertragung*, (2011) Vol. 47, pp. 1241-1249.

My thesis will be deposited to the University of Windsor Leddy library or University of Windsor's online theses and dissertations repository (<http://winspace.uwindsor.ca>) and will be available in full-text on the internet for reference, study and / or copy. I will also be granting Library and Archives Canada and ProQuest/UMI a non-exclusive license to reproduce, loan, distribute, or sell single copies of my thesis by any means and in any form or format. These rights will in no way restrict republication of the material in any other form by you or by others authorized by you.

Please confirm in writing or by email that these arrangements meet with your approval.

Thank you very much for your attention to this matter.

Sincerely,

Zhizhong Sun

*Ph.D. Candidate,
Dept. of Mechanical, Automotive, & Materials Engineering
University of Windsor
401 Sunset Avenue
Windsor, Ontario, N9B 3P4
Phone: (519) 997 3503*

CHAPTER 3

From: Matt Baker <mbaker@tms.org>
Subject: RE: Ask permission to include my paper to my Ph.D doctoral dissertation
Date: Wed, 13 Jul 2011 07:40:43 -0400
To: Sun Zhizhong <sun11@uwindsor.ca>



Dear Sun, Zhizhong:

TMS grants you permission to include your article, "Estimation of heat transfer coefficient in squeeze casting of magnesium alloy AM60 by experimental polynomial extrapolation method" , by Zhizhong Sun, Xiaoping Niu, Henry Hu, the proceedings of Magnesium Technology 2011, as a chapter in your doctoral dissertation, with the understanding that you include a credit line on the page of the dissertation, which should indicate the original source of the material. Please let me know if you have any further questions about this.

Best regards,

Matt Baker

Matt Baker | The Minerals, Metals & Materials Society

Content Specialist

TMS

184 Thorn Hill Road, Warrendale PA 15086

724.814.3176 Direct | 724.814.3177 Fax | 800.759.4TMS (Ext. 280) Toll Free

mbaker@tms.org | <http://www.tms.org>

CHAPTER 4

Supplier	Elsevier Limited The Boulevard, Langford Lane Kidlington, Oxford, OX5 1GB, UK
Registered Company Number	1982084
Customer name	Zhizhong Sun
Customer address	401 sunset Ave. Windsor, ON N9B3P4
License number	2787271059193
License date	Nov 13, 2011
Licensed content publisher	Elsevier
Licensed content publication	Journal of Materials Processing Technology
Licensed content title	Determination of heat transfer coefficients by extrapolation and numerical inverse methods in squeeze casting of magnesium alloy AM60
Licensed content author	Zhizhong Sun, Henry Hu, Xiaoping Niu
Licensed content date	August 2011
Licensed content volume number	211
Licensed content issue number	8
Number of pages	9
Start Page	1432
End Page	1440
Type of Use	reuse in a thesis/dissertation
Portion	full article
Format	both print and electronic
Are you the author of this Elsevier article?	Yes
Will you be translating?	No
Order reference number	JMPT-1108
Title of your thesis/dissertation	MODELING AND EXPERIMENTAL STUDY ON HEAT TRANSFER IN SQUEEZE CASTING OF MAGNESIUM ALLOY AM60 AND ALUMINUM ALLOY A443
Expected completion date	Nov 2011
Estimated size (number of pages)	200
Elsevier VAT number	GB 494 6272 12
Permissions price	0.00 USD
VAT/Local Sales Tax	0.0 USD / 0.0 GBP
Total	0.00 USD

From: "EP Support" <support@elsevier.com>

Subject: Request for permission to include the paper in my dissertation [PROTEC13101] [Reference: 111111-003425]



Date: Sun, 13 Nov 2011 15:43:34 +0000 (GMT)
To: sun11@uwindsor.ca

Subject

Request for permission to include the paper in my dissertation [PROTEC13101]

Discussion

Response Via Email(Deborah) - 13/11/2011 03.43 PM

Dear Mr. Sun,

Thank you for your e-mail.

We wish to advise, that as the author of the published paper, you have the right to include the article in full or in part in a thesis or dissertation (provided that this is not to be published commercially).

You may also contact our Permissions departments directly for further information:

Natalie Qureshi
Rights Manager
Global Rights Department
Elsevier Ltd
PO Box 800
Oxford OX5 1DX
UK

Tel: (+44) 1865 843830 (UK) or (+1) 215 239 3804 (US)
Fax: (+44) 1865 853333
E-mail: permissions@elsevier.com or healthpermissions@elsevier.com

You may find this Elsevier Customer Support solution useful:
http://support.elsevier.com/app/answers/detail/a_id/565/

If responding to this e-mail, please ensure that the reference number remains in the subject line.

Should you have any additional questions or concerns, please visit our self-help site at: <http://support.elsevier.com/>. Here you will be able to search for solutions on a range of topics, find answers to frequently asked questions and learn more about EES via interactive tutorials. You will also find our 24/7 support contact details should you need further assistance from one of our customer service representatives.

Yours sincerely,

Deborah Ruth M. David

Elsevier Customer Support

Copyright 2008 Elsevier Limited. All rights reserved.
How are we doing? If you have any feedback on our customer service we would be happy to receive your comments at customerfeedback@elsevier.com

Customer By Email (Zhizhong Sun) - 11/11/2011 07.42 PM

Dear Sir/Mdm:

I am completing a doctoral dissertation at the University of Windsor entitled " Modeling and Experimental Study on Heat Transfer in Squeeze Casting of magnesium alloy AM60 and aluminum Alloy A443" I would like your permission to include in my dissertation the following material:

Zhizhong Sun, Henry Hu, Xiaoping Niu, "Determination of heat transfer coefficients by extrapolation and numerical inverse methods in squeeze casting of magnesium alloy AM60", *Journal of Materials Processing Technology*, (2011) Vol. 211, pp. 1432-1440.

My thesis will be deposited to the University of Windsor Leddy library or University of Windsor's online thesis and dissertations repository (

I will also be granting Library and Archives Canada and ProQuest/UMI a non-exclusive license to reproduce, loan, distribute, or sell single copies of my thesis by any means and in any form or format. These rights will in no way restrict republication of the material in any other form by you or by others authorized by you.

Please confirm in writing or by email that these arrangements meet with your approval.

Thank you very much for your attention to this matter.

Sincerely,

Zhizhong Sun

Ph.D. Candidate,

Dept. of Mechanical, Automotive, & Materials Engineering
University of Windsor
401 Sunset Avenue
Windsor, Ontario, N9B 3P4
Phone: (519) 997 3503

CHAPTER 5

From: <Lorenz.Ratke@dlr.de>



Subject: Re: Request for permission to include the paper in my dissertation
Date: Mon, 14 Nov 2011 08:20:11 +0000
To: <sun11@uwindsor.ca>



Dear Zhizhong Sun,

You may do so. I attach the final version of your paper, as it will appear soon. Wish you success with your PhD.

Best regards

Lorenz Ratke

Prof. Dr. Dr. h.c. Lorenz Ratke
Institute of Materials Physics in Space
German Aerospace Center, DLR
In the Helmholtz Society
51147 Cologne
Phone: 0049-2203-601-2098
Fax.: 0049-2203-61768
email: lorenz.ratke@dlr.de
Web: <http://www.dlr.de/mp>

Von: Sun Zhizhong <sun11@uwindsor.ca>
Datum: Fri, 11 Nov 2011 14:56:56 -0500
An: Lorenz Ratke <lorenz.ratke@dlr.de>
Cc: Erica Lyons <elyons@uwindsor.ca>, Svetlana Georgieva <svetlana@uwindsor.ca>
Betreff: Request for permission to include the paper in my dissertation

Dear Dr. Lorenz Ratke,

I am completing a doctoral dissertation at the University of Windsor entitled " Modeling and Experimental Study on Heat Transfer in Squeeze Casting of magnesium alloy AM60 and aluminum Alloy A443" I would like your permission to include in my dissertation the following conference paper:

Zhizhong Sun, Henry Hu, Xiaoping Niu, "Section thickness-dependant interfacial heat transfer in squeeze casting of aluminum alloy A443", *The 3rd International Conference on Advances in Solidification Processes(ICASP-3), Aachen, Germany (June 7-10, 2011)*.

My thesis will be deposited to the University of Windsor Leddy library or University of Windsor's online theses and dissertations repository (<http://winspace.uwindsor.ca>) and will be available in full-text on the internet for reference, study and / or copy. I will also be granting Library and Archives Canada and ProQuest/UMI a non-exclusive license to reproduce, loan, distribute, or sell single copies of my thesis by any means and in any form or format. These rights will in no way restrict republication of the material in any other form by you or by others authorized by you. Please confirm in writing or by email that these arrangements meet with your approval. Thank you very much for your attention to this matter.

Sincerely,

Zhizhong Sun

Ph.D. Candidate,

Dept. of Mechanical, Automotive, & Materials Engineering

University of Windsor

401 Sunset Avenue Windsor, Ontario, N9B 3P4

Phone: (519) 997 3503

APPENDIX B

SOURCE CODE OF INVERSE MODELING METHOD

MATLAB 7.9.0.529(R2009B)

Inverse_method.m

function fd1d_heat_implicit ()

```
% % MAIN is the main program for FD1D_HEAT_IMPLICIT.
%
%   FD1D_HEAT_IMPLICIT solves the 1D heat equation with an implicit method.
%
%   This function solves
%
%   
$$dU/dT - k * d^2U/dX^2 = F(X,T)$$

%
%   over the position interval [A,B] with boundary conditions
%
%   
$$U(A,T) = U_A(T),$$

%   
$$U(B,T) = U_B(T),$$

%
%   over the temperature interval [T0,T1] with initial conditions
%
%   
$$U(X,T_0) = U_0(X)$$

%
%   The code uses the finite difference method and an implicit to calculate
%   backward Euler approximation to the first derivative in time.
%
%   The finite difference form can be written as
%
%   
$$\frac{U(X,T+dt) - U(X,T)}{dt} = F(X,T+dt) + k * \frac{(U(X-dx,T+dt) - 2 U(X,T+dt) + U(X+dx,T+dt))}{dx * dx}$$

%
%   so that we have the following linear system for U at time T+dt:
%
%   
$$\begin{aligned} & - k * dt / dx / dx * U(X-dx,T+dt) \\ & + ( 1 + 2 * k * dt / dx / dx ) * U(X, T+dt) \\ & - k * dt / dx / dx * U(X+dx,T+dt) \\ & = dt * F(X, T+dt) \\ & + U(X, T) \end{aligned}$$

%
%
%   timestamp ( );
%   fprintf ( 1, '\n' );
%   fprintf ( 1, 'FD1D_HEAT_IMPLICIT\n' );
%   fprintf ( 1, ' MATLAB version\n' );
%   fprintf ( 1, '\n' );
%   fprintf ( 1, ' Finite difference solution of\n' );
%   fprintf ( 1, ' the time dependent 1D heat equation\n' );
%   fprintf ( 1, '\n' );
```

```

fprintf ( 1, '  Ut - k * Uxx = F(x,t)\n' );
fprintf ( 1, '\n' );
fprintf ( 1, ' for space interval A <= X <= B with boundary conditions\n' );
fprintf ( 1, '\n' );
fprintf ( 1, '  U(A,t) = UA(t)\n' );
fprintf ( 1, '  U(B,t) = UB(t)\n' );
fprintf ( 1, '\n' );
fprintf ( 1, ' and temperature T0 <= T <= T1 with initial condition\n' );
fprintf ( 1, '\n' );
fprintf ( 1, '  U(X,T0) = U0(X).\n' );
fprintf ( 1, '\n' );
fprintf ( 1, ' A second order difference used for Uxx.\n' );
fprintf ( 1, '\n' );
fprintf ( 1, ' A first order backward Euler difference approximation\n' );
fprintf ( 1, ' is used for Ut.\n' );

k = 5.0E-07;
%
% Set X values.
%
x_min = 0.0;
x_max = 0.3;
x_num = 11;
x_delt = ( x_max - x_min ) / ( x_num - 1 );

x = zeros ( x_num, 1 );

for i = 1 : x_num
    x(i) = ( ( x_num - i ) * x_min ...
            + ( i - 1 ) * x_max ) ...
            / ( x_num - 1 );
end
%
% Set T values.
%
t_min = 0.0;
t_max = 720.0;
t_num = 51;
t_delt = ( t_max - t_min ) / ( t_num - 1 );

t = zeros ( t_num, 1 );

for j = 1 : t_num

    t(j) = ( ( t_num - j ) * t_min ...
            + ( j - 1 ) * t_max ) ...
            / ( t_num - 1 );
end
%
% Set the initial data, for T_MIN.
%
u = zeros ( x_num, t_num );
u(1:x_num,1) = u0 ( x_min, x_max, t_min, x );
%
% The matrix A does not change with time. We can set it once,

```

```

% factor it once, and solve repeatedly.
%
a = sparse ( [], [], [], x_num, x_num );

w = k * t_delt / x_delt / x_delt;

a(1,1) = 1.0;

for i = 2 : x_num - 1
    a(i,i-1) = - w;
    a(i,i) = 1.0 + 2.0 * w;
    a(i,i+1) = - w;
end

a(x_num,x_num) = 1.0;

b = zeros ( x_num, 1 );
fvec = zeros ( x_num, 1 );

for j = 2 : t_num
%
% Set the right hand side B.
%
    b(1) = ua ( x_min, x_max, t_min, t(j) );

    fvec = f ( x_min, x_max, t_min, t(j), x_num, x );

    b(2:x_num-1) = u(2:x_num-1,j-1) + t_delt * fvec(2:x_num-1);

    b(x_num) = ub ( x_min, x_max, t_min, t(j) );

    u(1:x_num,j) = a \ b(1:x_num);

end
%
% Write data to files.
%
x_file = 'x.txt';
header = 0;
dtable_write ( x_file, x_num, 1, x, header );
fprintf ( 1, '\n' );
fprintf ( 1, ' X data written to "%s".\n', x_file );

t_file = 't.txt';
dtable_write ( t_file, t_num, 1, t, header );

fprintf ( 1, ' T data written to "%s".\n', t_file );

u_file = 'u.txt';
dtable_write ( u_file, x_num, t_num, u, header );

fprintf ( 1, ' U data written to "%s".\n', u_file );
%
% Make a product grid of T and X for plotting.
%
```

```

[ t_grid, x_grid ] = meshgrid ( t, x );
%
% Make a mesh plot of the solution.
%
mesh ( t_grid, x_grid, u );
%
% Terminate.
%
fprintf ( 1, '\n' );
fprintf ( 1, 'FD1D_HEAT_IMPLICIT\n' );
fprintf ( 1, ' Normal end of execution.\n' );
fprintf ( 1, '\n' );
timestamp ( );

return
end

function dtable_write ( output_filename, m, n, table, header )

% *****
% Parameters:
%
% Input, string OUTPUT_FILENAME, the output filename.
%
% Input, integer M, the spatial dimension.
%
% Input, integer N, the number of points.
%
% Input, real TABLE(M,N), the points.
%
% Input, logical HEADER, is TRUE if the header is to be included.
%
output_unit = fopen ( output_filename, 'wt' );

if ( output_unit < 0 )
    fprintf ( 1, '\n' );
    fprintf ( 1, 'DTABLE_WRITE - Error!\n' );
    fprintf ( 1, ' Could not open the output file.\n' );
    error ( 'DTABLE_WRITE - Error!' );
    return;
end

for j = 1 : n
    for i = 1 : m
        fprintf ( output_unit, '%14f ', table(i,j) );
    end
    fprintf ( output_unit, '\n' );
end

fclose ( output_unit );

return
end
function value = f ( a, b, t0, t, x_num, x )

```

```

% *****
%
%% F returns the right hand side of the heat equation.
%
% Parameters:
%
%   Input, real A, B, the left and right endpoints.
%
%   Input, real T0, the initial temperature.
%
%   Input, real T, the current temperature.
%
%   Input, integer X_NUM, the number of points.
%
%   Input, real X(X_NUM), the current spatial positions.
%
%   Output, real VALUE(:), the prescribed value of U(X(:),T0).
%
    value = zeros ( x_num, 1 );

    return
end

function timestamp ( )

% *****%
%% TIMESTAMP prints the current YMDHMS date as a timestamp.
%
    t = now;
    c = datevec ( t );
    s = datestr ( c, 0 );
    fprintf ( 1, '%s\n', s );

    return
end

function value = u0 ( a, b, t0, x )

% *****%
%% U0 returns the initial condition at the starting time.
%
% Parameters:
%
%   Input, real A, B, the left and right endpoints
%
%   Input, real T0, the initial time.
%
%   Input, real T, the current time.
%
%   Input, real X(:), the positions at which the initial condition is desired.
%
%   Output, real VALUE, the prescribed value of U(X,T0).
%
    value = x;
    value = 100.0;

```



```

    return
end

function value = ua ( a, b, t0, t )

% *****%
%% UA returns the boundary condition at the left endpoint.
%
% Parameters:
%
%   Input, real A, B, the left and right endpoints
%
%   Input, real T0, the initial time.
%
%   Input, real T, the current time.
%
%   Output, real VALUE, the prescribed value of U(A,T).
%
    x = a;

    value = 20;

    return
end

function value = ub ( a, b, t0, t )

% *****%
%% UB returns the boundary condition at the right endpoint.
%
% Parameters:
%
%   Input, real A, B, the left and right endpoints
%
%   Input, real T0, the initial time.
%
%   Input, real T, the current time.
%
%   Output, real VALUE, the prescribed value of U(B,T).
%
    x = b;

    value = 20;

    return
end

clear; clc;

T_m = dlmread('step1-T1T4.txt');

% M = dlmread(filename) reads from the ASCII-delimited numeric data

```

```

% file filename to output matrix M. The filename input is a string
% enclosed in single quotes. The delimiter separating data elements is
% inferred from the formatting of the file. Comma (,) is the default
% delimiter.
%

[m,~] = size(T_m);
T_c = zeros(m,4);
t_q = zeros(m,4);
t_newq = zeros(m,4);
X = zeros(m,1);
Tmp = zeros(m+1,6);
q = zeros(m+1,1);

% Define the temperature's parameters.
%

T_c(1,:) = T_m(1,1);

q(1) = 5e1;
eq = 1e0;
p = 1;
Tmp(1,1) = q(1);

t_q(p,:) = get_T(T_m,T_c,q(p),p);
newq = q(p) + eq;
t_newq(p,:) = get_T(T_m,T_c,newq,p);
X(p) = (t_newq(p,2) - t_q(p,2))/eq;
q(2)=q(p);
T_c(p+1,:) = t_q(p,:);

fd1d_heat_implicit('step1-T1T4.txt')

for p = 2:m-1
    q(p) = 5e1;
    while 1 == 1
        t_q(p,:) = get_T(T_m,T_c,q(p),p);
        T_c(p+1,:) = t_q(p,:);
        newq = q(p) + eq;
        t_newq(p,:) = get_T(T_m,T_c,newq,p);
        X(p) = (t_newq(p,2) - t_q(p,2))/eq;
        delta_q = (((T_m(p,1)-t_q(p-1,2))*X(p-1))+((T_m(p+1,1)-t_q(p,2))*X(p)))/(X(p-1)^2+X(p)^2);
        if (delta_q/q(p)) < 0.01
            Tmp(p,1) = q(p);
            break;
        else q(p) = q(p) + delta_q;
        end
    end
end

Tmp(1,2:5) = T_m(1,1);
Tmp(2:m+1,2:5) = t_q;

t = 0:m-1;
figure(5)

```

```

plot(t,Tmp(1:561,3),':',t,T_m(:,1),'--')
text(300,360,'-- T1 measured','FontSize',9)
text(300,375,'.. T1 calculated','FontSize',9)

figure(6)
plot(t,Tmp(1:561,2),':',t,Tmp(1:561,3),'t,Tmp(1:561,4),'t,Tmp(1:561,5),'t,T_m(:,2),'t')
text(300,360,'.. T0 calculated','FontSize',9)
text(300,370,'-- T1 calculated','FontSize',9)
text(300,380,'-- T2 calculated','FontSize',9)
text(300,390,'-- T3 calculated','FontSize',9)
text(300,400,'-- T4 measured','FontSize',9)

figure(7)
t = 0:m;
plot(t,q)
title('q')

t = 0:m-1;
m_c = Tmp(1:561,3)-T_m(:,1);
figure(8)
plot(t,m_c)
Tmp(1:561,6) = m_c;

dlmwrite('0421-step1-Table.txt', Tmp, 'precision', '%.2f', 'newline', 'pc');

Get_T.m

function T = get_T(T_m,T_c,q,p)
F_0 = 0.2;
alpha = 8.27e-6;
deltaT = 0.1;
k = 29.5;
deltaX = 2e-3;

A = [(1+2*F_0), -2*F_0, 0, 0
      -F_0, (1+2*F_0), -F_0, 0
      0, -F_0, (1+2*F_0), -F_0
      0, 0, -F_0, (1+2*F_0)];

g = ((2*alpha*q*deltaT)/(k*deltaX));

C = [T_c(p,1)+g
      T_c(p,2)
      T_c(p,3)
      T_c(p,4)+F_0*T_m(p,2)];

T = A\C;
T = T';

'step1-T1T4.txt'

260.29 260.29          262.65 260.48          270.31 260.64
260.52 260.32          263.97 260.52          273.09 260.68
260.88 260.34          265.74 260.57          276.02 260.72
261.58 260.45          267.85 260.59          279.15 260.82

```

282.44	261.00	360.40	311.60	352.31	324.90
285.67	261.35	360.44	312.22	352.14	324.93
289.17	261.76	360.45	312.73	351.91	324.97
292.55	262.28	360.52	313.24	351.70	325.00
295.94	262.84	360.44	313.74	351.52	325.03
299.36	263.47	360.45	314.25	351.26	325.09
302.66	264.13	360.39	314.72	351.06	325.07
305.91	264.93	360.33	315.16	350.85	325.11
309.09	265.73	360.32	315.62	350.64	325.16
312.17	266.66	360.25	316.01	350.48	325.17
315.09	267.54	360.15	316.42	350.23	325.21
317.96	268.58	360.08	316.83	350.01	325.17
320.72	269.59	359.96	317.21	349.82	325.24
323.30	270.69	359.87	317.55	349.63	325.23
325.79	271.79	359.76	317.94	349.44	325.25
328.14	272.91	359.65	318.29	349.19	325.22
330.36	274.12	359.54	318.61	349.00	325.22
332.53	275.27	359.43	318.89	348.79	325.23
334.53	276.50	359.30	319.21	348.57	325.25
336.37	277.71	359.14	319.57	348.42	325.18
338.22	278.93	359.01	319.82	348.19	325.22
339.86	280.13	358.87	320.07	347.95	325.22
341.51	281.35	358.67	320.31	347.77	325.21
342.96	282.59	358.55	320.58	347.54	325.16
344.35	283.79	358.34	320.84	347.42	325.18
345.63	284.98	358.23	321.10	347.16	325.16
346.91	286.20	358.04	321.31	346.96	325.13
348.04	287.37	357.85	321.53	346.76	325.12
349.18	288.52	357.67	321.74	346.56	325.09
350.11	289.67	357.53	321.92	346.43	325.08
351.06	290.82	357.34	322.12	346.19	325.12
351.91	291.93	357.18	322.29	346.02	325.04
352.70	292.97	356.97	322.51	345.80	324.96
353.51	294.02	356.81	322.70	345.58	324.98
354.22	295.11	356.61	322.81	345.45	324.95
354.85	296.10	356.39	322.97	345.23	324.96
355.42	297.09	356.20	323.09	345.09	324.88
356.00	298.07	356.03	323.27	344.88	324.87
356.54	299.02	355.82	323.42	344.66	324.84
357.02	299.96	355.65	323.51	344.51	324.77
357.42	300.83	355.39	323.65	344.30	324.71
357.82	301.72	355.23	323.76	344.12	324.68
358.19	302.56	354.98	323.89	343.89	324.65
358.52	303.40	354.83	324.00	343.71	324.63
358.85	304.18	354.65	324.09	343.55	324.56
359.10	304.98	354.40	324.21	343.33	324.56
359.31	305.72	354.20	324.28	343.18	324.50
359.52	306.52	353.94	324.35	343.00	324.44
359.74	307.21	353.79	324.44	342.80	324.44
359.86	307.92	353.59	324.51	342.68	324.35
360.01	308.57	353.38	324.59	342.47	324.33
360.12	309.21	353.18	324.63	342.26	324.28
360.25	309.85	352.96	324.72	342.15	324.23
360.32	310.48	352.75	324.76	341.88	324.21
360.46	311.08	352.56	324.81	341.80	324.13

341.56	324.09	333.07	320.70	326.50	317.16
341.43	324.04	332.96	320.66	326.40	317.14
341.23	324.00	332.80	320.60	326.28	317.06
341.03	323.94	332.68	320.53	326.18	316.98
340.93	323.89	332.56	320.49	326.07	316.94
340.75	323.83	332.47	320.40	325.95	316.85
340.52	323.78	332.26	320.32	325.89	316.78
340.39	323.71	332.14	320.27	325.77	316.76
340.21	323.64	331.98	320.15	325.68	316.68
340.04	323.56	331.85	320.15	325.54	316.61
339.89	323.55	331.77	320.06	325.45	316.58
339.71	323.50	331.67	320.00	325.32	316.48
339.54	323.41	331.49	319.94	325.23	316.44
339.31	323.37	331.36	319.84	325.17	316.38
339.23	323.30	331.21	319.79	325.07	316.33
339.04	323.26	331.12	319.74	324.93	316.26
338.87	323.20	331.00	319.71	324.85	316.21
338.72	323.16	330.85	319.61	324.75	316.14
338.54	323.06	330.75	319.53	324.65	316.05
338.38	323.00	330.57	319.47	324.54	316.02
338.24	322.95	330.51	319.44	324.44	315.93
338.07	322.89	330.39	319.34	324.38	315.88
337.91	322.84	330.28	319.28	324.26	315.85
337.76	322.78	330.11	319.19	324.16	315.77
337.62	322.69	329.99	319.17	324.06	315.73
337.46	322.67	329.85	319.08	323.98	315.66
337.26	322.56	329.74	319.02	323.92	315.63
337.16	322.53	329.60	318.97	323.83	315.52
336.99	322.45	329.50	318.91	323.69	315.45
336.85	322.43	329.39	318.86	323.63	315.40
336.69	322.35	329.26	318.75	323.50	315.35
336.50	322.28	329.20	318.72	323.42	315.27
336.39	322.21	329.03	318.63	323.33	315.23
336.18	322.14	328.96	318.58	323.23	315.19
336.08	322.11	328.81	318.49	323.13	315.11
335.95	322.02	328.71	318.45	323.00	315.09
335.77	321.98	328.59	318.37	323.00	315.02
335.61	321.86	328.47	318.32	322.87	314.95
335.48	321.85	328.40	318.20	322.78	314.91
335.29	321.77	328.22	318.19	322.66	314.84
335.21	321.72	328.14	318.15	322.57	314.76
335.01	321.67	328.06	318.06	322.51	314.74
334.90	321.54	327.93	317.98	322.46	314.68
334.72	321.52	327.80	317.91	322.33	314.61
334.57	321.42	327.67	317.85	322.29	314.54
334.48	321.38	327.56	317.79	322.13	314.47
334.35	321.33	327.47	317.73	322.08	314.42
334.18	321.25	327.34	317.68	322.04	314.40
334.03	321.19	327.25	317.60	321.87	314.31
333.92	321.13	327.10	317.55	321.80	314.27
333.75	321.04	327.05	317.52	321.74	314.23
333.61	320.98	326.96	317.45	321.64	314.15
333.47	320.92	326.83	317.37	321.61	314.10
333.33	320.86	326.73	317.31	321.48	314.05
333.20	320.80	326.58	317.22	321.40	313.96

321.29	313.94	317.14	311.04	313.70	308.58
321.22	313.89	317.03	311.00	313.62	308.49
321.16	313.82	316.99	310.97	313.53	308.48
321.02	313.75	316.91	310.88	313.46	308.42
320.99	313.71	316.86	310.87	313.45	308.37
320.89	313.68	316.75	310.82	313.39	308.35
320.83	313.61	316.72	310.76	313.29	308.28
320.76	313.55	316.68	310.71	313.27	308.24
320.66	313.51	316.61	310.67	313.19	308.20
320.58	313.40	316.51	310.61	313.14	308.17
320.47	313.34	316.45	310.54	313.11	308.15
320.36	313.34	316.39	310.55	313.02	308.08
320.36	313.29	316.33	310.49	312.97	308.08
320.22	313.24	316.27	310.46	312.93	308.00
320.16	313.18	316.18	310.41	312.92	307.98
320.07	313.12	316.11	310.32	312.83	307.94
319.98	313.04	316.03	310.30	312.76	307.87
319.98	313.00	315.92	310.24	312.68	307.81
319.81	312.94	315.95	310.22	312.66	307.79
319.72	312.88	315.87	310.19	312.62	307.74
319.67	312.85	315.78	310.12	312.57	307.71
319.56	312.78	315.70	310.06	312.52	307.70
319.54	312.73	315.65	310.05	312.45	307.61
319.45	312.69	315.65	310.01	312.38	307.61
319.36	312.62	315.51	309.93	312.35	307.55
319.30	312.58	315.47	309.88	312.29	307.51
319.22	312.54	315.40	309.82	312.26	307.45
319.16	312.49	315.29	309.79	312.13	307.42
319.10	312.41	315.25	309.71	312.09	307.36
318.99	312.38	315.21	309.71	312.04	307.37
318.96	312.30	315.13	309.66	312.05	307.34
318.80	312.25	315.11	309.62	311.95	307.31
318.83	312.22	315.02	309.56	311.90	307.21
318.69	312.16	314.99	309.52	311.87	307.18
318.61	312.12	314.93	309.49	311.76	307.12
318.56	312.06	314.86	309.40	311.77	307.10
318.48	312.02	314.79	309.39	311.67	307.08
318.45	311.98	314.70	309.34	311.64	307.02
318.33	311.90	314.64	309.27	311.62	306.97
318.24	311.89	314.62	309.26	311.54	306.92
318.15	311.81	314.57	309.20	311.48	306.90
318.10	311.77	314.52	309.16	311.42	306.85
318.04	311.72	314.43	309.11	311.39	306.82
318.00	311.70	314.39	309.05	311.32	306.78
317.90	311.62	314.35	309.03	311.26	306.74
317.84	311.57	314.22	308.97	311.26	306.71
317.75	311.49	314.20	308.92	311.18	306.69
317.68	311.46	314.07	308.89	311.16	306.64
317.65	311.43	314.09	308.85	311.08	306.56
317.55	311.36	314.01	308.83	311.02	306.52
317.46	311.32	313.99	308.79	311.02	306.54
317.36	311.24	313.90	308.70	310.94	306.49
317.36	311.23	313.84	308.68	310.83	306.47
317.27	311.16	313.79	308.64	310.85	306.41
317.17	311.11	313.70	308.55	310.73	306.34

310.72 306.29
310.73 306.30
310.63 306.24
310.60 306.22
310.52 306.18
310.51 306.09
310.43 306.08
310.39 306.06
310.33 306.00
310.30 305.98
310.23 305.95
310.22 305.89
310.18 305.88
310.10 305.81
310.05 305.81
310.00 305.73
309.97 305.72
309.90 305.64
309.86 305.61
309.83 305.63
309.79 305.55
309.77 305.55
309.65 305.52
309.67 305.43
309.57 305.38
309.50 305.39
309.52 305.37
309.42 305.34
309.42 305.28
309.34 305.24
309.30 305.18
309.28 305.17
309.26 305.15
309.16 305.12
309.16 305.07
309.04 305.03
309.08 305.00
309.00 304.94
308.92 304.93
308.90 304.92
308.86 304.86
308.86 304.81
308.76 304.77
308.72 304.77
308.68 304.69
308.62 304.67
308.58 304.62
308.54 304.62
308.50 304.55
308.40 304.53
308.39 304.52
308.35 304.42
308.34 304.44
308.26 304.32

APPENDIX C

THE 5-STEP SQUEEZE CASTINGS EXPERIMENTAL RESULTS OF MAGNESIUM ALLOY AM60 & ALUMINUM ALLOY A443 UNDER DIFFERENT PRESSURES

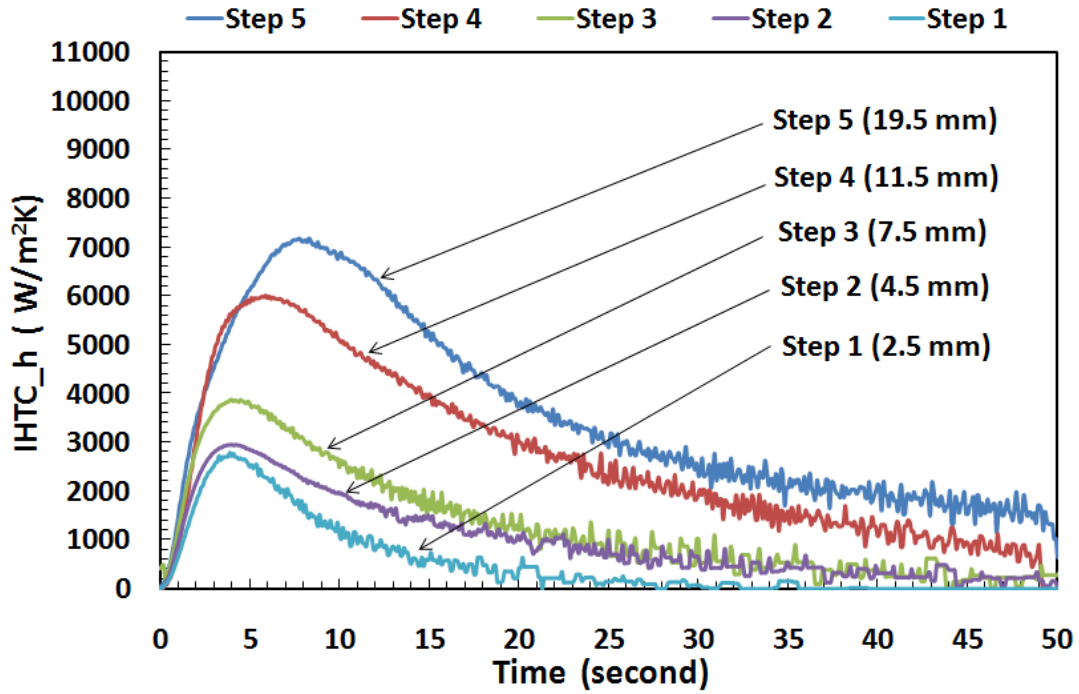


Figure AC- 1 The interfacial heat transfer coefficients(IHTC) curves of AM60 with all steps under the applied pressure of 30MPa.

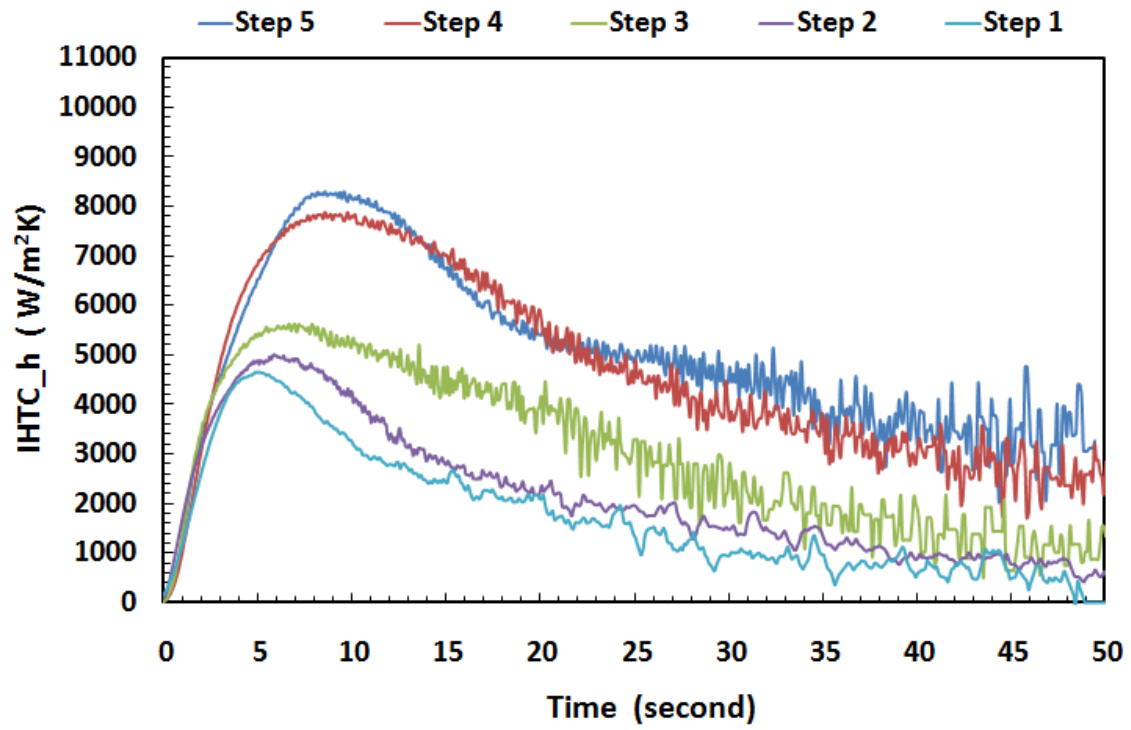


Figure AC- 2 The interfacial heat transfer coefficients(IHTC) curves of AM60 with all steps under the applied pressure of 60MPa.

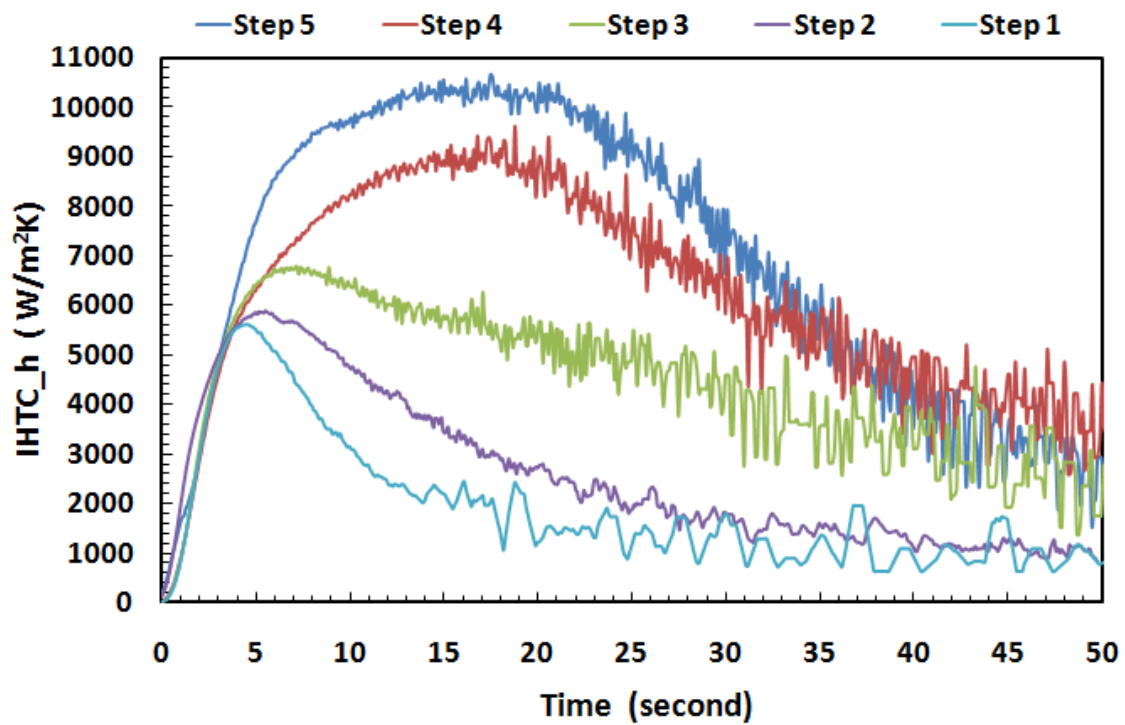


Figure AC- 3 The interfacial heat transfer coefficients(IHTC) curves of AM60 with all steps under the applied pressure of 90MPa.

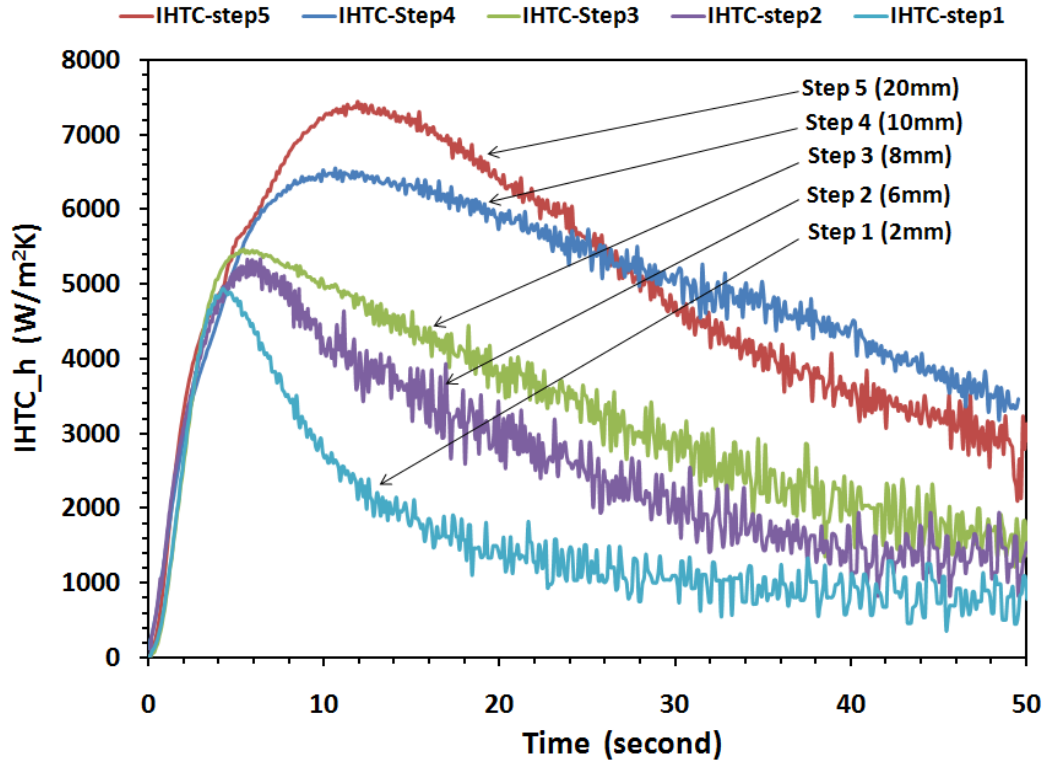


Figure AC- 4 The interfacial heat transfer coefficients(IHTC) curves of A443 with all steps under the applied pressure of 30MPa.

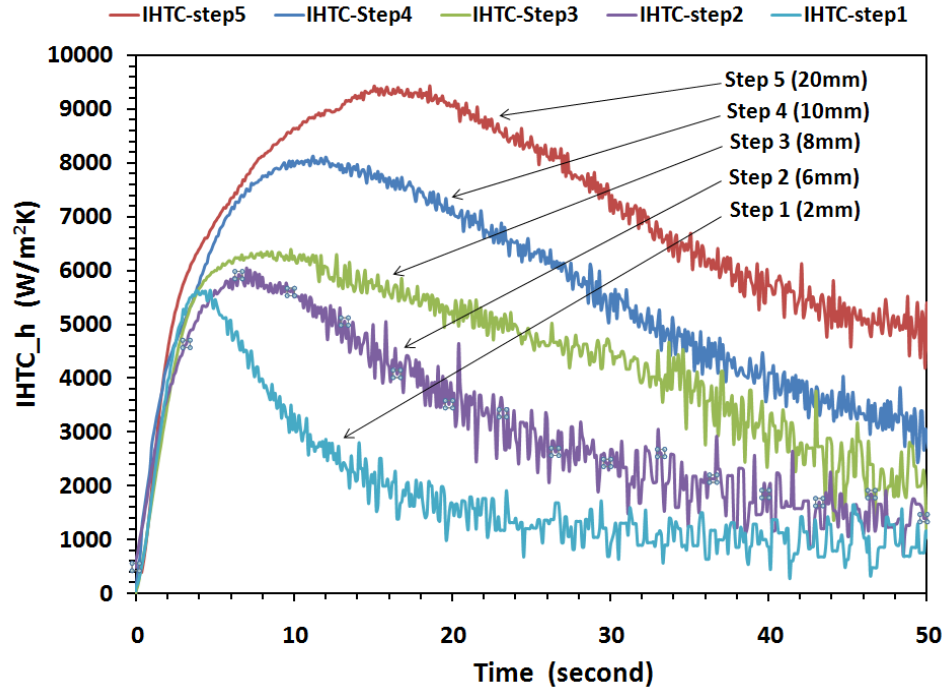


Figure AC- 5 The interfacial heat transfer coefficients(IHTC) curves of A443 with all steps under the applied pressure of 60MPa.

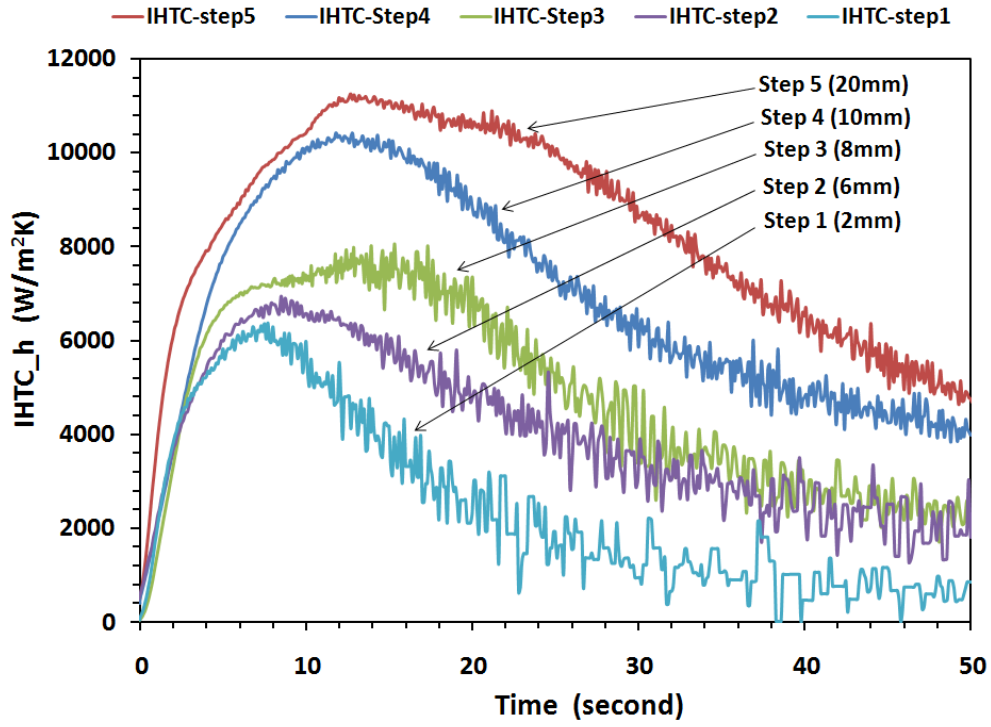


Figure AC- 6 The interfacial heat transfer coefficients(IHTC) curves of A443 with all steps under the applied pressure of 90MPa.

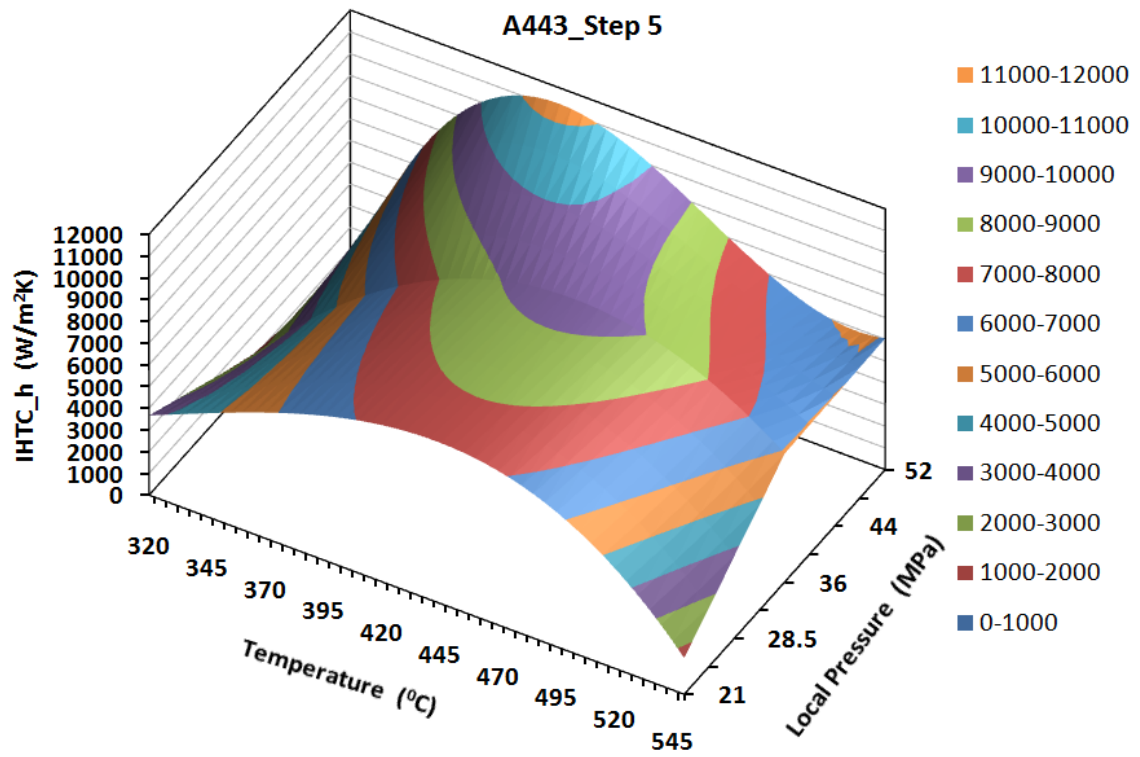


Figure AC- 7 IHTC curve plane of aluminum alloy 443(Step 5) as a function of the local pressure and solidification temperature.

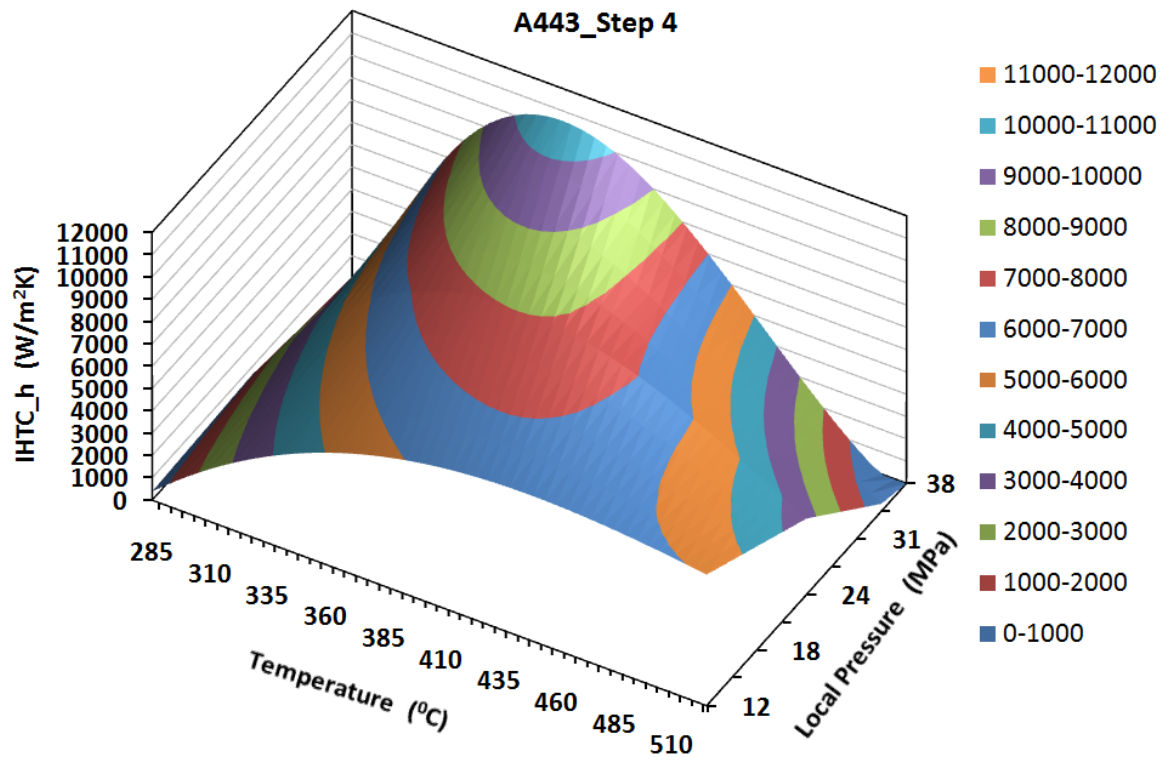


Figure AC- 8 IHTC curve plane of aluminum alloy 443(Step 4) as a function of the local pressure and solidification temperature.

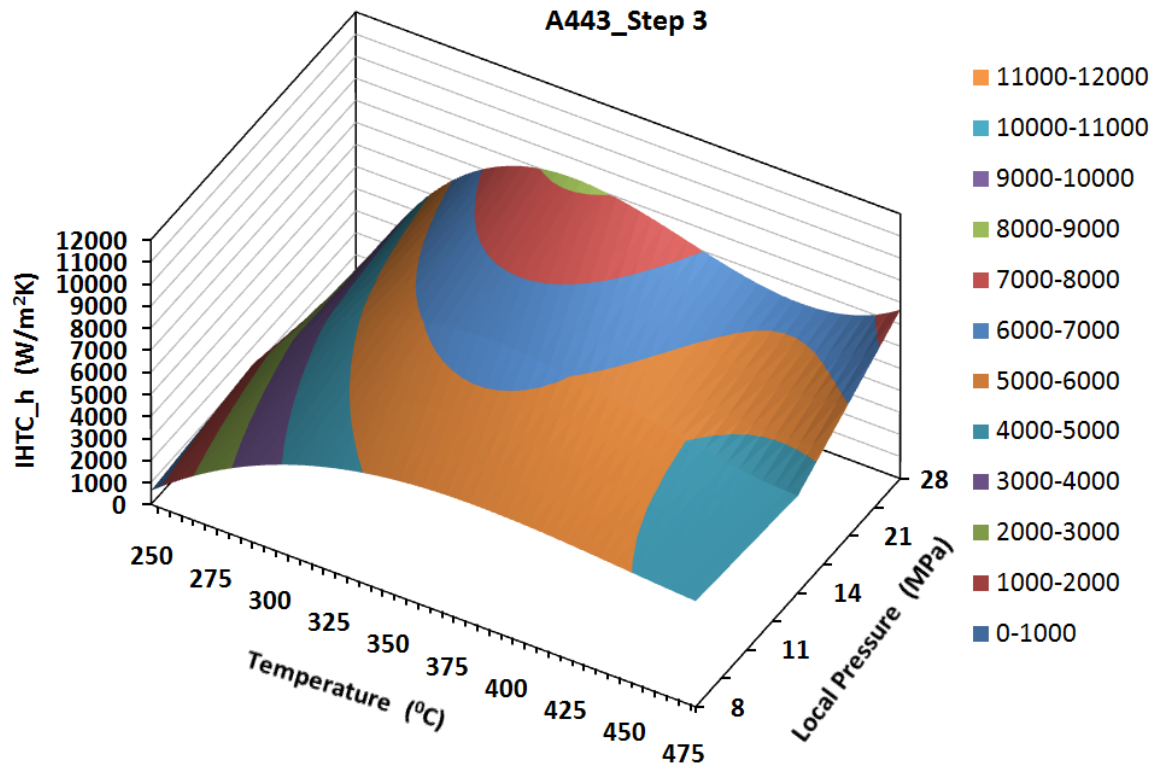


Figure AC- 9 IHTC curve plane of aluminum alloy 443(Step 3) as a function of the local pressure and solidification temperature.

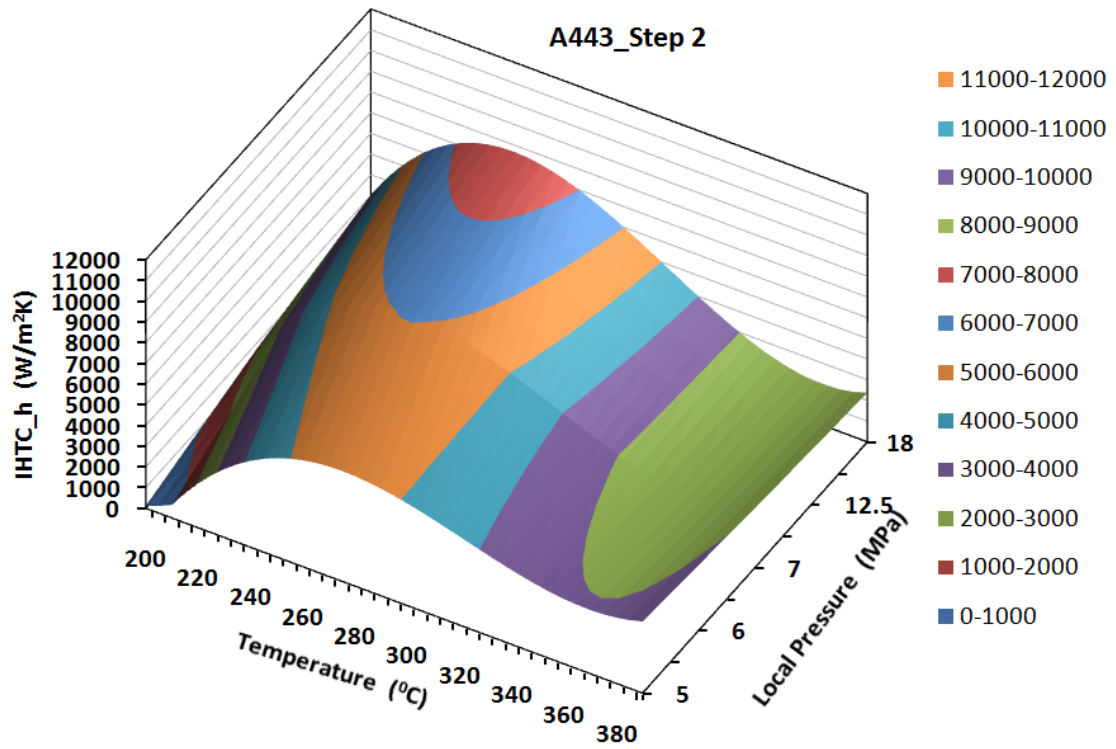


Figure AC- 10 IHTC curve plane of aluminum alloy 443(Step 2) as a function of the local pressure and solidification temperature.

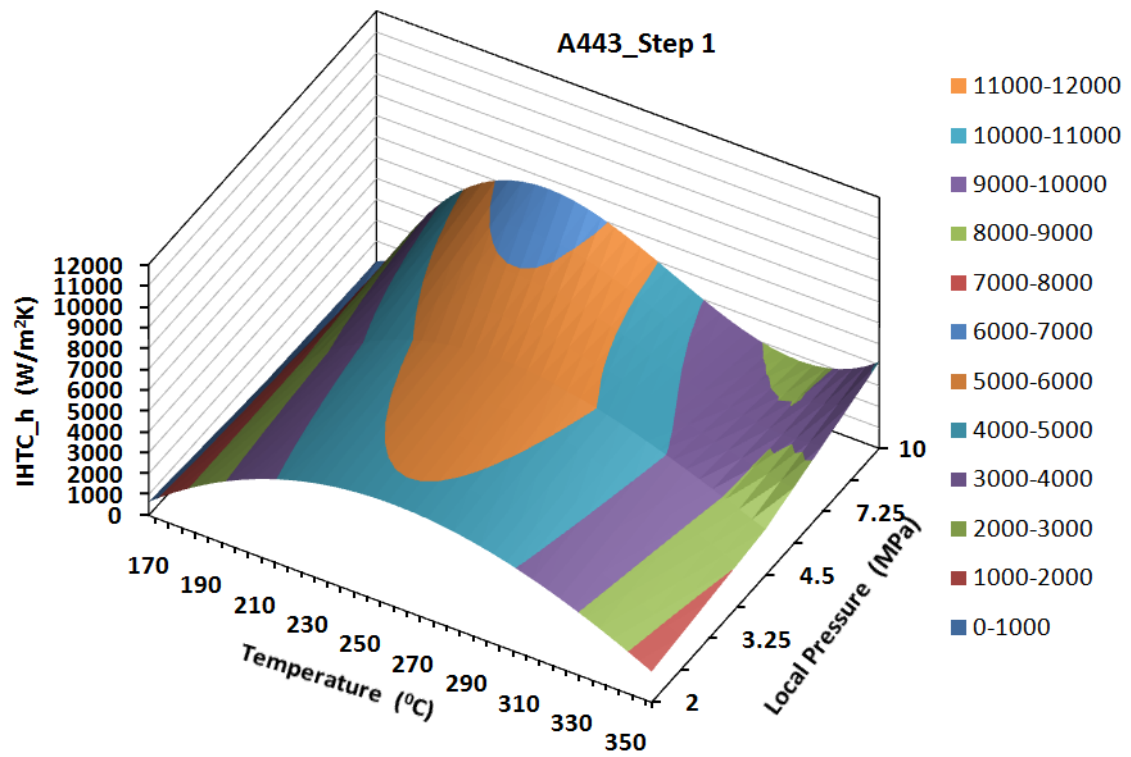


Figure AC- 11 IHTC curve plane of aluminum alloy 443(Step 1) as a function of the local pressure and solidification temperature.

PUBLICATION LIST

REFEREED JOURNAL PUBLICATIONS

1. **Zhizhong Sun**, Henry Hu, Xiaoping Niu, “Determination of heat transfer coefficients by extrapolation and numerical inverse methods in squeeze casting of magnesium alloy AM60”, *Journal of Materials Processing Technology*, (2011) Vol. 211, pp. 1432-1440.
2. **Zhizhong Sun**, Xuezhi Zhang, Xiaoping Niu, Alfred Yu, Henry Hu, “Numerical simulation of heat transfer in pressurized solidification of Magnesium alloy AM50”, *Heat and Mass Transfer / Waerme- und Stoffuebertragung*, (2011) Vol. 47, pp. 1241-1249.
3. **Zhizhong Sun**, Alfred Yu, Henry Hu, Lihong Han, “Mathematical Modeling of Squeeze Casting of Magnesium Alloy AM50”, *Defect and Diffusion Forum*, (2010), Vols. 297-301 p105-110.
4. **Zhizhong Sun**, Henry Hu, Xiang Chen, Qigui Wang, Wenying Yang, “Gating System Design for a Magnesium Alloy Casting”, *Journal of Materials Science & Technology*, (2008), Vol.24, N.1, p93-95.
5. **Zhizhong Sun**, Henry Hu, Xiang Chen. “Numerical Optimization of Gating System Parameters for A Magnesium Alloy Casting with Multiple Performance Characteristics”, *Journal of Materials Processing Technology*, (2007), Vol. 199, No.1, p256-264.
6. **Zhizhong Sun**, Ming Zhou, Henry Hu, Naiyi Li, “Strain-hardening and Fracture Behaviour of Die Cast Magnesium Alloy AM50”, *Research Letters in Materials Science*, (2007), Vol. 2007, Article ID 64195, 5 pages, doi:10.1155/2007/64195

7. Henry Hu, Ming Zhou; **Zhizhong Sun**; Naiyi Li, “Tensile behaviour and fracture characteristics of die cast magnesium alloy AM50”, Journal of Materials Processing Technology, (2008), Vol. 201, N 1-3, p364-368.

REFEREED CONFERENCE FULL PAPERS AND PRESENTATIONS

8. **Zhizhong Sun**, Xiaoping Niu, Henry Hu, “Effects of local pressure and wall-thickness on interfacial heat transfer in squeeze casting of magnesium alloy AM60”, Proceedings of the 7th International Conference on Computational Heat and Mass Transfer(ICCHMT-7), Istanbul, Turkey, (July 18-22, 2011), Accepted.
9. **Zhizhong Sun**, Henry Hu, Xiaoping Niu, “Section thickness-dependant interfacial heat transfer in squeeze casting of aluminum alloy A443”, The 3rd International Conference on Advances in Solidification Processes(ICASP-3), Aachen, Germany (June 7-10, 2011), Accepted.
10. **Zhizhong Sun**, Xiaoping Niu, Henry Hu, “Estimation of heat transfer coefficient in squeeze casting of magnesium alloy AM60 by experimental polynomial extrapolation method”, Magnesium Technology 2011, (2011), p146-152. 140th TMS 2011 conference proceedings.
11. **Zhizhong Sun**, Henry Hu, Jonathan Burns, Xueyuan Nie, Lihong Han, “Design of a Step Permanent Mold for Casting Magnesium Alloy AJ62”, AFS Transactions, (2010), Vol.118. p1-12. 114th Metalcasting Congress.
12. **Zhizhong Sun**, Henry Hu; Alfred Yu, “Numerical Simulation and Experimental Study of Squeeze Casting Magnesium Alloy AM50”, Magnesium Technology 2010, (2010), p301-311. 139th TMS 2010 conference proceedings.

13. **Zhizhong Sun**, Jean Kor, Henry Hu, Xiang Chen, Gerald Backer, Qigui Wang, Wenying Yang. “Numerical Analysis of Gating System Design in an Aluminum Casting”, AFS Transactions, (2007), Vol.115. p1-12. 111st Metalcasting Congress.
14. Jean Kor, Xiang Chen, **Zhizhong Sun**, Henry Hu, “Casting Design Through Multi-objective Optimization”, Proceedings of the 2009 Second International Conference on Future Information Technology and Management Engineering (FITME,) (2009), p 604-608.
15. Shuping Wang; **Zhizhong Sun**; Henry Hu, “Effect of pressure levels on tensile properties of squeeze cast Mg-Al -Sr alloy” Magnesium Technology 2008, (2008), p421-425. 137th TMS 2008 conference proceedings.

VITA AUCTORIS

NAME: Zhizhong Sun

PLACE OF BIRTH: Luoyang, China

DATE OF BIRTH: October 1969

EDUCATION: University of Windsor, Windsor, ON, Canada

2008-2011 Ph.D. in Engineering Materials

2006-2007 M.Sc. in Material Engineering

University of Science and Technology Beijing, China

1994-1997 M.Sc. in Mechanical Engineering

Luoyang Institute of Technology, China

1986-1990 B.Sc. in Material Engineering